TECHNICAL SUMMARY REPORT
20 July 1966

SID 66-1201

MASS LOADING EFFECTS ON LOCALIZED VIBRATORY ENVIRONMENTS OF ROCKET VEHICLES

(Contract NAS8-20019)

Prepared by

S. Y. Lee and S. S. Tang

Approved by

S. Y. Lee
Project Engineer

F. C. Hung
Project Manager

Structures and Dynamics Dept., Research & Engineering
SPACE AND INFORMATION SYSTEMS DIVISION
NORTH AMERICAN AVIATION, INC.
Downey, California

for

NATIONAL AERONAUTICS AND SPACE ADMINISTRATION
George C. Marshall Space Flight Center
Huntsville, Alabama

NORTH AMERICAN AVIATION, INC. SPACE and INFORMATION SYSTEMS DIVISION

TECHNICAL SUMMARY REPORT
20 July 1966

SID 66-1201

MASS LOADING EFFECTS ON LOCALIZED VIBRATORY ENVIRONMENTS OF ROCKET VEHICLES

(Contract NAS8-20019)

Prepared by

S. Y. Lee and S. S. Tang

Approved by

S. Y. Lee
Project Engineer

F. C. Hung
Project Manager

Structures and Dynamics Dept., Research & Engineering
SPACE AND INFORMATION SYSTEMS DIVISION
NORTH AMERICAN AVIATION, INC.
Downey, California

for

NATIONAL AERONAUTICS AND SPACE ADMINISTRATION
George C. Marshall Space Flight Center
Huntsville, Alabama

FOREWORD

This report describes the work performed under NASA Contract NAS8-20019, "Mass Loading Effects on Localized Vibratory Environments of Rocket Vehicles," by the Space and Information Systems Division (S&ID) of North American Aviation, Inc., for the George C. Marshall Space Flight Center, Huntsville, Alabama, during the period from 30 June 1965 to 31 July 1966.

The project was sponsored and administered under the direction of Messrs. J. Farrow, Branch Chief, and R. Schock, Section Chief of the Vibration and Acoustic Branch, Propulsion and Vehicle Engineering Division, NASA/MSFC.

The work was performed at S&ID under the direction of Dr. L. A. Harris, Director of the Structures and Dynamics Department, and Dr. F. C. Hung, Assistant Director of the Department and Program Manager of the project. Mr. S. Y. Lee, the Project Engineer, supervised the technical activities, and also, as the principal investigator, he established the theoretical and experimental methods, directed the experiments, and performed analyses to obtain numerical solutions. As an associate investigator, Mr. S. S. Tang assisted in the project administration and coordination, and carried out part of the detailed technical analysis.

The authors wish to express their appreciation to Mr. R. Jewell of NASA for his encouragement, to Prof. M. P. Bieniek of the University of Southern California for his technical consultation, to Mr. J.G. Liyeos for his assistance in computer programming and numerical evaluations, and to Messrs. C. Bailey and G. Parker for their assistance in test operations.

ABSTRACT

12236

Mass-loading and mass-coupling effects on dynamic characteristics of localized rocket vehicle structures were studied analytically and experimentally. Beams and plates loaded with various masses and bracketry were investigated. Solutions were obtained on free-vibration characteristics, transmissibility, and forced response. A specially built electromagnetic induction shaker, in addition to conventional vibration and acoustic test equipment, was employed to produce excitations including edge motions, concentrated force, and distributed force in the form of sinusoidal and random input. The analytical solutions agree closely with experimental results.

Author

CONTENTS

ILLUSTRATIONS

TABLES

INTRODUCTION

In spite of the recent rapid advances in many branches of the aerospace sciences, including dynamics, insufficient progress has been made in the practical applications of vibration technology. There are still many difficulties encountered in the areas of vibration design, environmental prediction, dynamic analysis, test and evaluation. Dynamic problems associated with a structure become more difficult and simultaneously more important when the local structure has a piece of equipment mounted on it. In such a case, the dynamicist is faced with the problem of estimating the effect of the equipment on the response of the local structure in order to predict, realistically, the vibratory environment experienced by the mounted component and to calculate the vibration response of the combined system.

In 1961, Mahaffey and Smith (Reference 1) studied the local vibration data of airplane flights, and in 1963 Franken (Reference 2) did an identical study of the Titan missile. The results of these studies have been widely used for the prediction of dynamic environments for mass-loaded and unloaded local structures of missiles and space vehicles throughout the aerospace industry. However, these two studies were primarily concerned with the statistical regression of the airplane or missile flight vibration data at a given vehicle zone; analyses of mass-loading effects due to the mounted equipment were lacking.

The first documentation of mass-loading effects on vibration environment appears to be Military Specification MIL-E-5272, but the mass-loading provision presented appears to have been determined rather arbitrarily. These mass-loading effects criteria were endorsed and specified in the new specification standards, MIL-STD-810, by a working committee (Reference 3) of shock and vibration specialists consisting of government and industry expert dynamicists selected by the USAF in late 1962. No information could be found in the new specification regarding the author, the date of initiation, or the technical basis used in establishing the arbitrary mass-loading criteria. During 1963-1964, Schock, Barrett, Jewel, and Lifer (References 4 through 8) of NASA/MSFC were interested in the mass-loading phenomenon and they introduced an empirical prediction technique employing a statistical approach in conjunction with Saturn firing test data; they also recommended theoretical and experimental research studies to investigate the dynamic response phenomenon.

Analytically, scientists and engineers have difficulty in computing the vibration response of a structure without an assumption of the dynamic

transmissibilities, quality factor, complex elasticity, or damping factor. This analytical problem is magnified when the structure is loaded with equipment masses. It is believed that this problem has not been solved and it was therefore one of the major technical objectives of this research program to explore the relation between the transmissibility characteristics of the mass-loaded and unloaded structures under both constant acceleration and constant force excitations.

At NAA, mass-loading effects on vibrating structures were observed by Lee in 1956 at the Engineering Development Laboratory of the Missiles Development Division. He found these phenomena repeatedly in his work in connection with 12 missiles and space systems at Douglas Aircraft Company. His initial analytical investigation of the vibration characteristics of mass-loaded structures was completed in 1959, and it emphasizes the frequency and modal isolation studies. Based on these approaches, the mass-attenuation analyses can be accomplished. This earlier work was documented as a research report (References 9 and 10) for the Mechanical Engineering Department of the University of Southern California.

In 1962, a preliminary experimental and theoretical investigation of the mass-loading and coupling problem was launched at NAA/S&ID (References 11, 12, 13, and 14). A consistent trend of the mass-loading effect on transmissibility characteristics then became apparent, and Lee formulated the relations in conjunction with his graduate research work. These formulations are verified further now by the planned experiments. The basic concepts of employing mass-coupling systems to investigate the characteristics of absorbtion of the vibration energy and to verify the validity and limitations of the mass-loading phenomenon were also initiated. These basic concepts are followed with further development through the present project. After Lee's initial contact with NASA/MSFC in 1963, and following a technical presentation, this study program was awarded in 1965 to correlate all of the aforementioned efforts and to develop a technique for predicting the mass-loading effect. The scope of work is illustrated in Figure 1.

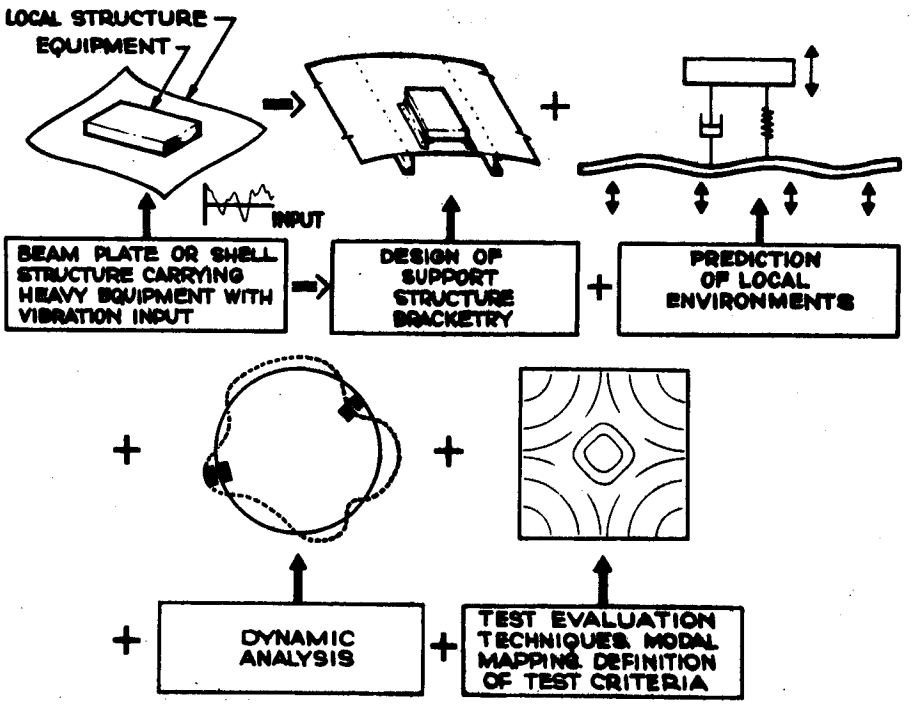

Figure 1. Statement of Problem

TECHNICAL APPROACH

Most of the local structures of rocket vehicles are beams, plates, or a combination of beams and plates. Since the study of mass-loading effects is in its exploratory phase, it has been necessary to consider only simple structures, and, therefore, analytical as well as experimental studies conducted under this contract accordingly place emphasis on mass-loaded beams and plates. However, the basic principles can be applied to other structures and with different boundary conditions.

The problem considered in this study involves a local structure that carries some equipment represented by rigid masses. In mass-loading studies, only the problems associated with equipment mass rigidly mounted or attached through a rigid bracketry to a local structure under an arbitrary vibration environment are considered. If the bracketry is sufficiently flexible or the equipment has some critical frequencies that interact with the local structures, the problem is treated under the mass-coupling cases.

For the mass-loading cases, the free-vibration and forced-vibration problems are solved with a direct solution and with several alternative approaches. The vibration transmissibility problems for the mass-loaded structures, however, are solved in terms of the unloaded structures. The mass-coupling problems are treated as an investigation of the interaction phenomena among the equipment mass, bracketry, and the local structure. This study is mainly for the purpose of inspecting the limitation of the applications of the mass-loading effects.

As shown in the block diagram (Figure 2), the mass-loading effects problem can be divided into four study areas to obtain solutions fulfilling the technical objectives:

1. Study the free-vibration characteristics including natural frequencies and modal response of the unloaded and mass-loaded structures of rocket vehicles.

2. Investigate the changes of vibratory transmissibility and the attenuation and isolation characteristics caused by the mounting of equipment masses.

3. Analyze the forced response of the mass-loaded systems under periodic and random excitations in the form of edge motion, uniformly distributed force, and concentrated force.

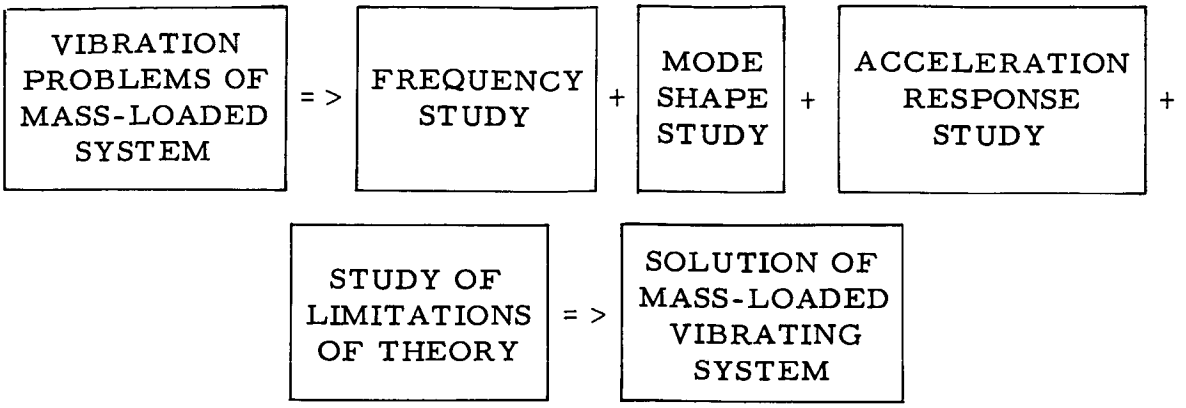

Figure 2. Technical Approach

4. Survey the coupling phenomena among bracketry, local structures, and equipment mass.

The problem of analytical prediction of mass-loading effects can be studied by several methods, including series-expansion, matrix-iteration, finite-difference, and some new development in the transfer-characteristic studies. Academic studies and new developments, as well as general applications, are equally emphasized in the investigation of mass-loaded beams, while more practical applications are developed in the investigation of mass-loaded plates. Mass-loaded beams, treated as continuous systems, are solved by the series-expansion approach; when treated as lumped-mass systems, solutions are obtained by the matrix-iteration technique. Other approaches are also discussed. Among the many analytical methods used for mass-loaded plates, a combination of the finite-difference and matrix-iteration approach is outstanding because of its efficiency and practical effectiveness in solving this type of problem.

An experimental test program that used 58 models to represent the unloaded and mass-loaded local structures was conducted as an extension of Lee's earlier work to confirm results of the theoretical studies and to explore the unknown transmissibility characteristics.

Both the analytical and experimental investigations consider free vibration and forced vibration. Sources of excitation include acoustic, mechanical, and electromagnetic induction. These excitations are in a form of edge-motion, concentrated force, uniformly distributed force, sinusoids, random oscillation, constant-force inputs, or constant-acceleration inputs.

Experimentally, mechanical shakers were used to produce the edge excitation. An electromagnetic induction shaker was specially built to

generate concentrated exciting forces that could be applied at any location of the specimen. Uniformly distributed forces were accomplished through acoustic tests. Constant-force inputs represent a different dynamic environment from the constant-acceleration cases; furthermore, the net levels of the exciting force do not identically correspond from one to the other. Mechanical shakers can easily produce the constant-acceleration excitation, but it is difficult to generate the controllable constant-force excitations. Hence, for the constant-force cases, electroinduction or acoustical forces were used. One of the most difficult experimental tasks is to test the specimens without the attachment of a shaker, instrumentation, or any other mass, however, this task can be accomplished ingenuously by the use of the electromagnetic induction shaker with proximity gages.

ANALYTICAL STUDIES

Several methods can be used in the analytical study of mass-loading problems:

Lumped-Masses and Stiffness-Matrix Method

Lumped-Masses and Flexibility-Matrix Method

Force-Matrix Method

Finite-Difference Method

Energy Method

Series-Expansion Technique

A good approximate solution for the first mode can be obtained by the energy method using Rayleigh approach, but usually this method becomes less effective for higher modes. Since the attenuation and isolation of higher modes is one of the major objectives of this study, this method is not considered for either the beam or plate cases. Any one of the other methods can be a convenient way in solving the mass-loaded beam problems and three of them are discussed in detail.

By treating the mass-loaded beam as a continuous system, the problem is solved through the use of the series-expansion technique which results in a general solution from which numerical values can be obtained easily. Where high-speed computers are available, mass-loaded beam problems are solved by the lumped-mass approach combined with the matrix-iteration process. Numerical solutions of the frequencies are obtained and the mode shapes are plotted to compare with the experimental results. The finite-difference method is briefly discussed for mass-loaded beam cases; however, the same method is presented in detail for the mass-loaded plate cases.

For the mass-loaded plate problems, the lumped-mass method may cause some computational difficulties in the determination of the stiffness or flexibility matrices; the series-expansion technique, which treats the mass-loaded plate as a continuous system, may introduce problems in computer programming or may require laborious manipulation for a numerical solution. Therefore, the plate problems are solved by using the finite-difference technique in conjunction with the Jacobian matrix-iteration method to obtain

numerical values. The problem is also solved theoretically by the series-expansion technique.

MASS-LOADING EFFECTS ON FREE VIBRATION

To predict the forced vibration response of a structure, it is beneficial first to find the free-vibration characteristics. Methods for solving free-vibration problems of a simple, unloaded structure are available in the published literature; however, for the mass-loading case the problem becomes more complicated — only a few solutions for some special cases exist.

In the following discussion, the modal response in free vibration of a mass-loaded beam or plate is analyzed in a general manner by two methods: (1) series-expansion, and (2) finite-difference methods. The lumped parameters approach is also employed for the case of mass-loaded beam. These methods do not offer equal advantages in obtaining solutions for the practical engineering problems because of the degree of complexity involved in each approach. It will be shown later that the lumped parameters method for the beam case and the finite-difference method for the plate case are the most practical approaches to the mass-loading problems. Computer programs have been written for evaluation of the modal responses of the mass-loaded beam and plate based on each of these two methods.

Mass-Loaded Beams

Series-Expansion Method

Equation of Motion. The equation of motion for a uniform beam carrying a system of concentrated masses M_i at locations $x = a_i$ (Figure 3) can be written as: (References 10 and 15)

$$EI\frac{\partial^4 y}{\partial x^4} - \frac{\partial}{\partial x}\left[\sum_{i=1}^{N} J_i \delta(x - a_i)\frac{\partial^3 y}{\partial x \partial t^2}\right] + \left[\rho + \sum_{i=1}^{N} M_i \delta(x - a_i)\right]\frac{\partial^2 y}{\partial t^2} = 0 \quad (1)$$

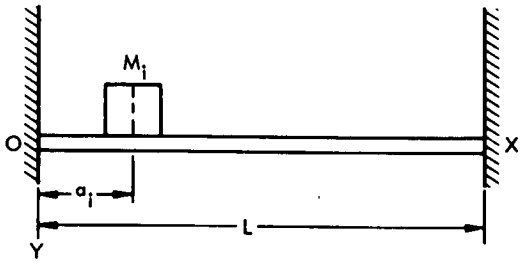

Figure 3. Analytical Model of Mass-Loaded Beam

where

EI = flexural rigidity of the beam

y = $y(x, t)$ = beam deflection

J_i = rotary inertia of the i^{th} concentrated mass

ρ = mass of the beam per unit length

δ = Dirac delta function with the property:

$$\int_0^L \delta(x - a_i)\, f(x)dx = f(a_i) \quad \text{for } x = a_i \text{ and}$$
$$\delta(x - a_i) = 0 \quad \text{for } x \neq a_i$$

N = total number of masses on the beam

Solution. Assume the deflection in a series form:

$$y(x, t) = \sum_{n=1}^{\infty} Y_n(x)\,(A_n \sin\omega_n t + B_n \cos\omega_n t) \tag{2}$$

where

$Y_n(x)$ = the n^{th} normal mode of the beam

ω_n = the n^{th} circular natural frequency

A_n, B_n = constants, determined from initial conditions

Substituting Equation (2) into Equation (1),

$$EI\, Y_n^{iv} + \omega_n^2 \left\{ \frac{d}{dx}\left[\sum_{i=1}^{N} J_i \delta(x - a_i) Y_n' \right] - \left[\rho + \sum_{i=1}^{N} M_i \delta(x - a_i) Y_n \right] \right\} = 0 \tag{3}$$

where the primes denote derivatives with respect to x.

The general solution of Equation (3) is

$$Y_n(x) = \frac{Y_n(0)}{2}(\cosh k_n x + \cos k_n x) + \frac{Y_n'(0)}{2k_n}(\sinh k_n x + \sin k_n x)$$

$$+ \frac{Y_n''(0)}{2k_n^2}(\cosh k_n x - \cos k_n x) + \frac{Y_n'''(0)}{2k_n^3}(\sinh k_n x - \sin k_n x)$$

$$- \frac{\omega_n^2}{2k_n^2 EI} \sum_{i=1}^{N} J_i Y_n'(a_i) \left[\cosh k_n(x - a_i) - \cos k_n(x - a_i)\right] u(x - a_i) \qquad (4)$$

$$+ \frac{\omega_n^2}{2k_n^3 EI} \sum_{i=1}^{N} M_i Y_n(a_i) \left[\sinh k_n(x - a_i) - \sin k_n(x - a_i)\right] u(x - a_i)$$

where

$$k_n^4 = \frac{\rho}{EI}\omega_n^2 \quad , \quad u = \text{unit step function}$$

Boundary Conditions. The boundary conditions for a beam are as follows:

Simply supported end:	$Y_n = 0$	$Y_n'' = 0$
Fixed end:	$Y_n = 0$	$Y_n' = 0$
Free end:	$Y_n'' = 0$	$Y_n''' = 0$

Imposing the proper boundary conditions at each end of the beam on Equation (4), a set of equations can be obtained, from which the frequency equation will be derived.

Frequency Equation and Natural Modes of a Simply Supported Beam. The first case to be studied is a mass-loaded beam with simply supported ends. The boundary conditions are

$$Y_n(0) = Y_n''(0) = Y_n(L) = Y_n''(L) = 0 \qquad (5)$$

Imposing these conditions on Equation (4), two sets of equations are obtained:

$$\frac{Y_n'(0)}{2k_n}(\sinh k_nL + \sin k_nL) + \frac{Y_n'''(0)}{2k_n^3}(\sinh k_nL - \sin k_nL)$$

$$- \frac{\omega_n^2}{2k_n^2 EI}\sum_{i=1}^{N} J_i Y_n'(a_i)\left[\cosh k_n(L - a_i) - \cos k_n(L - a_i)\right] u(L - a_i) \qquad (6)$$

$$+ \frac{\omega_n^2}{2k_n^3 EI}\sum_{i=1}^{N} M_i Y_n(a_i)\left[\sinh k_n(L - a_i) - \sin k_n(L - a_i)\right] u(L - a_i) = 0$$

and

$$\frac{k_nY'(0)}{2}(\sinh k_nL - \sin k_nL) + \frac{Y_n'''(0)}{2k_n}(\sinh k_nL + \sin k_nL)$$

$$- \frac{\omega_n^2}{2EI}\sum_{i=1}^{N} J_i Y_n'(a_i)\left[\cosh k_n(L - a_i) + \cos k_n(L - a_i)\right] u(L - a_i) \qquad (7)$$

$$+ \frac{\omega_n^2}{2k_nEI}\sum_{i=1}^{N} M_i Y_n(a_i)\left[\sinh k_n(L - a_i) + \sin k_n(L - a_i)\right] u(L - a_i) = 0$$

Substituting $x = a_q - \epsilon$ in Equation (4) and its derivative, $Y_n'(x)$, and by letting $\epsilon \to 0$, two sets of equations for the conditions of consistency are obtained.

$$
\begin{aligned}
&- Y_n(a_q) + \frac{Y_n'(0)}{2k_n}(\sinh k_n a_q + \sin k_n a_q) \\
&+ \frac{Y_n'''(0)}{2k_n^3}(\sinh k_n a_q - \sin k_n a_q) \\
&- \frac{\omega_n^2}{2k_n^2 EI} \sum_{i=1}^{q-1} J_i Y_n'(a_i) \left[\cosh k_n(a_q - a_i) - \cos k_n(a_q - a_i)\right] u(a_q - a_i) \\
&+ \frac{\omega_n^2}{2k_n^3 EI} \sum_{i=1}^{q-1} M_i Y_n(a_i) \left[\sinh k_n(a_q - a_i) - \sin k_n(a_q - a_i)\right] \\
&\cdot u(a_q - a_i) = 0 \qquad q = 1, 2, 3, \ldots, N
\end{aligned}
\tag{8}
$$

and

$$
\begin{aligned}
&- Y_n'(a_q) + \frac{Y_n'(0)}{2}(\cosh k_n a_q + \cos k_n a_q) + \frac{Y_n'''(0)}{2k_n^2}(\cosh k_n a_q - \cos k_n a_q) \\
&- \frac{\omega_n^2}{2k_n EI} \sum_{i=1}^{q-1} J_i Y_n'(a_i) \left[\sinh k_n(a_q - a_i) + \sin k_n(a_q - a_i)\right] \cdot u(a_q - a_i) \\
&+ \frac{\omega_n^2}{2k_n^2 EI} \sum_{i=1}^{q-1} M_i Y_n(a_i) \left[\cosh k_n(a_q - a_i) - \cos k_n(a_q - a_i)\right] \\
&\cdot u(a_q - a_i) = 0 \qquad q = 1, 2, 3, \ldots, N
\end{aligned}
\tag{9}
$$

Equations (6) through (9) form a system of (2N + 2) equations with (2N + 2) unknowns, $Y_n'(0)$, $Y_n'''(0)$, $Y_n(a_i)$, and $Y_n'(a_i)$. For nontrivial solutions of the problem the determinant of the coefficients of the above unknowns must vanish, thus, resulting in the frequency equation:

$$\det (k_n) = 0 \tag{10}$$

From this equation, the natural frequencies ω_n can be found. For each ω_n, the unknowns, $Y_n'(0)$, $Y_n'''(0)$, $Y_n(a_i)$ and $Y_n'(a_i)$ are first calculated then the corresponding mode shapes $Y_n(x)$ can be determined from Equation (4).

If the rotary inertias of the masses are neglected, Equation (9) may be discarded and then there exists only (N + 2) equations with (N + 2) unknowns, $Y_n'(0)$, $Y_n'''(0)$ and $Y_n(a_i)$.

Beam with Only One Mass. For a simply supported beam with only one concentrated mass (N = 1), Equation (10) becomes

$$\begin{aligned}
&\frac{JM}{\rho 2} k_n^4 (\sin k_n a \cosh k_n a - \sinh k_n a \cos k_n a) \\
&\cdot \left[\sin k_n(L-a) \cosh k_n(L-a) - \sinh k_n(L-a) \cos k_n(L-a)\right] \\
&+ \frac{2M}{\rho} k_n \left[\sin k_n L \sinh k_n a \sinh k_n(L-a)\right. \\
&\left. - \sinh k_n L \sin k_n a \sin k_n(L-a)\right] \\
&+ \frac{2J}{\rho} k_n^3 \left[\cos k_n(L-a) \sinh k_n L \cos k_n a - \cosh k_n(L-a)\right. \\
&\left. \cdot \sin k_n L \cosh k_n a\right] + 4 \sinh k_n L \sin k_n L = 0
\end{aligned} \tag{11}$$

If the mass is placed at midspan (a = L/2), Equation (11) can be factored into two equations: one for the symmetrical modes and the other for antisymmetric modes. If, in addition, the rotary inertia is not considered, the two frequency equations are

$$\frac{Mk_n}{\rho}\left(\tan \frac{k_n L}{2} - \tanh \frac{k_n L}{2}\right) - 4 = 0 \tag{12}$$

n = 1, 3, 5, ... , for symmetrical modes

and

$$\sin\frac{k_n L}{2} = 0 \qquad (13)$$

$n = 2, 4, 6, \ldots$, for antisymmetric modes

From Equations (12) and (13), the natural frequencies can be solved. The natural modes then are found from Equation (4).

Mass-Loading Effects on Natural Frequencies. To study the mass-loading effect on the natural frequencies of the beam, Equation (12) is rewritten as follows:

$$\tan\frac{k_n L}{2} - \tanh\frac{k_n L}{2} = \frac{4\rho}{Mk_n}$$

Let

$$\theta = \frac{k_n L}{2}$$

$M_b = \rho L$ = total mass of the beam

Then,

$$\theta(\tan\theta - \tanh\theta) = 2\frac{M_b}{M} \qquad (14)$$

It is seen from Equation (14) that the natural frequencies vary with the mass ratio, M_b/M. For each M_b/M there is a set of frequencies.

Several approximate values of θ (or $k_n L/2$) for the first three symmetric modes are as follows:

M_b/M	Value of θ		
	Mode 1	Mode 2	Mode 3
$M_b \ll M$	$\pi/4$	$1-1/4\pi$	$2-1/4\pi$
$M_b = M$	0.38π	1.38π	2.38π
$M_b \gg M$	$\pi/2$	$1-1/2\pi$	$2-1/2\pi$

Since

$$\omega_n^2 = \frac{EI}{\rho} k_n^4, \quad \omega_n = k_n^2 \sqrt{\frac{EI}{\rho}}$$

and

$$k_n = \frac{2\theta}{L} = \frac{2}{L}(j + b)\pi \tag{15}$$

where

$j = n - 1 = 0, 1, 2, \ldots$

b = constant, determined by M_b/M

$b = 1/4$ for $M_b/M \ll 1$

$= 0.38$ for $M_b/M = 1$

$= 1/2$ for $M_b/M \gg 1$

The frequency ω_n can be expressed in the form

$$\omega_n = 4(j + b)^2 \frac{\pi^2}{L^2} \sqrt{\frac{EI}{\rho}} \tag{16}$$

Mode Shape Investigation. The symmetric modes generated from Equation (4) can also be expressed in the following form for the simply supported beam with central mass (Figure 4):

$$Y_n(x) = C \cos \frac{k_n L}{2} \left[\frac{\sinh k_n x}{\cosh \frac{k_n L}{2}} - \frac{\sin k_n x}{\cos \frac{k_n L}{2}} \right] \tag{17}$$

where C is a constant. In particular, the normalized mode shape (C = 1) at the mas, $x = L/2$, is

$$Y_n\left(\frac{L}{2}\right) = \cos\frac{k_n L}{2} \left(\tanh \frac{k_n L}{2} - \tan\frac{k_n L}{2}\right)$$

or

$$Y_n\left(\frac{L}{2}\right) = \cos\theta \, (\tanh \theta - \tan\theta) \tag{18}$$

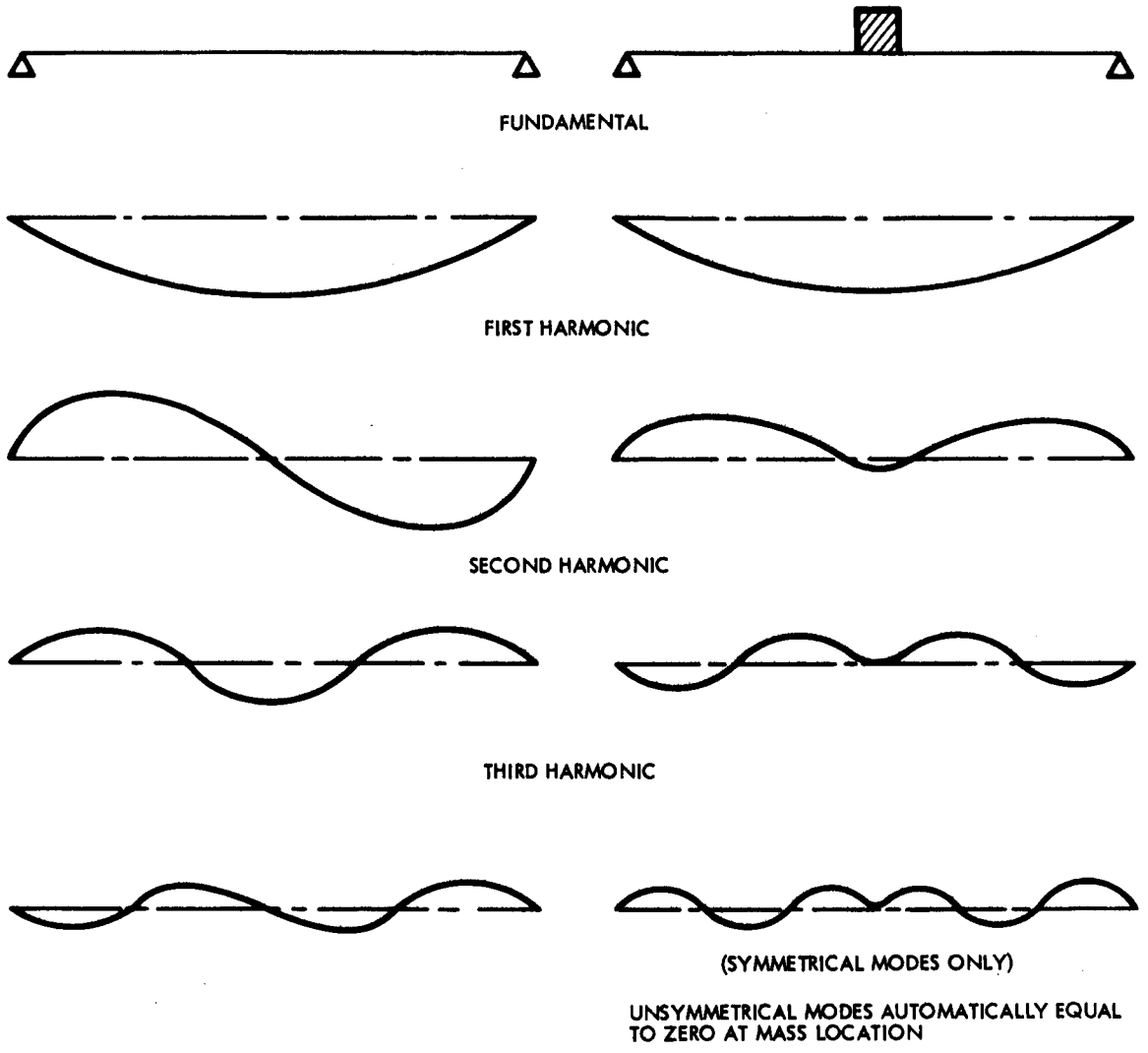

Figure 4. Mass-Loaded Beam Mode Shapes

From Equations (14) and (18), the mode shape at midspan of the beam can be expressed in terms of mass ratio M_b/M :

$$Y_n\left(\frac{L}{2}\right) = \cos\theta \frac{2}{\theta}\left(\frac{M_b}{M}\right) = \cos\theta \frac{4}{k_n L}\left(\frac{M_b}{M}\right) \tag{19}$$

Substituting Equation (15) into Equation (19),

$$Y_n\left(\frac{L}{2}\right) = \frac{2}{(j+b)\pi}\left(\frac{M_b}{M}\right)\left[\cos(j+b)\pi\right]$$

or

$$Y_n\left(\frac{L}{2}\right) = C' \frac{1}{n-1+b}\left(\frac{M_b}{M}\right) \tag{20}$$

where

$$C' = \frac{2}{\pi}\left|\cos b\pi\right|$$

$\left|\cos b\pi\right|$ = absolute value of $\cos b\pi$

and

By examining Equation (20) it is seen that the normal mode at $x = L/2$ is proportional directly to mass ratio, M_b/M, and indirectly to mode number, n. For the same mode the larger the mass, M (smaller in M_b/M), the smaller the modal deflection, $Y_n(L/2)$. For the same mass ratio the higher mode has smaller mode amplitude.

The most interesting and important result of the analysis is that, if the beam is loaded by a heavy mass, $(M >> M_b)$, the higher modes at the load become insignificant. For example, if $M = 10M_b$ or $M_b/M = 0.1$, Equation (20) gives

$$Y_1\left(\frac{L}{2}\right) = C' \frac{1}{1-1+0.25}(0.1) = \frac{1}{2.5} C' \text{ for mode 1}$$

$$Y_3\left(\frac{L}{2}\right) = C' \frac{1}{3-1+0.25}(0.1) = \frac{1}{22.5} C' \text{ for mode 3}$$

$$Y_5\left(\frac{L}{2}\right) = C' \frac{1}{5-1+0.25}(0.1) = \frac{1}{42.5} C' \text{ for mode 5}$$

The modal deflections at the mass for modes 1, 3, and 5 are of the ratios 1 : 0.111 : 0.0588.

Thus, it can be concluded that if the beam is loaded with a very heavy mass at the center, $M_b << M$, the higher modes become very small in comparison with the first one and have no significant effects on the vibration response. The mass-loaded beam can then be treated as a one-degree-of-freedom system wherein the problem is much simplified. Similar analysis can be applied to a mass-loaded beam with both ends fixed.

Beam with Fixed Ends. A mass-loaded beam with fixed ends can be analyzed in similar manner using the following boundary conditions:

$$Y_n(0) = Y_n'(0) = Y_n(L) = Y_n'(L) = 0 \tag{21}$$

From Equations (4) and (21), two sets of equations are obtained:

$$\frac{Y_n''(0)}{2k_n^2}(\cosh k_nL - \cos k_nL) + \frac{Y_n'''(0)}{2k_n^3}(\sinh k_nL - \sin k_nL)$$

$$- \frac{\omega_n^2}{2k_n^2EI}\sum_{i=1}^{N} J_iY_n'(a_i)\left[\cosh k_n(L-a_i)\right.$$

$$\left. - \cos k_n(L-a_i)\right] u(L-a_i) \tag{22}$$

$$+ \frac{\omega_n^2}{2k_n^3EI}\sum_{i=1}^{N} M_iY_n(a_i)\left[\sinh k_n(L-a_i) - \sin k_n(L-a_i)\right] u(L-a_i) = 0$$

$$\frac{Y_n''(0)}{2k_n}(\sinh k_nL + \sin k_nL) + \frac{Y_n'''(0)}{2k_n^2}(\cosh k_nL - \cos k_nL)$$

$$- \frac{\omega_n^2}{2k_n EI} \sum_{i=1}^{N} J_i Y_n'(a_i) \left[\sinh k_n(L - a_i) + \sin k_n(L - a_i)\right] u(L - a_i) \qquad (23)$$

$$+ \frac{\omega_n^2}{2k_n^2 EI} \sum_{i=1}^{N} M_i Y_n(a_i) \left[\cosh k_n(L - a_i) - \cos k_n(L - a_i)\right] u(L - a_i) = 0$$

The conditions of compatibility give the following two sets of equations for $Y_n(a_q)$ and $Y_n'(a_q)$:

$$- Y_n(a_q) + \frac{Y_n''(0)}{2k_n^2}(\cosh k_n a_q - \cos k_n a_q) + \frac{Y_n'''(0)}{2k_n^3}(\sinh k_n a_q - \sin k_n a_q)$$

$$- \frac{\omega_n^2}{2k_n^2 EI} \sum_{i=1}^{q-1} J_i Y_n'(a_i) \left[\cosh k_n(a_q - a_i) - \cos k_n(a_q - a_i)\right] u(a_q - a_i) \qquad (24)$$

$$+ \frac{\omega_n^2}{2k_n^2 EI} \sum_{i=1}^{q-1} M_i Y_n(a_i) \left[\sinh k_n(a_q - a_i) - \sin k_n(a_q - a_i)\right] u(a_q - a_i) = 0$$

$$- Y_n'(a_q) + \frac{Y_n''(0)}{2k_n}(\sinh k_n a_q + \sin k_n a_q) + \frac{Y_n'''(0)}{2k_n^2}(\cosh k_n a_q - \cos k_n a_q)$$

$$- \frac{\omega_n^2}{2k_n EI} \sum_{i=1}^{q-1} M_i Y_n'(a_i) \left[\sinh k_n(a_q - a_i) + \sin k_n(a_q - a_i)\right] u(a_q - a_i) \qquad (25)$$

$$+ \frac{\omega_n^2}{2k_n^2 EI} \sum_{i=1}^{q-1} M_i Y_n(a_i) \left[\cosh k_n(a_q - a_i) - \cos k_n(a_q - a_i)\right] u(a_q - a_i) = 0$$

$$q = 1, 2, 3, \ldots, N$$

Equating to zero the determinant of the coefficients of the unknowns, $Y_n''(0)$, $Y_n'''(0)$, $Y_n(a_i)$ and $Y'(a_i)$, the frequency equation is obtained:

$$\det (k_n) = 0$$

The mode shapes are then determined from Equation (4). For the case with only one central mass, the problem is much simpler. The mass-loading effect can be analyzed by similar techniques as in the case of simply supported beams. However, the detailed analysis of this case is not presented here since another method, the lumped-mass/matrix iteration approach, which is discussed next, provides the same accuracy for solution of the problem but requires less effort in analysis and computation.

Lumped Mass Approach

It can be seen from the preceding discussion that to find a closed-form solution for the free-vibration problem of a mass-loaded beam is a lengthy process, especially if more than one concentrated mass is involved, or if the effects of rotary inertia and shear deformation are considered. Practically, it is more convenient to solve the problem by an approximate method such as the one which will be discussed in this section herein.

The lumped-mass method was derived originally by Myklested and Prohl (Reference 16) and it has been modified since to include the effects of rotary inertia and shear. The mass-loading beam is represented by a number of lumped masses connected by massless linear springs with constant bending stiffness EI and shear stiffness KAG. The notations are listed as follows:

A = cross-sectional area of beam

E = Young's modulus

G = shear modulus

I = area moment of inertia about Z-axis

I_Z = mass moment of inertia about Z-axis through center of gravity of mass

K = shear factor = 5/6 for rectangular cross-section

L = length of beam

m = lumped-mass

M = bending moment

V = shear force

y = deflection of beam

θ = slope of beam

$(\ddot{\ldots}) = d^2/dt^2(\ldots)$

The subscripts are as follows

b, s = quantity due to bending and shear, respectively

i = station or section number of beam

t = total quantity

The coordinates and sign conventions for moment and shear are indicated in Figure 5.

For simple harmonic motion the inertia loads at station i are

$$-m_i\ddot{y} = \omega^2 m_i y_i$$

$$-I_{zi}\ddot{\theta} = \omega^2 \theta_b I_{zi}$$

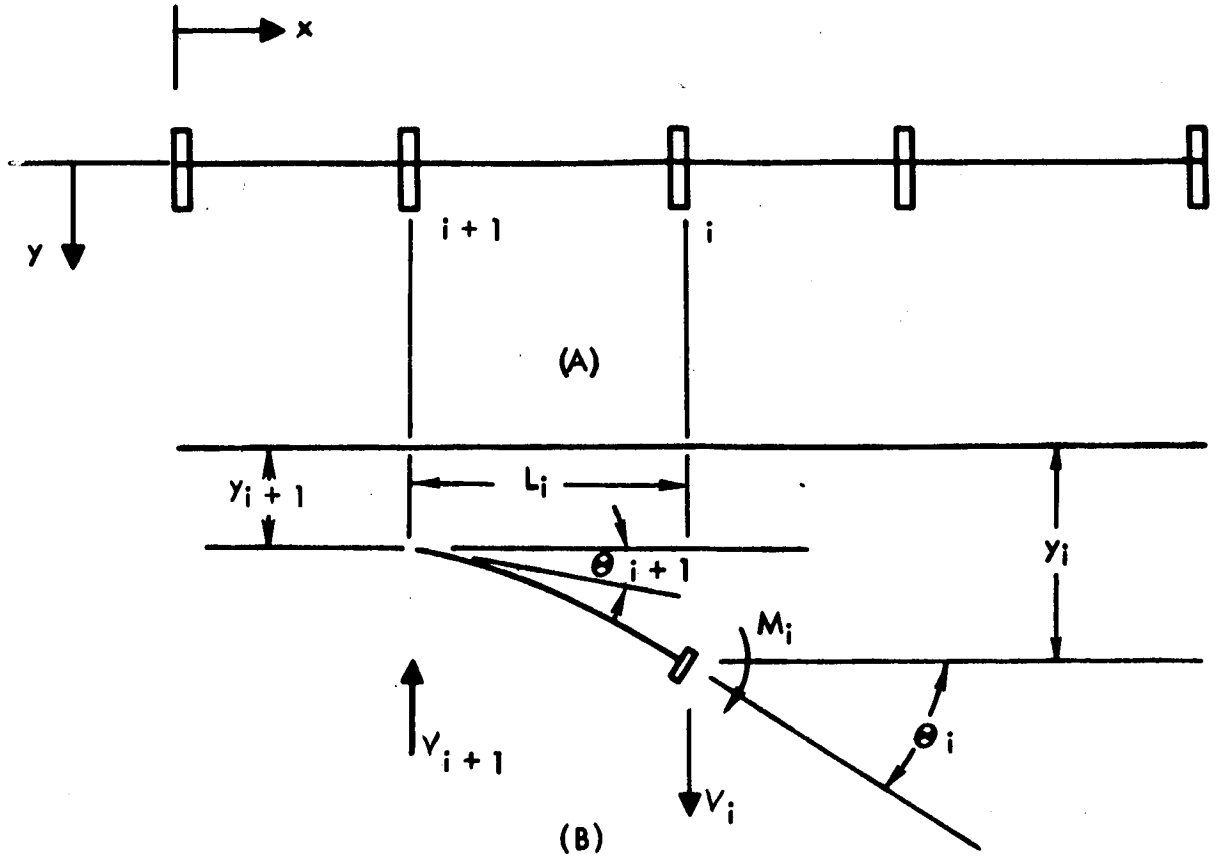

Figure 5. Coordinates and Sign Conventions of the Beam

The influence coefficients for the i^{th} section of the beam due to unit load (Figure 6) are as follows.

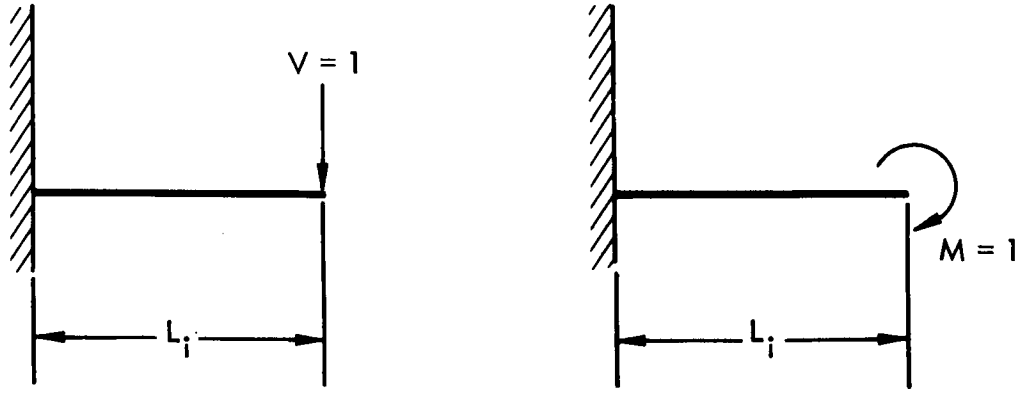

Figure 6. Unit Load on a Beam

Due to unit force,

$$\theta_b = \frac{L_i^2}{2(EI)_i}, \quad y_b = \frac{L_i^3}{3(EI)_i}, \quad \theta_s = \frac{1}{(KAG)_i}, \quad y_s = \frac{L_i}{(KAG)_i}$$

Due to unit moment,

$$\theta_b = \frac{L_i}{(EI)_i}, \quad y_b = \frac{L_i^2}{2(EI)_i}$$

Figure 7 shows diagrams of the shear, moment, slope, and deflection for a vibrating cantilever beam. Various discontinuities can be observed in some of the curves.

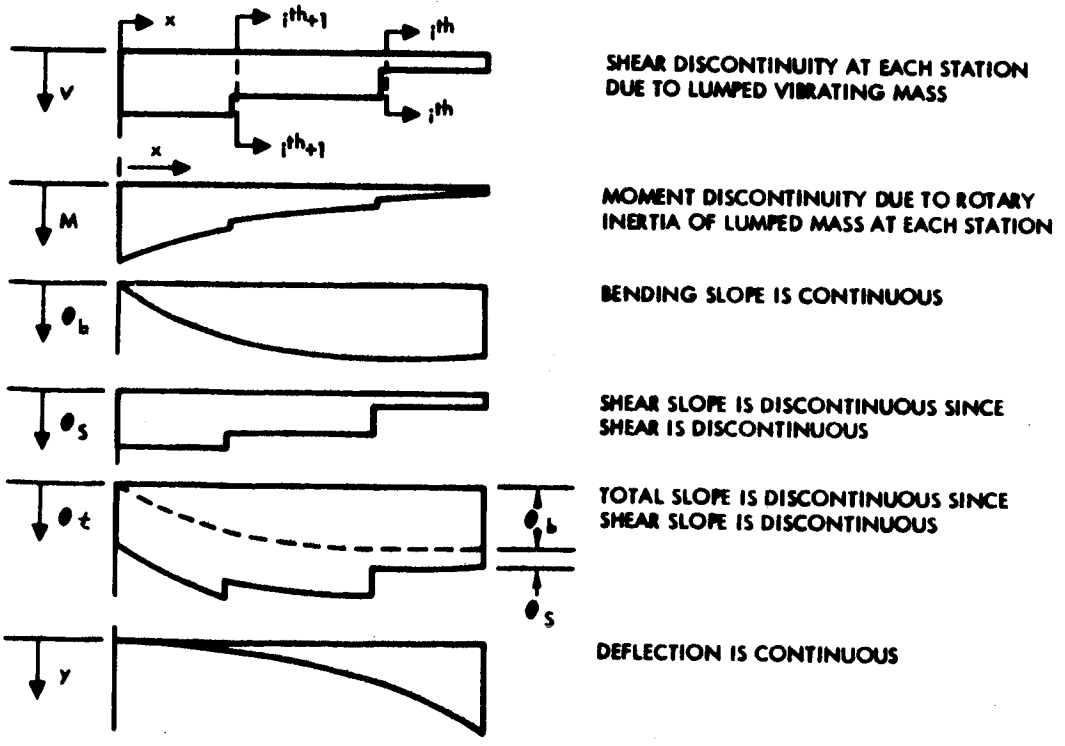

Figure 7. Forces and Deformations of a Cantilever Beam

Starting from station i, the shear and moment at station i + 1 on the left side of i can be calculated:

$$V_{i+1} = V_i + m_i\omega^2 y_i \tag{26}$$

It is noted that V_i is the shear at i but it does not include the effect of the mass at i,

$$M_{i+1} = M_i + V_i L_i + m_i\omega^2 y_i L_i$$

If rotary inertia is considered,

$$M_{i+1} = M_i + V_i L_i + m_i\omega^2 y_i L_i + I_{zi}\omega^2\theta_{bi} \tag{27}$$

It is noted that M_i is the moment at i but it does not include the moment from the i^{th} mass and rotary inertia.

The slope due to bending can be calculated by the following equations:

$$\theta_{bi} = \theta_{b,i+1} + \frac{L_i^2}{2(EI)_i}\left(V_i + m_i\omega^2 y_i\right) + \frac{L_i}{(EI)_i}\left(M_i + I_{zi}\omega^2\theta_{bi}\right)$$

$$= \theta_{b,i+1} + \frac{V_i L_i^2}{2(EI)_i} + \frac{M_i L_i}{(EI)_i} + I_{zi}\frac{\omega^2 L_i}{(EI)_i}\theta_{bi} + m_i\omega^2 y_i \frac{L_i^2}{2(EI)_i} \tag{28}$$

$$\theta_{b,i+1} = \theta_{bi}\left[1 - I_{zi}\omega^2 \frac{L_i}{(EI)_i}\right] - \frac{V_i L_i^2}{2(EI)_i} - \frac{M_i L_i}{(EI)_i} - y_i \frac{m_i\omega^2 L_i^2}{2(EI)i}$$

The total slope is the sum of the slope due to bending, and that due to shear

$$\theta_{t,i+1} = \theta_{b,i+1} + \left(V_i + m_i\omega^2 y_i\right)\frac{1}{(KAG)_i} \tag{29}$$

The deflection at i is calculated as

$$y_i = y_{i+1} + \theta_{t,i+1} L_i + \left(V_i + m_i \omega^2 y_i\right) \frac{L_i^3}{3(EI)_i} + \left(M_i + I_{zi} \omega^2 \theta_{bi}\right) \frac{L_i^2}{2(EI)_i}$$

$$y_i = y_{i+1} + \theta_{b,i+1} L_i + V_i \left[\frac{L_i^3}{3(EI)_i} + \frac{L_i}{(KAG)_i}\right] + m_i \omega^2 y_i \left[\frac{L_i^3}{3(EI)_i} + \frac{L_i}{(KAG)_i}\right]$$

$$+ M_i \frac{L_i^2}{2(EI)_i} + I_{zi} \omega^2 \theta_{bi} \frac{L_i^2}{2(EI)_i}$$

Replacing $\theta_{b,i+1}$ in Equation (29) by other quantities at i and solving for y_{i+1}

$$y_{i+1} = V_i \left[\frac{L_i^3}{6(EI)_i} - \frac{L_i}{(KAG)_i}\right] + M_i \left[\frac{L_i^2}{2(EI)_i}\right] + \theta_{bi} \left[I_{zi} \omega^2 \frac{L_i^2}{2(EI)_i} - L_i\right] \qquad (30)$$

$$+ y_i \left[1 + \frac{m_i \omega^2 L_i^3}{6(EI)_i} - \frac{m_i \omega^2 L_i}{(KAG)_i}\right]$$

Equations (26) through (30) related the quantities at i+1 to those at i , and they can be expressed in matrix form as

$$\left|U\right|_{i+1} = \left[D_i\right] \left|U\right|_i \qquad (31)$$

where

$\left|U\right|_{i+1}$ = column matrix of $(V_{i+1}, M_{i+1}, \theta_{b,i+1}, \theta_{t,i+1}, y_{i+1})$

$\left|U\right|_{i}$ = column matrix of $(V_i, M_i, \theta_{bi}, \theta_{ti}, y_i)$

$\left[D\right]_i$ = square matrix as follows:

$$\left[\begin{array}{c|c|c|c|c} 1 & 0 & 0 & 0 & m_i\omega^2 \\ \hline L_i & 1 & I_{zi}\omega^2 & 0 & m_i\omega^2 L_i \\ \hline -\frac{L_i^2}{2(EI)_i} & -\frac{L_i}{EI_i} & 1 - I_{zi}\omega^2\frac{L_i}{(EI)_i} & 0 & -m_i\omega^2\frac{L_i^2}{2(EI)_i} \\ \hline \frac{1}{(KAG)_i} - \frac{L_i^2}{2(EI)_i} & -\frac{L_i}{(EI)_i} & 1 - I_{zi}\omega^2\frac{L_i}{(EI)_i} & 0 & \frac{m_i\omega^2}{(KAG)_i} - m_i\omega^2\frac{L_i^2}{2(EI)_i} \\ \hline \frac{L_i^3}{6(EI)_i} - \frac{L_i}{(KAG)_i} & \frac{L_i^2}{2(EI)_i} & I_{zi}\omega^2\frac{L_i^2}{2(EI)_i} - L_i & 0 & 1 + m_i\omega^2\left[\frac{L_i^3}{6(EI)_i} - \frac{L_i}{(KAG)_i}\right] \end{array}\right]$$

At one end of the beam, station 1, the quantities of $\left[U\right]_1$ either are known from boundary conditions or can be normalized to other quantities. The quantities at station 2 then can be calculated as:

$$\left|U\right|_2 = \left[D\right]_1 \left|U\right|_1 \tag{32}$$

Similarly,

$$\left|U\right|_3 = \left[D\right]_2 \left|U\right|_2 = \left[D\right]_2 \left[D\right]_1 \left|U\right|_1 \tag{33}$$

$$\left|U\right|_4 = \left[D\right]_3 \left|U\right|_3 = \left[D\right]_3 \left[D\right]_2 \left[D\right]_1 \left|U\right|_1 \tag{34}$$

At the other end of the beam, station n,

$$\left|U\right|_n = \left[D\right]_t \left|U\right|_1 \tag{35}$$

where

$$\left[D\right]_t = \left[D\right]_{n-1} \cdots \left[D\right]_{i+1} \left[D\right]_i \cdots \left[D\right]_2 \left[D\right]_1 \tag{36}$$

$\left[D\right]_t$ is called the transfer matrix with elements d_{pg}, where p, q = 1, 2, 3, 4, 5. The elements d_{p4} are equal to zero; i.e.,

$$d_{14} = d_{24} = d_{34} = d_{44} = d_{54} = 0$$

Frequencies and Mode Shapes. To solve Equation (32) for the forces and deformations, $\left[U\right]_n$, at station n, the natural frequency, ω, involved in the transfer matrix, $\left[D\right]_t$, must be found first according to the following procedures:

1. Substitute the boundary conditions of the beam in Equation (35) to obtain a set of equations in terms of the unvanishing quantities of $\left[U\right]_1$ and $\left[U\right]_n$.
2. The frequencies are found by equating to zero the determinant of the coefficients of the unknowns in the system of equations.

For the mass-loaded beam with fixed ends the boundary conditions at stations and n are:

$$\theta_b = \theta_t = 0$$

$$y = 0$$

Substituting in Equation (35),

$$\begin{bmatrix} V_n \\ M_n \\ 0 \\ 0 \\ 0 \end{bmatrix} = \begin{bmatrix} d_{11} & d_{12} & d_{13} & d_{14} & d_{15} \\ d_{21} & d_{22} & d_{23} & d_{24} & d_{25} \\ d_{31} & d_{32} & d_{33} & d_{34} & d_{35} \\ d_{41} & d_{42} & d_{43} & d_{44} & d_{45} \\ d_{51} & d_{52} & d_{53} & d_{54} & d_{55} \end{bmatrix} \begin{bmatrix} V_1 \\ M_1 \\ 0 \\ 0 \\ 0 \end{bmatrix} \tag{37}$$

The last two equations of (37) can be written in the form

$$d_{41}V_1 + d_{42}M_1 = 0$$

$$d_{51}V_1 + d_{52}M_1 = 0$$

For nontrivial solutions of V_1 and M_1, the determinant of the coefficient must vanish. This gives the frequency equation

$$\begin{vmatrix} d_{41} & d_{42} \\ d_{51} & d_{52} \end{vmatrix} = 0$$

or

$$d_{41}d_{52} - d_{42}d_{51} = 0 \tag{38}$$

Once the natural frequencies are found from Equation (38) the matrix $[D]_i$ of Equation (31) is known. The mode shapes, y_i, at any station then can be calculated step by step using Equations (32) through (35).

A computer program has been available at NAA for performing the preceding calculations of frequencies and mode shapes. The program was originally developed for modal analysis of any beam-like structure with any boundary conditions. In the present case of a mass-loaded beam with fixed

ends, the computed natural frequencies and mode shapes were found to agree closely with the experimental data.

Table 1 presents a comparison of the natural frequencies. The mode shapes of first four modes plotted by the computer program are shown in the appendix.

Finite-Difference Method

The free-vibration problem of a mass-loaded beam can be solved by the finite-difference method. Starting with the equation of motion for an unloaded beam,

$$EI \frac{\partial^4 y}{\partial x^4} + \rho \frac{\partial^2 y}{\partial t^2} = 0 \tag{39}$$

The notations are the same as previously stated. For a mass-loaded beam, ρ is a function of x, i.e.,

$$\rho = \rho(x) = \text{mass/unit length}$$

Assume the solution to be of the form

$$y(x,t) = Y(x)\, e^{i\omega t} \tag{40}$$

where $Y(x)$ = natural mode. Substituting Equation (40) into Equation (39),

$$\frac{d^4 Y}{dx^4} - \frac{\rho}{EI} \omega^2 Y = 0$$

or

$$\frac{d^4 Y}{dx^4} = \frac{\omega^2}{EI} \rho Y \tag{41}$$

In the finite-difference form,

$$\frac{\Delta^4 Y}{\Delta x^4} = \frac{\omega^2}{EI} \rho Y \tag{42}$$

Table 1. Mass-Loaded Beam Frequencies Comparison

Case No.	Additional Weight	Frequency No.	Additional Weight at 4.25 (in.)		Additional Weight at 7.25 (in.)		Additional Weight at 12 (in.)	
			Analytical	Test	Analytical	Test	Analytical	Test
1	0	1	66.26	66.4	66.26	66.4	66.26	66.4
	0	2	182.6	182.1	182.6	182.1	182.6	182.1
	0	3	357.7	357.9	357.7	357.9	357.7	357.9
	0	4	590.8	591.5	590.8	591.5	590.8	591.5
2	0.165	1	63.8	61.16	57.5	56.24	51.90	52.57
	0.165	2	156.6	158.8	152.9	158.3	176.9	178.0
	0.165	3	305.6	307.6	333.0	334.4	326.0	325.3
	0.165	4	515.5	543.0	545.0	557.0	543.9	564.0
3	0.231	1	62.8	60.10	54.6	53.8	48.3	46.86
	0.231	2	152.3	150.9	147.8	150.8	176.8	176.00
	0.231	3	294.5	295.6	328.1	332.6	318.0	305.5
	0.231	4	513.2	524.9	533.8	568.8	542.6	556.0
4	0.330	1	61.3	59.38	50.99	50.0	44.04	43.48
	0.330	2	143.4	145.3	141.7	144.7	173.2	174.2
	0.330	3	284.1	292.7	317.5	326.7	309.0	302.5
	0.330	4	495.1	520.8	510.0	535.3	515.0	547.0
5	0.495	1	58.7	57.0	46.1	45.17	38.9	38.71
	0.495	2	132.4	134.8	134.9	138.10	165.7	168.1
	0.495	3	272.3	283.4	297.2	306.7	298.0	296.2
	0.495	4	460.7	475.0	485.0	492.4	469.3	485.0
6	0.660	1	56.3	54.5	42.4	41.66	35.2	35.33
	0.660	2	124.9	125.4	130.5	135.6	159.5	157.6
	0.660	3	264.1	269.8	281.1	271.8	290.0	291.0
	0.660	4	432.6	406.1	465.0	440.7	440.6	413.0
7	1.320	1	47.9	46.5	33.1	33.38	26.8	26.57
	1.320	2	109.6	110.7	117.8	121.8	129.7	135.8
	1.320	3	228.9	236.2	217.6	222.8	276.0	273.8
	1.320	4	338.9	385.5	410.0	412.0	363.0	364.7
8	1.980	1	42.3	40.5	28.1	27.0	22.5	23.03
	1.980	2	103.1	104.6	109.6	109.2	113.8	119.5
	1.980	3	203.4	190.8	193.3	182.8	269.0	270.2
	1.980	4	313.2	293.7	390.0	400.0	340.0	350.2

The beam is equally divided into n portions with the mass lumped at each division points, which is designated as a station. There will be (n+1) such stations, including two end-stations.

By the central-difference method, for station i,

$$\Delta^4 Y = Y_{i-2} - 4Y_{i-1} + 6Y_i - 4Y_{i+1} + Y_{i+2} \tag{43}$$

where

$i = 0, 1, 2, \ldots\ldots (n+1)$.

Substituting Equation (43) into Equation (42),

$$Y_{i-2} - 4Y_{i-1} + 6Y_i - 4Y_{i+1} + Y_{i+2} = \frac{\omega^2}{EI} \rho \Delta x^4 Y_i \tag{44}$$

where

$\Delta x = L/n$ = length of subspan

Letting

$M_i = \rho \Delta x$ = lumped mass at station i for a length, Δx,

Equation (44) is rewritten as

$$Y_{i-2} - 4Y_{i-1} + 6Y_i - 4Y_{i+1} + Y_{i+2} = \frac{\Delta x^3}{EI} \omega^2 M_i Y_i \tag{45}$$

In applying boundary conditions to Equation (45), for a simply supported beam,

$$y(o) = y(L) = 0 , \quad \frac{\partial^2 y(o)}{\partial x^2} = \frac{\partial^2 y(L)}{\partial x^2} = 0$$

or

$$Y_o = Y_n = 0 , \quad Y_{-1} = -Y_1 , \text{ and } Y_{n-1} = -Y_{n+1}$$

and for a clamped beam,

$$y(o) = y(L) = 0 , \quad \frac{\partial y(o)}{\partial x} = \frac{\partial y(L)}{\partial x} = 0$$

or

$$Y_o = Y_n = 0 , \quad Y_{-1} = Y_1 , \text{ and } Y_{n-1} = Y_{n+1}$$

For each station i, an equation such as Equation (45) is written. There are (n-1) such equations with (n-1) unknown deflections. In matrix form the system of equations is

$$[K] \left|Y\right| = \lambda^2 \left[M \right] \left|Y\right| \tag{46}$$

where

$[K]$ = square matrix of stiffness coefficients, obtained from the coefficients of Y in Equation (45).

$\left|Y\right|$ = column matrix of deflection Y

$\left[M \right]$ = diagonal matrix of lumped masses

$$\lambda^2 = \omega^2 \Delta x^3 / EI$$

The mode shapes are found as

$$\left|Y\right| = \lambda^2 [K]^{-1} \left[M \right] \left|Y\right| \tag{47}$$

where

$[K]^{-1}$ = inverse of $[K]$.

The frequency equation is

$$\left[I \right] - \lambda^2 [K]^{-1} \left[M \right] = 0 \tag{48}$$

where

$[\ I\ ]$ = unit matrix.

Using the Jacobian subroutine of the computer programs, the natural frequencies and modes can be calculated.

Mass-Loaded Plates

Finite-Difference/Matrix-Iteration Method

For investigation of the free vibration of the mass-loaded plates, the finite-difference method, in connection with the matrix-iteration method, is used. The formulation of the problem from this method is simple and could be conveniently evaluated by computer programs with considerable accurate results.

Equation of Motion of Free Vibration

$$\nabla^2\nabla^2 w + \frac{\rho h}{D}\ddot{w} = 0 \tag{49}$$

where

$$\nabla^2\nabla^2 = \left(\frac{\partial^2}{\partial x^2} + \frac{\partial^2}{\partial y^2}\right)^2$$

$$\ddot{w} = \frac{\partial^2 w}{\partial t^2}$$

$w = w(x, y, t)$ = deflection

ρ = density of plate

h = thickness of plate

$$D = \frac{Eh^3}{12(1 - \nu^2)} = \text{flexual rigidity of plate}$$

This equation applies only to an unloaded isotropic plate with uniform density and thickness. For a mass-loaded plate, replace ρh by $M(x, y)$ which is the mass per unit area.

$$\nabla^2\nabla^2 w + \frac{M}{D}\ddot{w} = 0 \tag{50}$$

Assume the solution to be of the form

$$w(x, y, t) = W(x, y) \sin \omega t \tag{51}$$

where

$W(x, y)$ = natural mode

ω = circular natural frequency.

Substituting Equation (51) into (50), the equation of motion becomes

$$\nabla^2 \nabla^2 W - \frac{M}{D} \omega^2 W = 0 \tag{52}$$

or in the form of finite difference,

$$\frac{\Delta^4 W}{\Delta x^4} + 2 \frac{\Delta^4_{xy} W}{\Delta x^2 \Delta y^2} + \frac{\Delta^4 W}{\Delta y^4} - \frac{M\omega^2}{D} W = 0 \tag{53}$$

The plate of size $a \cdot b$ is equally divided into $m.n$ rectangular elements of size $(\Delta x) \times (\Delta y)$ as shown in Figure 8. In addition, one row of elements is added along the edges of the plate to account for the boundary conditions which will be discussed later. The intersections of the division lines, numbered by i and j along x and y directions, respectively, are stations where the mass of the plate and the loads will be lumped.

By the central-difference method the relative deflections can be expressed as

$$\begin{aligned}
\Delta^4_x W &= W_{i-2,j} - 4W_{i-1,j} + 6W_{i,j} - 4W_{i+1,j} + W_{i+2,j} \\
\Delta^4_y W &= W_{i,j-2} - 4W_{i,j-1} + 6W_{i,j} - 4W_{i,j+1} + W_{i,j+2} \\
\Delta^4_{xy} W &= W_{i-1,j-1} + W_{i-1,j+1} + W_{i+1,j-1} + W_{i+1,j+1} \\
&\quad - 2\left[W_{i,j-1} + W_{i,j+1} + W_{i-1,j} + W_{i+1,j}\right] + 4W_{i,j}
\end{aligned} \tag{54}$$

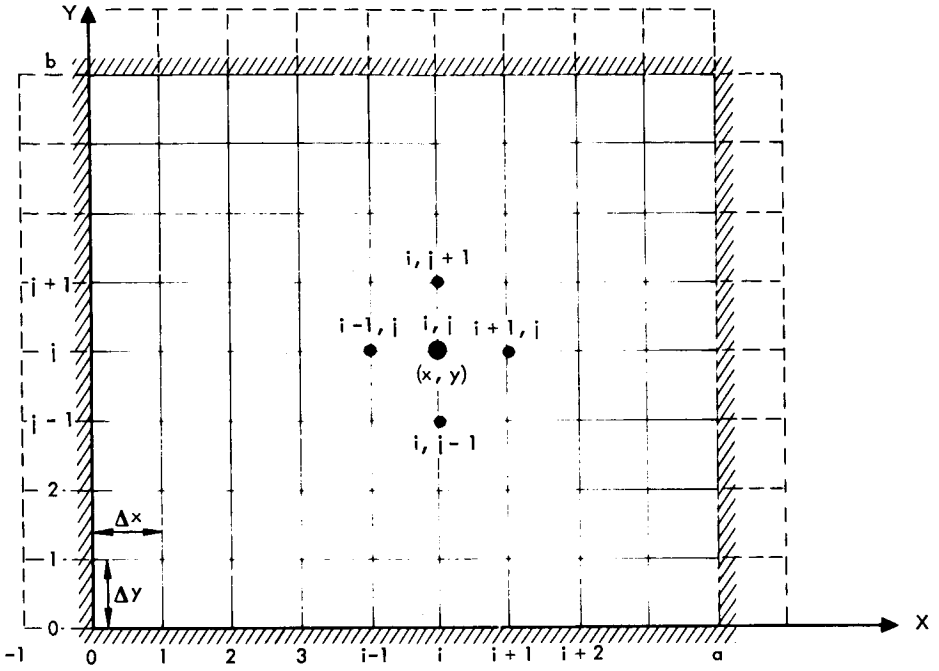

Figure 8. Plate Geometry

Substituting these quantities into Equation (54) and letting $\Delta x = \Delta y$,

$$\left[20 - \frac{M_{ij}}{D}\omega^2\Delta x^2\right] W_{i,j} - 8\left[W_{i+1,j} + W_{i-1,j} + W_{i,j+1} + W_{i,j-1}\right]$$

$$+ 2\left[W_{i+1,\,j+1} + W_{i+1,\,j-1} + W_{i-1,\,j+1} + W_{i-1,\,j-1}\right] + W_{i+2,\,j} + W_{i-2,\,j}$$

$$+ W_{i,j+2} + W_{i,j-2} = 0 \qquad (55)$$

For each station, i, j, there is an equation such as (55). M_{ij} is the lumped-mass at station i, j for an area Δx_j^2 ; i. e. ,

$$M_{ij} = M\Delta x^2$$

In order to solve these equations, boundary conditions must be applied:

Simply Supported Boundary:

$$\left.\begin{aligned} W_{(o,y)} = 0\,, \quad \frac{\partial^2 W(o,y)}{\partial x^2} = 0 \\ W_{(o,j)} = 0\,, \quad W_{-1,j} = -\,W_{1,j} \end{aligned}\right\} \text{ at } x = 0$$

(Similar conditions exist at $y = 0$, $x = a$, and $y = b$.)

Clamped Boundary:

$$W_{o,j} = 0, \quad W_{-1,j} = W_{1,j} \quad \text{at} \quad x = 0$$

$$W_{i,o} = 0, \quad W_{i,-1} = W_{i,1} \quad \text{at} \quad y = 0$$

(Similar conditions exist at $x = a$ and $y = b$.)

To illustrate the procedure, the plate in Figure 9 is assumed to be clamped at all edges with 9 times 8 = 72 plate elements ($m = 9$, $n = 8$). For each station i, j, an expression of Equation (55) is written for all deflections at its own station and other adjacent stations. For these two kinds of boundary conditions the deflections on the edges are zero, and the deflections outside the boundary can be expressed in terms of those inside the boundary. Hence, there are only $(m - 1)(n - 1) = 56$ such equations with 56 unknown deflections.

The system of equations can be written in matrix form:

$$-C\omega^2 \left[M \right] \left| W \right| + \left[K \right] \left| W \right| = 0 \tag{56}$$

where

$$C = \frac{\Delta x^2}{D}$$

$\left[M \right]$ = diagonal matrix of mass M_{ij}

$\left| W \right|$ = column matrix of deflection W_{ij}

$[K]$ = square matrix of stiffness coefficients, obtained from the coefficients of W_{ij} in Equation (55)

In another form,

$$[K] \left| W \right| = \lambda^2 \left[M \right] \left| W \right| \tag{57}$$

where

$$\lambda^2 = C\omega^2 = \omega^2 \Delta x^2 / D$$

Premultiply Equation (57) by the inverse matrix of $[K]$,

$$[K]^{-1} [K] \left| W \right| = \lambda^2 [K]^{-1} \left[M \right] \left| W \right|$$

$$\left| W \right| = \lambda^2 [K]^{-1} \left[M \right] \left| W \right| \tag{58}$$

Rearrange Equation (58),

$$\left[\left[I \right] - \lambda^2 [K]^{-1} \left[M \right] \right] \left| W \right| = 0 \tag{59}$$

where

$\left[I \right]$ = unit matrix = $[K]^{-1} [K]$

The frequency equation is obtained as

$$\left[I \right] - \lambda^2 \left[K\right]^{-1} \left[M \right] = 0 \qquad (60)$$

The natural frequencies of the mass-loaded plate are found by matrix iteration. Mode shapes are obtained by substituting the frequency in Equation (58).

For numerical evaluation, a computer program based on this discussion has been written for a computation of natural frequencies and modes of the mass-loaded plates. The Jacobian subroutine was incorporated in the program to evaluate the eigenvalue λ and the eigenfunction W. A modal mapping subroutine, which will be discussed later, was employed to plot the mode shapes. The first six natural frequencies calculated by the computer program for the unloaded and mass-loaded plates of 14-1/2 inches by 16-1/2 inches with fixed edges agree well with the experimental data shown in Table 2.

Series-Expansion Method

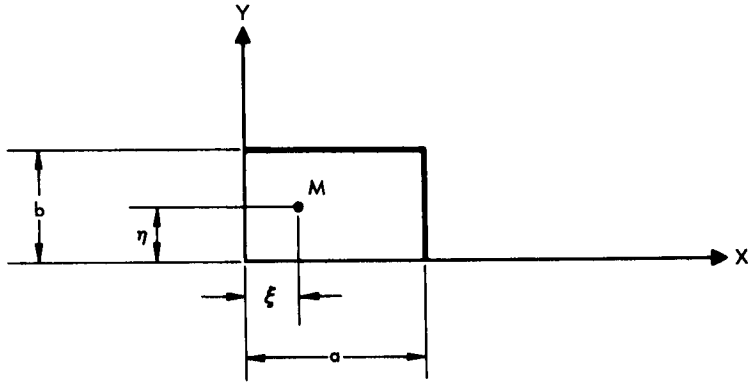

Figure 9. Mass-Loaded Plate

For free vibration of a mass-loaded plate, as shown in Figure 9, the equation of motion is as follows:

$$\nabla^2\nabla^2 w \left[\rho h + M\delta(x-\xi)\delta(x-\eta) \right] \frac{\ddot{w}}{D} = 0 \qquad (61)$$

Table 2. Comparison of Mass-Loaded Plate Frequencies

Case	Additional Weight (lb)	1st Frequency (cps)		2nd Frequency (cps)		3rd Frequency (cps)		4th Frequency (cps)		5th Frequency (cps)		6th Frequency (cps)	
		Computed	Test	Computed	Test	Computed	Test	Computed	Test	Computed	Test	Computed	Test
1	0.00	270.58	268.00	484.06	460.00	550.59	510.0	751.91	690.0	778.76	750.0	907.97	890.0
2	1.80	212.00	210.00	435.50	401.00	527.50	500.0	726.13	672.0	768.21	710.0	883.30	860.0
3	2.70	184.50	195.00	387.80	370.00	475.10	450.0	702.30	664.0	736.10	698.0	859.10	830.0
4	3.29	171.00	185.00	364.10	350.00	448.90	430.0	664.91	630.0	695.94	660.00	822.14	800.0
5	5.30	141.20	140.00	305.00	300.00	382.22	360.0	571.50	540.0	602.30	583.0	726.30	700.0
6	10.41	105.80	110.00	231.70	225.00	293.40	300.0	431.10	408.0	466.80	430.0	582.20	525.0
7	15.62	87.25	87.00	193.40	187.00	245.51	220.0	369.36	350.0	402.46	380.0	498.30	460.0
8	21.02	76.00	77.00	168.31	160.00	214.00	205.0	323.50	300.0	344.50	340.0	440.10	405.0

where M is a concentrated mass loaded at the location $x = \xi$ and $y = \eta$. The other notations are the same as in the finite difference method section. The delta functions have the following property:

$$\text{For } x = \xi,\ y = \eta,\ \int_o^{\alpha}\int_o^{b} f(x, y)\,\delta(x - \xi)\,(y - \eta)\,dxdy = f(\xi, \eta)$$

$$\text{For } x \neq \xi,\ y \neq \eta,\ \delta(x - \xi) = 0 \text{ and } \delta(y - \eta) = 0$$

Assume the solution to be

$$w(x, y, t) = W(x, y)\,e^{i\omega t} \tag{62}$$

where

$W(x, y)$ = Mode shape of plate

ω = Circular natural frequency

Substituting Equation (62) into (61),

$$\nabla^2\,\nabla^2\,W - \omega^2\left[\rho h + M\delta(x - \xi)\,\delta(y - \eta)\right]\frac{W}{D} = 0 \tag{63}$$

assume $W(x, y)$ to be an approximate solution of Equation (63) with the form

$$W(x, y) = \sum_{i=1}^{N} a_i\,\psi_i(x, y) \tag{64}$$

where

$\psi_i(x, y)$ = known functions of x and y satisfying the boundary conditions,

a_i = unknown parameters,

N = number of terms in the series.

The boundary conditions to be satisfied by the plate mode shapes are as follows:

Simply Supported Edge:

$$\text{At } x = \text{constant}, \quad W = 0, \quad \frac{\partial^2 W}{\partial x^2} = 0$$

$$\text{At } y = \text{constant}, \quad W = 0, \quad \frac{\partial^2 W}{\partial y^2} = 0$$

Clamped Edge:

$$\text{At } x = \text{constant}, \quad W = 0, \quad \frac{\partial W}{\partial x} = 0$$

$$\text{At } y = \text{constant}, \quad W = 0, \quad \frac{\partial W}{\partial y} = 0$$

Free Edge:

At x = constant,

$$\frac{\partial^2 W}{\partial x^2} + \nu \frac{\partial^2 W}{\partial y^2} = 0, \qquad \frac{\partial^3 W}{\partial x^3} + (2 - \nu) \frac{\partial^3 W}{\partial x \partial y^2} = 0$$

At y = constant,

$$\frac{\partial^2 W}{\partial y^2} + \nu \frac{\partial^2 W}{\partial x^2} = 0, \qquad \frac{\partial^3 W}{\partial y^3} + (2 - \nu) \frac{\partial^3 W}{\partial x^2 \partial y} = 0$$

where

ν = Poisson's ratio.

By Galerkins method, the following equation is obtained:

$$\int_o^a \int_o^b \left\{ \nabla^2 \nabla^2 \sum_{i=1}^{N} a_i \psi_i - \frac{\omega^2}{D} \left[\rho h + M \delta (x - \xi) \delta (y - \eta) \right] \sum_{i=1}^{N} a_i \psi_i \right\} \cdot \psi_j \, dxdy = 0 \tag{65}$$

where

$$j = 1, 2, \cdots\cdots N.$$

After integration, a system of equations is derived, from which the coefficients a_i as well as the natural frequencies and modes can be found. Solution of Equation (61) can also be found by the Ritz method, another form of energy approach. In this method, the natural mode W (x, y) of Equation (62) is expressed in the form

$$W(x, y) = \sum_{m=1}^{\infty} \sum_{n=1}^{\infty} A_{mn} X_m(x) Y_n(y) \tag{66}$$

where

A_{mn} = constant to be determined

$X_m(x)$ and $Y_n(y)$ = mode shapes of beams having boundary conditions similar to those of the plate.

The natural modes of the mass-loaded beam derived in the "Mass-Loaded Beam" Section can be used.

Strain Energy:

$$U = \frac{D}{2} \int_o^a \int_o^b \left[\left(\frac{\partial^2 w}{\partial x^2} + \frac{\partial^2 w}{\partial y^2} \right) - 2(1-\nu) \left[\frac{\partial^2 w}{\partial x^2} \frac{\partial^2 w}{\partial y^2} - \left(\frac{\partial^2 w}{\partial x \partial y} \right)^2 \right] \right] dxdy \tag{67}$$

Kinetic Energy:

$$K = \frac{1}{2} \int_o^a \int_o^b \left[\rho h + M \delta (x-\xi) \delta (x-\eta) \right] \left(\frac{\partial w}{\partial t} \right)^2 dxdy$$

$$= \frac{1}{2} \omega^2 \int_o^a \int_o^b \left[\rho h + M \delta (x-\xi) \delta (x-\eta) \right] W^2 dxdy \tag{68}$$

By Ritz Method:

$$\frac{\partial (U-K)}{\partial A_{mn}} = 0 \tag{69}$$

i. e. ,

$$\frac{\partial U}{\partial A_{mn}} - \frac{\omega^2}{2} \frac{\partial}{\partial A_{mn}} \iint \left[\rho h + M \delta (x - \xi) \delta (x - \eta) \right] W^2 \, dxdy = 0 \qquad (70)$$

Substituting Equations (66) into (67) to find U and putting the value into (70), a system of equations is obtained. The frequencies then are determined by vanishing the determinant of the coefficients of the unknowns.

It is noted that in Equation (66), the natural mode is expressed in the form of an infinite series. In practical calculation, solutions of acceptable accuracy can be obtained by using only a definite number of terms in the series. If N terms are considered, the system of equations, as well as the solutions, will be the same as those of the Galerkin method when identical mode shapes are assumed in both cases.

Since the method of finite difference has been proved to be the simplest one to compute natural frequencies and modes with good accuracy, neither the series-expansion method nor the Ritz method is employed in the study.

Modal Mapping Development

The mode shapes of a vibrating plate, either unloaded or mass-loaded, are of great importance to the vibration analysis. Their three-dimensional nature makes it difficult to visualize the modal behaviors, especially for the higher modes. The simple, one-dimensional beam-mode plot is not applicable to this case. A contour plotting technique similar to that used in lunar surface mapping was developed and programmed by NAA (Reference 17).

After minor modification, this computer program is found to be suitable for plotting plate mode shapes with clear and descriptive details. The program was written as a group of FORTRAN IV subroutines, which generate output for subsequent plotting by an SC-4020 CRT (cathode ray tube). The technique will contour data arranged in a rectangular array. The procedure is begun with establishment of the algebraic minimum and maximum values of the data to be plotted and the number of increments between these extreme values. Then the array is contoured systematically by considering rectangles having four adjacent points for vertices. The chosen rectangle is then divided into two triangles by a diagonal that has minimum length between two points. Since each triangle represents a plane, the problem is reduced to determining the lines of intersection of the contour planes and the individual triangles. This determination is accomplished by performing linear interpolations between the vertices of the triangles to locate points where the individual contour lines intersect each side. These end points are then paired and individual segments of contour lines are drawn between them. This technique involves several approximations, and its fidelity depends on the number of data points given to be plotted.

In Figures 10 through 21, the mode shapes of mass-loaded plate, obtained by the computer program, are presented by means of contour mapping. The contour identification, some of the plate parameters, and the natural frequency associated with the modal shape are included in each plot. The meanings of the values above each diagram are indicated in the following example of the second mode (Figure 11):

Contour Ident.

Surface Level	Mode Shape
1-	12.5 (negative displacement on level 1)
2-	10.5
3-	8.5
4-	6.5
5-	4.5
6-	2.5
7-	0.5
8	1.5 (positive displacement on level 8)
9	3.5
A	5.5
B	7.5
C	9.5
D	11.5
E	13.5
F	15.5

Parameters: 2.0 (mode number)
4.0 (case number)
305.0 (natural frequency)

CONTOUR	IDENT.
1	0.730462
2	1.460923
3	2.191385
4	2.921846
5	3.652308
6	4.382769
7	5.113231
8	5.843692
9	6.574154
A	7.304615
B	8.035076
C	8.765538
D	9.496000
E	10.226461

PARAMETERS
1.000000
4.000000
141.000000

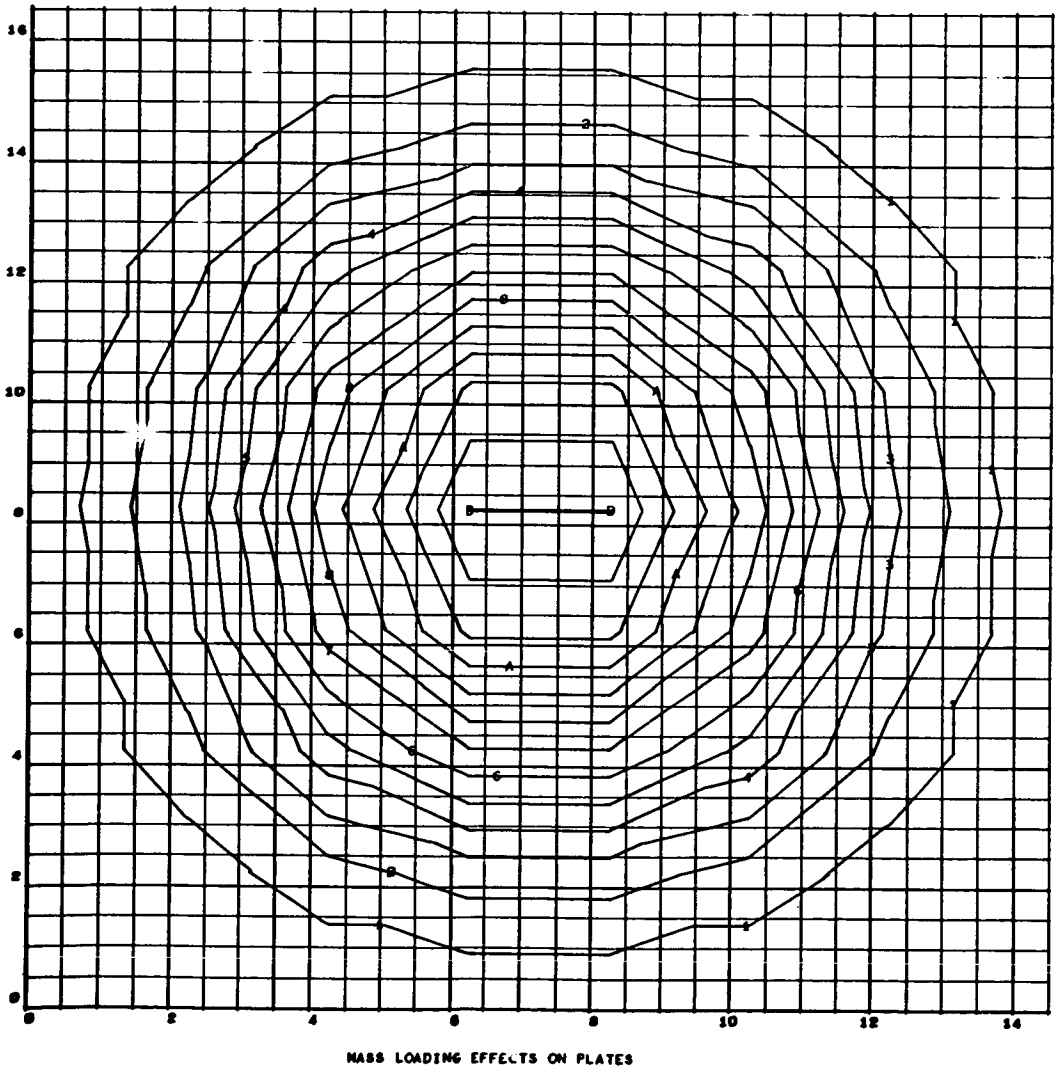

Figure 10. Mass-Loading Effects on Plates, First Mode

CONTOUR IDENT.

1 -	12.500000
2 -	10.500000
3 -	8.500000
4 -	6.500000
5 -	4.500000
6 -	2.500000
7 -	0.500000
8	1.500000
9	3.500000
A	5.500000
B	7.500000
C	9.500000
D	11.500000
E	13.500000
F	15.500000

PARAMETERS

2.000000
4.000000
305.000000

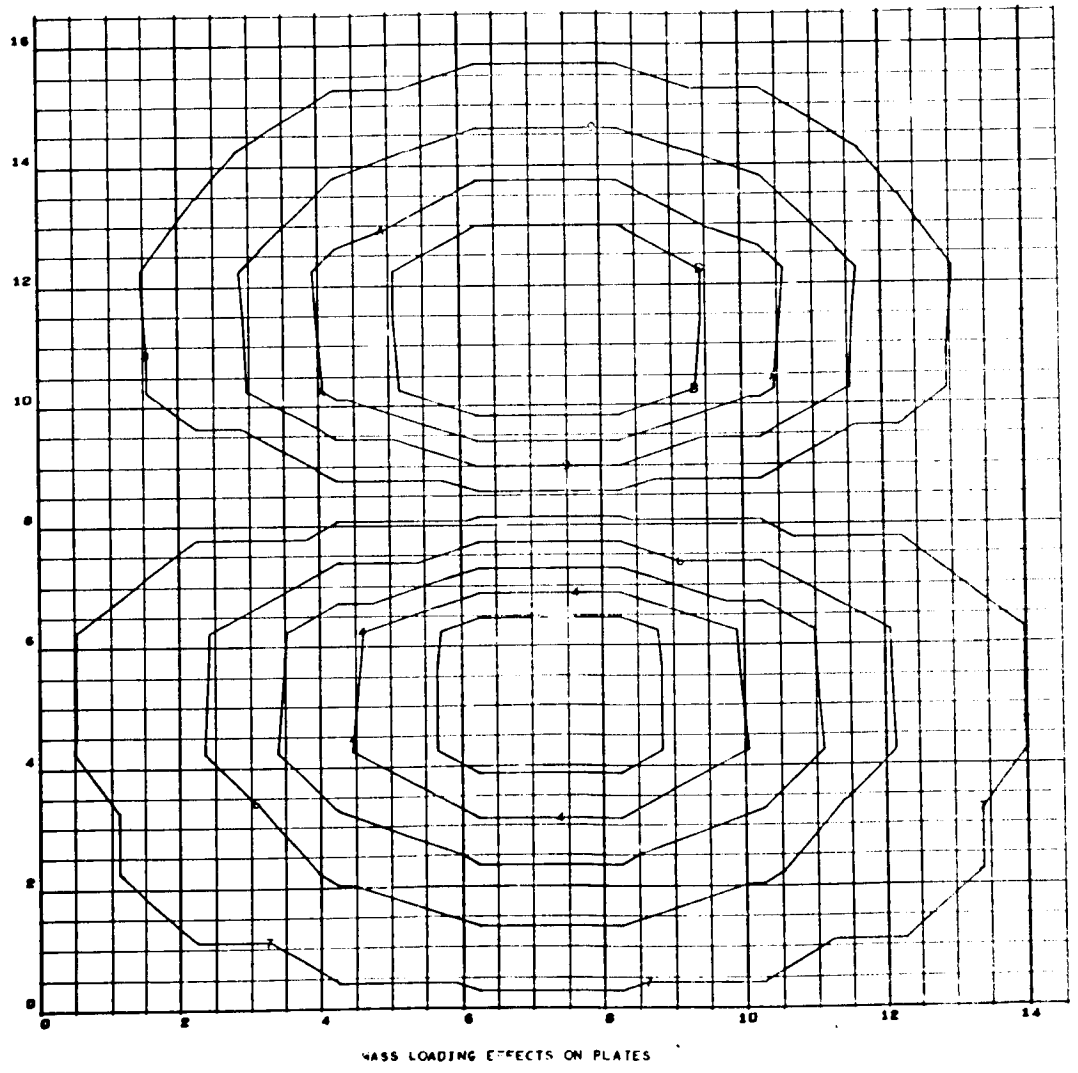

Figure 11. Mass-Loading Effects on Plates, Second Mode

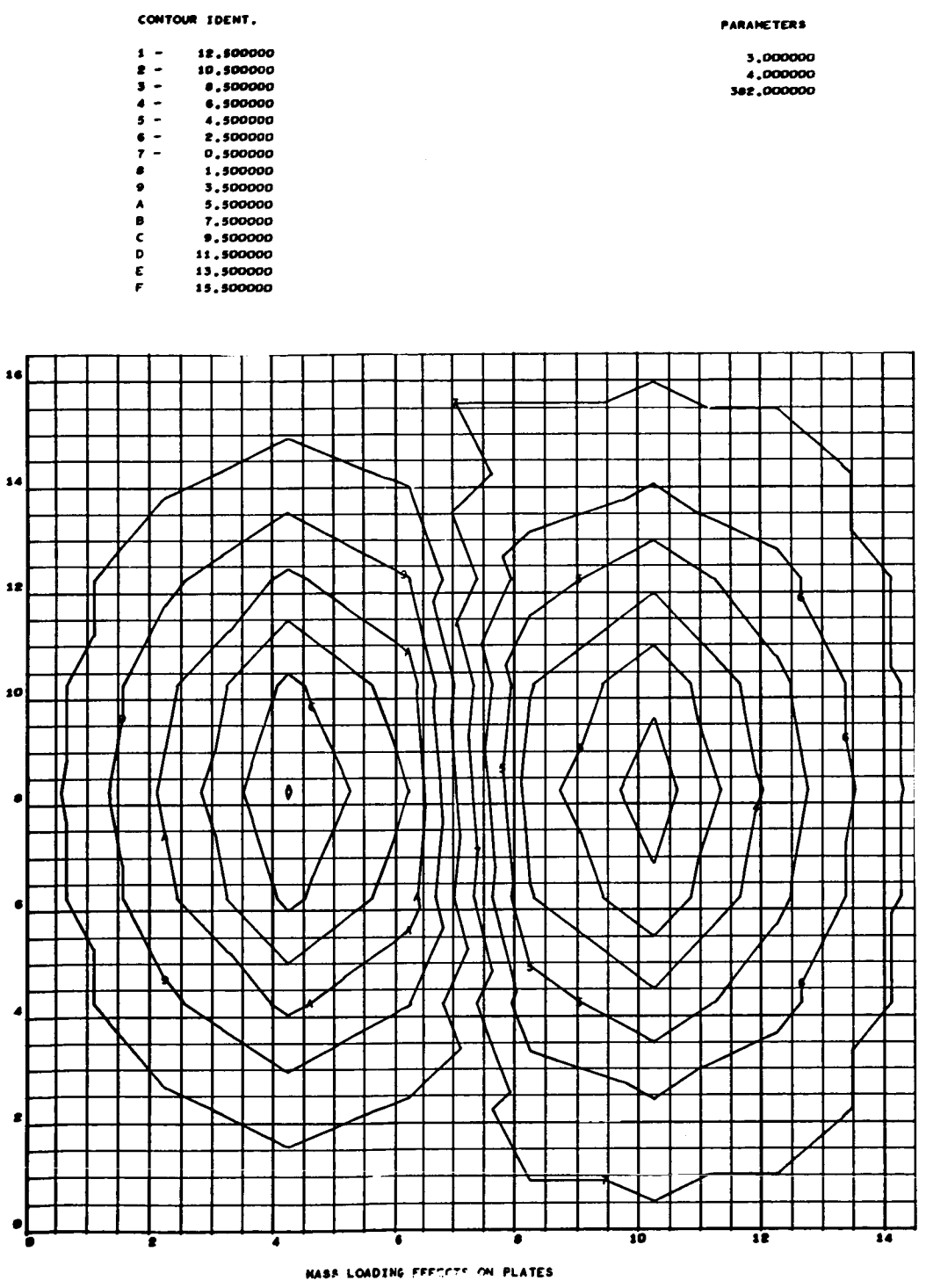

Figure 12. Mass-Loading Effects on Plates, Third Mode

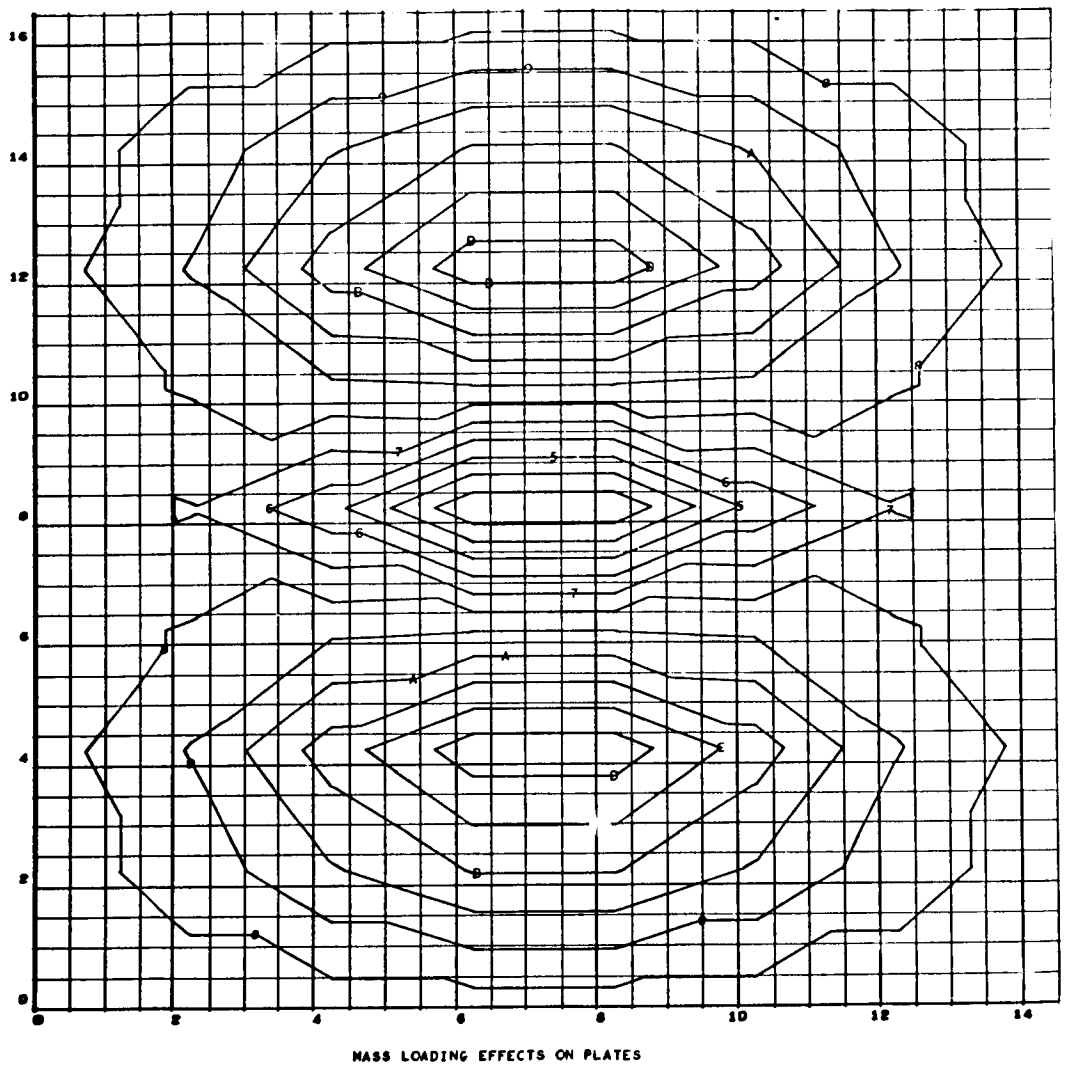

Figure 13. Mass-Loading Effects on Plates, Fourth Mode

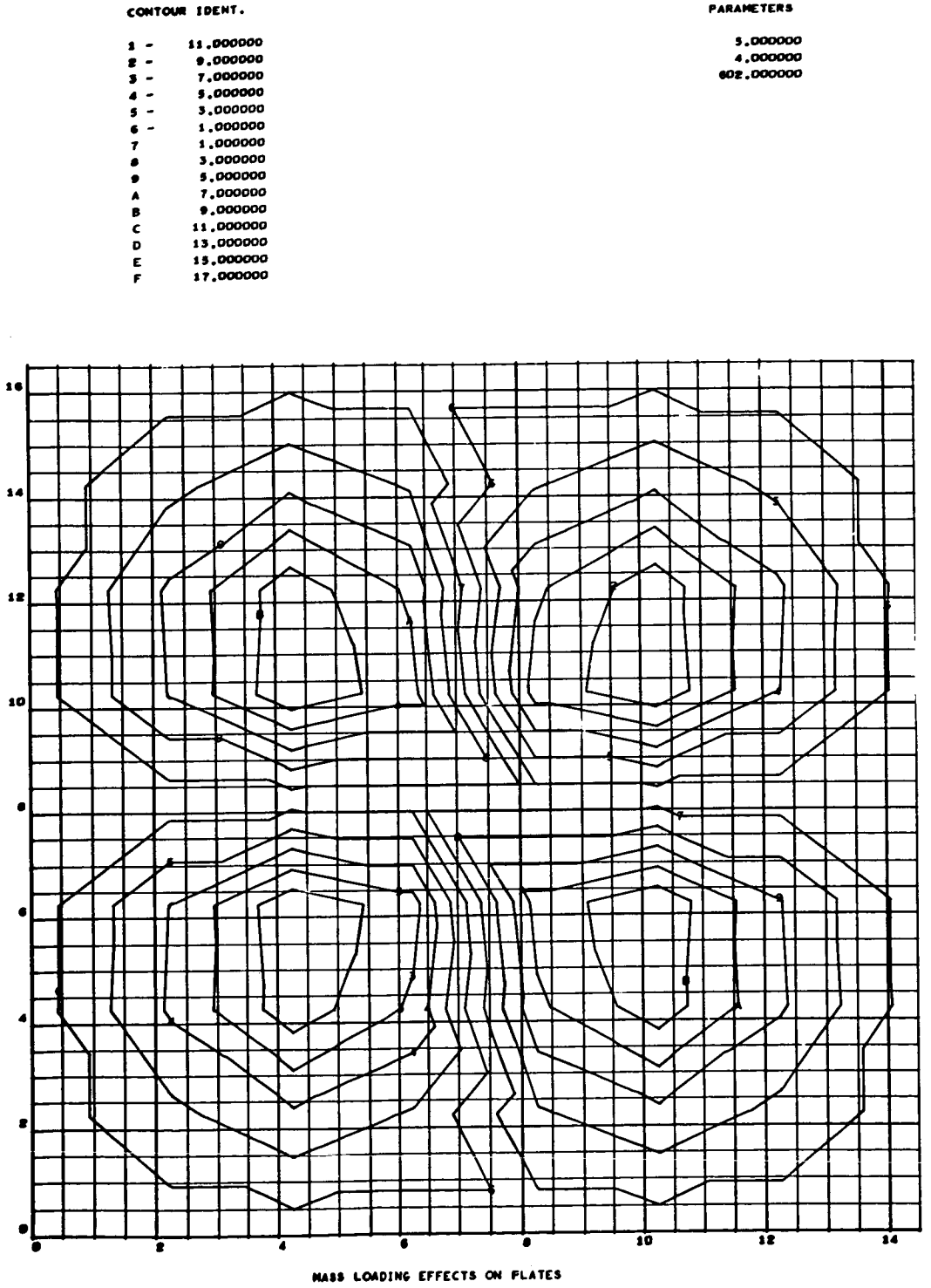

Figure 14. Mass-Loading Effects on Plates, Fifth Mode

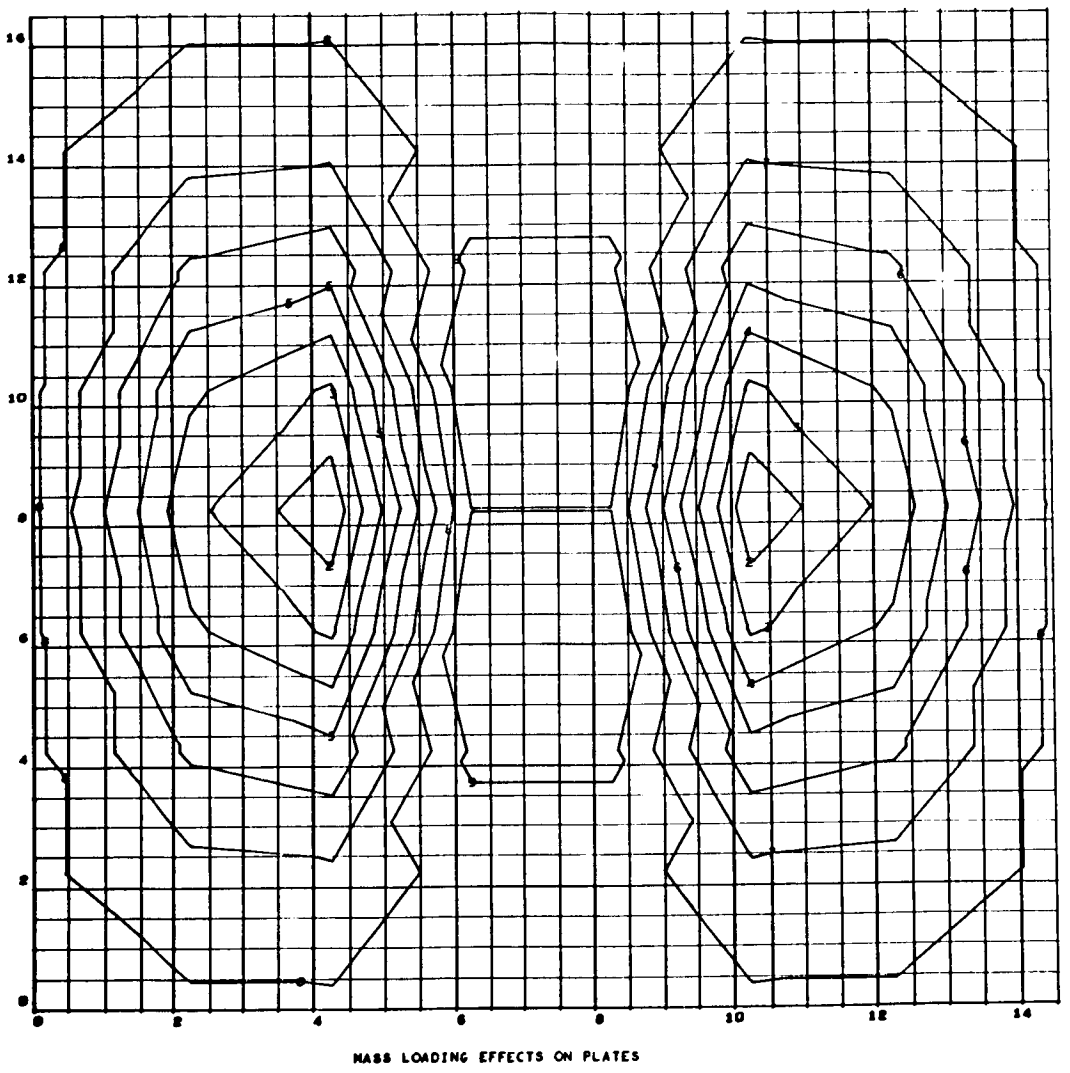

Figure 15. Mass-Loading Effects on Plates, Sixth Mode

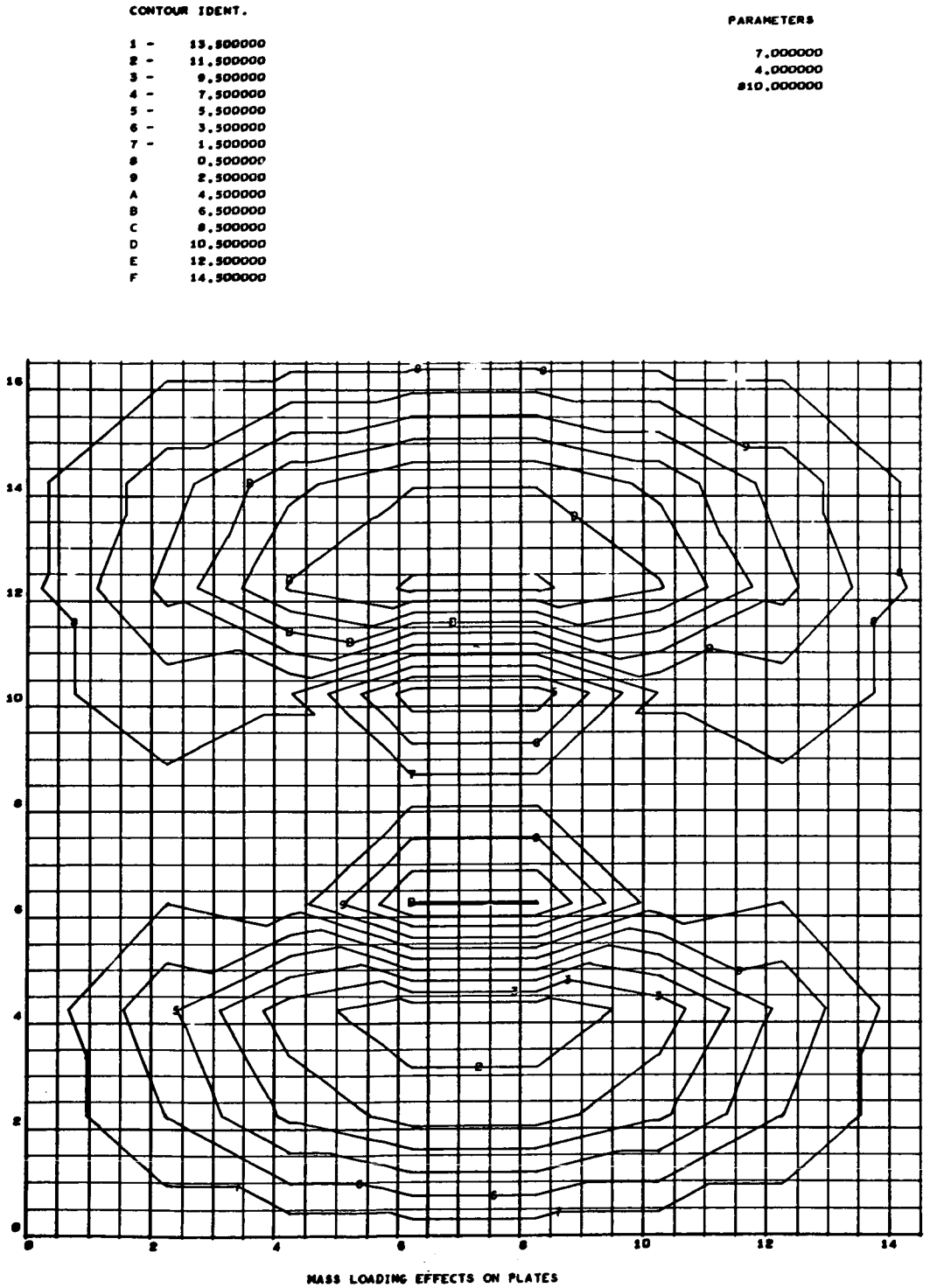

Figure 16. Mass-Loading Effects on Plates, Seventh Mode

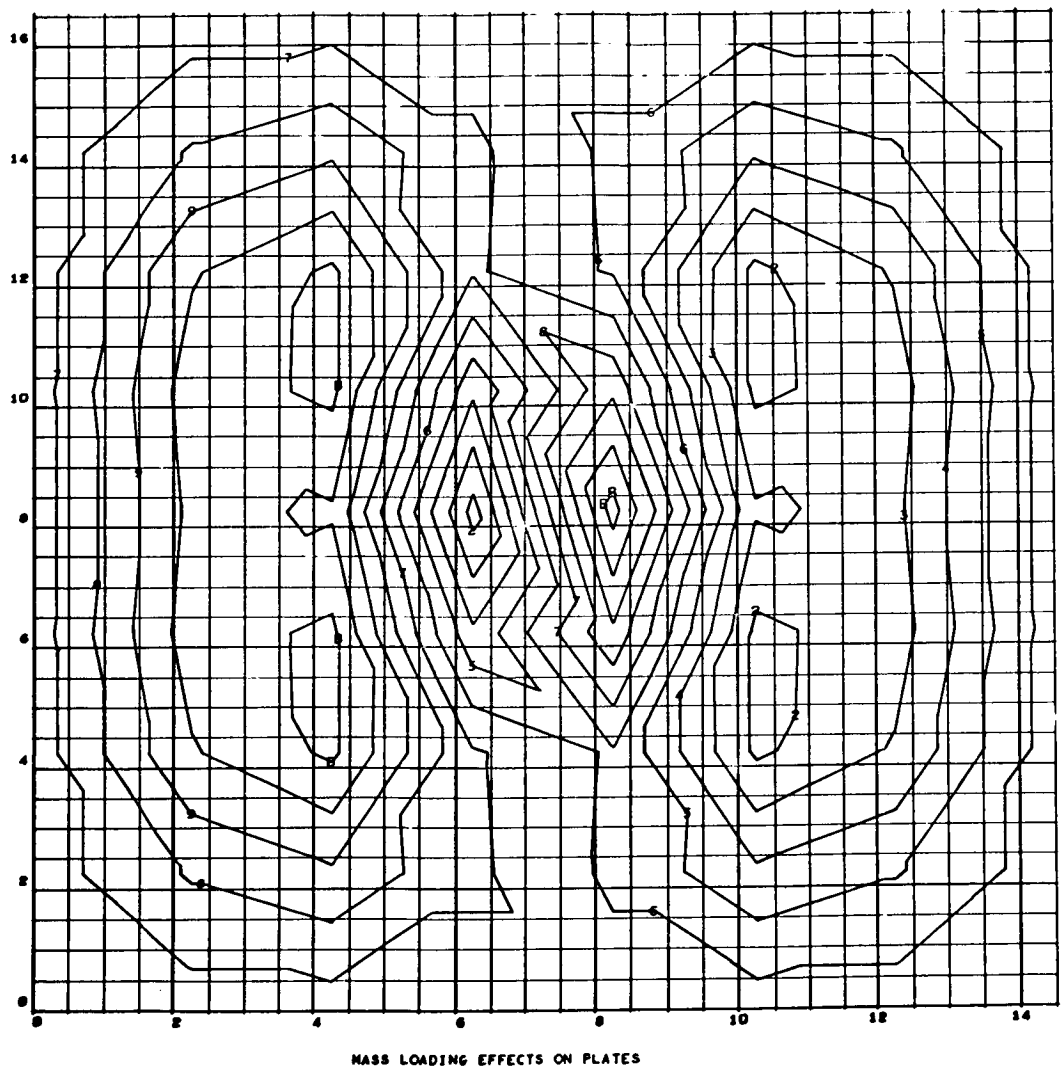

Figure 17. Mass-Loading Effects on Plates, Eighth Mode

CONTOUR IDENT.	
1 -	12.000000
2 -	10.000000
3 -	8.000000
4 -	6.000000
5	4.000000
6 -	2.000000
7	0.000000
8	2.000000
9	4.000000
A	6.000000
B	8.000000
C	10.000000
D	12.000000
E	14.000000
F	16.000000

PARAMETERS
9.000000
4.000000
898.000000

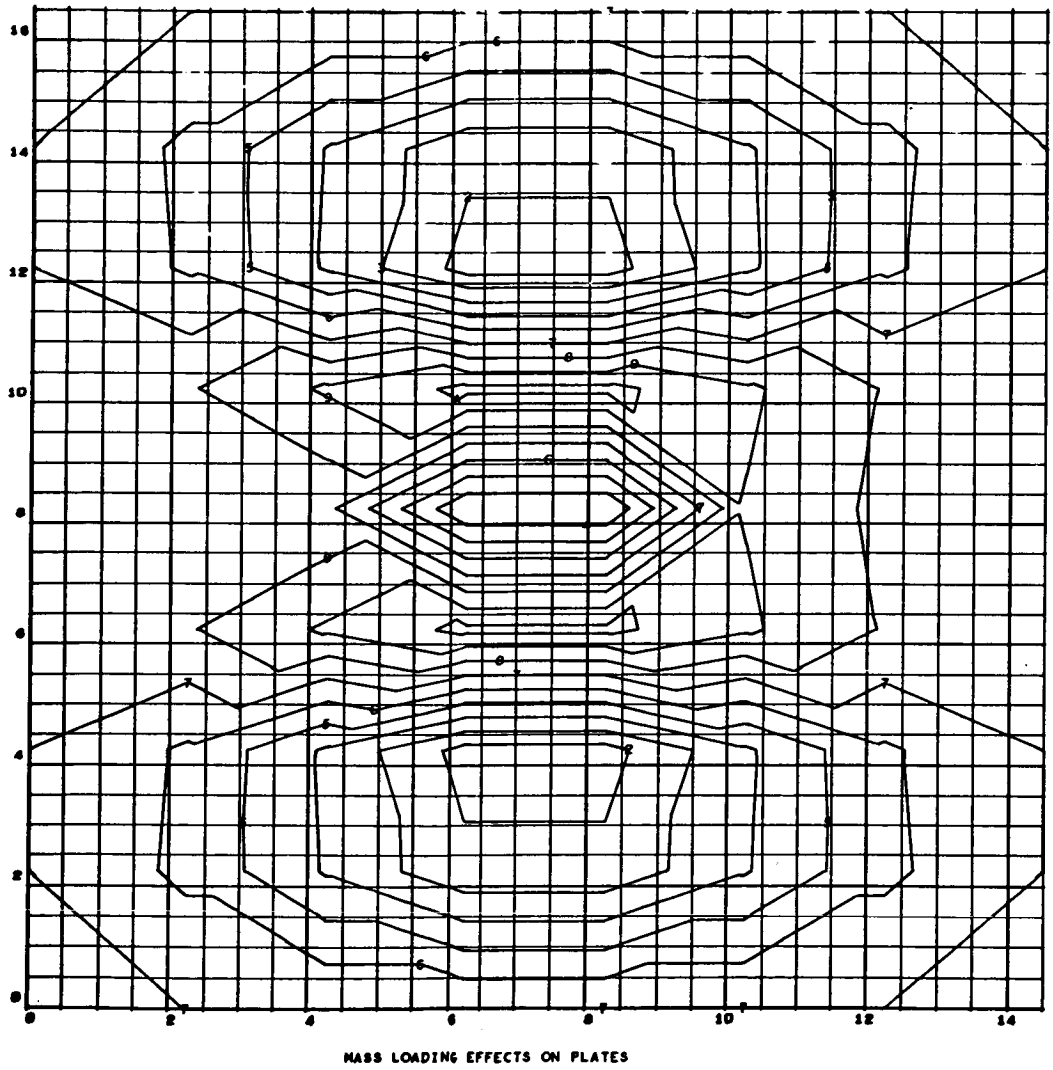

Figure 18. Mass-Loading Effects on Plates, Ninth Mode

CONTOUR IDENT.

1 -	15.000000
2 -	12.900000
3 -	10.800000
4 -	8.700000
5 -	6.600000
6 -	4.500000
7 -	2.400000
8 -	0.300000
9	1.800000
A	3.900000
B	6.000000
C	8.100000
D	10.200000
E	12.300000
F	14.400000

PARAMETERS

10.000000
4.000000
939.000000

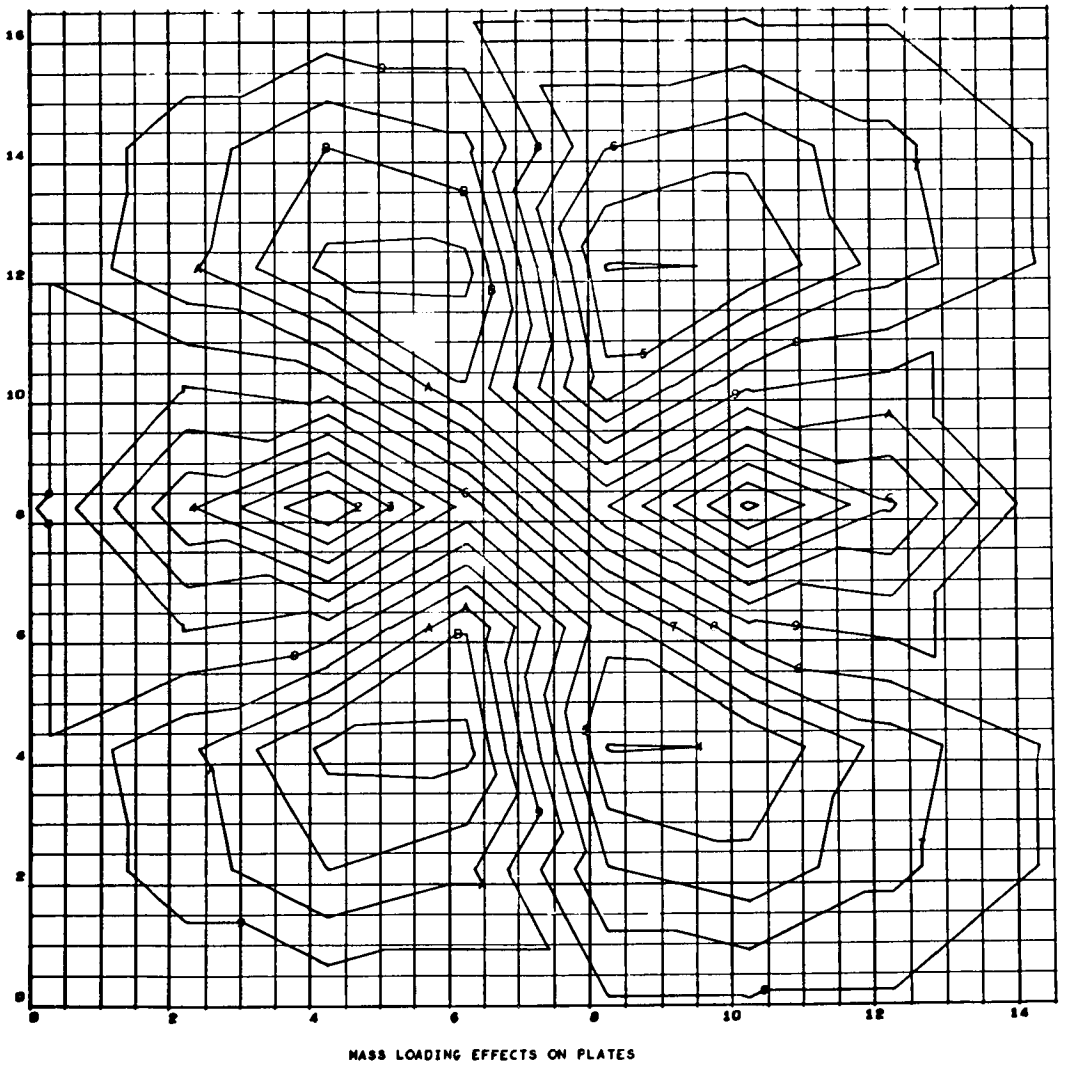

Figure 19. Mass-Loading Effects on Plates, Tenth Mode

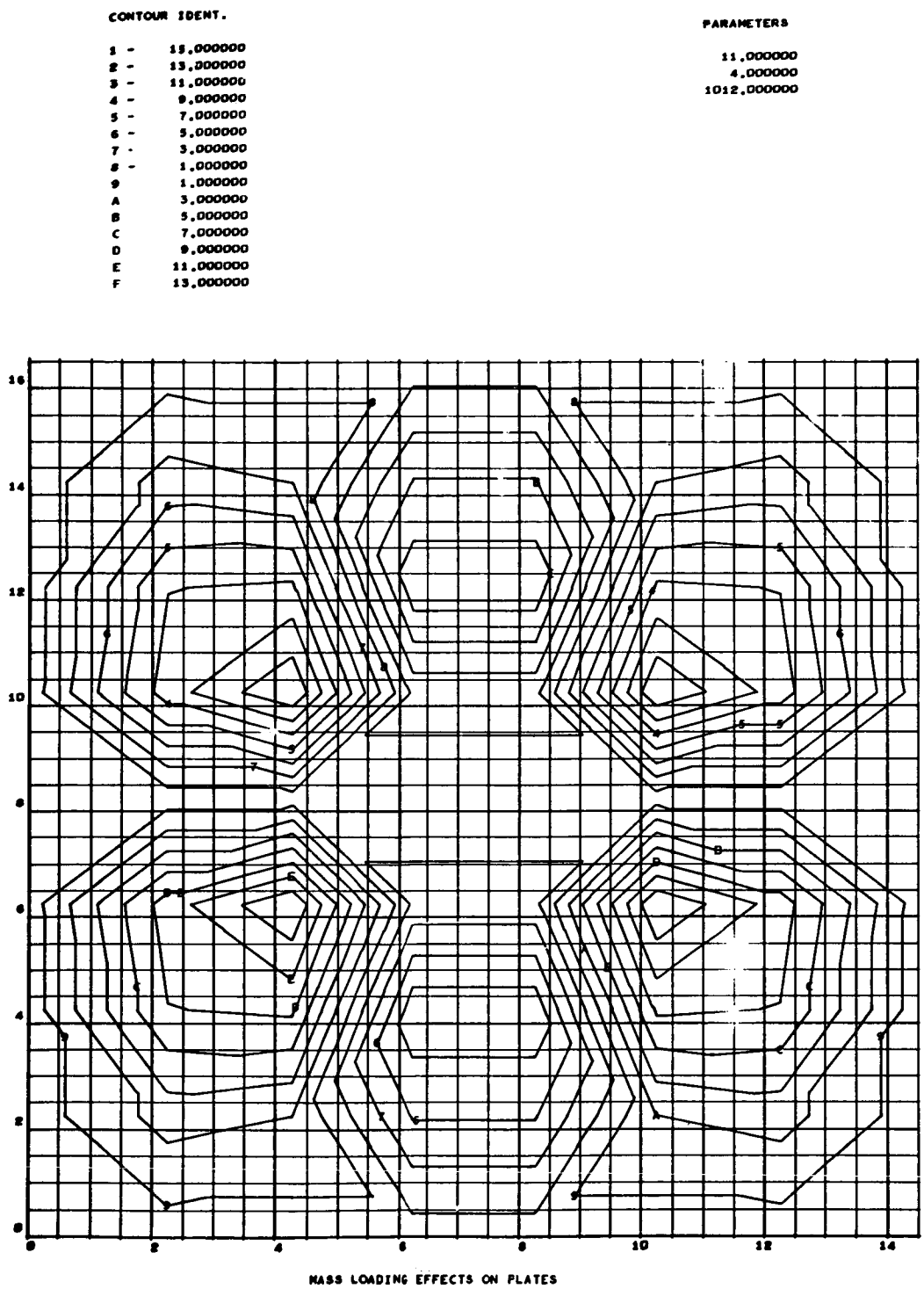

Figure 20. Mass-Loading Effects on Plates, Eleventh Mode

CONTOUR IDENT.

1 -	15.000000
2 -	13.000000
3 -	11.000000
4 -	9.000000
5 -	7.000000
6 -	5.000000
7 -	3.000000
8 -	1.000000
9	1.000000
A	3.000000
B	5.000000
C	7.000000
D	9.000000
E	11.000000
F	13.000000

PARAMETERS

12.000000
4.000000
1058.000000

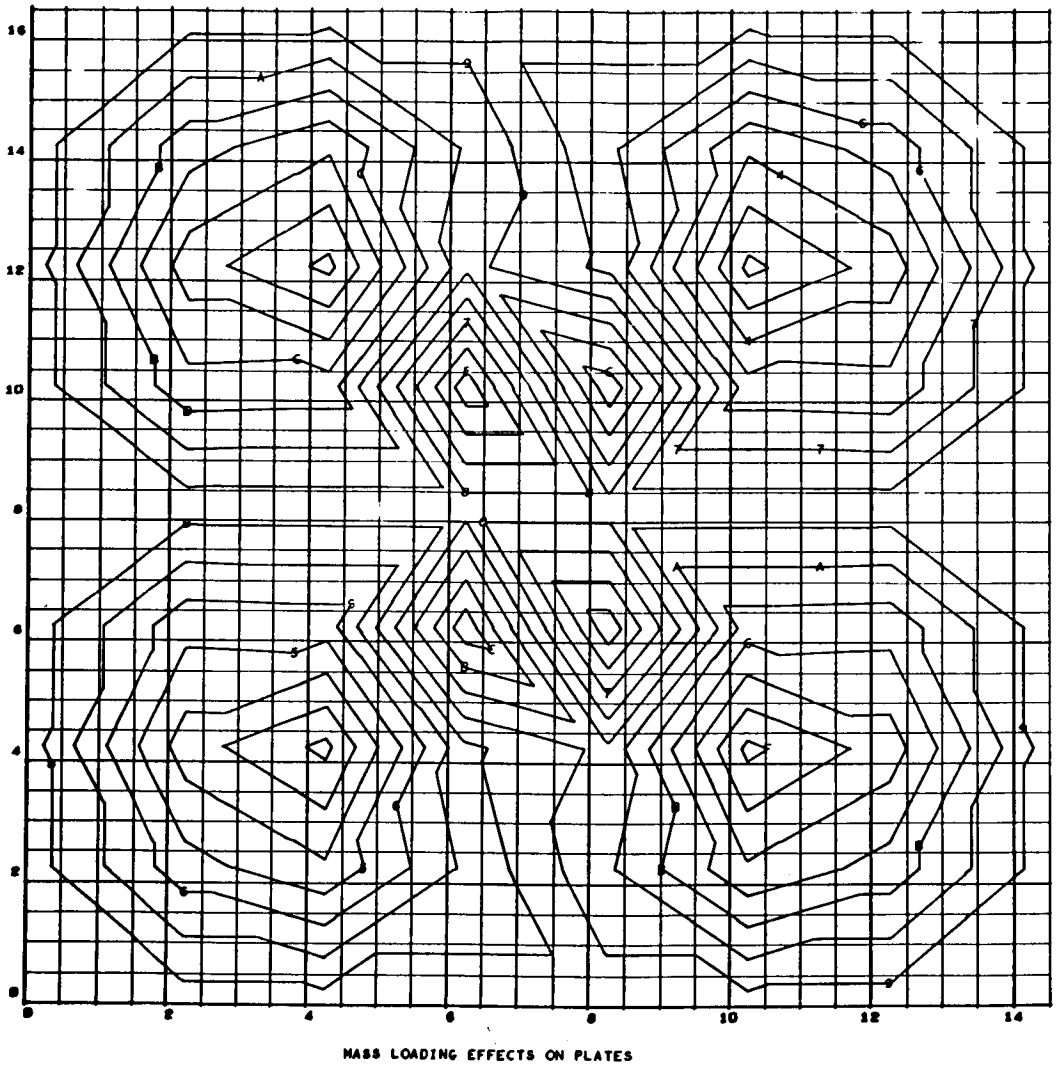

Figure 21. Mass-Loading Effects on Plates, Twelfth Mode

MASS-LOADING EFFECTS ON FORCED VIBRATION AND TRANSMISSIBILITY CHARACTERISTICS

The problem of vibration transmissibility and response of a mass-loaded structure subjected to various excitations can be solved conveniently by the well known classical method based on an assumption of viscous damping or material damping in the equation of motion. The accuracy of the solution depends mainly on the correctness of the assumed damping factor. In practice, the damping factor can be obtained by one of the following experimental methods:

1. Uniaxial material test — Find the complex modulus of elasticity, from which the damping factor can be determined.

2. Free vibration test — Find the logarithmic decrement from the damped vibration curve, then calculate the damping factor.

3. Forced vibration test — Determine the transmissiblity at resonance from the frequency response curve, then find the damping factor.

The third method apparently gives a direct relation between transmissibility and damping. For a one-degree system subjected to force excitation at the mass, this is

$$Q = \frac{1}{2\zeta} \tag{71}$$

where

Q = maximum transmissibility at resonance

$\zeta = \frac{c}{c_c}$ = viscous damping/critical damping

Beyond resonance, the transmissibility becomes

$$T = \frac{1}{\left[\left(1 - \frac{\omega^2}{\omega_n^2}\right)^2 + 4\zeta^2 \frac{\omega^2}{\omega_n^2}\right]^{1/2}} \tag{72}$$

where

ω = angular forcing frequency

ω_n = angular natural frequency

An important phenomenon of mass-loading is established by comparing the transmissibility of a mass-loaded structure to that of the unloaded counterpart. This phenomenon will be discussed in this section. The dynamic responses to any other type of excitations then can be estimated by applying the transmissibility relation between the mass-loaded and unloaded structures. Thus, any unrealistic assumption of damping is eliminated and the results are more accurate.

Mass-Loaded Beams

Transmissibility Characteristics

The analytical solution of transmissibility given by Equations (71) and (72) for a single-degree-of-freedom system can be applied also to the case of mass-loaded beam, which is equivalent to a multidegree-of-freedom system. Using a subscript n to indicate mode number, the transmissibility for the $n^{\underline{th}}$ mode is expressed in the form

$$T_n = \frac{1}{\left[\left(1 - \frac{\omega^2}{\omega_n}\right)2 + 4\zeta_n^2 \frac{\omega^2}{\omega_n}\right]^{1/2}} \qquad (73)$$

At resonance,

$$Q_n \equiv (T_n)_{max} = \frac{1}{2\zeta_n} \qquad (74)$$

where ζ_n represents damping factor for the $n^{\underline{th}}$ mode of the structure.

Tests were performed in the experimental phase of the program to obtain transmissibility data for the various mass-loaded beams. The results are shown in Table 3 for the cases with the mass attached to the beam at its midspan tested on a mechanical shaker. Notations appearing in Table 3 are as follows:

W_2 = additional weight mounted on the beam = $m_2 g$

W_1 = weight of the beam = $m_1 g$

W_2/W_1 = weight ratio or mass ratio

= m_2/m_1

G_2 = maximum response of the mass-loaded beam in g's measured at the location of the added mass

G_1 = maximum response of the beam alone in g's measured at the corresponding location as for G_2

Q_2 = maximum transmissibility of the mass-loaded beam = G_2/G

Q_1 = maximum transmissibility of the beam alone = G_1/G

G = input acceleration in g's

Table 3. Transmissibility of Mass-Loaded Beams with Mass at Midspan (Mechanical Shaker)

m_2/m_1 or W_2/W_1	Mode 1			Mode 3		
	G_2	Q_2	G_2/G_1	G_2	Q_2	G_2/G_1
0	3.34	334	1.0	2.54	254	1.0
0.25	2.94	294	0.88	1.16	116	0.457
0.35	2.68	268	0.80	0.94	94	0.370
0.5	2.61	261	0.78	0.80	80	0.315
0.75	2.28	228	0.68	0.58	58	0.228
1.0	2.03	203	0.61	0.44	44	0.173
2.0	1.88	188	0.56	0.33	33	0.130
3.0	1.59	159	0.48	0.12	12	0.047

Notes: Input acceleration, G = 0.01 g

Beam response, G_1 = 3.34 g's

Beam transmissibility, Q_1 = 334

It can be seen from Tables 3, 4, and 5 that the ratio of maximum responses or maximum transmissibility, $(G_2/G_1 \equiv Q_2/Q_1)$, decreases as the mass ratio, m_2/m_1, increases. This phenomenon of transmissibility attenuation, shown in Figures 22 and 23, is one of the most significant findings of the study.

It is discovered that the relation between the transmissibility of mass-loaded and unloaded structures can be expressed by the following equation, with the constants A, n to be determined experimentally or from the presented curves:

$$y = A + \frac{B}{x^n} \tag{75}$$

where

$$y = G_2/G_1$$

$$x = 1 + \frac{W_2}{W_1} = 1 + \frac{m_2}{m_1}$$

A, n = constants

$$B = 1-A$$

This equation, together with the constants A and n, determined from Figures 22, 23, and 24, may also be applicable to local structures having similar geometries; however, its general application to other geometries or different structural properties is not yet certain. Further investigation with more test samples is required to confirm the validity of the equation's extended applications to various types of structures.

The lower curve in Figure 22 represents mass-loading effects on acceleration response of the beam subjected to constant force excitation.

In Figure 24, data of acceleration response (rms) from the random vibration tests are presented for the mass-loaded beam with mass at its midspan. Input and output acceleration spectral density plots obtained from the tests with mass at various locations on the beam were reduced to useful data similar to those in Figure 24.

Table 4. Transmissibility of Mass-Loaded Beam with Mass at 7-1/4 Inches (Mechanical Shaker)

m_2/m_1 or W_2/W_1	Mode 1			Mode 3		
	G_2	Q_2	G_2/G_1	G_2	Q_2	G_2/G_1
0.	2.17	217	1.0	1.47	147	1.0
0.25	2.00	200	0.922	0.72	72	0.49
0.35	1.83	183	0.844	0.45	45	0.31
0.50	1.63	163	0.751	0.37	37	0.25
0.75	1.53	153	0.705	0.25	25	0.17
1.0	1.30	130	0.599	0.13	13	0.089
2.0	1.15	115	0.530	0.08	8	0.054
3.0	1.02	102	0.470	0.03	3	0.020

Notes: Input acceleration, $G = 0.01$ g

Beam response, $G_1 = 2.17$ g's

Beam transmissibility, $Q_1 = 217$

Table 5. Transmissibility of Mass-Loaded Beam with Mass at 4-1/4 Inches (Mechanical Shaker)

m_2/m_1 or W_2/W_1	Mode 1			Mode 3		
	G_2	Q_2	G_2/G_1	G_2	Q_2	G_2/G_1
0	1.00	100	1.0	3.00	300	1.00
0.25	0.96	96	0.96	1.11	111	0.37
0.35	0.93	93	0.93	1.07	107	0.36

Table 5. Transmissibility of Mass-Loaded Beam with Mass at 4-1/4 Inches (Mechanical Shaker) (Cont)

m_2/m_1 or W_2/W_1	Mode 1			Mode 3		
	G_2	Q_2	G_2/G_1	G_2	Q_2	G_2/G_1
0.50	0.75	75	0.75	1.04	104	0.35
0.75	0.55	55	0.55	0.96	96	0.32
1.0	0.46	46	0.46	0.37	37	0.12
2.0	0.39	39	0.39	0.29	29	0.097
3.0	0.29	29	0.29	0.25	25	0.083

Note: Input acceleration, $G = 0.01$ g

Beam response, $G_2 = 1.00$ g's

Beam transmissibility, $Q_1 = 100$

Forced Vibration Response

Concentrated Force Excitation. The equation of motion of a mass-loaded beam subjected to a system of concentrated forces and moments can be written directly from Equation (3) by adding forcing function terms to the right side of the equation of free vibration:

$$EI\frac{\partial^4 y}{\partial x^4} - \frac{\partial}{\partial x}\left[\sum_{i=1}^{N} J_i \delta(x - a_i)\frac{\partial^3 y}{\partial x \partial t^2}\right] + \left[\rho + \sum_{i=1}^{N} M_i \delta(x - a_i)\right]\frac{\partial^2 y}{\partial t^2} = \sum_{j=1}^{r} F_j(t)\delta(x - b_j) + \sum_{k=1}^{s} C_k(t)\delta'(x - c_k) \tag{76}$$

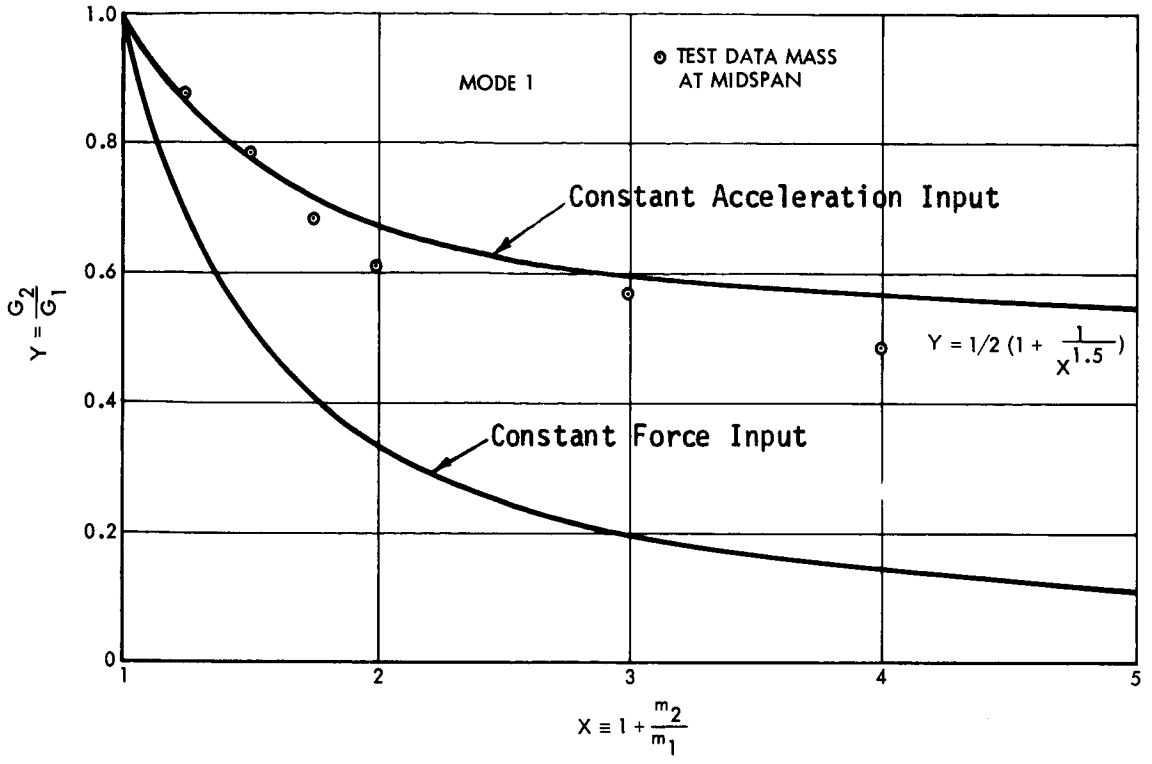

Figure 22. Mass-Loading Effects on Beam (Mechanical Shaker), Mode 1

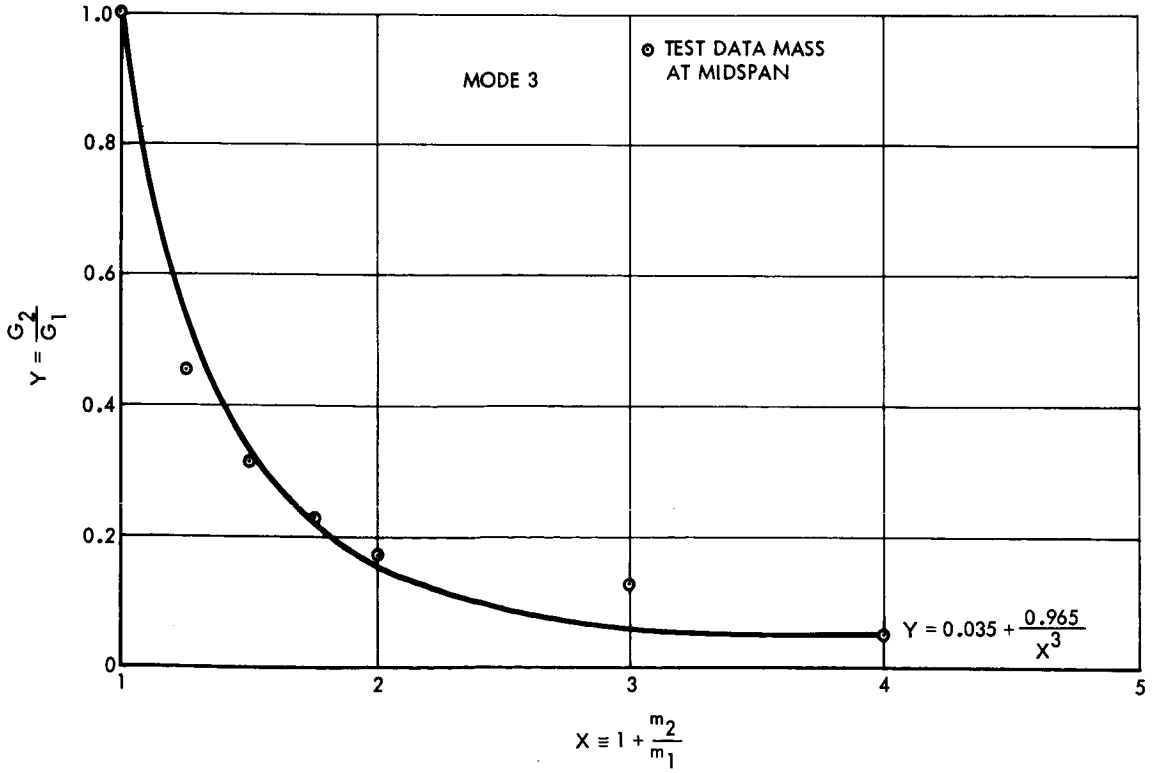

Figure 23. Mass-Loading Effects on Beam (Mechanical Shaker), Mode 3

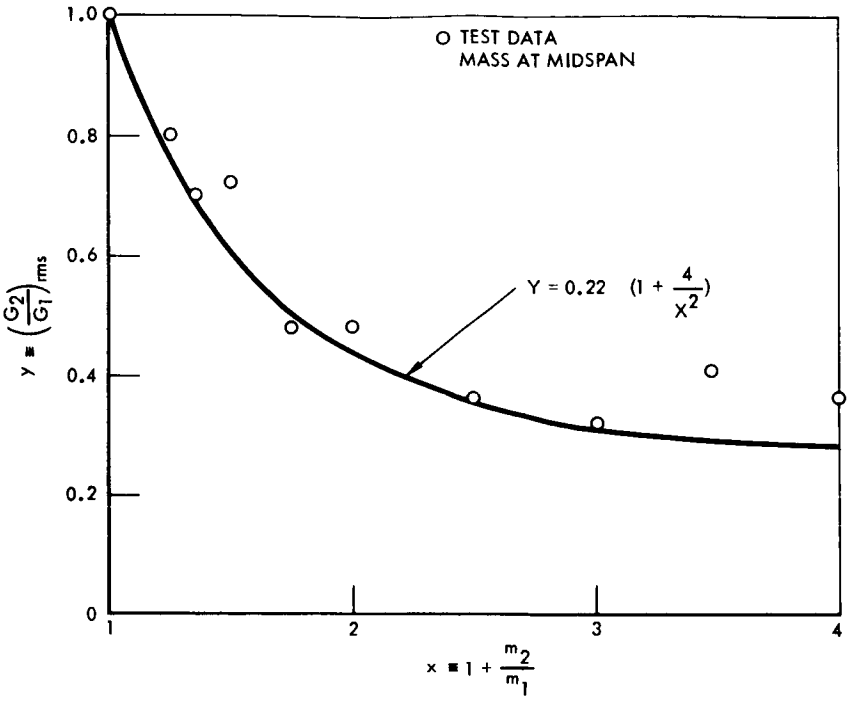

Figure 24. Mass-Loading Effects on Beam (Random Vibration Test)

where $F_j(t)$ and $C_k(t)$ are systems of forces and moments acting at the locations $x = b_j$ and $x = c_k$, respectively; r and s are total numbers of driving forces and driving moments, respectively.

Using the method of normal mode expansion, the solution of Equation (76) can be expressed as

$$y(x,t) = \sum_{n=1}^{\infty} q_n(t) Y_n(x) \qquad (77)$$

where

$Y_n(x)$ = $n^{\underline{th}}$ normal mode obtained previously in the section of free vibration

$q_n(t)$ = time function to be determined

The normal modes satisfy Equation (3), which is written as

$$-Y_n^{iv} = \lambda_n \left\{ \left[\left[\sum_{i=1}^{N} J_i \delta (x - a_i) Y_n' \right]' - \left[\rho + \sum_{i=1}^{N} M_i \delta(x - a_i) \right] Y_n \right\} \tag{78}$$

where

$$\lambda_n = \frac{\omega_n^2}{EI} = \frac{k_n^4}{\rho}$$

The normal modes also satisfy the following orthogonality condition, which is derived from Equation (78) by multiplying by Y_m and performing integration from 0 to L:

$$\int_0^L \left\{ \left[\left[- \sum_{i=1}^{N} J_i \delta(x - a_i) Y_n' \right]' Y_m + \left[\rho + \sum_{i=1}^{N} M_i \delta(x - a_i) \right] Y_n Y_m \right\} dx = 0 \text{ for } m \neq n \tag{79}$$

or, after integration,

$$\int_0^L \rho Y_n Y_m dx + \sum_{i=1}^{N} M_i Y_n(a_i) Y_m(a_i) + \sum_{i=1}^{N} J_i Y_n'(a_i) Y_m'(a_i) = 0 \text{ for } m \neq n \tag{80}$$

For the special case, in whigh $J_i = 0$, $M_i = M$ and $M_i = 0$ for $i \neq 1$, Equation (80) becomes

$$\int_0^L \rho Y_n Y_m dx + M Y_n(a) Y_m(a) = 0 \text{ for } m \neq n \tag{81}$$

After substitution of Equation (77) into Equation (76), multiply the resulting equation by $Y_m(x)$ and integrate:

$$EI \sum_{n=1}^{\infty} q_n(t) \int_0^L Y_n^{iv} Y_m dx + \sum_{n=1}^{\infty} \ddot{q}_n(t) \int_0^L \left\{ - \left[\sum_{i=1}^{N} J_i \delta(x-a_i) Y_n' \right]' + \left[\rho + \sum_{i=1}^{N} M_i \delta(x-a_i) \right] Y_n \right\} Y_m dx \tag{82}$$

$$= \sum_{j=1}^{r} F_j(t) \int_0^L Y_m \delta(x-b_j) dx + \sum_{k=1}^{s} C_k(t) \int_0^L Y_m \delta'(x-c_k) dx$$

Substituting Equation (78) into Equation (82):

$$\sum_{n=1}^{\infty} \left[\omega_n^2 q_n(t) + \ddot{q}_n(t) \right] \int_0^L \left\{ \left[-\sum_{i=1}^{N} J_i \delta(x-a_i) Y_n' \right]' + \left[\rho + \sum_{i=1}^{N} M_i \delta(x-a_i) Y_n \right] \right\} Y_m dx \tag{83}$$

$$= \sum_{j=1}^{r} F_j(t) Y_m(b_j) - \sum_{k=1}^{s} C_k(t) Y_m'(c_k)$$

Using the orthogonality condition, Equation (79), and replacing m by n, Equation (83) reduces to

$$\ddot{q}_n(t) + \omega_n^2 q(t) = \frac{f_n(t)}{Q_n} \tag{84}$$

where Q_n is the generalized mass and $f_n(t)$ is the generalized force in the following forms:

$$Q_n = \int_0^L \rho Y_n^2 dx + \sum_{i-1}^{N} M_i \left[Y_n(a_i)\right]^2 + \sum_{i=1}^{N} J_i \left[Y_n'(a_i)\right]^2$$

$$f_n(t) = \sum_{j=1}^{r} F_j(t)\, Y_n(b_j) - \sum_{k=1}^{s} C_k(t)\, Y_n'(c_k)$$

By convolution integral, the general solution of Equation (84) is obtained:

$$q_n(t) = A_n \sin\omega_n t + B_n \cos\omega_n t + \frac{1}{\omega_n Q_n}\int_0^t f_n(t') \sin\omega_n(t-t')\, dt' \tag{85}$$

where A_n and B_n are constants determined by the initial conditions.

The displacement response is then solved by putting Equation (85) into Equation (77):

$$Y(x,t) = \sum_{n=1}^{\infty} (A_n \sin\omega_n t + B_n \cos\omega_n t)\, Y_n(x) + \sum_{n=1}^{\infty} \frac{Y_n(x)}{\omega_n Q_n}\int_0^t \left[\sum_{j-1}^{r} F_j(t')\, Y_n(b_j) - \sum_{k=1}^{s} C_k(t')\, Y_n'(c_k)\right] \sin\omega_n(t-t')\, dt' \tag{86}$$

For sinusoidal excitation,

$$F_j(t) = F_j \sin\omega_j t$$

and

$$C_k(t) = C_k \sin\omega_j t$$

The response can be obtained in a close form:

$$Y(x,t) = \sum_{n=1}^{\infty} (A_n \sin\omega_n t + B_n \cos\omega_n t)\, Y_n(x)$$

$$+ \sum_{n=1}^{\infty} \frac{Y_n(x)}{\omega_n Q_n} \left\{ \sum_{j=1}^{r} Y_n(b_j)\, F_j \right.$$

$$\cdot \left[\frac{\omega_j}{\omega_j^2 - \omega_n^2} \sin\omega_n t - \frac{\omega_n}{\omega_j^2 - \omega_n^2} \sin\omega_j t \right] \qquad (87)$$

$$- \sum_{k=1}^{s} Y_n'(c_k) C_k \left[\frac{\omega_k}{\omega_k^2 - \omega_n^2} \sin\omega_n t \right.$$

$$\left. \left. - \frac{\omega_n}{\omega_k^2 - \omega_n^2} \sin\omega_k t \right] \right\}$$

For other types of excitation, the response can be found by Equation (86).

Arbitrary Forcing Function. If the forcing function is not a concentrated one but of arbitrary distribution, $p(x,t)$, the equation of motion (76) is

$$EI \frac{\partial^4 y}{\partial x^4} - \frac{\partial}{\partial x} \left[\sum_{i=1}^{N} J_i \delta(x-a_i) \frac{\partial^3 y}{\partial x \partial t^2} \right]$$

$$+ \left[\rho + \sum_{i=1}^{N} M_i \delta(x-a_i) \right] \frac{\partial^2 y}{\partial t^2} = p(x,t) \qquad (88)$$

Equations (77) through (81) and Equation (84) are applicable except that the generalized force in Equation (84) is now in the form

$$f_n(t) = \int_0^L p(x,t)\, Y_n(x)\, dx \qquad (89)$$

The generalized mass Q_n is the same as before. Then the solution of Equation (84) becomes

$$q_n(t) = A_n \sin\omega_n t + B_n \cos\omega_n t + \frac{1}{\omega_n Q_n}\int_0^t \int_0^L p(x,t')\, Y_n(x)\, dx \sin\omega_n (t-t')\, dt' \tag{90}$$

The complete solution of Equation (88) is

$$y(x,t) = \sum_{n=1}^{\infty} (A_n \sin\omega_n t + B_n \cos\omega_n t)\, Y_n(x) + \sum_{n-1}^{\infty} \frac{Y_n(x)}{\omega_n Q_n}\int_0^t \int_0^L p(x,t')\, Y_n(x)\, dx \cdot \sin\omega_n (t-t')\, dt' \tag{91}$$

For $p(x,t) = p_o \sin\omega t$ with p_o = constant,

$$f_n(t) = \int_0^L p_o \sin\omega_n t\, Y_n(x)\, dx = p_o \sin\omega_n t \int_0^L Y_n(x)\, dx$$

The forced response is

$$y(x,t) = \sum_{n=1}^{\infty} (A_n \sin\omega_n t + B_n \cos\omega_n t)\, Y_n(x) + \sum_{n=1}^{\infty} \frac{p_o}{\omega_n Q_n}\left[\int_0^L Y_n(x)\, dx\right] Y_n(x) \cdot \left[\frac{\omega}{\omega^2 - \omega_n^2} \sin\omega_n t - \frac{\omega_n}{\omega^2 - \omega_n^2} \sin\omega t\right] \tag{92}$$

Edge Excitation. If the beam in Figure 3 is excited by a given displacement d(t) of its supports, the problem can be solved by using the equation of motion for free vibration.

$$EI\frac{\partial^4 y}{\partial x^4} - \frac{\partial}{\partial x}\left[\sum_{i=1}^{N} J_i\,\delta(x-a_i)\frac{\partial^3 y}{\partial x \partial t^2}\right] + \left[\rho + \sum_{i=1}^{N} M_i\,\delta(x-a_i)\right]\frac{\partial^2 y}{\partial t^2} = 0 \tag{93}$$

Assume a fixed end boundary condition:

$$\text{At } x = 0, \quad y = d(t), \quad \frac{\partial y}{\partial x} = 0$$

$$\text{At } x = L, \quad y = d(t), \quad \frac{\partial y}{\partial x} = 0$$

For transformation of variables, let

$$w(x,t) = y - d \tag{94}$$

i.e.,

$$y = w + d$$

Substitute Equation (94) into Equation (93):

$$EI\frac{\partial^4 w}{\partial x^4} - \frac{\partial}{\partial x}\left[\sum_{i=1}^{N} J_i\,\delta(x-a_i)\frac{\partial^3 w}{\partial x \partial t^2}\right] + \left[\rho + \sum_{i=1}^{N} M_i\,\delta(x-a_i)\right]\frac{\partial^2 w}{\partial t^2} = -\left[\rho + \sum_{i=1}^{N} M_i\,\delta(x-a_i)\right]\ddot{d}(t) \tag{95}$$

The new boundary conditions are

$$\text{At } x = 0, \quad w = 0, \quad \frac{\partial w}{\partial x} = 0$$

$$\text{At } x = L, \quad w = 0, \quad \frac{\partial w}{\partial x} = 0$$

The problem then becomes one with a forcing function equal to

$$-\left[\rho + \sum_{i=1}^{N} M_i \, \delta(x-a_i)\right] \ddot{d}(t),$$

which can be solved by the normal mode expansion method given previously.

Assume the solution to be

$$w(x,t) = \sum_{n=1}^{\infty} q_n(t) \, Y_n(x) \tag{96}$$

Rewrite Equation (84), which still applies to the present case:

$$\ddot{q}_n(t) + \omega_n^2 \, q(t) = \frac{f_n(t)}{Q_n} \tag{97}$$

The generalized mass Q_n is the same as before, but the generalized force $f_n(t)$ is different.

$$f_n(t) = -\ddot{d}(t)\left[\rho\int_0^L Y_n(x)dx + \sum_{i=1}^{N} M_i \, Y_n(a_i)\right] \tag{98}$$

or

$$f_n(t) = c_n \, \ddot{d}(t)$$

where

$$c_n = -\left[\rho\int_0^L Y_n(x)\,dx + \sum_{i=1}^{N} M_i \, Y_n(a_i)\right]$$

Equation (97) can be expressed as

$$\ddot{q}_n(t) + \omega_n^2 \, q(t) = \frac{c_n}{Q_n} \ddot{d}(t) \tag{99}$$

The solution $q_n(t)$ of Equation (99) is found by substituting Equation (98) into Equation (85).

$$q_n(t) = A_n \sin\omega_n t + B_n \cos\omega_n t$$

$$+ \frac{c_n}{\omega_n Q_n} \int_0^t \ddot{d}(t') \sin\omega_n (t-t') \, dt' \tag{100}$$

For sinusoidal acceleration excitation at both ends of the beam,

$$\ddot{d}(t) = a_o \sin\omega t$$

where

a_o = constant (acceleration amplitude)

then

$$d(t) = \iint \ddot{d}(t) dt \, dt = - \frac{a_o}{\omega^2} \sin\omega t \tag{101}$$

and

$$q_n(t) = A_n \sin\omega_n t + B_n \cos\omega_n t$$

$$+ \frac{c_n a_o}{\omega_n Q_n} \left[\frac{\omega}{\omega^2 - \omega_n^2} \sin\omega_n t - \frac{\omega_n}{\omega^2 - \omega_n^2} \sin\omega t \right] \tag{102}$$

Using Equations (96), (102), and (94), the displacement response to sinusoidal acceleration excitation is found as

$$y(x,t) = \sum_{n=1}^{\infty} (A_n \sin\omega_n t + B_n \cos\omega_n t)\, Y_n(x)$$

$$+ \sum_{n=1}^{\infty} \frac{c_n a_o}{\omega_n Q_n} Y_n(x) \left[\frac{\omega_n}{\omega^2 - \omega_n^2} \sin\omega_n t - \frac{\omega_n}{\omega^2 - \omega_n^2} \sin\omega t \right] \quad (103)$$

$$- (a_o/\omega^2) \sin\omega t$$

Mass-Loaded Plates

Transmissibility Characteristics

Vibration transmissibility of a mass-loaded plate can be shown to have similar form as that of a mass-loaded beam given by Equations (73) and (74). Let m and n be the mode number in x and y directions, respectively. The transmissibility for mode mn is

$$T_{mn} = \frac{1}{\left[\left(1 - \frac{\omega^2}{\omega_{mn}^2} \right)^2 + 4\zeta_{mn}^2 \frac{\omega^2}{\omega_{mn}^2} \right]^{1/2}}$$

At resonance,

$$Q_n \equiv (T_{mn})_{max.} = \frac{1}{2\zeta_{mn}}$$

where ω_{mn} and ζ_{mn} are natural frequency and damping factor of the structure in the mode mn.

Data obtained from the experimental phase of the program (Table 6) shows that there is similar attenuation of transmissibility as in the beam cases. An expression for plate transmissibility in the form of Equation (75) is derived:

$$y = 0.163 + \frac{0.837}{x^3}$$

Table 6. Transmissibility of Mass-Loaded Plates
(Sinusoidal Vibration Tests)

m_2/m_1	0	0.7	1.0	2.0	3.0	4.0
G_1, g's	149					
G_2, g's	149	35	24	22	36.5	31
G_2/G_1	1.0	0.235	0.168	0.148	0.245	0.208

Notations: m_1 = mass of the unloaded plate

m_2 = additional mass on the plate

G_1 = maximum acceleration response of the unloaded plate

G_2 = maximum acceleration response of the mass-loaded plate

For any given mass ratio, m_2/m_1, the transmissibility ratio, G_2/G_1, can be found from the plot (Figure 25). The transmissibility of the mass-loaded plate, T_2, then can be expressed in terms of that of the unloaded plate, T_1.

$$T_2 = \left(\frac{G_2}{G_1}\right) T_1$$

Vibration tests on the mass-loaded plates with random excitation also result in similar data. In this case, the response is in terms of root-mean-square value of the acceleration in g's (Table 7). The plot in Figure 26 shows the relation between the experimental data and the expression

$$y = 0.22 \left(1 + \frac{4}{x^2}\right)$$

Table 7. Transmissibility of Mass-Loaded Plates
(Random Vibration Tests)

m_2/m_1	0	0.34	0.5	0.6	1	2	3	4
$(G_1)_{rms}$, g's	13							
$(G_2)_{rms}$, g's	13	7	6	5.3	5.7	5.0	4.2	2.8
$(G_2/G_1)_{rms}$	1.0	0.54	0.46	0.41	0.44	0.38	0.32	0.21

Note that this is also in the form of the general equation

$$y = A + \frac{B}{x^n}$$

Figure 27 shows the experimental results demonstrating the attenuation of acceleration response and higher modes for the mass-loaded plate in comparison with the unloaded panel.

In Appendix B, X-Y plots from random vibration tests on the mass-loaded plates are presented to demonstrate the input and output spectral density at the mass.

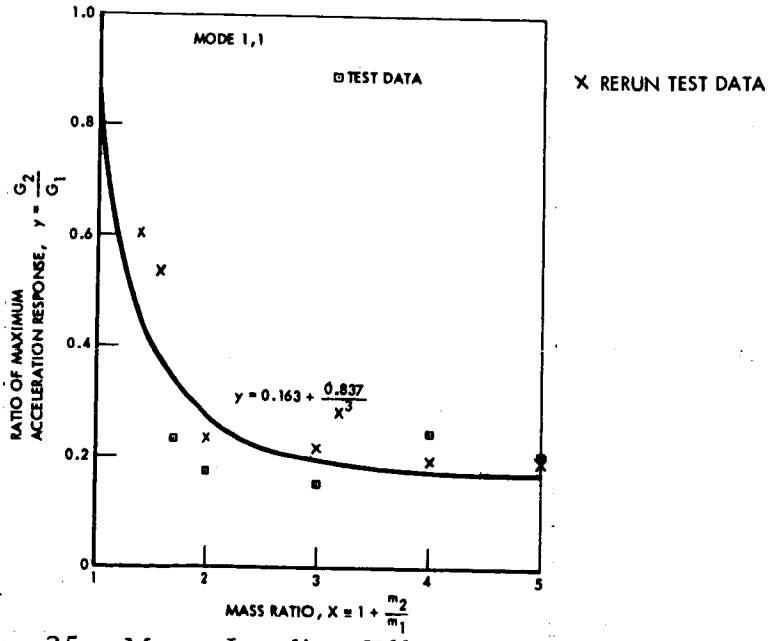

Figure 25. Mass-Loading Effects on Plate
(Sinusoidal Vibration Test)

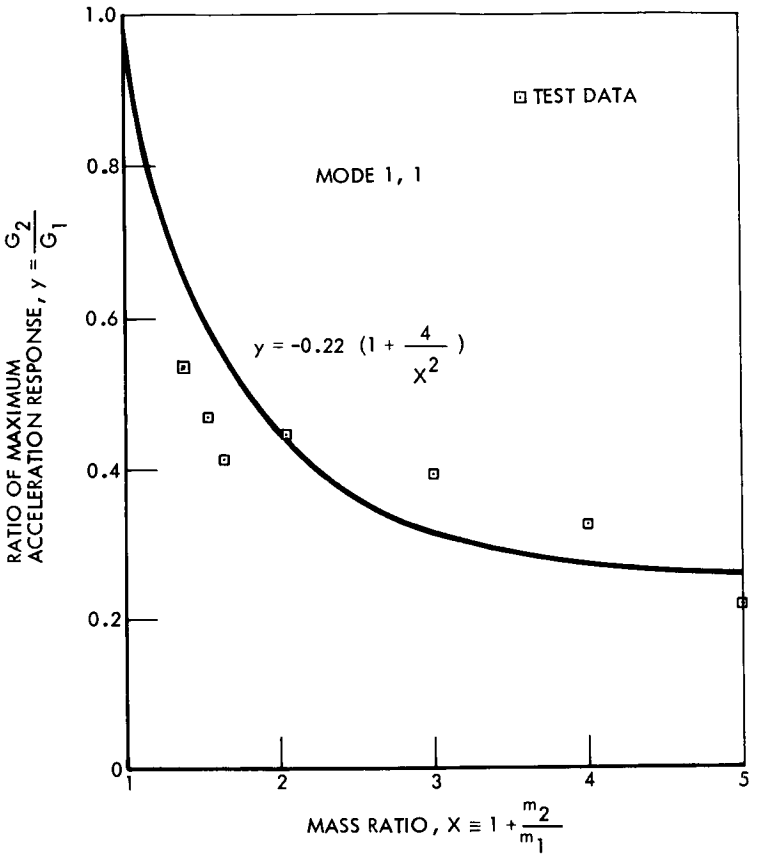

Figure 26. Mass-Loading Effects on Plate (Random Vibration Test)

Forced Vibration Response

Concentrated Force Excitation. When the mass-loaded plate of Figure 9 is subjected to a concentrated force excitation, P(t), applied at $x = x_o$, $y = y_o$, the equation of motion is

$$\nabla^2\nabla^2 w + \left[\rho h + M\delta(x-\xi)\ (y-\eta)\right]\frac{\ddot{w}}{D} = \frac{P(t)}{D}\,\delta(x-x_o)\,\delta(y-y_o) \tag{104}$$

Assume the solution to be of the form

$$w(x, y, t) = \sum_{m=1}^{\infty} \sum_{n=1}^{\infty} q_{mn}(t)\, W_{mn}(x, y) \tag{105}$$

where

$q_{mn}(t)$ = time function to be determined,

$W_{mn}(x, y)$ = natural modes of plate obtained from free vibration analysis

The natural modes satisfy the equation of motion of free vibration:

$$\nabla^2\nabla^2 W_{mn} = \frac{\omega^2_{mn}}{D} \left[\rho h + M\delta(x-\xi)\,\delta(y-\eta)\right] W_{mn} \tag{106}$$

They also satisfy the orthogonality condition of the natural modes, which is derived as follows: For any mode pq with frequency ω_{pq}, the mode shape is W_{pq}, which satisfies Equation (106). Hence,

$$\nabla^2\nabla^2 W_{pq} = \frac{\omega^2_{pq}}{D} \left[\rho h + M\delta(x-\xi)\,\delta(y-\eta)\right] W_{pq} \tag{107}$$

Multiply Equation (106) by W_{pq} and multiply Equation (107) by W_{mn}; then integrate over the plate surface and subtract the results.

$$\int_0^a \int_0^b \left[\left(\nabla^2\nabla^2 W_{mn}\right)W_{pq} - \left(\nabla^2\nabla^2 W_{pq}\right)W_{mn}\right] dxdy$$

$$= \frac{1}{D}\left(\omega^2_{mn} - \omega^2_{pq}\right)\int_0^a \int_0^b \left[\rho h + M\delta(x-\xi)\,\delta(y-\eta)\right] \tag{108}$$

$$\cdot W_{mn}\, W_{pq}\, dxdy$$

Integrating by part and using the boundary conditions, the left side of Equation (108) vanishes.

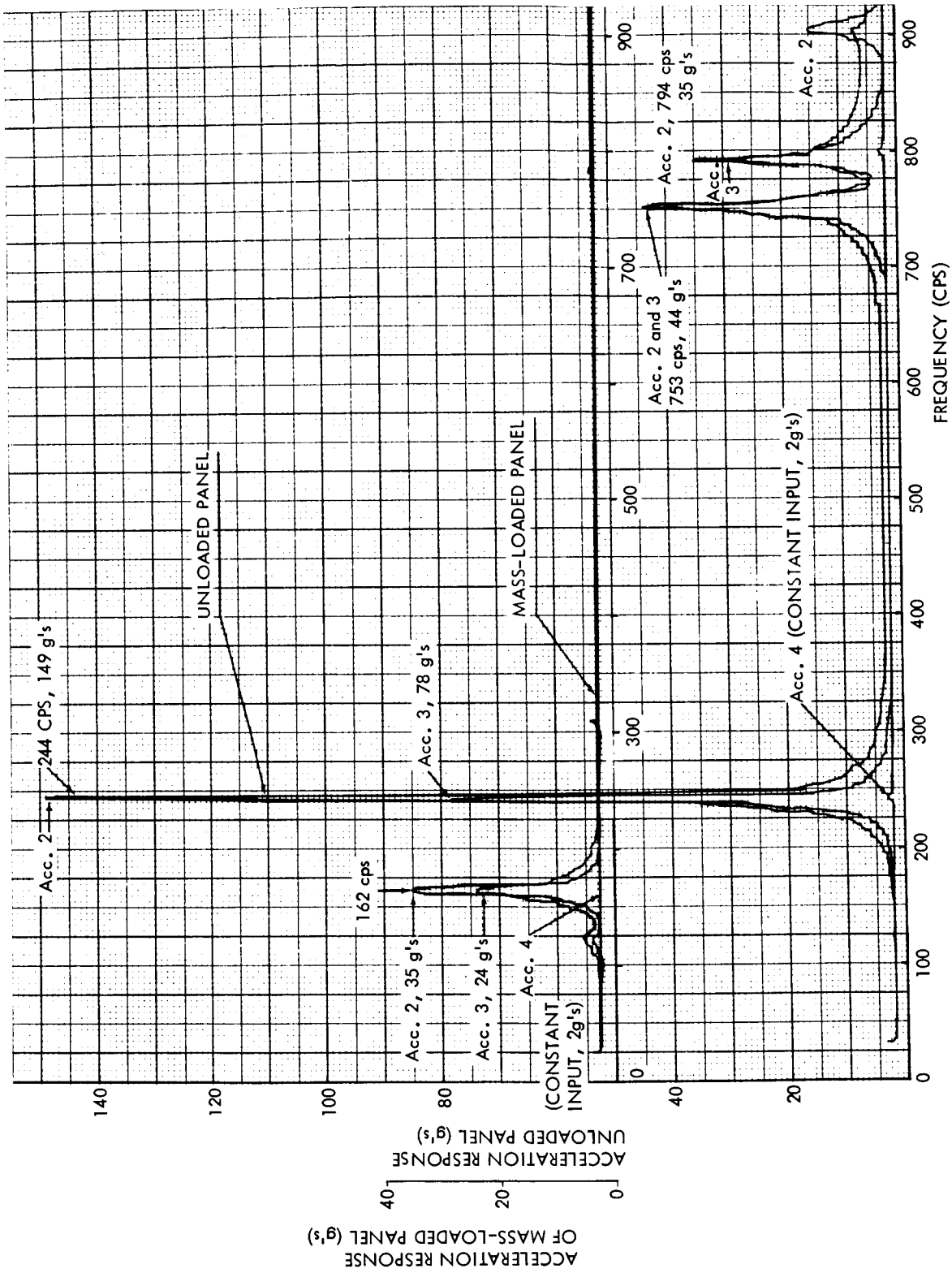

Figure 27. Attenuation of Response and Higher Modes of Mass-Loaded Plate

The second term on the right side of Equation (108) can be integrated to be

$$\int_0^a \int_0^b M\,\delta(x-\xi)\,\delta(y-\eta)\,W_{mn}\,W_{pq}\,dxdy$$

$$= M\,W_{mn}(\xi,\eta)\,W_{pq}(\xi,\eta)$$

Equation (108) then becomes

$$(\omega_{mn}^2-\omega_{pq}^2)\left\{\rho h\int_0^a\int_0^b W_{mn}\,W_{pq}\,dxdy + M\,W_{mn}(\xi,\eta)\,W_{pq}(\xi,\eta)\right\} = 0 \qquad (109)$$

The orthogonality condition is obtained as

$$\rho h\int_0^a\int_0^b W_{mn}\,W_{pq}\,dxdy + M\,W_{mn}(\xi,\eta)\,W_{pq}(\xi,\eta) = 0$$

$$\text{for } \omega_{mn} \neq \omega_{pq} \qquad (110)$$

After substitution from Equation (105) into Equation (104), multiply the resulting equation by W_{pq} and integrate,

$$\sum_{m=1}^{\infty}\sum_{n=1}^{\infty} q_{mn}(t)\int_0^a\int_0^b \left(\nabla^2\nabla^2 W_{mn}\right) W_{pq}\,dxdy$$

$$+\frac{1}{D}\sum_{m=1}^{\infty}\sum_{n=1}^{\infty}\ddot{q}_{mn}(t)\int_0^a\int_0^b \left[\rho h+M\delta(x-\xi)\,\delta(y-\eta)\right]W_{mn}W_{pq}\,dxdy \qquad (111)$$

$$= \frac{P(t)}{D}\int_0^a\int_0^b \delta(x-x_o)\,\delta(y-y_o)\,W_{pq}\,dxdy$$

Substituting Equation(106) into Equation (111),

$$\sum_{m=1}^{\infty} \sum_{n=1}^{\infty} \left[\omega_{mn}^2 q_{mn}(t)+\ddot{q}_{mn}(t)\right] \cdot$$

$$\cdot \int_0^a \int_0^b \left[\rho h+M\delta(x-\xi)\delta(y-\eta)\right] W_{mn} W_{pq} dxdy \qquad (112)$$

$$= P(t)W_{pq}(x_o, y_o)$$

Using the orthogonality condition, Equation (110), the above equation is simplified to

$$\ddot{q}_{mn}(t) + \omega_{mn}^2 q_{mn}(t) = \frac{f_{mn}(t)}{Q_{mn}} \qquad (113)$$

where

Q_{mn} = the generalized mass and

$f_{mn}(t)$ = the generalized force in the following forms:

$$Q_{mn} = \rho h \int_0^a \int_0^b W_{mn}^2 dxdy+M\left[W_{mn}(\xi, \eta)\right]^2 \qquad (114)$$

$$f_{mn}(t) = P(t)\, W_{mn}(x_o, y_o) \qquad (115)$$

The general solution of Equation (113) can be found by convolution integral.

$$q_{mn}(t) = A_{mn} \sin\omega_{mn} t+B_{mn} \cos\omega_{mn} t + \frac{1}{\omega_{mn} Q_{mn}} \int_0^t f_{mn}(t') \sin\omega_{mn}(t-t')\, dt' \qquad (116)$$

where A_{mn} and B_{mn} are constants determined from the initial conditions, or

$$q_{mn}(t) = A_{mn}\sin\omega_{mn}t + B_{mn}\cos\omega_{mn}t + \frac{W_{mn}(x_o, y_o)}{\omega_{mn} Q_{mn}} \int_0^t P(t')\sin\omega_{mn}(t-t')dt' \tag{117}$$

Substituting the solution of Equation (117) into Equation (105), the displacement response is obtained.

For sinusoidal excitation,

$$P(t) = P_o \sin\omega t \text{ with } P_o = \text{constant},$$

the solution is in the form

$$w(x, y, t) = \sum_{m=1}^{\infty} \sum_{n=1}^{\infty} (A_{mn}\sin\omega_{mn}t + B_{mn}\cos\omega_{mn}t) W_{mn}(x, y) + \sum_{m=1}^{\infty} \sum_{n=1}^{\infty} \frac{P_o W_{mn}(x_o, y_o)}{\omega_{mn} Q_{mn}} W_{mn}(x, y) \cdot \left[\frac{\omega}{\omega^2 - \omega_{mn}^2} \sin\omega_{mn}t - \frac{\omega_{mn}}{\omega^2 - \omega_{mn}^2} \sin\omega t \right] \tag{118}$$

Arbitrary Force Excitation. For an arbitrarily distributed force excitation, $p(x, y, t)$, the equation of motion becomes

$$\nabla^2\nabla^2 w + \left[\rho h + M\delta(x-\xi)\delta(y-\eta)\right] \frac{\ddot{w}}{D} = p(x, y, t) \tag{119}$$

Equations (105) to (110) and Equations (113) and (114) are applicable except that the generalized force in Equation (113) is now

$$f_{mn}(t) = \int_0^a \int_0^b p(x, y, t) W_{mn}(x, y) dx dy \tag{120}$$

The solution of Equation (113) then becomes

$$q_{mn}(t) = A_{mn}\sin\omega_{mn}t + B_{mn}\cos\omega_{mn}t + \frac{1}{\omega_{mn}Q_{mn}}\int_0^t\left[\int_0^a\int_0^b p(x,y,t')W_{mn}(x,y)dxdy\right] \cdot \sin\omega_{mn}(t-t')\,dt' \qquad (121)$$

For $p(x,y,t) = p_o \sin\omega t$ with p_o = constant,

$$f_{mn}(t) = \int_0^a\int_0^b p_o\sin\omega t\, W_{mn}(x,y)dxdy = p_o\sin\omega t\int_0^a\int_0^b W_{mn}(x,y)dxdy \qquad (122)$$

The displacement response is

$$w(x,y,t) = \sum_{m=1}^{\infty}\sum_{n=1}^{\infty}(A_{mn}\sin\omega_{mn}t + B_{mn}\cos\omega_{mn}t)W_{mn}(x,y) + \sum_{m=1}^{\infty}\sum_{n=1}^{\infty}\frac{p_o}{\omega_{mn}Q_{mn}}\left[\int_0^a\int_0^b W_{mn}(x,y)dxdy\right]W_{mn}(x,y) \cdot\left[\frac{\omega}{\omega^2-\omega_{mn}^2}\sin\omega_{mn}t - \frac{\omega_{mn}}{\omega^2-\omega_{mn}^2}\sin\omega t\right] \qquad (123)$$

Edge Excitation. If the mass-loading plate is subjected to a displacement excitation, d(t), at its edges, the problem can be investigated from the free vibration equation (87). Assume a clamped-edge boundary condition:

At $x=0$ and $x = a$,

$$w = d(t), \qquad \frac{\partial w}{\partial x} = 0$$

$$\text{At } y = 0 \text{ and } y = b,$$

$$w = d(t), \qquad \frac{\partial w}{\partial y} = 0$$

For transformation of variables, let

$$z(x, y, t) = w - d$$

i.e., $$w(x, y, t) = z + d \tag{124}$$

Substitute Equation (124) into Equation (87):

$$\nabla^2\nabla^2 z + \left[\rho h + M\delta(x-\xi)\,\delta(y-\eta)\right]\frac{\ddot{z}}{D} = -\left[\rho h + M\delta(x-\xi)\,\delta(y-\eta)\right]\ddot{d}(t) \tag{125}$$

The new boundary conditions are

$$\text{At } x = 0, \text{ and } x = a$$

$$z = 0, \quad \frac{\partial z}{\partial x} = 0$$

$$\text{At } y = 0, \text{ and } y = b,$$

$$z = 0, \quad \frac{\partial z}{\partial y} = 0$$

The problem then becomes one with a forcing function equal to

$$-\left[\rho h + M\delta(x-\xi)\,\delta(y-\eta)\right]\ddot{d}(t)$$

The solution of Equation (125) is assumed to be

$$z(x, y, t) = \sum_{m=1}^{\infty}\sum_{n=1}^{\infty} q_{mn}(t)\, W_{mn}(x, y) \tag{126}$$

Rewrite Equation (113), which still applies to this case.

$$\ddot{q}_{mn}(t) + \omega_{mn}^2\, q_{mn}(t) = \frac{f_{mn}(t)}{Q_{mn}} \tag{127}$$

The generalized mass Q_{mn} is the same as in Equation (114), but the generalized force $f_{mn}(t)$ is different.

$$f_{mn}(t) = -\ddot{d}(t)\int_0^a\int_0^b \left[\rho h+M\delta(x-\xi)\delta(y-\eta)\right]W_{mn}(x,y)dxdy$$

$$= -\ddot{d}(t)\left[\rho h\int_0^a\int_0^b W_{mn}(x,y)dxdy+M W_{mn}(\xi,\eta)\right] \qquad (128)$$

$$= c_{mn}\ddot{d}(t)$$

where

$$c_{mn} = -\left[\rho h\int_0^a\int_0^b W_{mn}(x,y)dxdy+M W_{mn}(\xi,\eta)\right]$$

Equation (127) then becomes

$$\ddot{q}_{mn}(t)+\omega_{mn}^2 q_{mn}(t) = \frac{c_{mn}}{Q_{mn}}\ddot{d}(t) \qquad (129)$$

The general solution of Equation (129) is similar to Equation (116).

$$q_{mn}(t) = A_{mn}\sin\omega_{mn}t+B_{mn}\cos\omega_{mn}t + \frac{c_{mn}}{\omega_{mn}Q_{mn}}\int_0^t \ddot{d}(t')\sin\omega_{mn}(t-t')dt' \qquad (130)$$

For sinusoidal acceleration excitation applied at the edges,

$$\ddot{d}(t) = a_o\sin\omega t$$

where

a_o = constant, amplitude of acceleration.

Then,

$$d(t) = \int\int \ddot{d}(t)\, dt\, dt$$

$$= \int\int a_o \sin\omega t\, dt\, dt \qquad (131)$$

$$= -\frac{a_o}{\omega^2} \sin\omega t$$

The displacement response is

$$w(x, y, t) = \sum_{m=1}^{\infty} \sum_{n=1}^{\infty} (A_{mn} \sin\omega_{mn} t + B_{mn} \cos\omega_{mn} t) W_{mn}(x, y)$$

$$+ \sum_{m=1}^{\infty} \sum_{n=1}^{\infty} \frac{c_{mn} a_o}{\omega_{mn} Q_{mn}} W_{mn}(x, y)$$

$$\cdot \left[\frac{\omega}{\omega^2 - \omega_{mn}^2} \sin\omega_{mn} t - \frac{\omega_{mn}}{\omega^2 - \omega_{mn}^2} \sin\omega t \right] \qquad (132)$$

$$- \frac{a_o}{\omega^2} \sin\omega t$$

MASS-COUPLING EFFECTS

Mass-coupling is an extension of the mass-loading problem in the sense that it deals with a system having an additional spring of finite stiffness between the two masses. This corresponds to a situation in which a component is attached to a local structure by relatively flexible brackets. Obviously, if the stiffness of the brackets relative to that of the local structure could be gradually increased, the problem would eventually change from one of mass-coupling to one of mass-loading.

The analysis of mass-coupling phenomenon may be performed for a continuous system representing mass-loaded beams and plates; however, it requires a tedious mathematical treatment and laborious manipulation to obtain numerical solutions. Furthermore, the coupling phenomenon is difficult to be intuitively visualized. For practical purposes, the mass-coupling system of a lightly damped metal structure can be quite accurately represented by a conventional two-degree-of-freedom model. The component (or equipment) is represented by the mass with its flexibility represented by the bracket. If the dynamic properties of the component become much less important than those of the mounting, the component itself is represented by the mass with high rigidity and the mounting device is represented by the bracketry having a finite stiffness and a damping factor. The unloaded local structure may be approximated, in such a case, by a simple spring-mass-damper combination. Since local structures are of solid-metal material with slightly damped properties, the simplified analytical model is justified without introducing significant errors. In the mass loading situation, however, the behavior of the supporting structure is very important; and it becomes necessary to use a multi-degree-of-freedom simulation and include the effects of all the parameters involved in the equation of motion which describes the dynamic behavior of the mass-loaded structural system. In particular, the effects of damping increase in importance and a good knowledge of its nature and its variation with mass-ratio is essential.

A thorough investigation of the mass-coupling phenomenon and of the conditions under which the problem changes to mass-loading must be performed to find the limitations of the mass-loading approach and its applications. The interaction among the mass-loading, mass-coupling, and damping are studied under both the sinusoidal and random excitations.

The mass-coupling problem under sinusoidal excitation in a form of vibration absorbers and mass-dampers has been well known in dynamics for a long time. Some of the earlier work for simple dynamic systems was presented by Timoshenko (Reference 18) in 1928 and Den Hartog (Reference 19) in 1956.

Random vibration problems of two-mass systems has been investigated by Curtis and Boykin (Reference 20) in 1961, Crandall and Mark (Reference 21) in 1963, and Morrow (Reference 22) in 1955. Curtis and Boykin solved the response to white noise problem in a form of integral functions in terms of mean square displacements numerically presented in a range of mean square displacements numerically presented in a range of dimensionless parameters. Crandall and Mark employed the same approach with more detail analytical derivations and presented the results inmean square accelerations as well as mean square displacements. Morrow treated the problem based on an assumption that the upper mass does not load the lower mass. Three of these studies were theoretical work and were investigations limited, as most of the earlier dynamic absorber studies, to the two-mass systems with upper mass smaller than the lower mass; hence, the practical application of these results to localized vibration problems for aerospace vehicles is limited.

At NAA, the mass-coupling problem was analytically as well as experimentally investigated for sinusoidal and random vibration cases by the principal investigator and his associates (Reference 23) since 1962. Earlier, from 1957 to 1959, some analytical work was performed by the principal investigator as part of a research paper (Reference 24) at the University of Southern California, under the supervision of Professor C.R. Freberg. The investigations now under way are intended to extend these works in terms of mass-loading effects and to investigate the interaction among the mass-loading, mass-coupling, and the damping phenomenon for different objectives and applications in solving the vibration problems for localized aerospace vehicle structures. Since there is a wide range of component masses that may be mounted to the local structures of aerospace vehicles, the investigation includes the cases for the upper mass smaller and larger than the lower mass.

Sinusoidal Excitation

The equations of motion for a multidegree-of-freedom system may be written, in matrix notation, as

$$[m]\{\ddot{x}\} + [c]\{\dot{x}\} + [k]\{x\} = \{F(t)\}$$

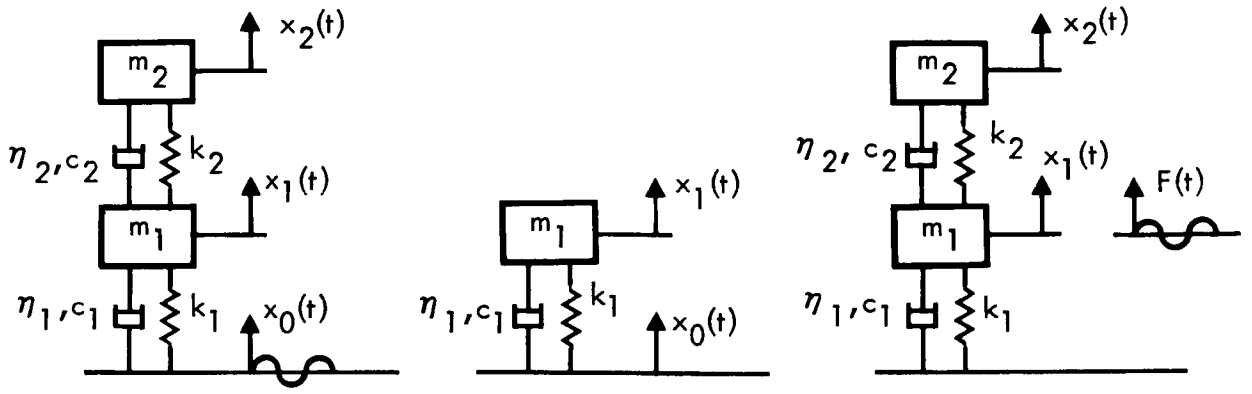

Figure 28. Mass-Coupling System

For the two-mass coupling system shown in Figure 28, the equations for free vibration are:

$$m_1\ddot{x}_1 + c_1(\dot{x}_1 - \dot{x}_o) + c_2(\dot{x}_1 - \dot{x}_2) + k_1(x_1 - x_o) + k_2(x_1 - x_2) = 0 \quad (133)$$

$$m_2\ddot{x}_2 + c_2(\dot{x}_2 - \dot{x}_1) + k_2(x_2 - x_1) = 0 \quad (134)$$

The equation of motion for the single-mass system is:

$$m_1\ddot{x}_1 + c_1(\dot{x}_1 - \dot{x}_o) + k_1(x_1 - x_o) = 0$$

The stiffness of the system can be represented by a complex number k^* incorporating the stiffness produced by both the spring and the damper. The complex stiffness, k^*, can be expressed as

$$k^* = k + ik'$$

$$= k\left(1 + i\frac{k'}{k}\right)$$

$$= k(1 + i\alpha)$$

where

k and k' = stiffness values found from experiments

α = damping factor defined as the ratio of the imaginary part to the real part of the complex stiffness. Its relation to structural damping factor (η), as defined by Kelvin,

$$\alpha = \left(\frac{\omega}{k}\right)\eta$$

ω = uncoupled frequencies $= \sqrt{\frac{k}{m}}$

For the two-mass coupling system shown in Figure 28, the equations for base excitations can be written as

$$-m_1\omega^2 X_1 + k_2^*(X_1 - X_2) + k_1^*(X_1 - X_o) = 0$$

$$-m_2\omega^2 X_2 + k_2^*(X_2 - X_1) = 0$$

where X_0, X_1, X_2 = amplitude of x_0, x_1, x_2, respectively.

For the single mass system, it becomes

$$-m_1\omega^2 X_1 + k_1^*(X_1 - X_o) = 0$$

Solving for these equations, the transmissibility defined by the displacement ratio is obtained.

$$T = \frac{x_1}{x_o} = \frac{k_1^*\left(k_2^*/m_2 - \omega^2\right)}{\left(k_2^*/m_2 - \omega^2\right)\left(k_1^* - m_1\omega^2\right) - k_2^*\omega^2}$$

or

$$T^2 = \left|\frac{x_1}{x_o}\right|^2 =$$

$$\frac{\left[\left(\frac{\omega_2}{\omega}\right)^2 - \left(\frac{\omega_1}{\omega}\right)^2\left(\frac{k_2}{k_1}\right)\right]^2 + \left[\left(\frac{\omega_2}{\omega}\right)^2 \alpha\right]^2}{\left[\frac{m_1}{m_1 + m_2}\left(\frac{\omega_1}{\omega}\right)^4\left(\frac{k_2}{k_1}\right) - \left(\frac{\omega_1}{\omega}\right)^2\left[\left(\frac{\omega_2}{\omega}\right) + \frac{k_2}{k_1}\right] + \left(\frac{\omega_2}{\omega}\right)^2\right] + \left[\left(\frac{\omega_2}{\omega_1}\right)^2 \alpha\right]^2\left[1 - \left(\frac{\omega_1}{\omega}\right)^2\right]^2}$$

Similarly, for the force excitation case, solutions can be found from the following equations of motion:

$$-m_1\omega^2 X_1 + k_2^*(X_1 - X_2) + k_1^* X_1 = F(t)$$

$$-m_2\omega^2 X_2 + k_2^*(X_2 - X_1) = 0$$

Numerical solutions in terms of various parameters can be easily obtained through the use of computers.

Cases of base excitation may represent problems of mechanical vibration applied at supports while force excitation cases may be considered as acoustic forces or electromagnetic induction forces applied to the support structure.

Random Excitation

Random vibration analyses of simple structures have been presented by several authors with an identical approach (References 20 through 29). The effort of this program and related earlier studies has been directed toward similar basic approach to investigate the mass-coupling phenomenon interacted with mass-loading effects on localized random vibration environment for aerospace vehicles. To maintain a concise presentation of the subject investigation for a physical system and to avoid mathematical complications, only random vibration excitation having white noise characteristics is to be considered.

As shown for the sinusoidal case, the equations of motion remain as

$$m_1\ddot{x}_1 + c_1(\dot{x}_1 - \dot{x}_2) + c_2(\dot{x}_1 - \dot{x}_2) + k_1(x_1 - x_2) + k_2(x_1 - x_2) = 0$$

$$m_2\ddot{x}_2 + c_2(\dot{x}_2 - \dot{x}_1) + k_2(x_2 - x_1) = 0$$

$$m_1\ddot{x}_1 + c_1(\dot{x}_1 - \dot{x}_o) + k_1(x_1 - x_o) = 0$$

The transmissibility functions can be expressed in terms of acceleration for the upper mass (T_1) as well as for the lower mass (T_2).

$$T_1 = \left[\omega_1^2\omega_2^2 - i\omega^3 2\zeta_1\omega_1 - \omega^2\left(\omega_1^2 + 4\zeta_1\zeta_2\omega_1\omega_2\right) + i\omega_2\left(\zeta_1\omega_1\omega_2^2 + \zeta_2\omega_2\omega_1^2\right)\right](B)^{-1}$$

$$T_2 = \left[\omega_1^2\omega_2^2 - \omega^2 4\zeta_1\zeta_2\omega_1\omega_2 + i\omega_2\left(\zeta_1\omega_1\omega^2{}_2 + \zeta_2\omega_2\omega_1^2\right)\right](B)^{-1}$$

where

$$B = \omega^4 - i\omega_2^3\left[\zeta_1\omega_1 + \zeta_2\omega_2\left(\frac{m_1 + m_2}{m_1}\right)\right] - \omega^2\left[\omega_1^2 + \omega_2^2\left(\frac{m_1 + m_2}{m_1}\right) + 4\zeta_1\zeta_2\omega_1\omega_2\right] + i\omega_2\left[\zeta_1\omega_1\omega_2^2 + \zeta_2\omega_2\omega_1^2\right] + \omega_1^2\omega_2^2$$

$$T_o = \frac{-1}{\omega_1^2 - \omega^2 + 2i\zeta_1\omega_1\omega}$$

For linear systems, the acceleration spectral density of the random vibration response is obtained from the product of the input acceleration spectral density and the square of the transmissibility curve, which is essentially the same for sinusoidal case. Hence, the response acceleration spectral density to white noise random vibratory excitation is directly proportional to the square of the transmissibility curve. The mean square response is equal to the area under the response spectral density plot.

The mean square acceleration response for the upper mass ($|A_2|^2$) and for the lower mass ($|A_1|^2$) is

$$|A_1|^2 = \int_{-\infty}^{\infty} A_i |T_1|^2 d\omega$$

$$= 2\pi\omega_1\omega_2 A_i D^{-1} \Bigg\langle \zeta_1\omega_1\omega_2{}^3\left(\frac{m_2}{m_1}\right) + \zeta_2\left[\left(\omega_1{}^2 - \frac{m_1+m_2}{m_1}\omega_2{}^2\right)^2 + \left(\frac{m_2}{m_1}\right)\omega_1{}^2\omega_2{}^2\right] + 4\Bigg\{\zeta_1{}^3\left(\frac{m_2}{m_1}\right)\omega_1\omega_2{}^3 + \zeta_1{}^2\zeta_2\left[\left(\omega_1{}^2 - \omega_2{}^2\right)^2 + \omega_1{}^2\omega_2{}^2 + \left(\frac{m_2}{m_1}\right)\omega_2{}^4\right] + \zeta_1\zeta_2{}^2\left[\omega_1{}^3\omega_2 + \left(\frac{m_1+m_2}{m_1}\right)\omega_1\omega_2{}^3\right] + \zeta_2{}^3\left(\frac{m_1+m_2}{m_1}\right)\omega_1{}^2\omega_2{}^2\Bigg\} + 16\omega_1\omega_2\zeta_1{}^2\zeta_2\left[\left(\zeta_1{}^2+\zeta_2{}^2\right)\omega_1\omega_2 + \left(\omega_1{}^2+\omega_2{}^2\right)\zeta_1\zeta_2\right]\Bigg\rangle$$

where

A_i = input acceleration spectral densities (g^2/cps)

$$D = 4\omega_1\omega_2\Bigg\{\left(\frac{m_2}{m_1}\right)\omega_1\omega_2(\zeta_1\omega_2+\zeta_2\omega_1)^2 + \zeta_1\zeta_2\left[\omega_1{}^2 - \frac{m_1+m_2}{m_1}\omega_2{}^2\right]^2 + 4\zeta_1\zeta_2\omega_1\omega_2\Bigg[\omega_1\omega_2\left(\zeta_1{}^2 + \frac{m_1+m_2}{m_1}\zeta_2{}^2\right) + \zeta_1\zeta_2\left(\omega_1{}^2 + \frac{m_1+m_2}{m_1}\omega_2{}^2\right)\Bigg]\Bigg\}$$

$$\left|A_2\right|^2 = \int_{-\infty}^{\infty} A_i \left|T_2\right|^2 d\omega$$

$$= 2\pi\omega_1^2\omega_2^2 A_i D^{-1} \Bigg\langle \zeta_1\omega_1\left(\omega_1^2 + \frac{m_2}{m_1}\omega_2^2\right)$$

$$+ \zeta_2\omega_2\left[\left(\frac{m_2}{m_1}\right)\omega_1^2 + \left(\frac{m_1+m_2}{m_1}\right)^2\omega_2^2\right]$$

$$+ 4\Bigg\{\zeta_1^3\omega_1\omega_2^2 + \zeta_1^2\zeta_2\left[\omega_1^2\omega_2 + \left(\frac{m_1+m_2}{m_1}\right)\omega_2^3\right]$$

$$+ \zeta_1\zeta_2^2\left[\omega_1^3 + \left(\frac{m_1+m_2}{m_1}\right)\omega_1\omega_2^2\right] + \zeta_2^3\left(\frac{m_1+m_2}{m_1}\right)\omega_1^2\omega_2\Bigg\}$$

$$+ 16\zeta_1^2\zeta_2^2\omega_1\omega_2(\zeta_1\omega_2 + \zeta_2\omega_1)\Bigg\rangle$$

$$\left|A_o\right|^2 = \int_{-\infty}^{\infty} A_i \left|T_o\right|^2 d\omega = \pi A_i\left(2\zeta_1\omega_1^3\right)^{-1}$$

Interaction of Mass-Loading, Coupling, and Damping

A study of the parameters involved in the dynamic equations in the previous paragraph can provide an intuitive insight of the relations among mass-loading, frequency coupling, and damping effects in relation to a single-mass system. From these relations, the interactions, limitations, and applications can be readily inspected.

Figure 29 shows the behavior of the upper mass (m_2) by curves 1 to 8, and the lower mass (m_1) by curves A to H. From this figure, it is apparent that frequency coupling effects are free from mass-loading after the frequency

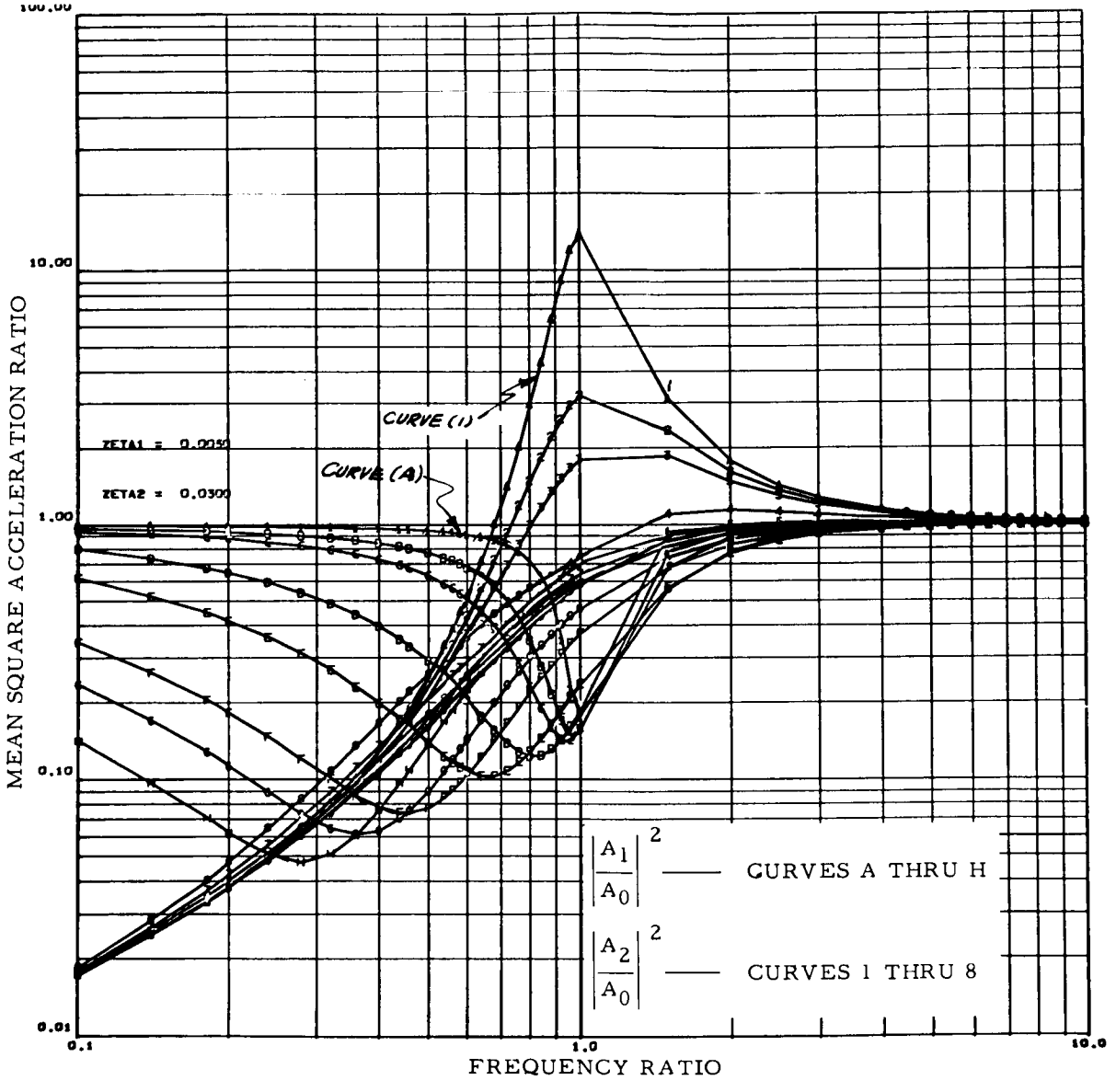

Figure 29. Interaction of Mass Loading, Coupling, and Damping — I

ratio reaches approximately five ($\omega_2/\omega_1 \doteq 5$). Thus, the mass-loading phenomenon applies only in the mass-loading region, which may be defined by ($\omega_2/\omega_1 > 5$), without introducing a significant error. When the frequency ratios become less than five ($\omega_2/\omega_1 < 5$), coupling effects in terms of frequency ratios are gradually enlarged; however, mass-loading effects are still playing an important role in the mass coupling region ($\omega_2/\omega_1 \doteq 0$ to 5). The chart has been prepared by assuming damping ratios ($\zeta_2 = 0.005$ and $\zeta_1 = 0.03$) which are the generally expected range of damping for standard metal structures. Sixteen cases of different mass ratios are considered, from very small upper mass ($m_2 = 0.01 m_1$) to very large upper mass ($m_2 = 9m_1$). Forty-two frequency ratios ranging from 1 to 10 are investigated and presented.

An identical study is made and plotted in Figure 30 for the case of a constant damping ratio ($\zeta_1 = \zeta_2 = 0.03$). It is found from Figure 31 that common values of damping for metal structures have little effect on the response in either mass-loading or mass-coupling regions; they introduce further attenuation of the motion of the upper mass only when the system has a very small mass ratio ($m_2/m_1 << 0.1$). The presence of these damping factors or the increase of damping, however, does not help reduce any vibration amplitude of the lower mass; the response, on the contrary, is amplified with the increase of damping for a small mass ratio ($m_2/m_1 < 1$) and becomes independent of damping for larger mass ratios ($m_2/m_1 \gtrsim 1$).

Figure 32 shows that the maximum attenuation can be accomplished by a mass-coupling design; the presented minimum response values are each associated with a specific frequency ratio, a specific mass ratio, and the constant damping ratios. The maximum mass-attenuation can be obtained by a mass-loading design within the mass-coupling region as shown in Figure 33; again, each of the minimum response values of the presented curves is subjected to the specific requirements. This figure also illustrates the significance of the mass-loading effects even within the region of mass-coupling.

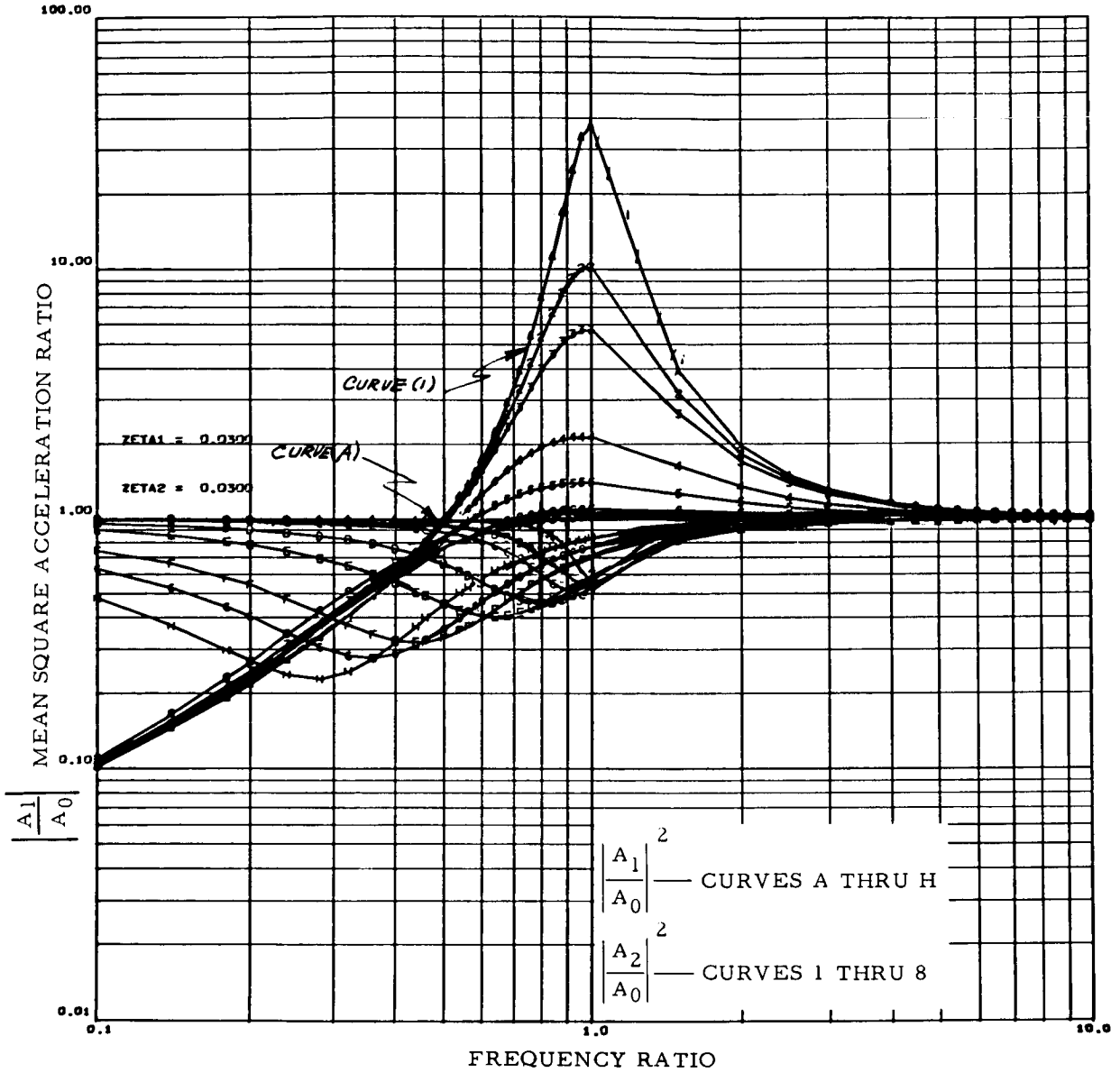

Figure 30. Interaction of Mass Loading, Coupling, and Damping — II

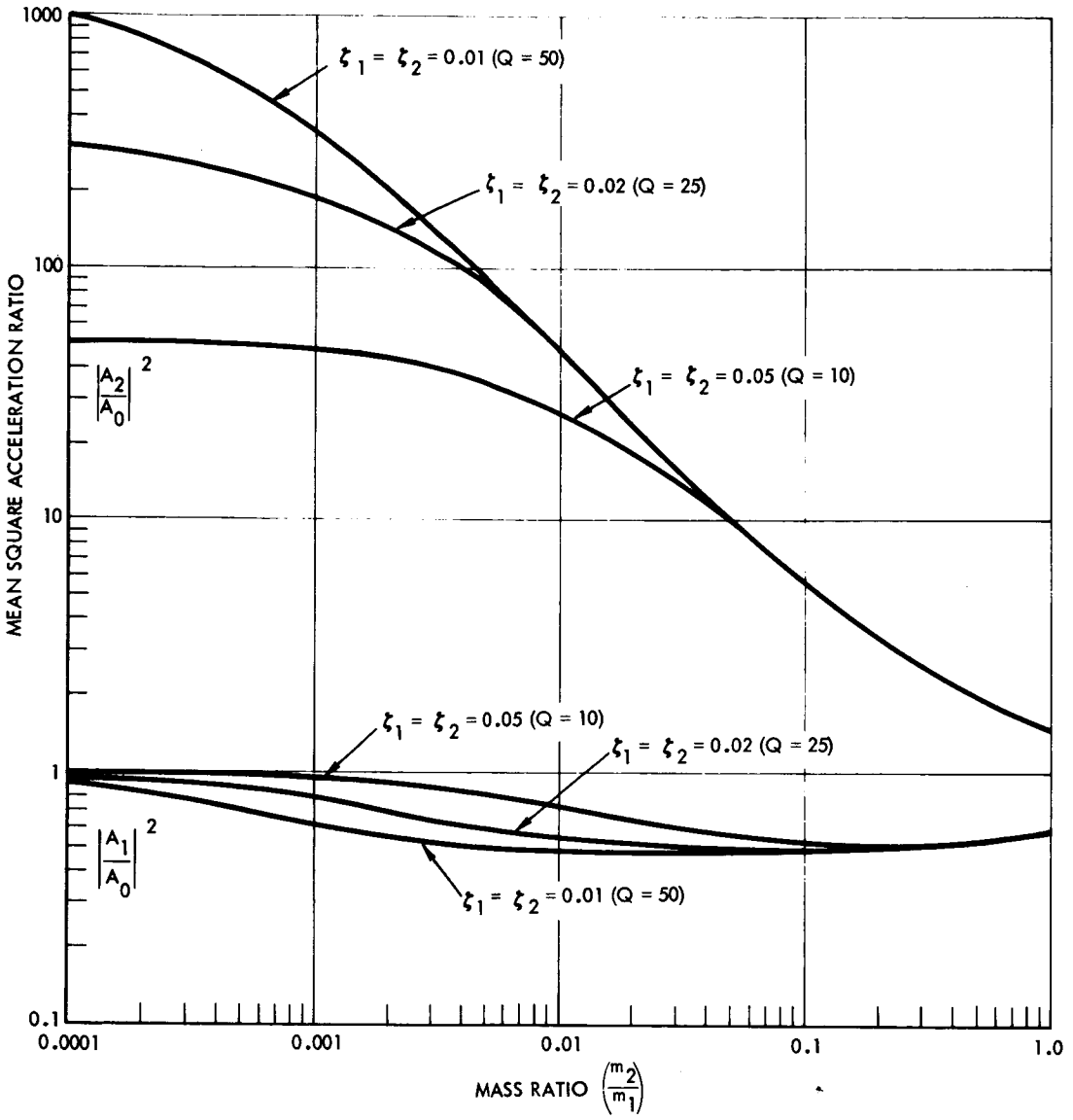

Figure 31. Maximum Damping Effect in Mass Coupling Region

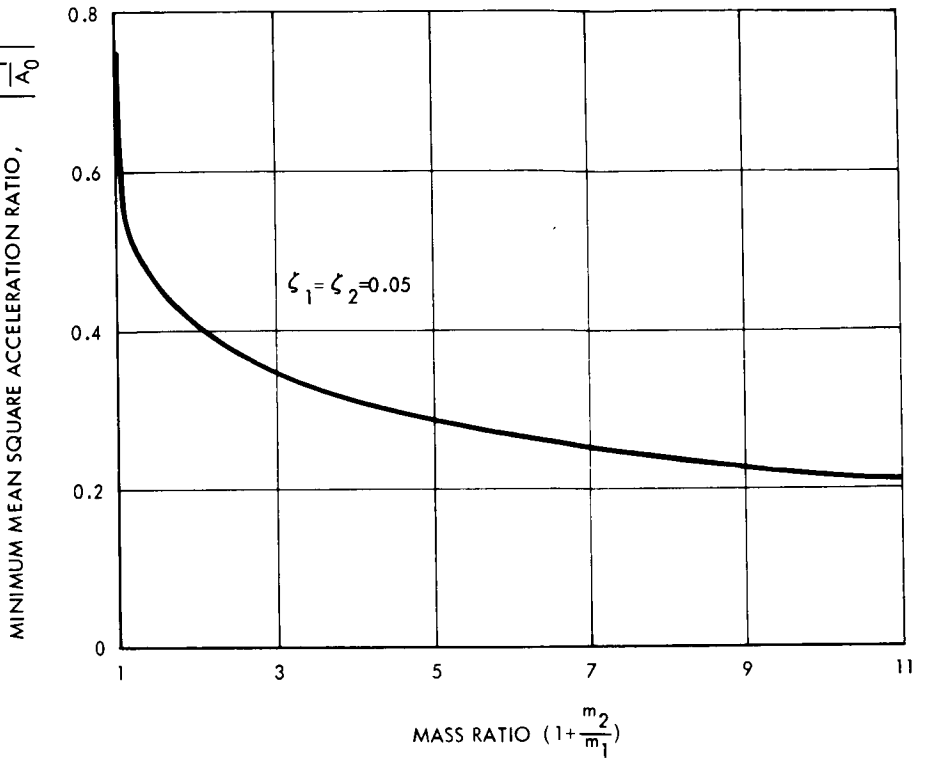

Figure 32. Maximum Attentuation by Mass Coupling

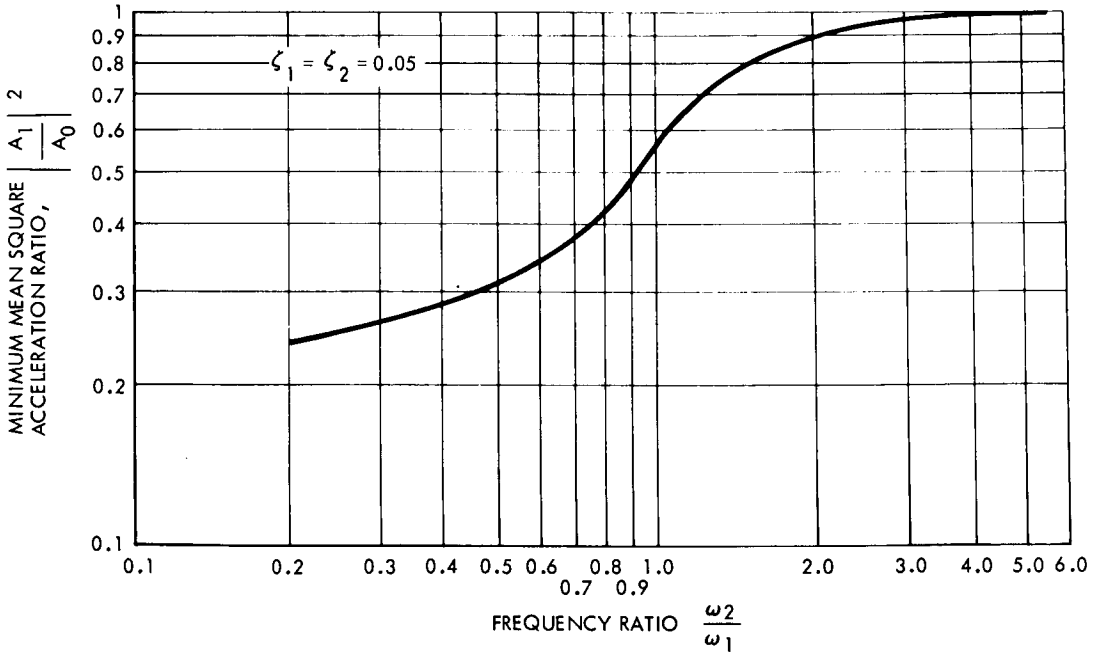

Figure 33. Maximum Mass-Loading Attenuation in Mass-Coupling Region

EXPERIMENTAL INVESTIGATION

The objectives of the experimental study portion of the program are as follows:

1. Mass-Loading Effects

   To obtain data for concentrated rigid mass-loading effects on the natural frequencies, mode shapes, acceleration responses, and damping of the supporting structures, which typify the localized structures of a rocket vehicle mounted with equipment masses.

2. Mass-Coupling Effects

   To obtain data for mass-bracketry-coupling effects on natural frequencies, vibration response of the primary structure, the secondary structure, and the integrated system.

3. Effects of Various Excitations

   To obtain data for vibration transmissibility of the mass-loaded and mass-coupled structures due to various types of excitation including

   a. Sinusoidal input from a mechanical shaker, electro-magnetic-induction shaker, or acoustic chamber,

   b. Random input from a mechanical shaker or acoustic chamber.

SPECIMEN DESIGN AND FABRICATION

To accomplish the objectives, two types of basic structural models typifying the localized structures of a rocket vehicle were designed and fabricated as described in the following paragraphs.

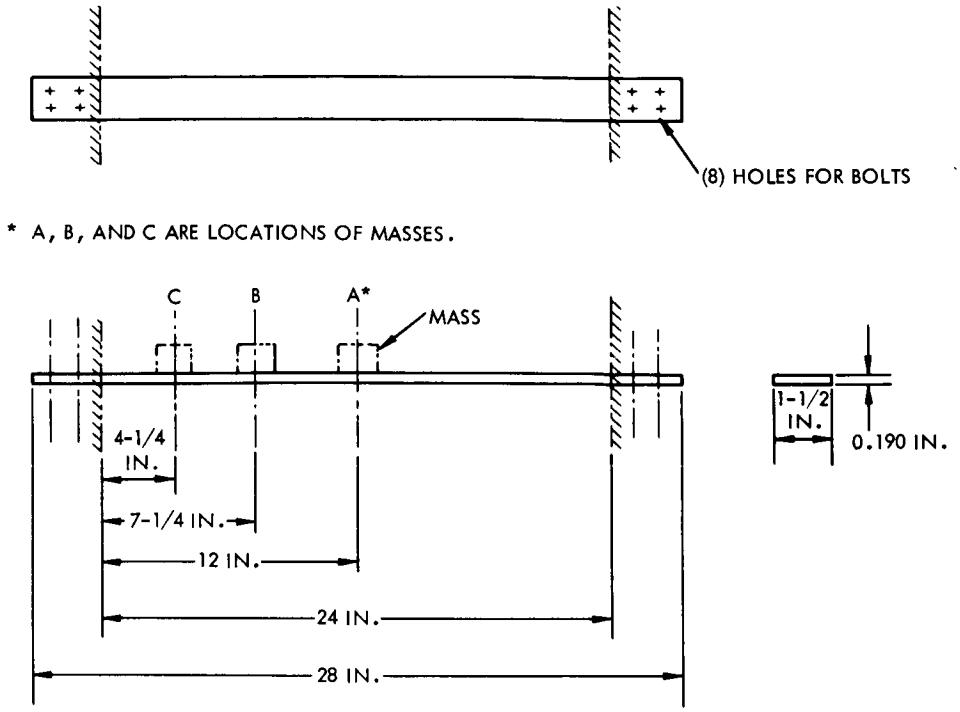

Figure 34. Mass-Loaded Beam Model

Mass-Loaded Beam Models

The mass-loaded beam models consist of a uniform beam and eight rigid masses. The beam is made of aluminum alloy 6063-T6 and is 28 inches long. The unsupported length of the beam is only 24 inches (Figure 34). The masses are made of aluminum, brass, or lead and are of different sizes to give various weight ratios (Table 8). The reason for using a different material for the masses is to minimize the size of the weights and, thus, reduce the rocking-motion effect during vibration testing.

During the testing, the eight masses were mounted on the beam, one at a time, at one of the three locations (4-1/4 inches, 7-1/4 inches, and 12 inches from one end) to constitute twenty-four mass-loaded beam models.

Mass-Coupling Beam Models

The mass-coupling beam model typifies a structural system with a heavy mass mounted on a bracket, which, in turn, is attached to the primary

Table 8. Details of Mass-Loaded Beam Models

Item		Material	Size	Weight (Pounds)	W_a/W_b
Beam, W_b		Alum. 6063 T-6	0.190 x 1-1/2 x 28	0.66	0
Masses, W_a	W_1	Aluminum		0.165	0.25
	W_2	Brass		0.231	0.35
	W_3	Brass		0.33	0.50
	W_4	Brass		0.495	0.75
	W_5	Brass		0.66	1.0
	W_6	Brass		0.982	1.5
	W_7	Lead		1.32	2.0
	W_8	Lead		1.98	3.0

W_a = Weight of rigid masses

W_b = Weight of beam of 24-inch span

structure. The design principle of such a model is to construct the secondary spring-mass systems (bracketry and mass) to produce natural frequencies that are lower than, equal to, or higher than, the natural frequency of the beam.

The bracketry is made of thin aluminum tubing and shaped to a circular ring (Figure 35). Two masses, W_3 and W_4 (Table 8), used in the

mass-loaded beam models were attached, one or two at a time, to the bracket to produce three secondary spring-mass systems:

1. Mass A: $W_A = W_S + W_3 = 0.360$ lb
2. Mass B: $W_B = W_S + W_4 = 0.525$ lb
3. Mass C: $W_C = W_S + W_4 + W_3 = 0.855$ lb

($W_S = 0.03$ lb = weight of upper accelerometer housing)

These three mass-bracketry systems were cemented to the beam at three locations, as in the mass-loaded beam tests, to form nine models for the mass-coupling tests.

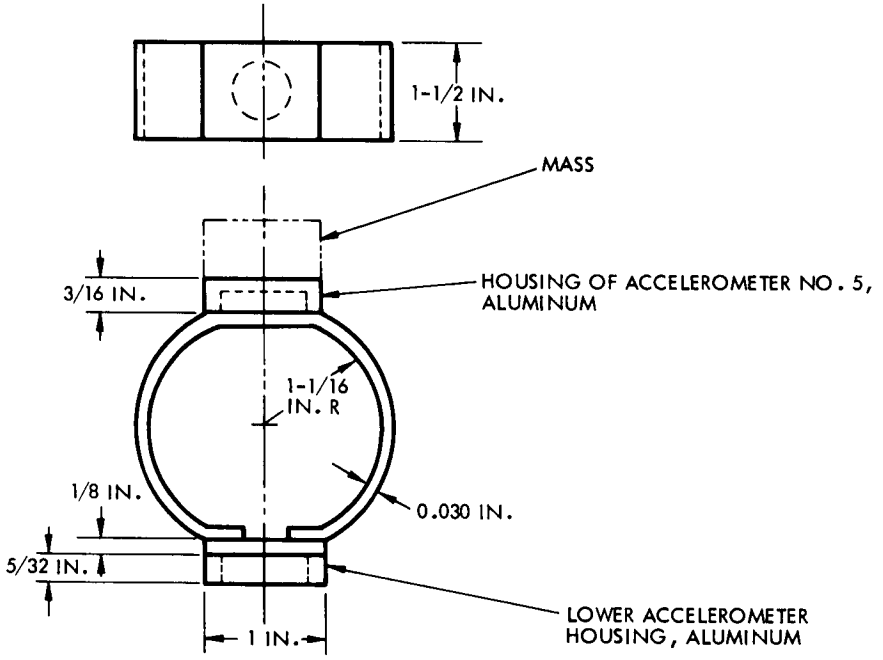

Figure 35. Mass-Bracket System for Mass-Coupled Beam Model

Mass-Loaded Plate Models

The mass-loaded plate models consist of a rectangular aluminum flat plate and seven rigid masses, which are bolted to the middle of the panel, one

at a time, to constitute seven mass-loaded plate models. Details of these models are given in Table 9.

It is noted that the size of the basic flat panel is 0.190 x 16 x 18 inches; however, the unsupported size of the panel is only 14-1/2 x 16-1/2 inches because a 3/4-inch-deep border is clamped along four edges during testing.

Mass-Coupled Plate Models

The mass-coupled plate models are similar to the mass-loaded plates, although the masses are not directly mounted on the plate; instead, they are attached to a pair of Z-shaped steel brackets that are bolted to the plate. Figure 36 shows a typical arrangement of a mass-coupled plate model.

The basic plate has the same dimensions as the mass-loaded plate. The only difference is the location of the holes for mounting the brackets.

All seven masses used in the mass-loading tests are employed to form seven mass-coupled plate models.

Mass-Loaded Beam-Plate Models

The mass-loaded beam-plate models are similar to the mass-coupled plate models; however, the Z-bracket of the latter is extended to 16-1/2 inches as shown in Figure 37. The Z-brackets are spot-welded to the basic plate.

Test Fixtures

Beam Test Fixture

The fixture used for the beam tests is a U-shaped aluminum block. As shown in Figure 38, a rectangular piece of aluminum plate with four bolts is placed at each end of the fixture to serve as a clamp to hold the beam in position. This arrangement results in excellent boundary conditions for the fixed-end beam. A 3/8-inch-thick aluminum plate, also of U-shape, is screwed down on one side of the fixture. This plate stiffens both ends of the fixture and prevents rocking motion of the beam supports. It also serves as the support and guide for the proximity gage, which measures displacement of the mass-loaded beam during tests.

The stiffened fixture has a fundamental natural frequency of 750 cps, which is well above the fourth natural frequency of any test model, and causes no jig resonance during the tests. It is noted that the fourth mode is the highest planned for tests.

Table 9. Details of Mass-Loaded Plate Models

Item	Size (Inches)	Weight (Pounds)	Bolts		Total Weight (Pounds)	$\frac{W_a}{W_p}$
			Size (Inches)	Weight (Pounds)		
Aluminum Plate, W_p (weight mount only)	0.190 x 16 x 18	5.29			5.29	0
Aluminum Plate (bracket mount only)	0.190 x 16 x 18	5.25			5.25	0
Beam-Plate Model	0.190 x 16 x 18	6.50			6.50	0
Aluminum Weight, W_1	0.45 x 5 x 7	1.57	(4) 3/8 x 1	0.23	1.8	0.34
Aluminum Weight, W_2	0.7 x 5 x 7	2.47	(4) 3/8 x 1	0.23	2.7	0.51
Steel Weight, W_3	1/4 x 5 x 7	3.06	(4) 3/8 x 1	0.23	3.29	0.62
Steel Weight, W_4	1/2 x 5 x 7	5.07	(4) 3/8 x 1	0.23	5.30	1.0
Steel Weight, W_5	1 x 5 x 7	10.09	(4) 3/8 x 1-1/2	0.32	10.41	2.0
Steel Weight, W_6	1-1/2 x 5 x 7	15.24	(4) 3/8 x 2	0.38	15.62	3.0
Steel Weight, W_7	2 x 5 x 7	20.58	(4) 3/8 x 2-5/8	0.49	21.02	4.0

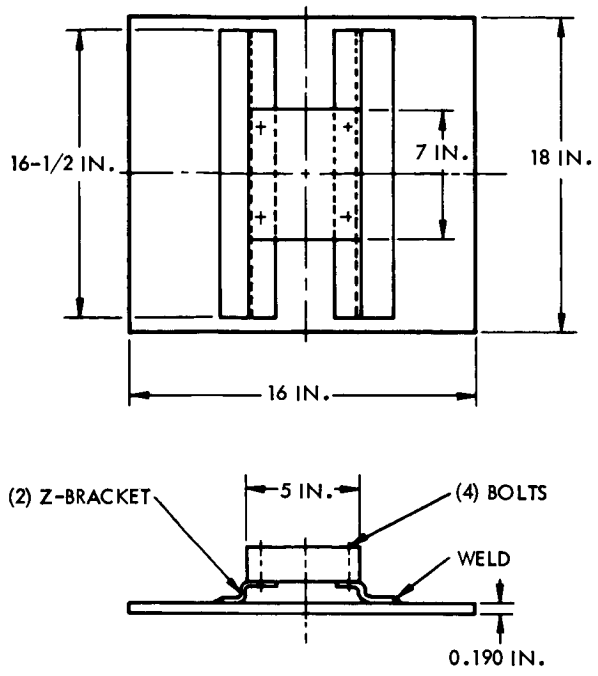

Figure 36. Typical Mass-Coupled Plate Model

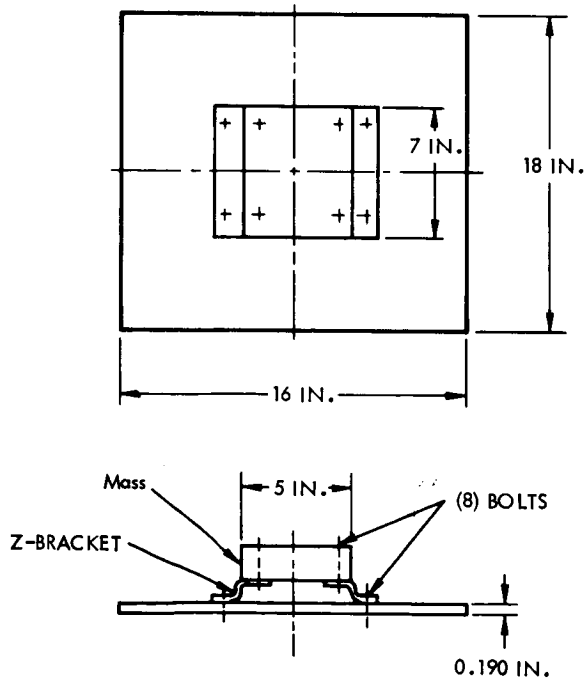

Figure 37. Mass-Loaded Beam-Plate Models

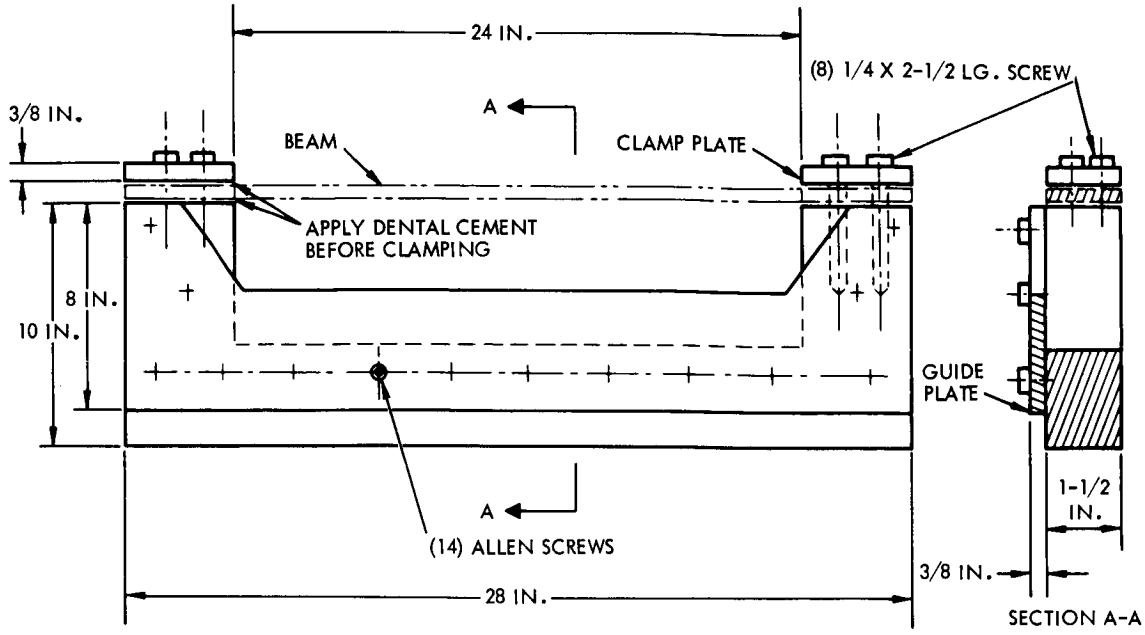

Figure 38. Beam Test Fixture

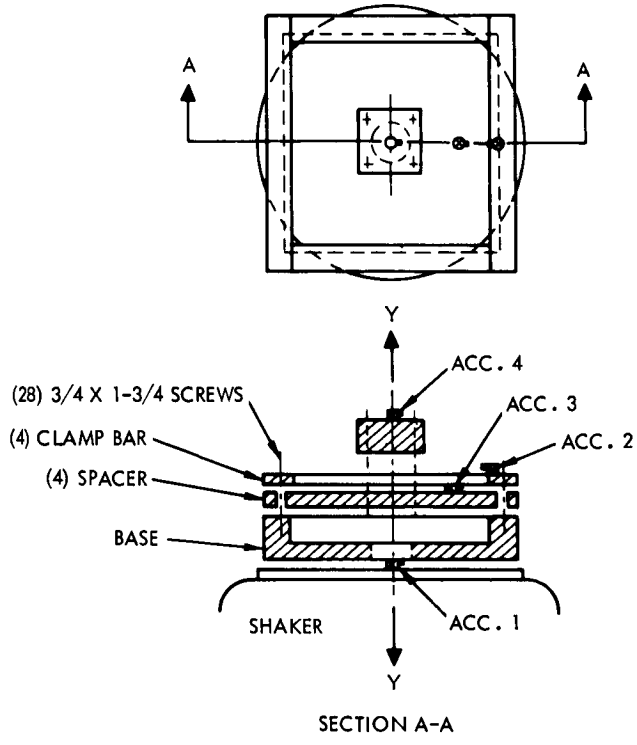

Figure 39. Plate Test Fixture

Plate Test Fixture

The plate test fixture consists of the following aluminum parts: a base, four spacers, and four clamp bars (Figure 39). Test specimens (the mass-loaded or mass-coupled plate model) are placed on top of the base of the fixture and clamped along the four edges by the clamp bars. The fundamental frequency of the fixture is about 1200 cps, which is above the highest frequency planned for the tests. Resonance of the fixture does not influence the responses of the test models.

TEST CONFIGURATION

Shakers and Test Equipment

Mechanical Shaker

Base excitation of the clamped beam and plate models was provided by mechanical shakers of the Type MB C25 H (2500-pound) and associated equipment, such as power supply units, oscillators, amplifiers, oscilloscope, oscillograph recorder, x-y plotter, electronic counter, attenuator, calibrator, filters, etc.

Electromagnetic-Induction Shaker

For the beam sinusoidal tests an electromagnetic-induction shaker was employed. The shaker is constructed by winding heavy-gage copper wire around a U-shaped permanent magnet (Figure 40). It operates on the principle of eddy current induced in the specimen by the electromagnetic field of the shaker. Interference between the magnetic flux of the eddy current and those of the magnetic field of the shaker causes motion of the specimen. This system offers several advantages for vibration tests:

1. No contact between the shaker and specimen is necessary; thus, the test set-up is simplified and jig resonance effect is eliminated.

2. Excitation that is equivalent to a concentrated force input can be applied at any location on the specimen.

3. Excitation can be turned on and off instantaneously to produce excellent damping curves on oscillographs.

4. Magnitude of the exciting force can be controlled easily.

5. The system is more stable; response data on x-y plots or oscillographs are clearer and cleaner than those from mechanical shakers.

The electromagnetic-induction shaker does have some disadvantages:

1. Excitation cannot be applied at the mass of the mass-loaded or mass-coupled specimen.

2. System response varies with the location of the shaker and causes difficulty in data comparison.

Acoustic Chamber

An acoustic reverberant chamber was used for acoustic tests of the mass-loaded plate models. The chamber can produce sound pressure levels up to 150 db. Sinusoidal, as well as random signals, can be used to perform desired tests at various sound pressure levels.

Test Set-Up

Beam Models on Mechanical Shaker (Figure 41)

Mechanical shakers were used for sinusoidal and random vibration tests of the mass-loaded and mass-coupled beam models. Procedures of the test set-up are as follows:

1. Clamp both ends of the beam on the test fixture (Figure 38). Apply dental cement at both ends before clamping to ensure fixed-end conditions.

2. Glue or cement the strain gages and accelerometers at various locations on the beam (Figure 42).

3. Install the proximity gage on the guide plate (Figure 42).

4. Fasten the base of the fixture on top of the shaker. Apply dental cement at the joint before screwing together.

Beam Models with Electromagnetic-Induction Shaker

The test set-up for the beam models using the electroinduction shaker is as follows:

1. Repeat procedures (1), (2) and (3) used for the mechanical shaker.

2. Cement the base of the fixture on a heavy test table, a reinforced concrete block weighing 1-1/2 tons.

3. Clamp the shaker on a stand.

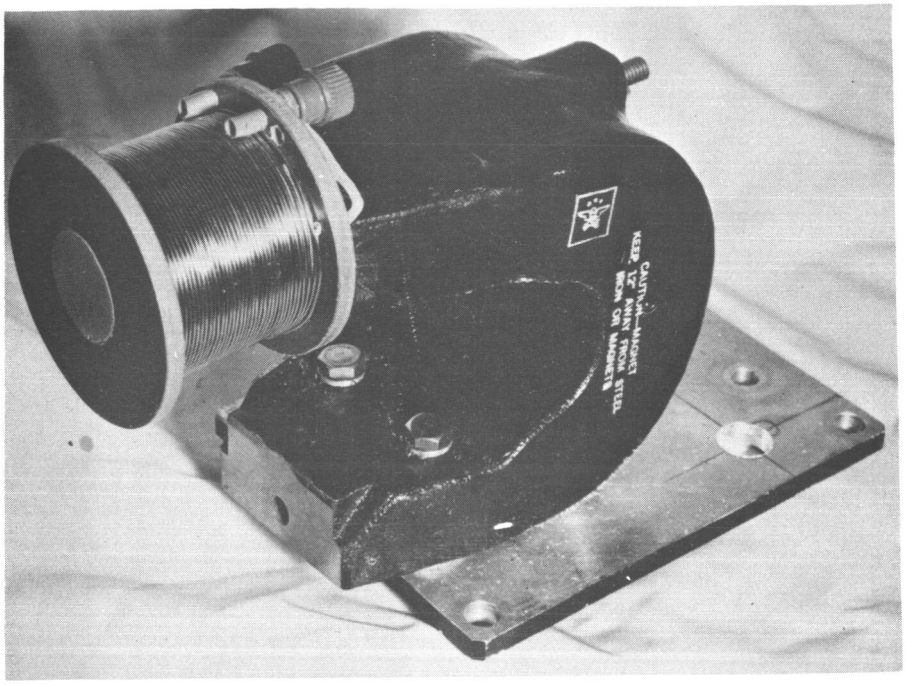

Figure 40. Electromagnetic Induction Shaker

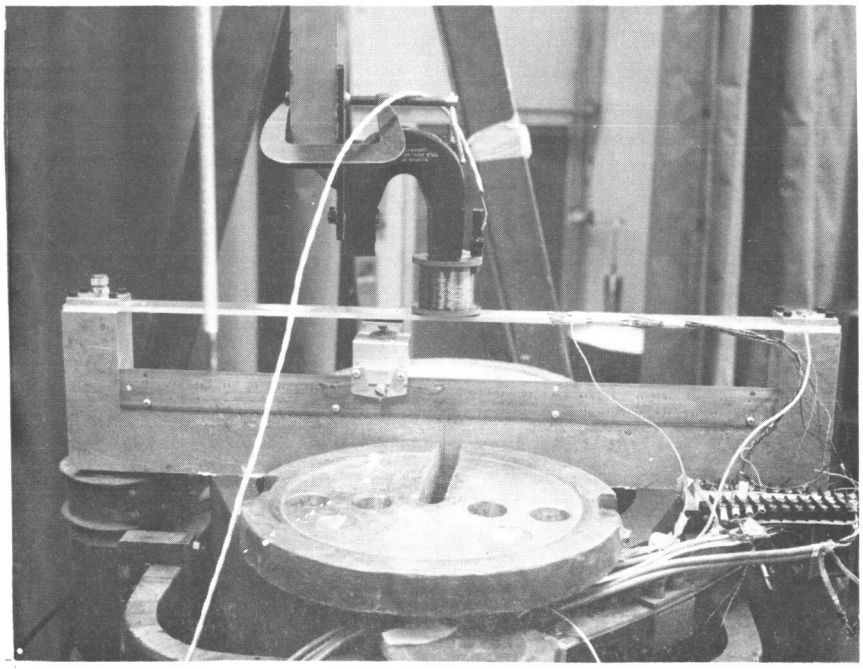

Figure 41. Beam Test Set-Up

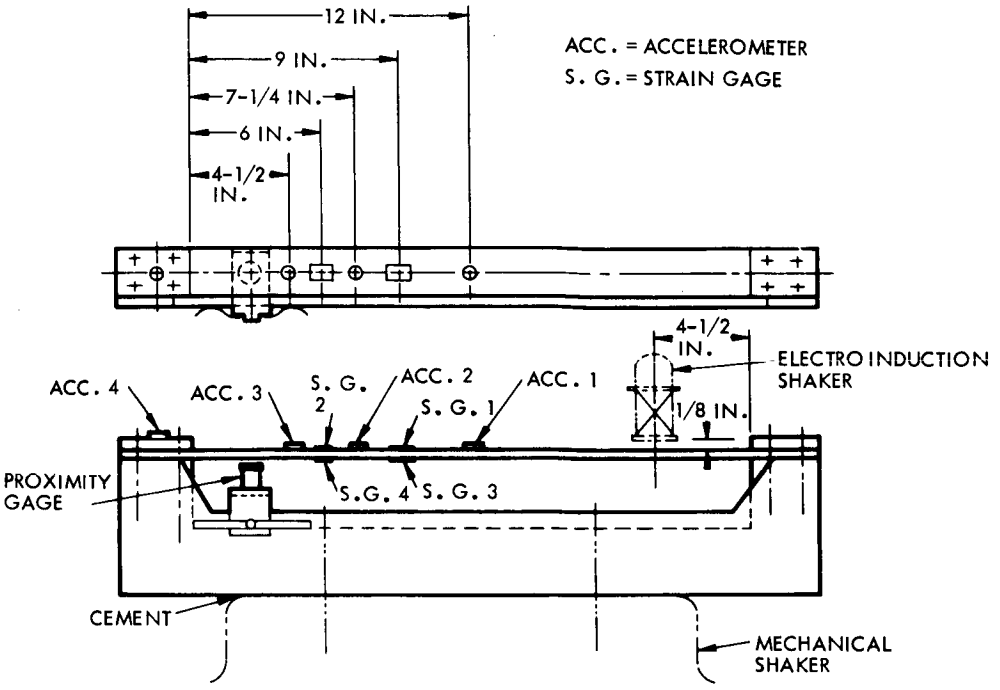

Figure 42. Test Set-Up for Beam Model

4. Place the shaker 1/8 inch above the beam and 4-1/2 inches from the right support (Figure 42).

Plate Models on Mechanical Shaker

Sinusoidal and random vibration tests of the mass-loaded and mass-coupled plate models were performed on a mechanical shaker. The test set-up is as follows:

1. Clamp the four edges of the plate on the fixture (Figure 39). Apply a thin film of oil along the edges to provide a fixed boundary condition.

2. Cement and screw down the base of the fixture on top of the shaker.

3. Install accelerometers and strain gages on the plate models as shown in Figures 43, 44, 45, and 46.

Acoustic Test Set-Up for Mass-Loaded Plates

For acoustical vibration tests with either sinusoidal or random excitation the mass-loaded plate models were clamped to the opening of the acoustic

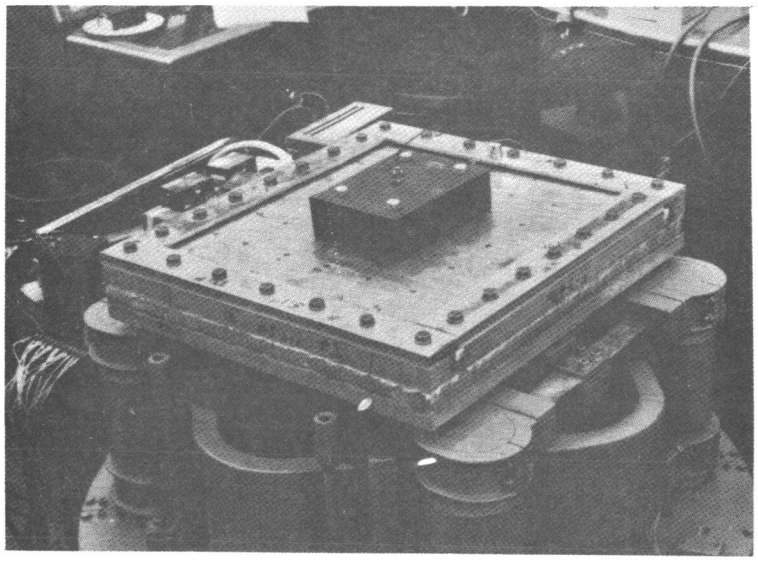

Figure 43. Test Set-Up for Mass-Loaded Plate

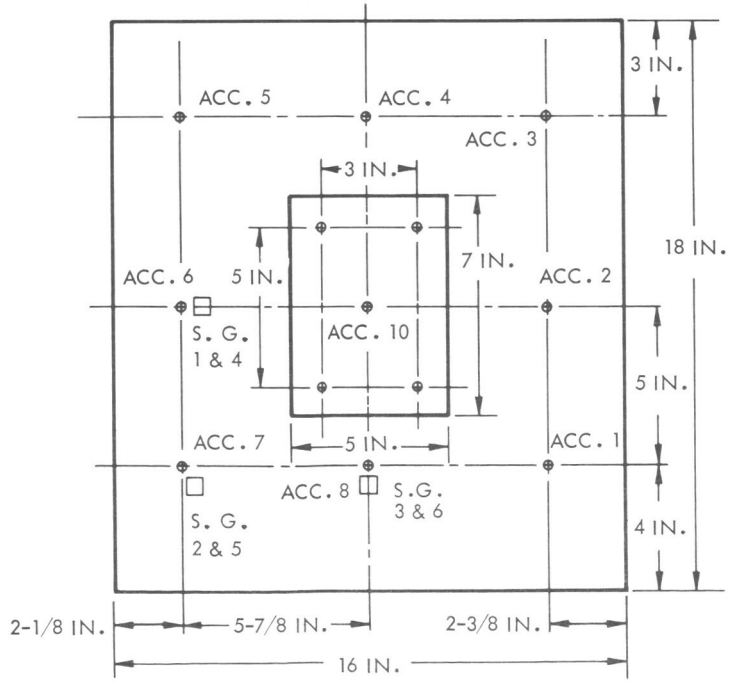

NOTE: CONTROL ACCELEROMETER 9 NOT SHOWN.

Figure 44. Instrumentation on Mass-Loaded Plate

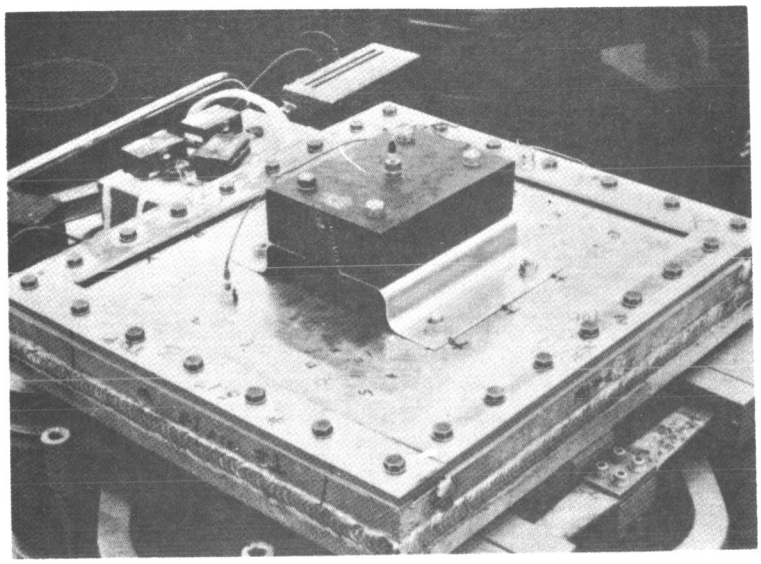

Figure 45. Test Set-Up for Mass-Coupled Plate

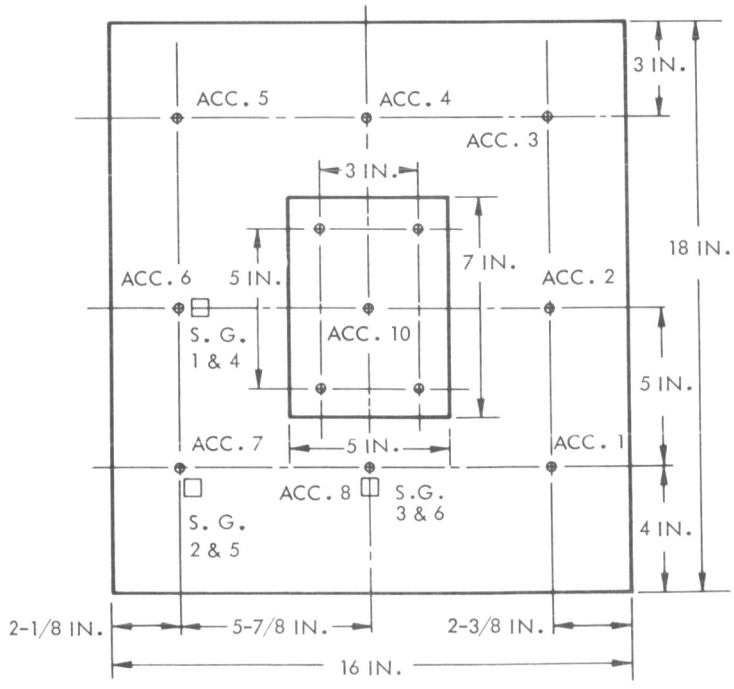

NOTE: CONTROL ACCELEROMETER 9 NOT SHOWN.

Figure 46. Instrumentation on Mass-Coupled Plate

reverberant chamber with accelerometers and microphones placed at various locations as shown in Figures 47 and 48.

Instrumentation

Sinusoidal Vibration Tests on Beam Models

The instrumentation hook-up for the mass-loaded beam tests with sinusoidal excitation from the mechanical shaker is shown in Figures 49 and 50.

The instrumentation hook-up for excitation from the electroinduction shaker is essentially the same as that for the mechanical shaker, except that some equipment related to the mechanical shaker is replaced by that shown in Figure 51.

Random Vibration Tests on Beam Models

Instrumentation for the mass-loaded and mass-coupled beam tests with random excitation is shown in Figures 52 and 53. It is noted that, for these tests, only the mechanical shaker was used. The same equipment was used for plate tests.

Vibration Tests on Plate Models

Vibration tests on the mass-loaded and mass-coupled plate models with sinusoidal and random excitation were performed on the mechanical shaker. This instrumentation hook-up also is shown in Figures 52, 53, and 54.

Acoustic Tests on Mass-Loaded Plates

The instrumentation hook-up for acoustic tests on the mass-loaded plate models is shown in Figure 55.

System Calibrations

Sinusoidal Vibration Tests on Beam Models

Test data measured by accelerometers and strain gages were recorded on oscillographs for the mass-loaded and mass-coupled beam tests with sinusoidal excitation from either a mechanical shaker or electroinduction shaker. The output of one of the accelerometers at the location of the mass also was recorded on X-Y plots and monitored by voltmeters.

The proximity gage, which measures mode shapes at various locations along the beam, was monitored by voltmeters. Since only the relative lateral

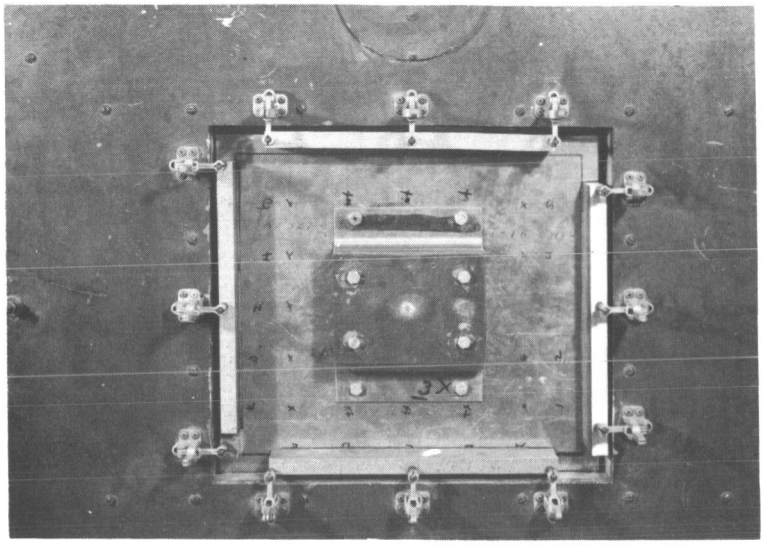

Figure 47. Acoustic Test Set-Up

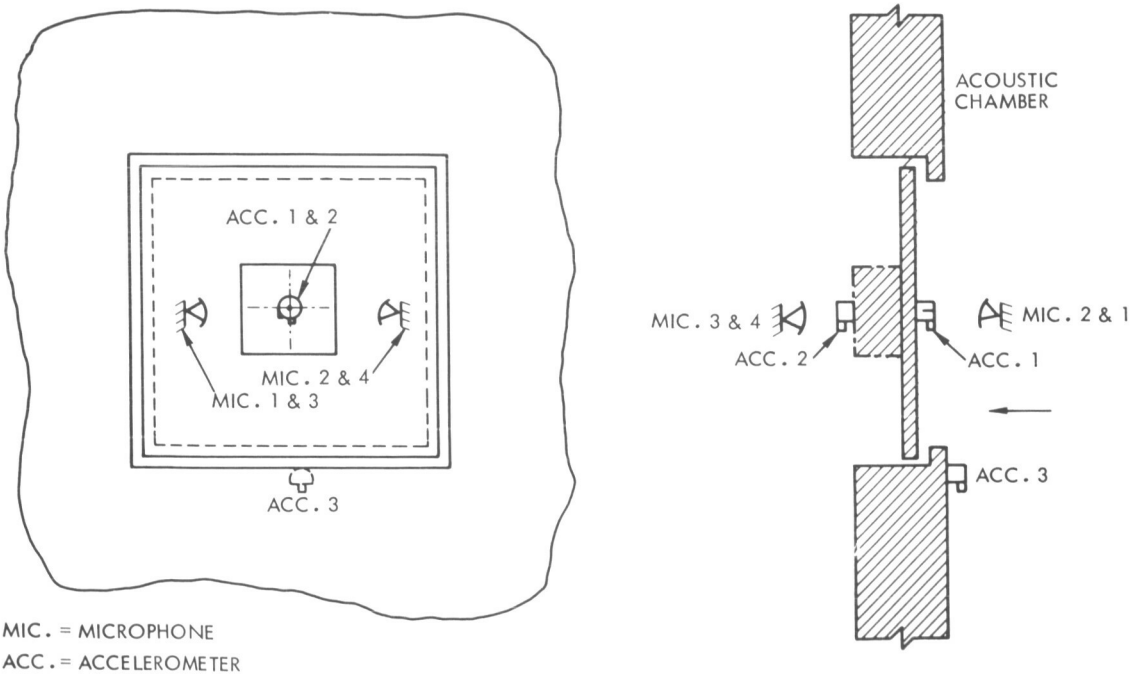

Figure 48. Instrumentation on Acoustic Test Set-Up

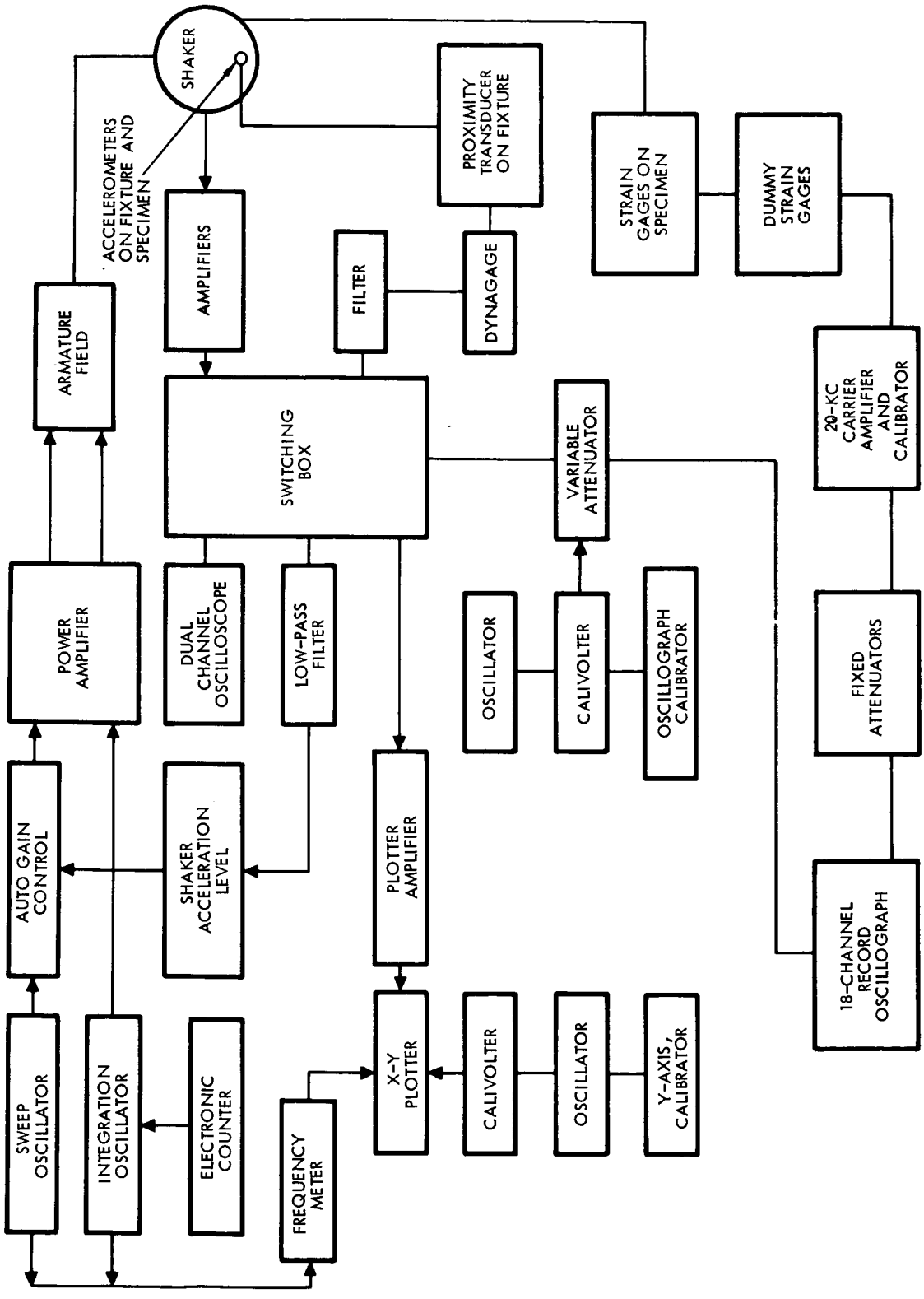

Figure 49. Instrumentation Hook-Up for Beam Tests With Sinusoidal Input From Mechanical Shaker

Figure 50. Instrumentation for Beam Model Test

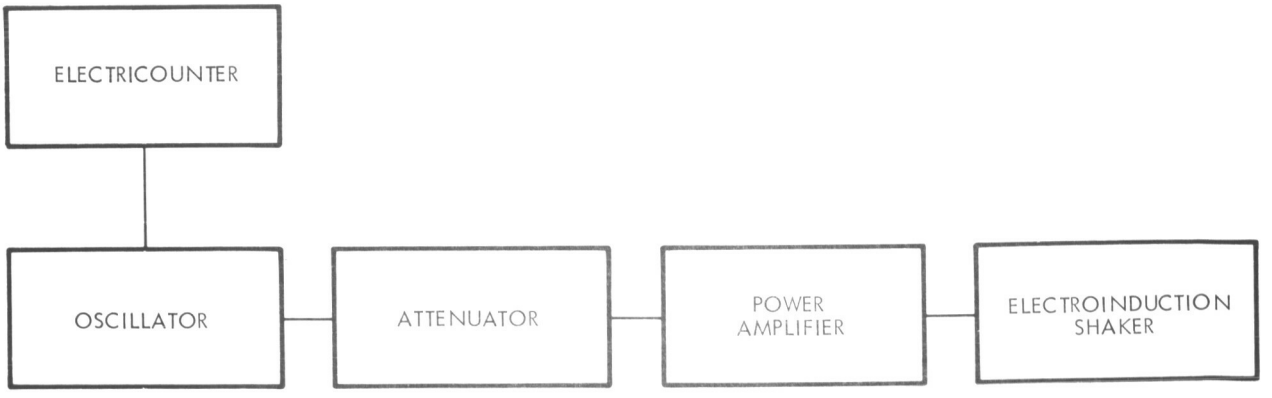

Figure 51. Instrumentation Hook-Up for Electroinduction Shaker

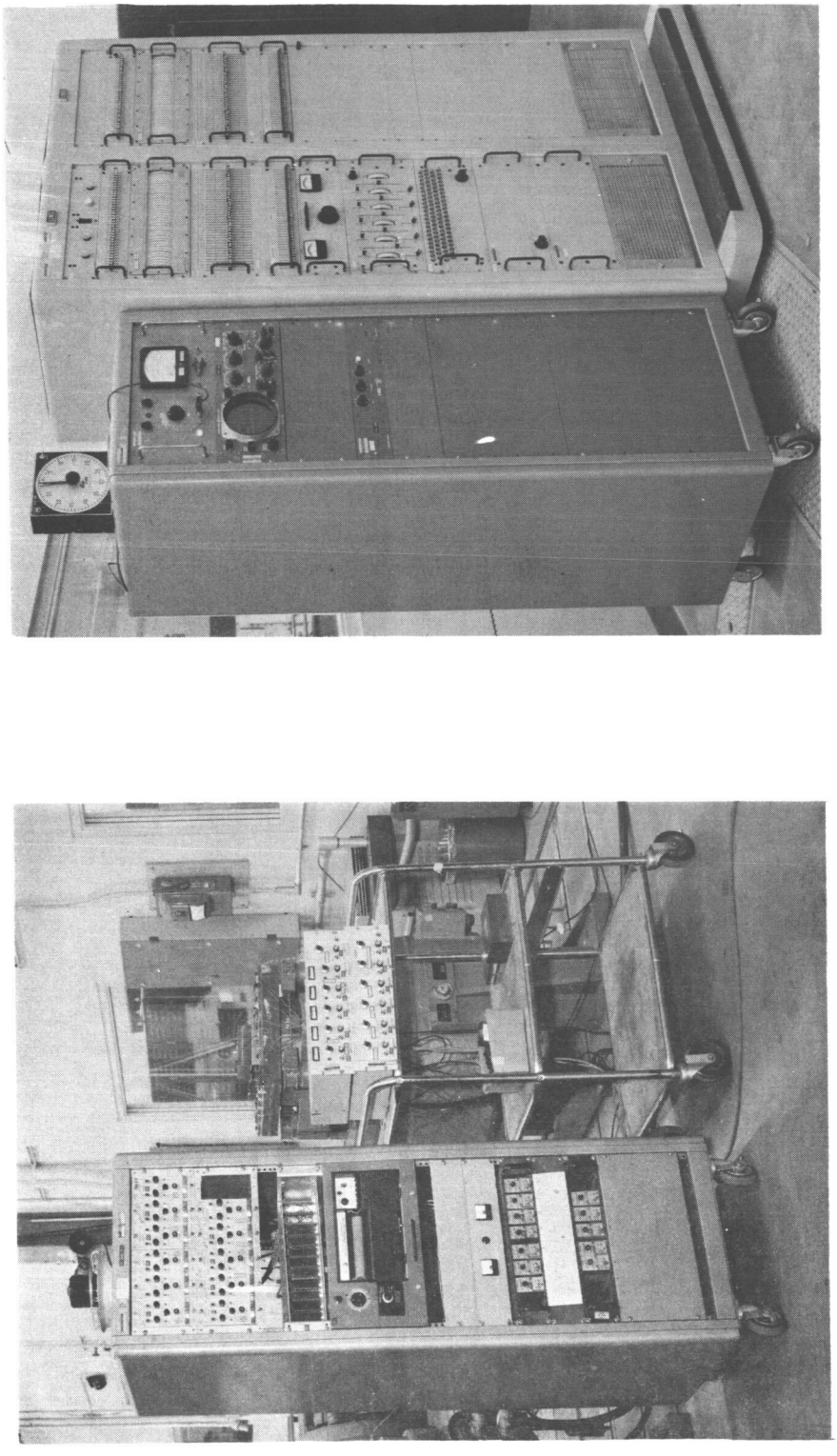

Figure 52. Instrumentation for Plate Tests and for Beam Tests With Random Input

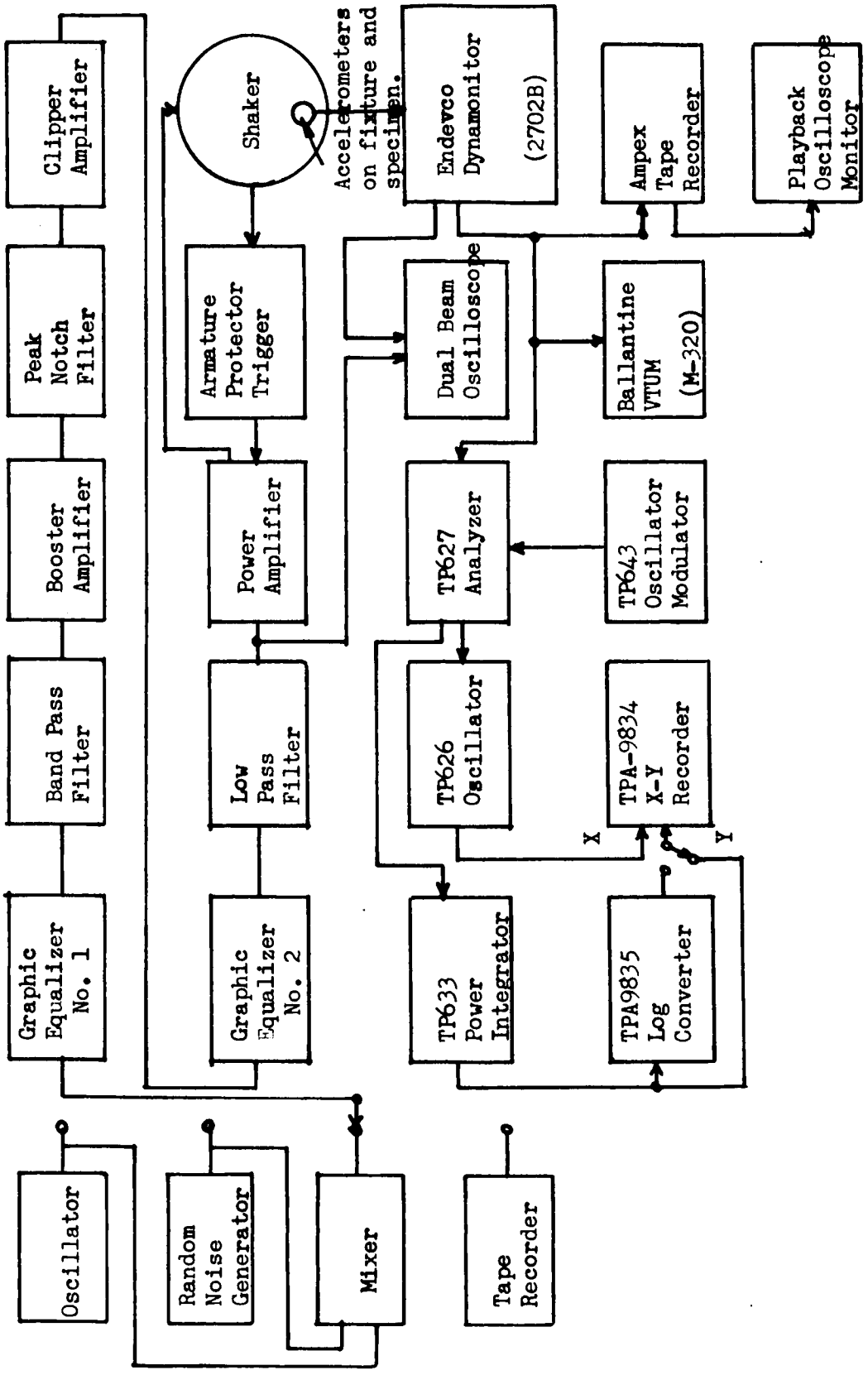

Figure 53. Vibration Test, Random Noise Instrumentation Hook-up (Beam and Plate Models)

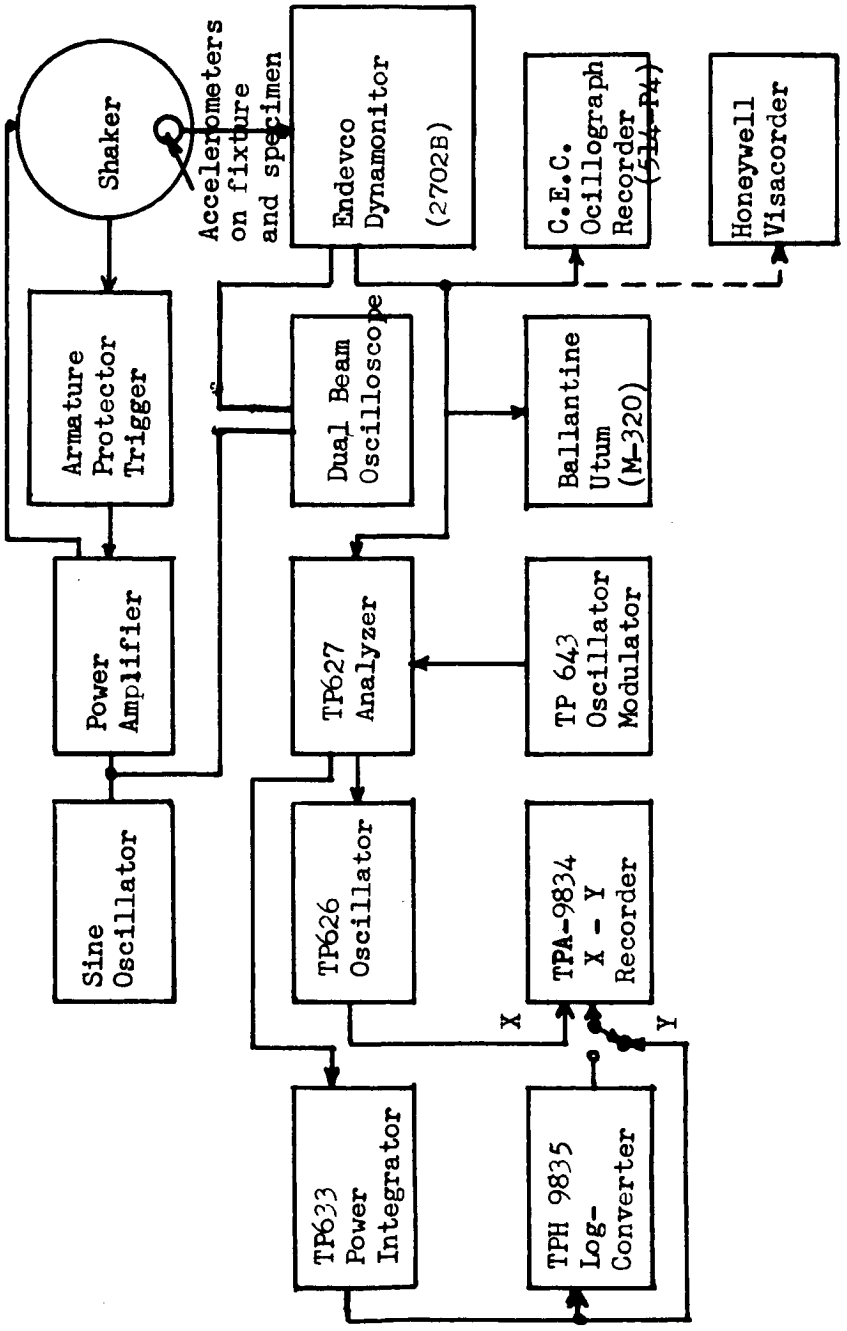

Figure 54. Vibration Test, Sinusoidal Instrumentation Hook-up (Plate Tests)

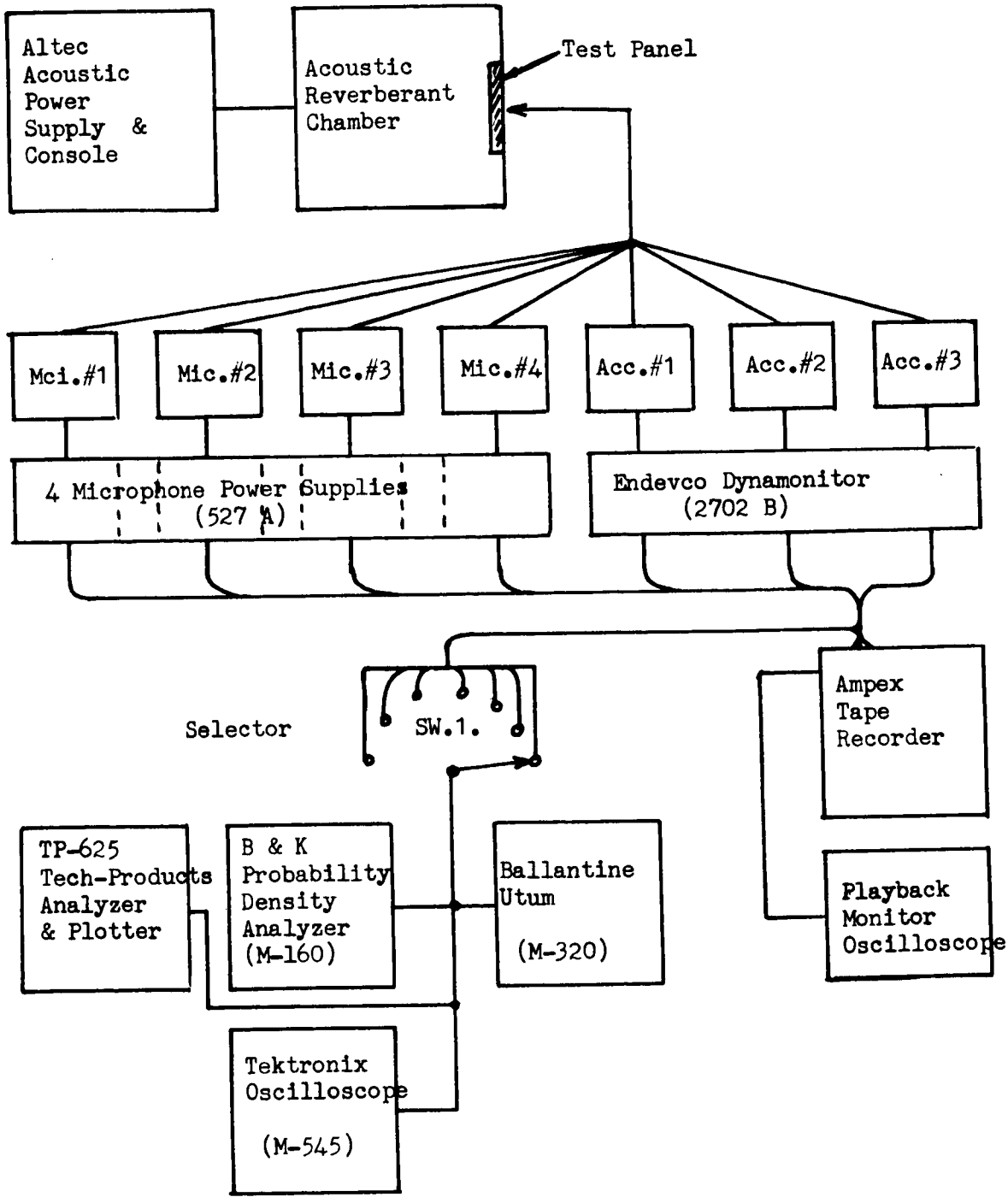

Figure 55. Acoustic Test, Instrumentation Hook-up

displacements were of interest, direct readings from voltmeters were used as the mode shape data requiring no calibration. Other necessary calibrations are as follows:

Accelerometers. Five miniature accelerometers were used for acceleration measurements. The acceleration output in g's is calculated by the following formula:

$$a = 1/SG \quad g's/volt$$

where

S = sensitivity of accelerometer, volt/g

G = accelerometer amplifier gain factor

a = acceleration in g's per volt

Table 10 gives the values of acceleration calibrated for each accelerometer. Accelerometers 1 to 4 were attached to the beam and its support as shown in Figure 42. Accelerometer 5 was mounted on top of the bracket for the mass coupled beam test as shown in Figure 35.

X-Y Plots. X-Y plots were made for the acceleration responses at the mass locations on the beam. The calibration voltages, the ordinates on the plot, are multiplied by "a", the calibrated acceleration, to obtain the response amplitude in g's:

$$A = aV$$

Table 10. Accelerometer Calibrations

Accelerometer Number	S	G	a
1	0.00138	100	7.25
2	0.006	100	1.665
3	0.0056	100	1.785
4	0.007	100	1.428
5	0.00107	100	9.34

where

A = acceleration response amplitude, g's, and

V = calibration voltage, volts.

Oscillographs. Eight channels of vibration measurements have been recorded on oscillographs for each test. Four of them are for accelerometers and the others for strain gages. To convert the oscillograph data into useful forms, the following calibrations were performed.

Accelerometer Records. The frequency factor K_i for the i^{th} accelerometer is determined with

$$K_i = \frac{D_i}{D_{fi}}$$

where

D_i = double amplitude of the record of frequency calibration at a reference frequency (20 cps in this case) for the i^{th} channel

D_{fi} = double amplitude of the record of frequency calibration at the test frequency for the i^{th} channel

The values of K_i are given in Figure 56. This factor is used to correct the nonlinearity of the accelerometer output due to changes in frequency.

The calibration factor B_i is calculated with

$$B_i = \frac{a_i}{D_i} \text{ g's/volt}$$

where a_i are values of "a" in Table 10.

The actual acceleration output, A_i, is given by

$$A_i = \frac{B_i V_i d_i}{K_i c_i} \text{ g's}$$

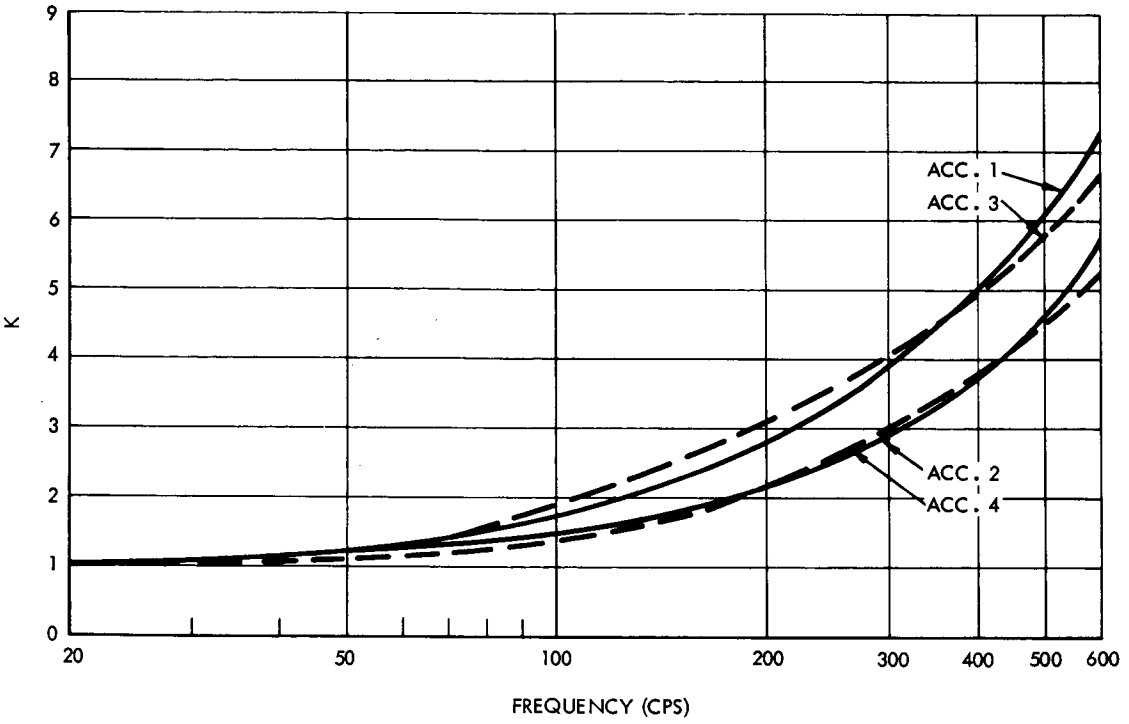

Figure 56. Frequency Factor for Accelerometer Calibrations

where

V_i = calibration voltage, volts

d_i = double amplitude on data records, inches

c_i = double amplitude on calibration record, inches

Strain Gage Records. The measurement of the strain gages is calculated by the formula,

$$\bar{e} = \frac{R_G}{2NK(R_G + R_c)}$$

where

$\bar{e}$ = strain intensity = strain per inch of the double amplitude of strain gage record

R_G = 120 ohms = gage resistance

R_c = 87,500 ohms = calibration resistance

N = 2 = number of active resistors on bridge of strain gage circuit

K = 1.97 = gage constant

By substitution,

$$\bar{e} = \frac{120}{2 \times 2 \times 1.97\,(120 + 87,500)}$$

$$= 0.174 \times 10^{-3} \text{ in./in. of double amplitude.}$$

The maximum strain e, is the product of the strain intensity, $\bar{e}$, and the double amplitude, d, of the oscillograph of the strain gage; namely,

$$e = \bar{e}d$$

In some cases the data record, d, was attenuated during tests by a factor, m. The total strain then becomes

$$e = m\bar{e}d$$

Random Vibration Test on Beam Models and All Vibration Test on Plate Models

Calibration of all accelerometers mounted on the test specimens was accomplished prior to testing. System calibration on all accelerometer channels was performed prior to testing using the voltage insertion method as shown in Figure 57. A precision internal calibration source was used to record calibration signals on tape. This source supplies a calibrated charge to the input of the amplifier, the peak-to-peak value of which represents the peak-to-peak full-scale output value sent to the recorders. Nominal frequency of the calibration is 1000 cps with a rates full-scale output of 5 volts peak or 10 volts peak-to-peak.

The tape transport FM record amplifiers were calibrated for 15 ips with a center frequency of 54 kc to receive an input signal of 5 volts peak or 10 volts peak-to-peak for a 40-percent carrier deviation.

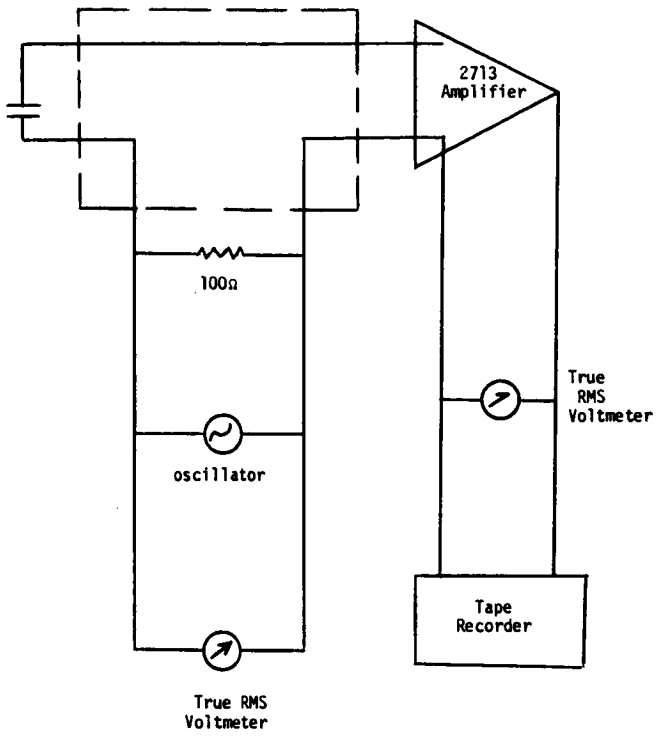

Figure 57. System Calibration

Strain gage calibration was accomplished by the shunt method, using the relationship

$$R_c = \frac{R_g}{E_s \cdot K} - R_g$$

with a strain gage resistance, R_g, of 350 ohms and a gage factor, K, of 3.18. A value of 300 microstrain can be simulated by a shunt resistance of 365,000 ohms. A shunt voltage, E_s, of 15 volts dc was selected for bridge excitation to produce a maximum output from the amplifier of 2.8 volts for a 200 microstrain calibration.

With respect to the strain gages, the tape transport FM record amplifiers were calibrated for 15 ips with a center frequency of 13.5 kc to receive an input signal of 2.8 volts dc for a full-scale 40-percent carrier deviation. This level now represents 300 microstrain zero to peak.

VIBRATION TESTS

Vibration tests with various types of excitations have been performed on the beam and plate models to investigate the effects of mass-loading and mass-coupling. The test procedure generally were begun with resonance surveys to find the natural frequencies and modes of the structure, then were carried on to obtain data for the dynamic responses. Details of the test procedures are described in the following paragraphs:

Beam-Model Tests

Mass-Loading Tests With Sinusoidal Excitation From Mechanical Shaker

1. Perform a resonance survey for the beam model (without additional mass). Maintain a constant acceleration excitation equal to 0.01 g at all test frequencies from 0 to 600 cps.

2. Obtain X-Y plots for the acceleration responses of the three accelerometers (Numbers 1, 2, and 3) at the three locations of the beam (Figure 42) within a frequency range of 0 to 600 cps, which covers the first four natural frequencies of the beam.

3. Take oscillograph records at each resonance of the first four modes for all pickups including one input and three output accelerometers, and four strain gages. For each natural mode, there is a set of records for the response data together with a set of records for calibration.

4. At each resonance, obtain proximity gage measurements for mode shapes.

5. Repeat the above procedures, 1 through 4, for sinusoidal vibration tests on the mass-loaded beam models (Table 8). For each model the mass is cemented on top of the accelerometer housing, which, in turn, is cemented on the beam at one of the three locations of the accelerometers (Figure 42). There are eight different masses constituting twenty-four test models to have twenty-four test runs as described in Steps 1 through 4 above.

Mass-Coupling Tests With Sinusoidal Excitation From Mechanical Shaker

The secondary mass-bracket system, as shown in Figure 35, was used to form nine mass-coupled beam models. For each model, the following tests were performed:

1. Cement the mass-bracket system on the beam at one of the three accelerometer locations (Figure 42).

2. Find the natural frequency of the secondary system by inserting a solid block between the beam and the shaker so that excitation transfers directly to the secondary system.

3. Perform a resonance survey employing sinusoidal sweep.

4. Take oscillograph records for all pick-ups as in Step 3 for mass-loading tests.

5. Obtain voltmeter readings of maximum responses for all accelerometers.

Mass-Loading Test With Sinusoidal Excitation From an Electro-Induction Shaker

The test procedures are identical with those for the mechanical shaker, except that an electroinduction shaker replaces the mechanical shaker as described before in the section on test set-up. Two additional steps are performed, however:

1. At the beginning of testing, perform a survey on forcing function. At a constant voltage (1 volt) input to the shaker, use a proximity gage to measure deflections at several locations along the beam (no mass added) at the first resonance. The amplitude of the force is then calculated by a conventional method from strength of materials.

2. Obtain damping curves on oscillographs for the first four modes of all test models. At 1-volt input to the shaker, tune the model to a resonance. Then, turn off the electrical input to the shaker. Meanwhile, take oscillograph records of the accelerometer outputs.

Random Vibration Tests With Mechanical Shaker

1. Apply 20 seconds of random vibration with a power spectral density of 0.001 g^2/cps to the test model. The total frequency bandwidth varies with each model so that the excited frequencies are limited to the first four natural modes.

2. Record all outputs of the accelerometers and strain gages on magnetic tape.

3. Obtain X-Y plots for output spectral densities through data reduction processes.

4. All mass-loaded beam models are subjected to above random vibration tests.

5. For mass-coupling tests, the secondary mass-bracket system is mounted only at locations A and B on the beam (Figure 34). The above procedures 1 through 3 apply to the mass-coupled models.

Plate Model Tests

Sinusoidal Excitation

1. Perform a resonance survey of the unloaded and mass-loaded plate models using a sinusoidal sweep at one minute per octave from 20 to 1,200 cps.

2. Use a constant acceleration of 1 g as excitation input in a frequency range from 20 to 1,200 cps.

3. Record all outputs of the accelerometers and strain gages on magnetic tape.

4. Through data reduction processes, obtain X-Y plots for the acceleration responses of all pickups.

5. Repeat above steps 1 through 4 for all mass-coupled plate models.

Random Excitation

1. Apply random excitations to test models, one at a time, including the plain plate and all mass-loaded plates. Use constant input power spectral density of 0.1 g^2/cps over a frequency band from

20 to 1,200 cps. The upper frequency band varies with each model so as to cover the same number of modes for all models.

2. Record the output spectral densities of all pickups on magnetic tape.

3. Obtain X-Y plots for above outputs.

4. Repeat steps 1 to 3 for tests of mass-coupled plate models.

Acoustic Excitation

1. Set up the test model in the acoustic reverberation chamber. Apply sonic pressure at levels of 117, 120, 123, 127, 130, 133, 136, 139, and 142 db using a sinusoidal sweep from 20 to 2000 cps.

2. Perform random vibration tests. Apply sonic pressure at the same levels as in Step 1; however, use narrow-band white-noise random inputs having 1/3-octave bandwidth and 1/2-power bandwidth about the first modal frequencies. As with vibration tests, no appreciable response was recorded at higher frequencies other than that of the fundamental modes when a wide-band (20-2000 cps) white-noise random spectrum at 140 db was applied. No wide-band random acoustic tests, therefore, become necessary.

Beam-Plate Model Tests

Vibration tests on the mass-loaded beam-plate models were performed on a mechanical shaker with sinsoidal and random excitations. Test procedures are identical with those for the plate model tests.

DATA ANALYSIS

Some of the data from the vibration tests on the beam and plate models were recorded on magnetic tape during tests. To extract useful information from the tape, it is necessary to perform the following data reduction using the system of equipment shown in Figure 58.

1. Reduce vibration data on both the beam and plate models to power spectral density (g^2/cps) of the acceleration response versus frequency on X-Y plots. Reduce data of the strain gages to the mean square value of strain in (microinch/inch)^2/cps.

2. Reduce sinusoidal vibration data on the plate models to X-Y plots giving continuous curves for acceleration response versus frequency.

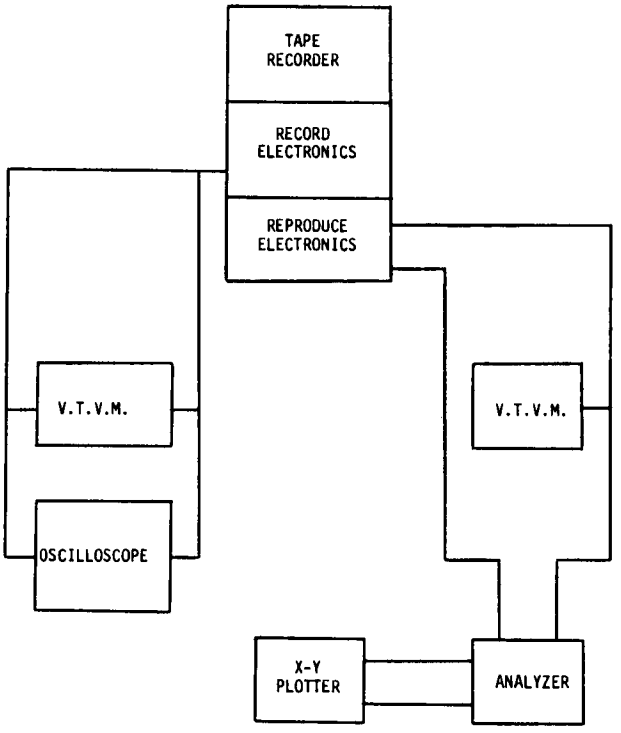

Figure 58. Data Reduction System

COMPARISON OF ANALYTICAL AND EXPERIMENTAL RESULTS

For verification of the results, the experimental data obtained from various tests in the program are compared with the analytical solutions. Two sets of data are presented for comparison:

1. Natural frequencies and modes of free vibration

2. Acceleration response or transmissibility in forced vibration

During free vibration of the mass-loaded beam, variation of location of the additional mass causes significant change in natural frequencies and mode shapes. In forced vibration of both the mass-loaded beam and plate, transmissibility characteristics are greatly affected by the type of excitation employed, as well as by the variation of mass locations. Notations used in the diagrams of this section are the following

f = natural frequency

G = maximum acceleration response

M = mass

Subscripts:

"1" = the unloaded structure, beam or plate

"2" = the mass-loaded beam or plate

Note that the acceleration response ratio G_2/G_1 can be regarded also as the transmissibility ratio T_2/T_1 or Q_2/Q_1 as previously discussed under sections of Forced Vibrations of "Mass-Loaded Beams" and "Mass-Loaded Plates".

ACOUSTIC EXCITATION

Acoustic tests have been performed at various sound pressure levels for the mass-loaded plate models under either sinusoidal or random excitation. The predicted natural frequencies are agreeable with the experimental values shown in Figures 59 and 60. The transmissibility follows the predicted attenuation curve; however, some scattered data were observed because of the existence of standing waves and the effect of reflected waves in the acoustic reverberant chamber (Figures 61 through 77).

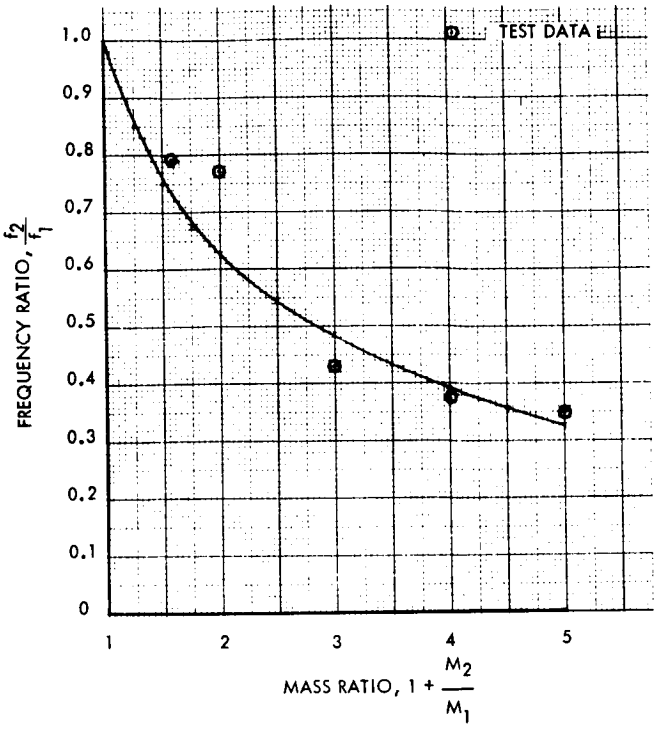

Figure 59. Mass-Loaded Plates Frequency Comparison (Acoustic Sinusoidal Excitation)

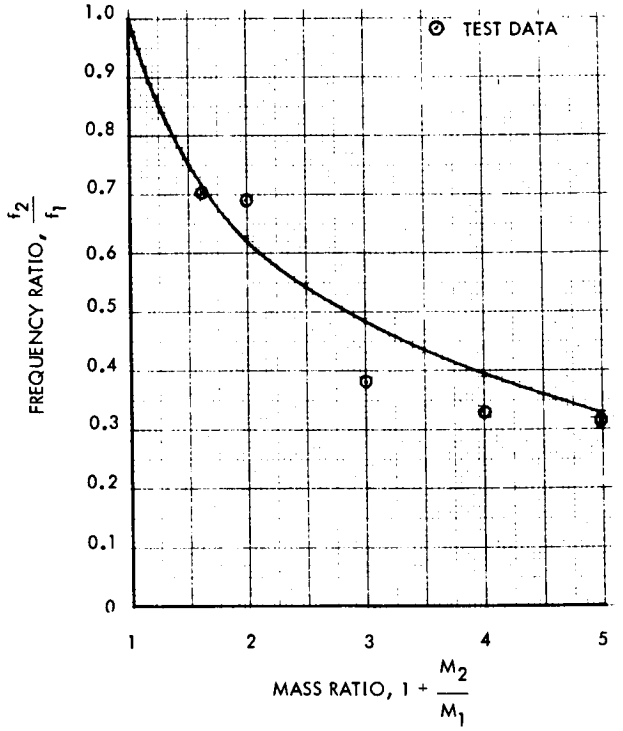

Figure 60. Mass-Loaded Plates Frequency Comparison (Acoustic Random Excitation)

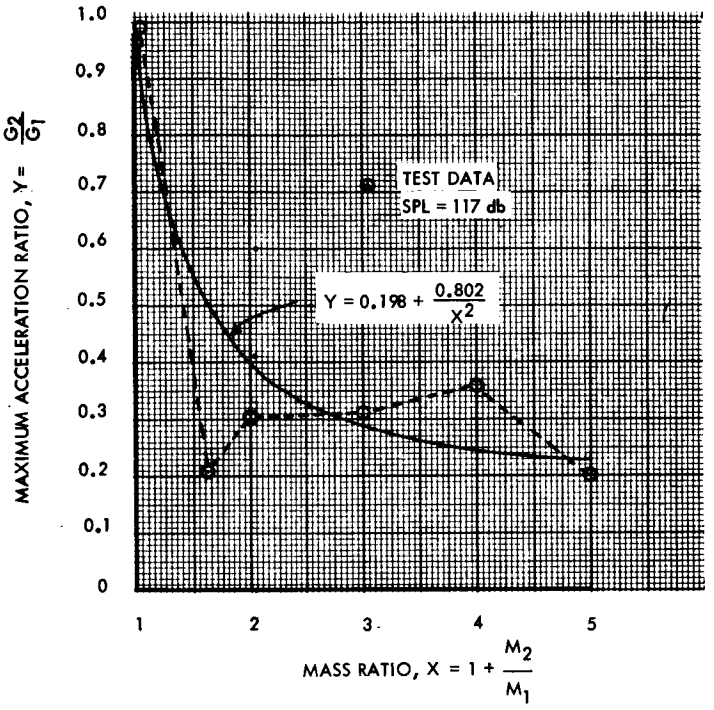

Figure 61. Mass-Loading Effects on Plate (Acoustic Sinusoidal Excitation), SPL = 117 db

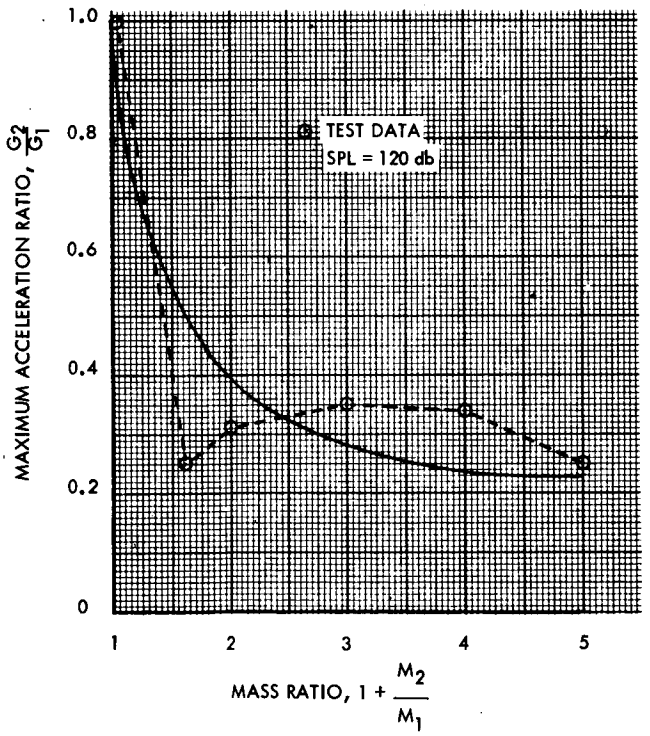

Figure 62. Mass-Loading Effects on Plate (Acoustic Sinusoidal Excitation), SPL = 120 db

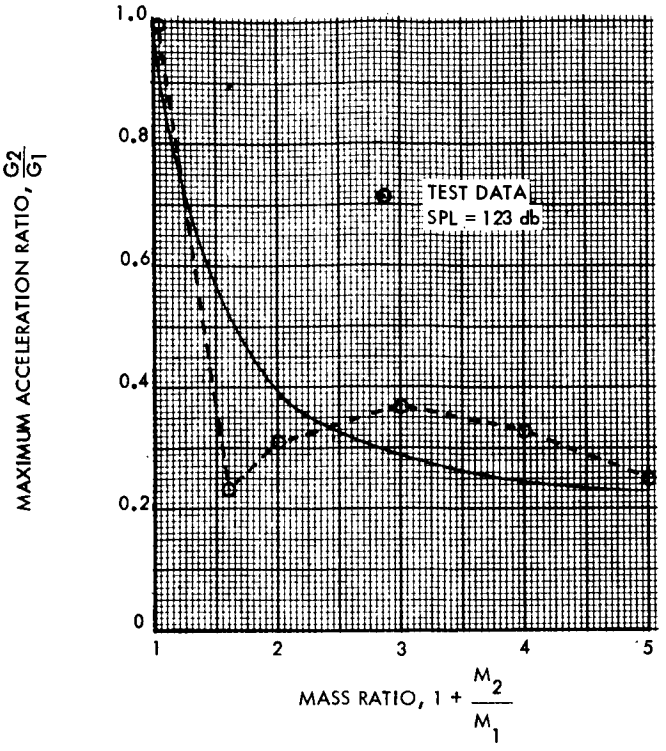

Figure 63. Mass-Loading Effects on Plate (Acoustic Sinusoidal Excitation), SPL = 123 db

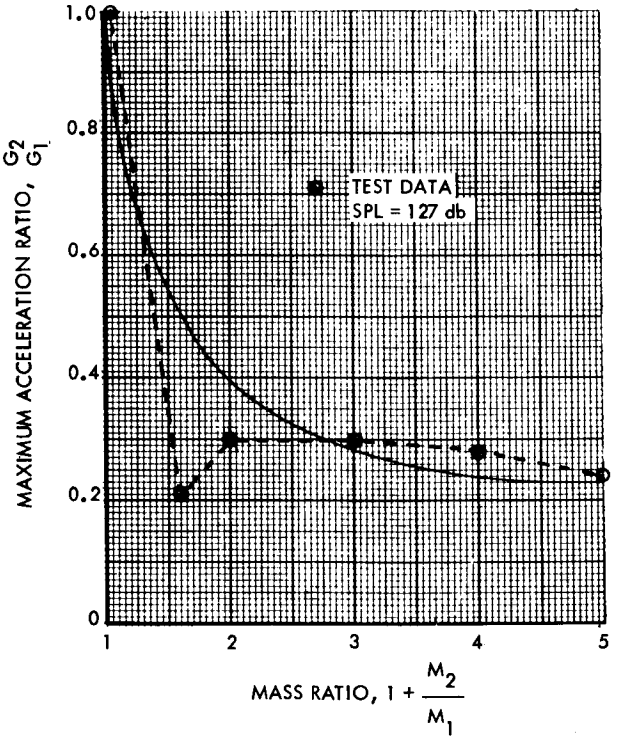

Figure 64. Mass-Loading Effects on Plate (Acoustic Sinusoidal Excitation), SPL = 127 db

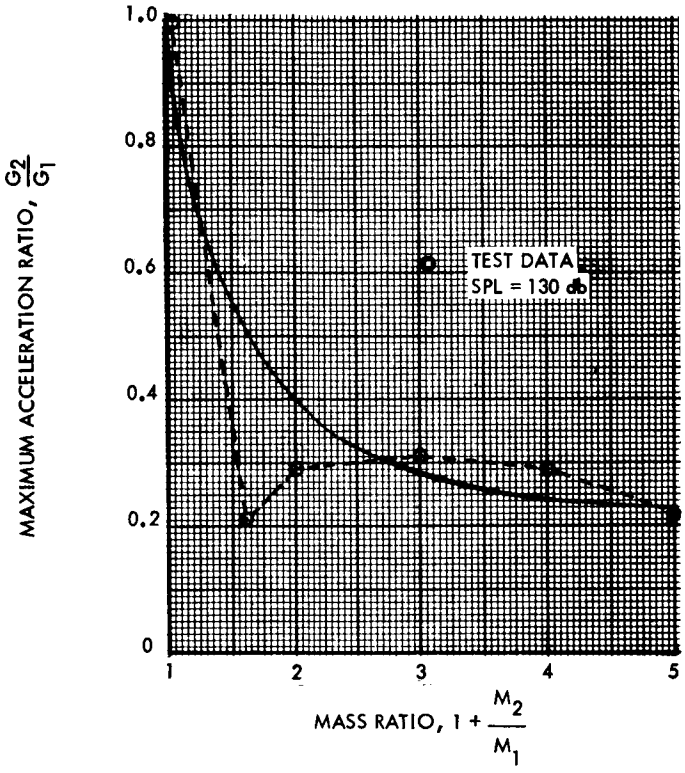

Figure 65. Mass-Loading Effects on Plate (Acoustic Sinusoidal Excitation), SPL = 130 db

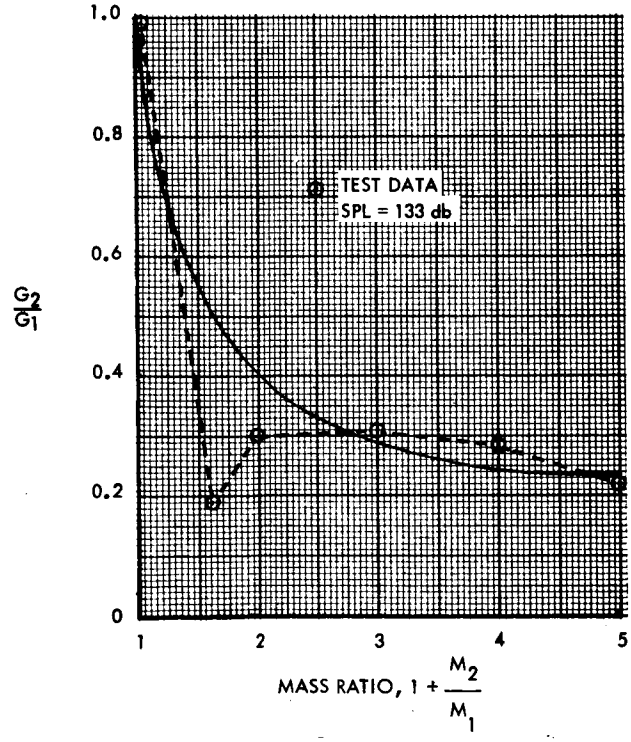

Figure 66. Mass-Loading Effects on Plate (Acoustic Sinusoidal Excitation), SPL = 133 db

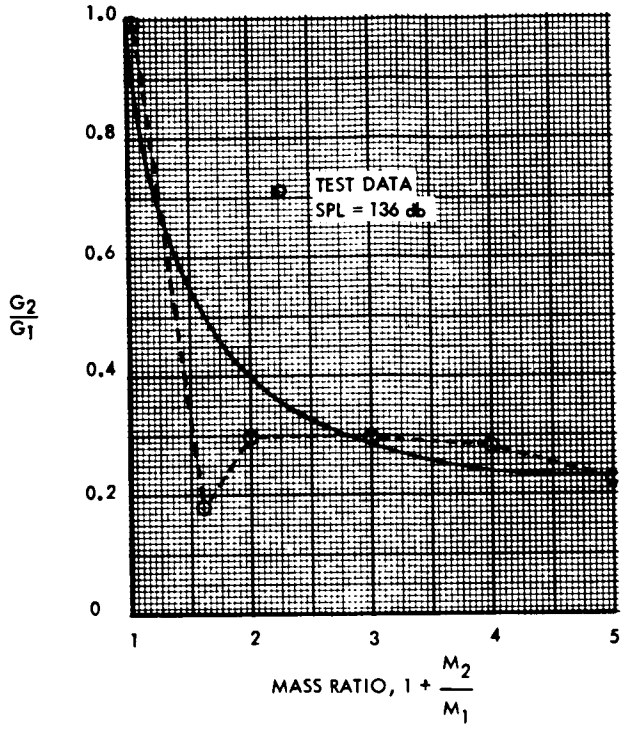

Figure 67. Mass-Loading Effects on Plate (Acoustic Sinusoidal Excitation), SPL = 136 db

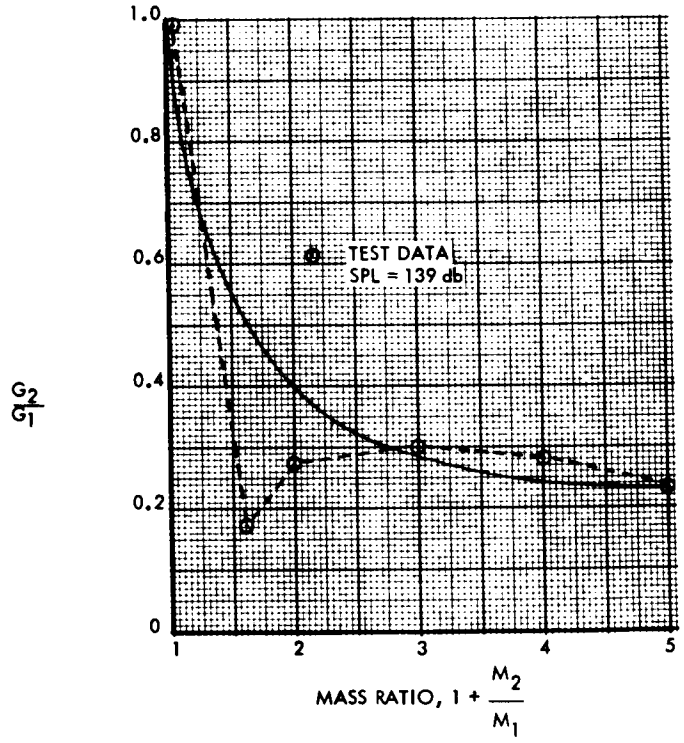

Figure 68. Mass-Loading Effects on Plate (Acoustic Sinusoidal Excitation), SPL = 139 db

In Figures 61 through 69, the acceleration responses of the mass-loaded plate under acoustic sinusoidal excitation are shown. The expression $y = 0.198 + 0.802/x^2$ for the curve of Figure 61 also applies to the other curves shown in Figures 62 through 69. Presented in Figures 70 through 77 are the root-mean-square acceleration responses for the cases with random input. Note that in Figure 70 that transmissibility attenuation curve has an expression $y = 0.375 + 0.625/x^2$ which also applies to the other curves in Figures 71 through 77.

MECHANICAL EXCITATION

The vibration tests performed on mechanical shakers for the mass-loaded beams and plates resulted in satisfactory data, which agrees well with the analytical solutions.

Figures 78 through 81 show the frequency comparison of the mass-loaded beams for the first four modes (refer to Table 2). It may be noted that the natural frequency predictions are of good accuracy, especially for the cases with mass-loading at the middle of the beam. The mode shapes obtained from the computer program are presented in Appendix A. They are identical with those measured by a proximity gage during testing. For the higher modes of the beam with a heavy mass attached, the modal displacement at the mass location diminishes as the mass increases.

Figures 82 through 87 show the frequency comparison of the mass-loaded plates. The analytical values are quite accurate, as discussed previously under "Mass-Loaded Plates" (refer to Table 2).

The transmissibility predictions shown in Figures 88 and 89 for the mass-loaded beams follows similar attenuation trends as expected. For the mass-loaded plate, the transmissibility curves are discussed under "Mass-Loaded Plates, Transmissibility Characteristics," and are shown in Figures 25 and 26.

CONCENTRATED FORCE EXCITATION

Mass-loaded beam tests were performed by using a specially built electromagnetic-induction shaker, which produces a concentrated force excitation. The natural frequencies so obtained are identical with those from tests with the mechanical shaker. The acceleration response differs, however, from that of mechanical excitation (Figures 90 and 91) and varies with the location of the shaker and the magnitude of the force input. In the experiments, the input force was maintained at a constant level. As a result, the input acceleration reduces as the additional mass increases according to Newton's Law. No attempts have been made to adjust the force input to produce a constant acceleration for all mass-loaded beam tests, since a mechanical shaker is better qualified to do so.

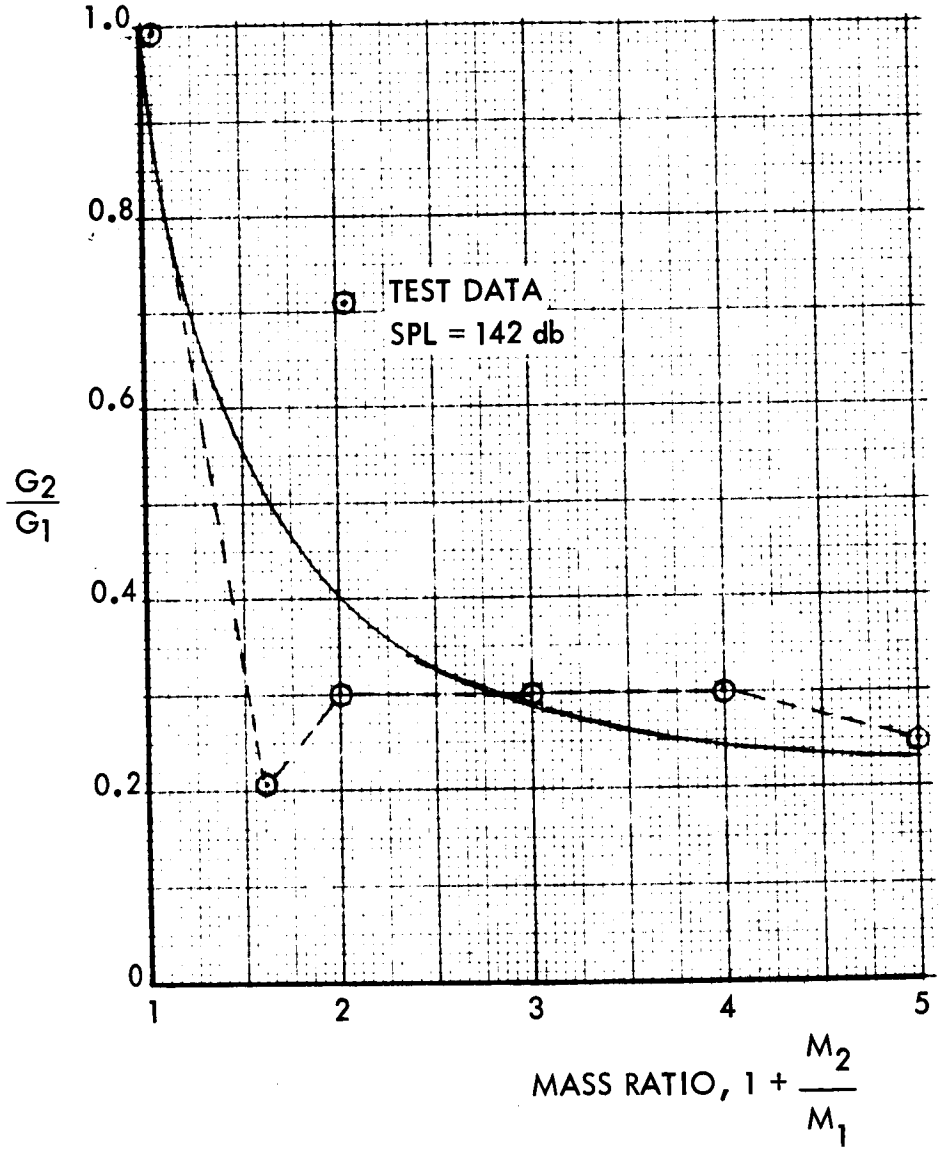

Figure 69. Mass-Loading Effects on Plate (Acoustic Sinusoidal Excitation), SPL = 142 db

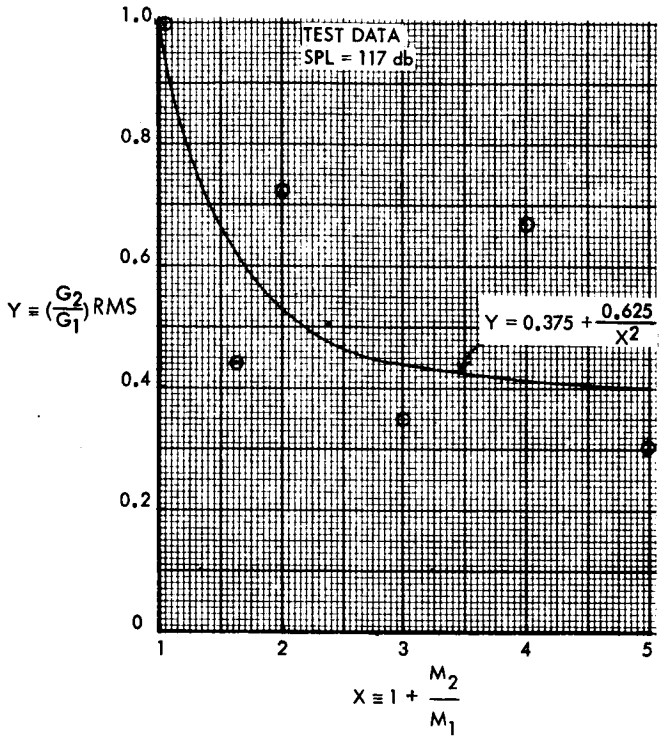

Figure 70. Mass-Loading Effects on Plate (Acoustic Random Excitation), SPL = 117 db

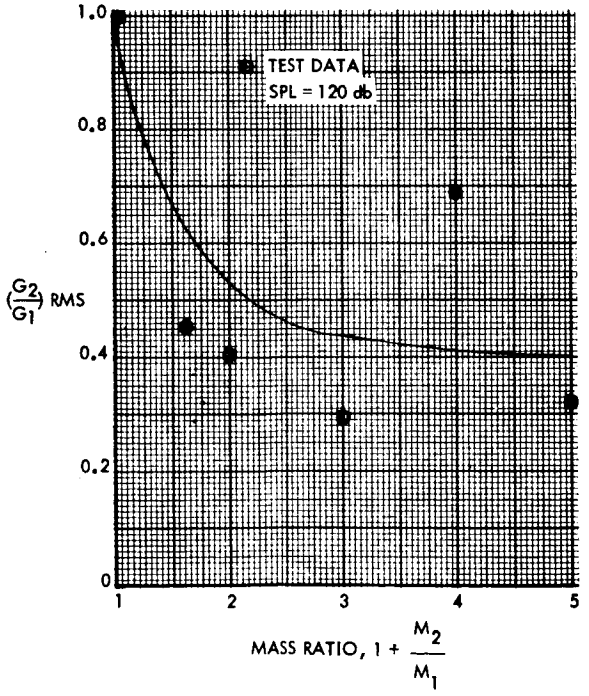

Figure 71. Mass-Loading Effects on Plate (Acoustic Random Excitation), SPL = 120 db

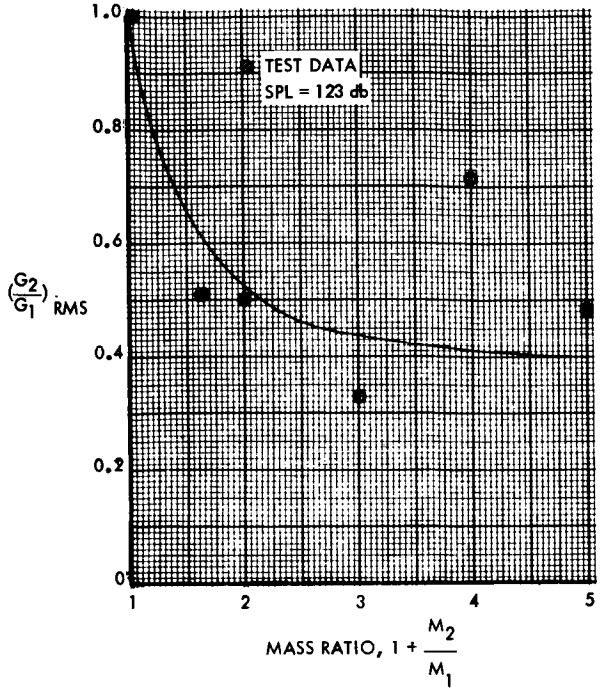

Figure 72. Mass-Loading Effects on Plate (Acoustic Random Excitation), SPL = 123 db

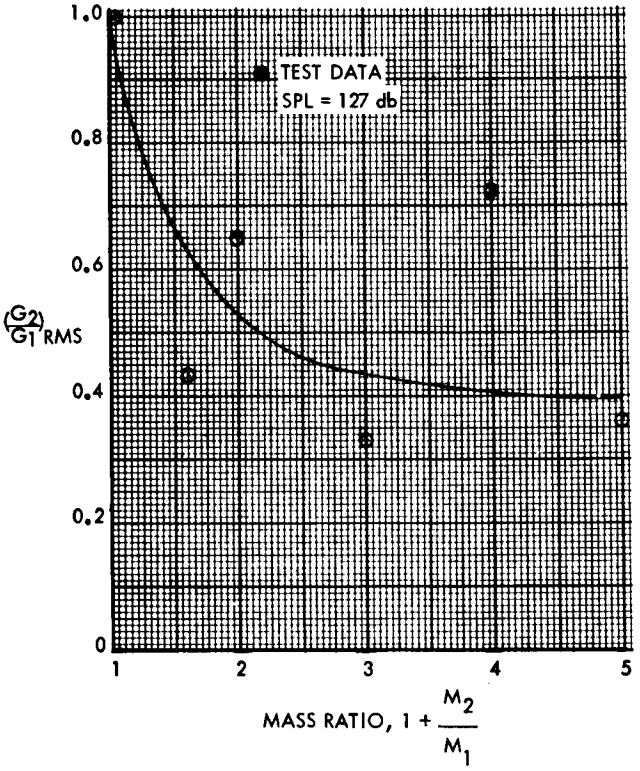

Figure 73. Mass-Loading Effects on Plate (Acoustic Random Excitation), SPL = 127 db

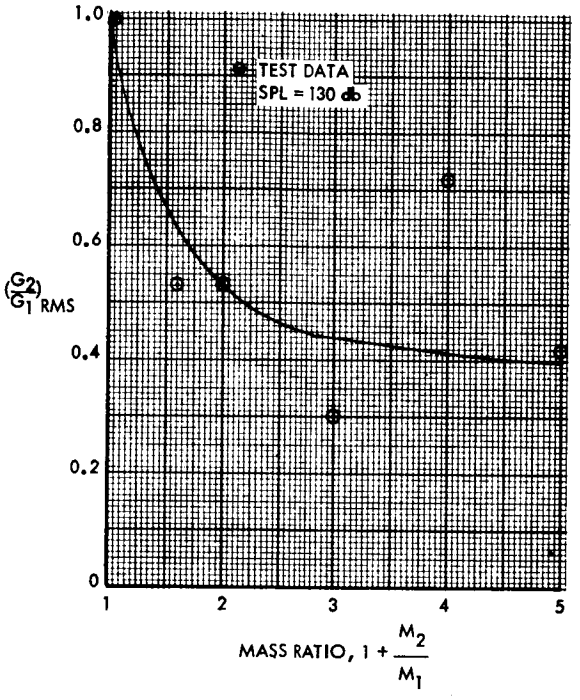

Figure 74. Mass-Loading Effects on Plate (Acoustic Random Excitation), SPL = 130 db

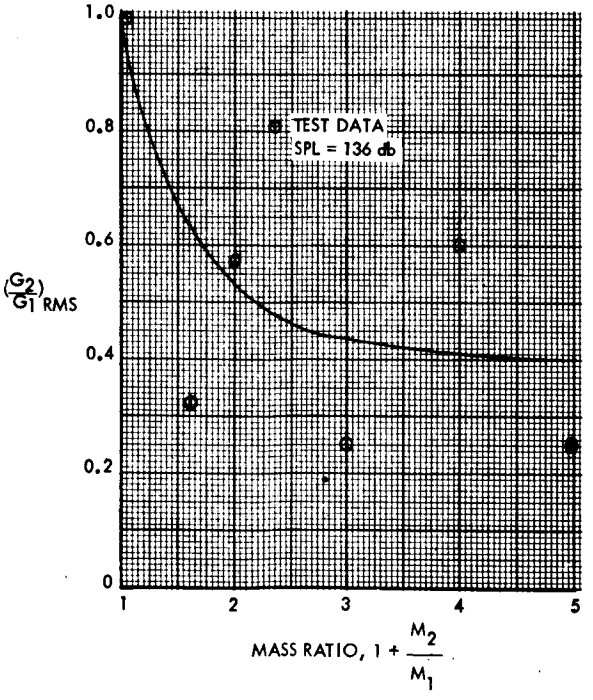

Figure 75. Mass-Loading Effects on Plate (Acoustic Random Excitation), SPL = 136 db

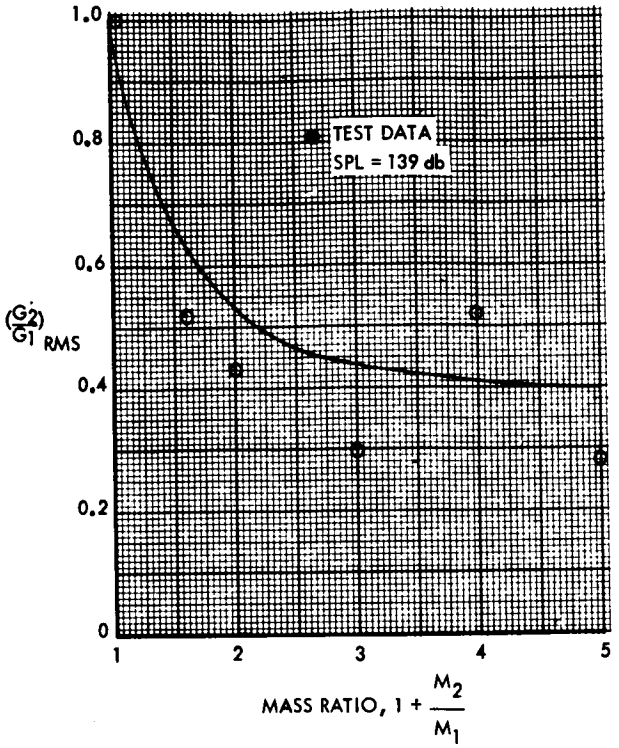

Figure 76. Mass-Loading Effects on Plate (Acoustic Random Excitation), SPL = 139 db

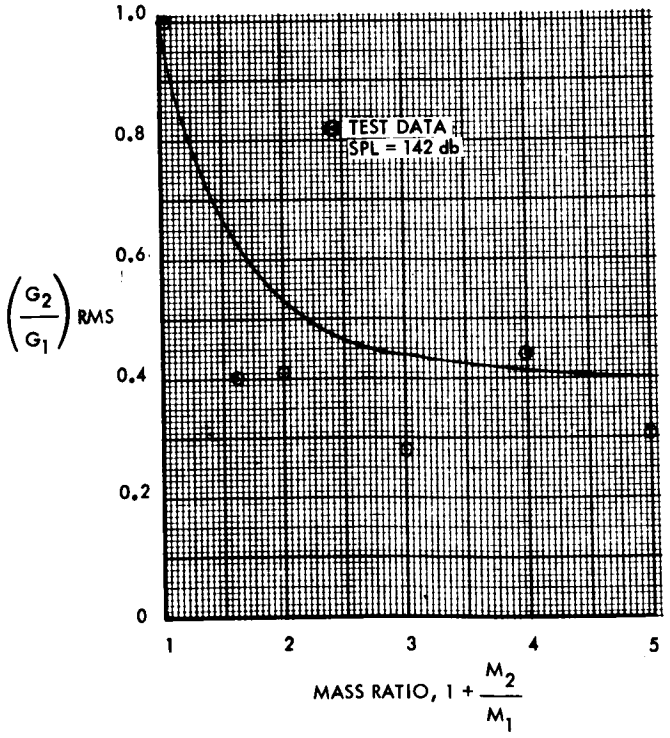

Figure 77. Mass-Loading Effects on Plate (Acoustic Random Excitation), SPL = 142 db

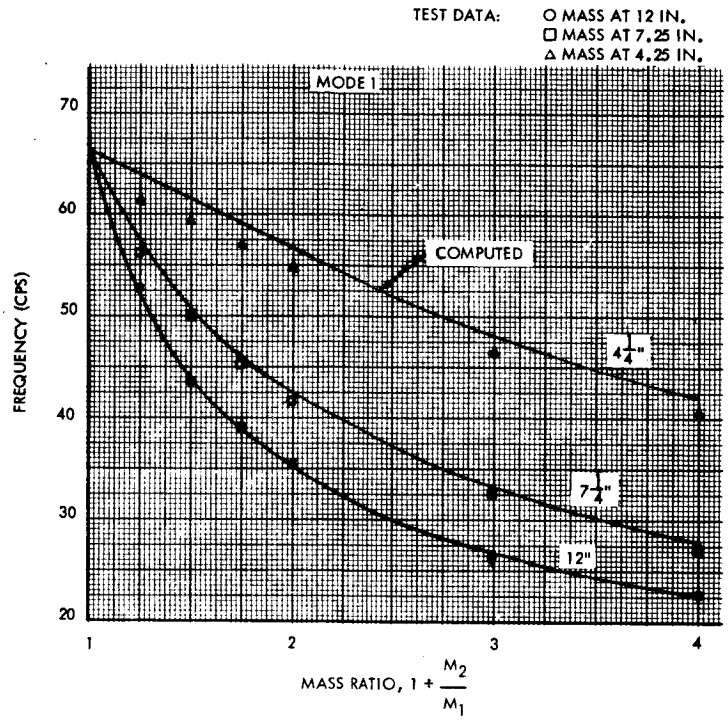

Figure 78. Mass-Loaded Beam, Frequency Comparison, Mode 1

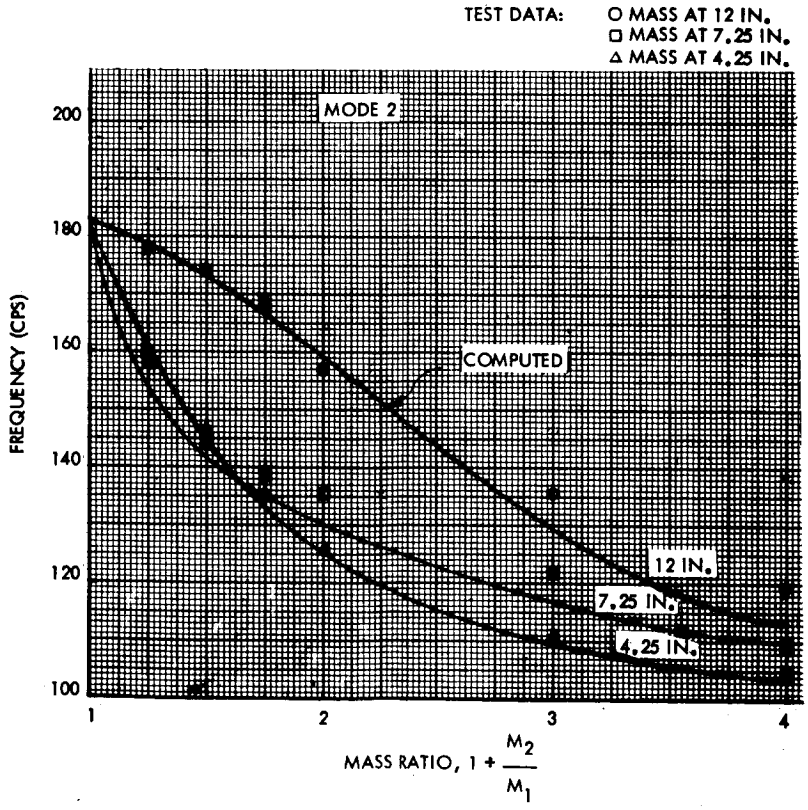

Figure 79. Mass-Loaded Beam, Frequency Comparison, Mode 2

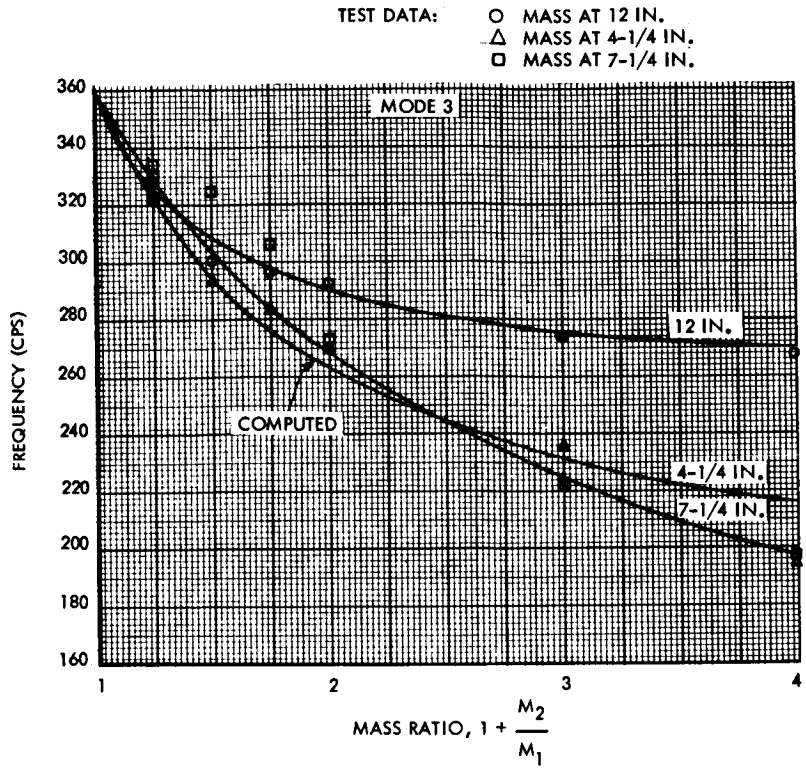

Figure 80. Mass-Loaded Beam, Frequency Comparison, Mode 3

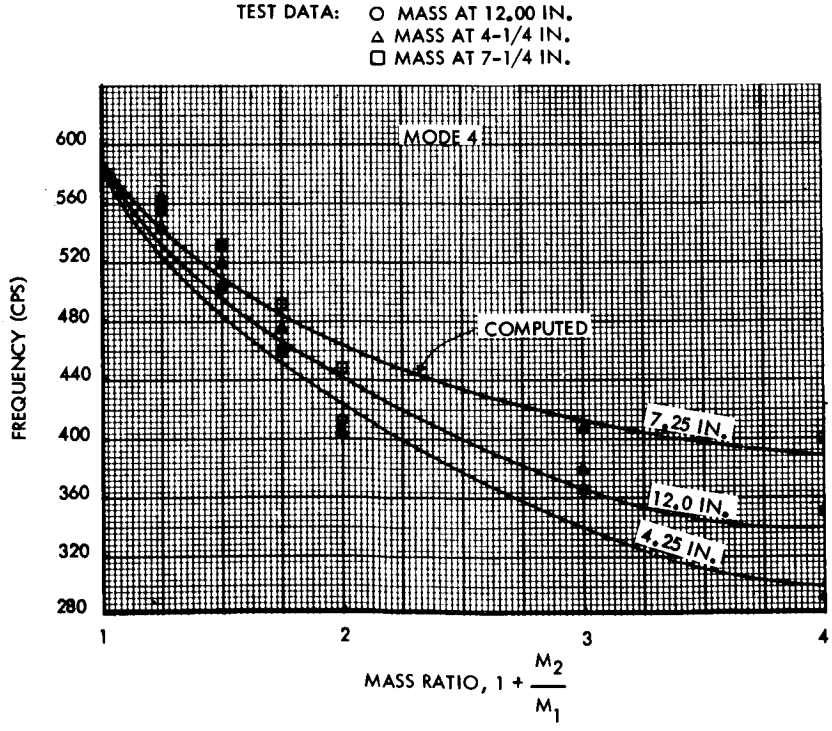

Figure 81. Mass-Loaded Beam, Frequency Comparison, Mode 4

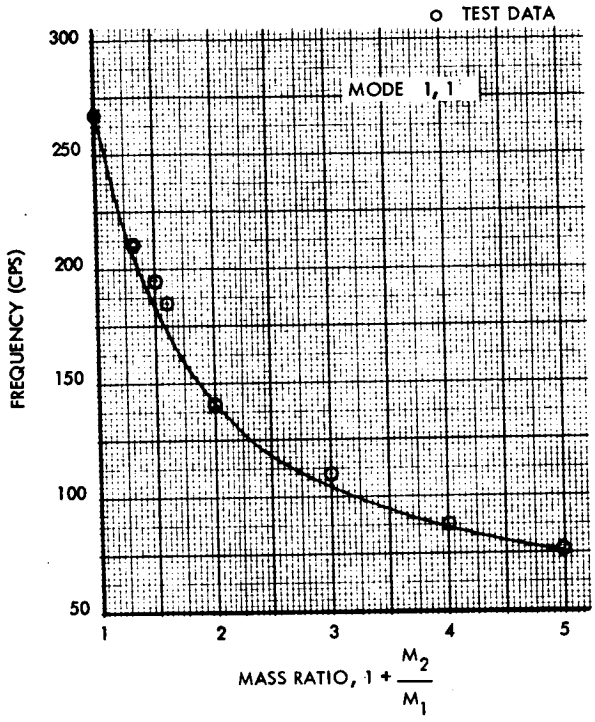

Figure 82. Mass-Loaded Plates, Frequency Comparison, Mode 1, 1

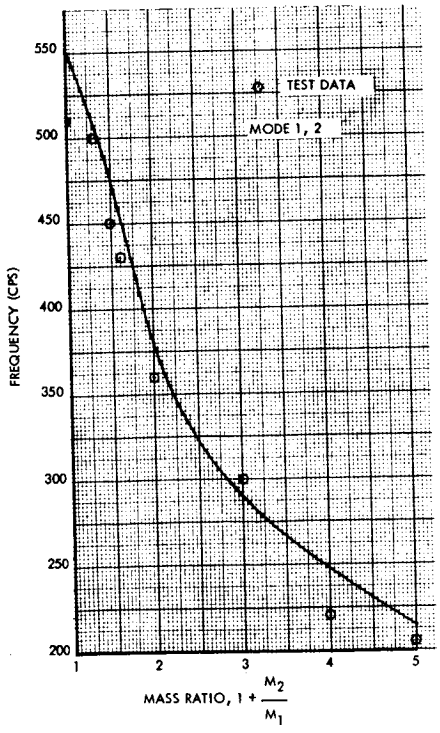

Figure 83. Mass-Loaded Plates, Frequency Comparison, Mode 1, 2

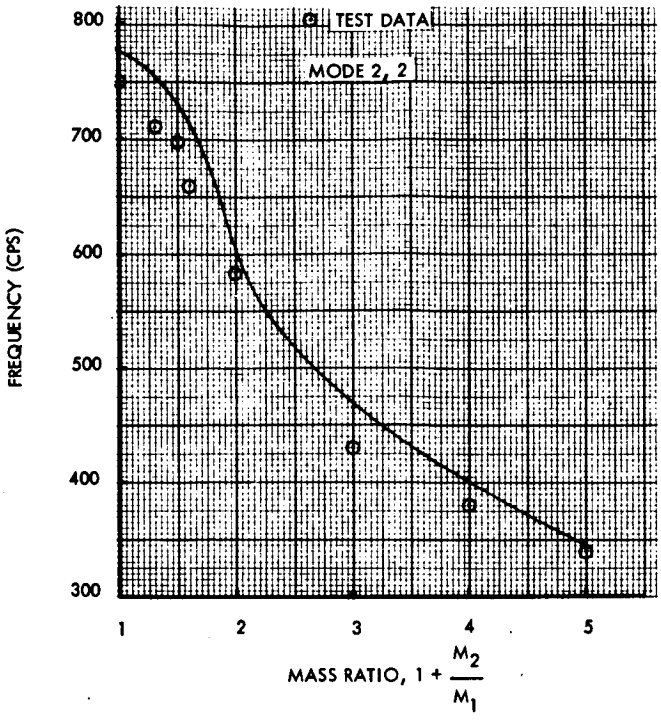

Figure 84. Mass-Loaded Plates, Frequency Comparison, Mode 2, 1

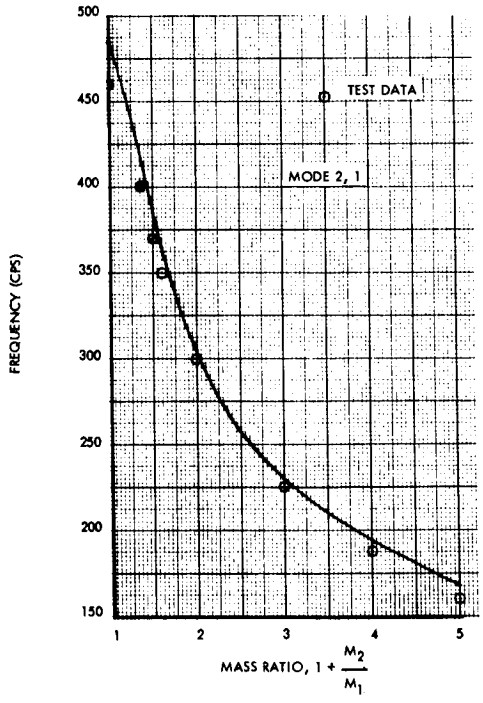

Figure 85. Mass-Loaded Plates, Frequency Comparison, Mode 2, 2

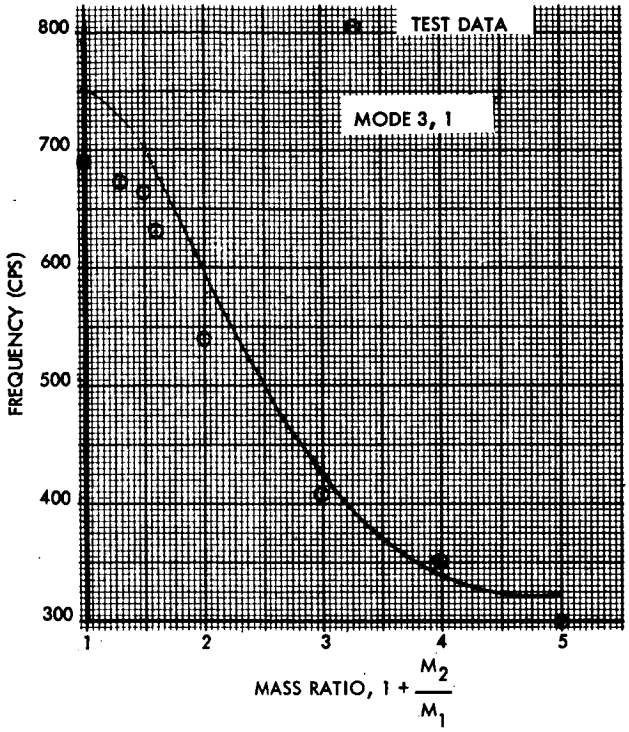

Figure 86. Mass-Loaded Plates, Frequency Comparison, Mode 3, 1

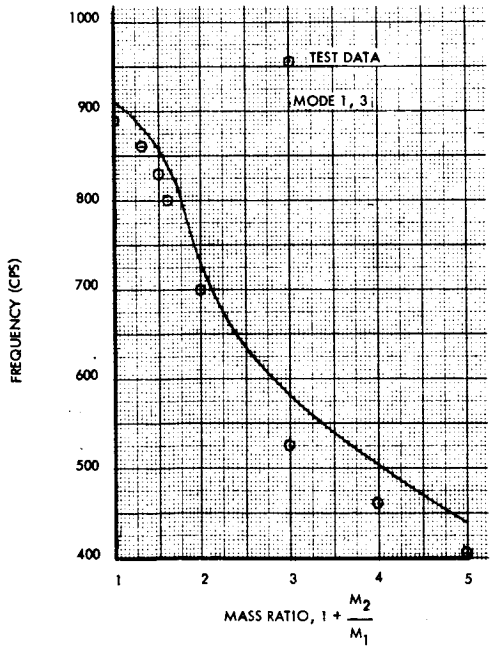

Figure 87. Mass-Loaded Plates, Frequency Comparison, Mode 1, 3

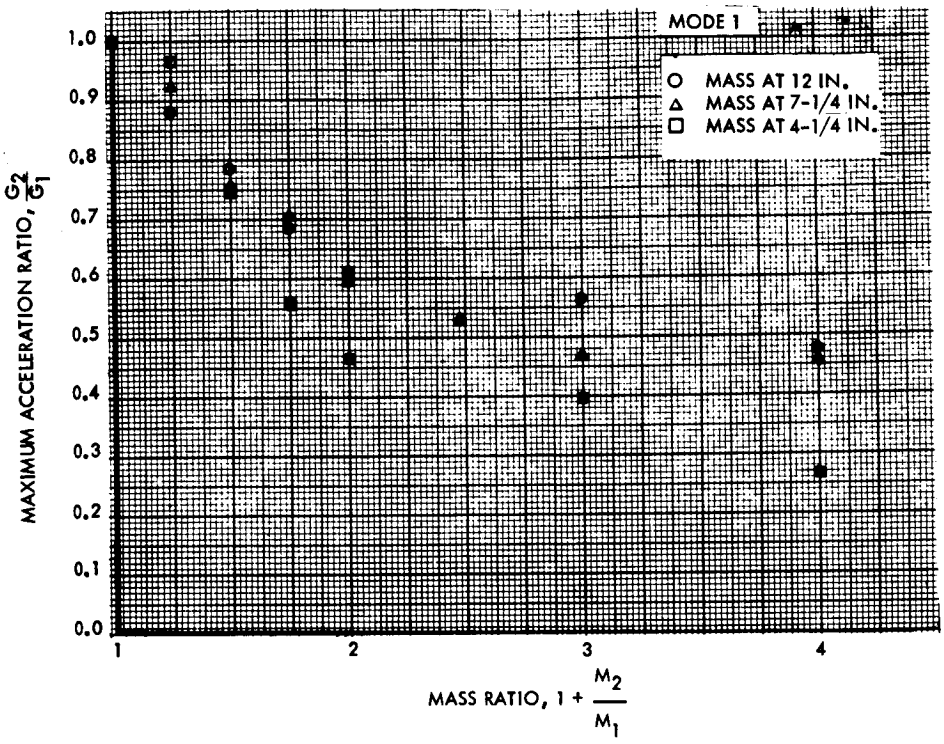

Figure 88. Mass-Loading Effects on Beam (Mechanical Shaker), Mode 1

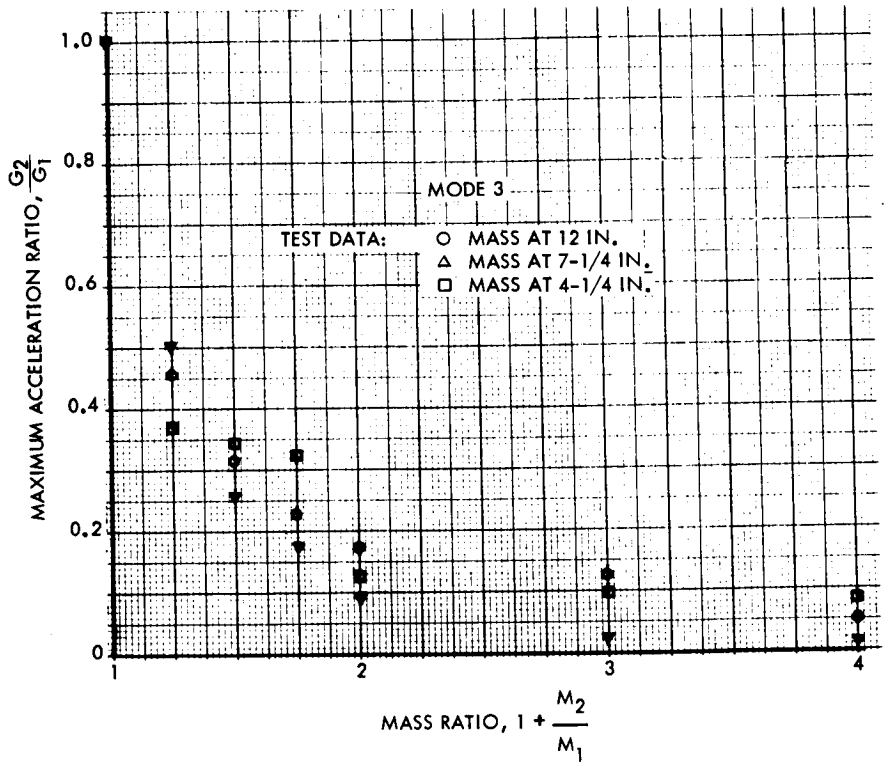

Figure 89. Mass-Loading Effects on Beam (Mechanical Shaker), Mode 3

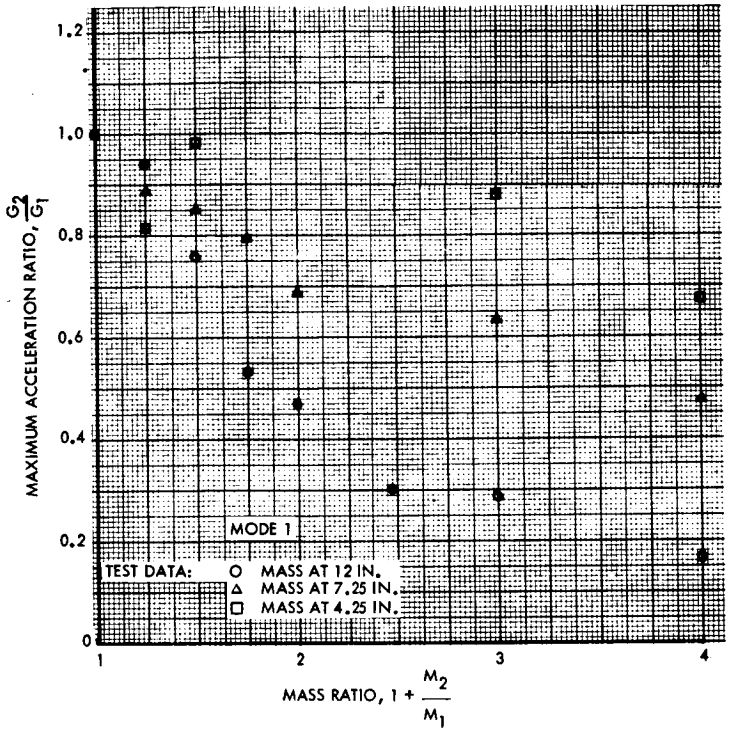

Figure 90. Mass-Loading Effects on Beam (Electroinduction Shaker), Mode 1

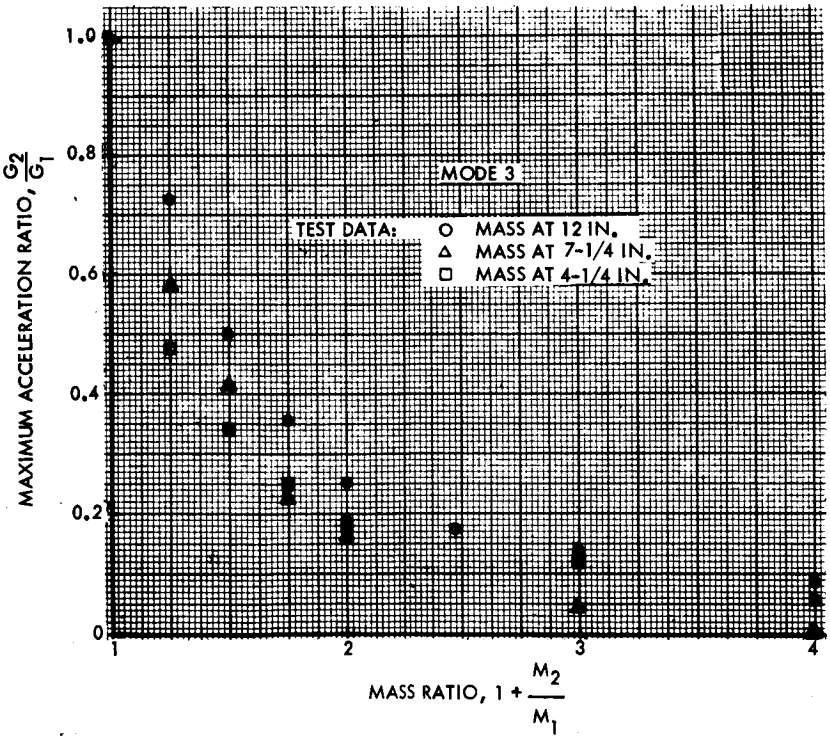

Figure 91. Mass-Loading Effects on Beam (Electroinduction Shaker), Mode 3

RANDOM EXCITATION

Vibration tests on the mass-loaded beams and plates with random excitation were performed on a mechanical shaker. For a constant white noise input, the experimental data of power spectral density and root-mean-square value of acceleration response follows similar trends as in the cases with sinusoidal input (Figure 26). X-Y plots from the tests for the input and output spectral density are shown in Appendix B for the mass-loaded plate. Similar plots were obtained for the mass-loaded beam tests, and have been reduced to useful data.

VARIATION OF MASS-LOADING LOCATIONS

Mass-loading effects due to variation of location of the attached mass are described clearly in the section on "Analytical Study." These effects, obtained from experiments, are shown in Figures 78 through 81 and in Figures 88 and 89 for the mass-loading beams. Both the natural frequencies and acceleration responses vary with the location of mass.

BEAM-PLATE

Vibration tests were performed on the mass-loaded beam-plate model. The resulting data are presented in Table 11.

Table 11. Mass-Loading Effects on Beam-Plate

Case No.	Additional Mass (Pounds)	Natural Frequency (cps)	Maximum Acceleration Response (g's)	
			On Plate	On Mass
0	0	—	5.5	—
1	5.07	470	6.0	4.75
2	15.24	287	6.25	4.6
3	20.58	253	5.4	4.1

It may be noted that variation of the masses results in little change in the acceleration responses. This effect is due to the fact that the two beams stiffen the plate considerably, thus causing a transmissibility ratio of almost 1 to 1 for all three mass-loaded cases. The beam-plate model represents a panel that is supported by a stiff primary structure of an aerospace vehicle and that carries a component mass.

APPLICATION OF THE MASS-LOADING EFFECTS

Among the major problems in vibration and acoustics associated with aerospace vehicles are the prediction of vibration environments, computation of the response, and the establishment of vibration criteria requirements for equipment design and testing. Mass-loading and coupling involve the changes in the vibratory characteristics of a structure caused by the addition of one or more localized component masses, and, therefore, are intimately associated with these problems. Applications of the specific results have been mentioned in the individual sections. This section is intended to convey the practical application for specific purposes.

Most solutions have been developed analytically and verified experimentally and may be applicable to similar cases. Extension of the direct application of the figures to other structures with different properties and geometry should be performed with caution because the test specimens have been limited. Application of the theories and analytical methods, however, is not confined to the range of the representative models.

ENVIRONMENTAL PREDICTION

Much work has been performed in the measurement of the vibration environment and in the prediction of the vibration environment extrapolated from measured values of one vehicle to a modified or future design vehicle. Extensive analytical and experimental investigations of dynamic response phenomena and transmissibility characteristics, however, have been scarce. The present sutdy results may be applied to fill this requirement for the purpose of evaluation and refinement of these empirical prediction techniques.

Predictions of the vibrational environment encountered by structure-mounted equipment usually are based on statistics and assumptions that are open to considerable question as to their applicability. While this approach has its proper place in the earliest phase of preliminary design where the available structural information is far from definitive, more refined methods are needed to incorporate the design revisions or to account for the difference resulting from application of vibration data from one vehicle to another. Mass-loading effects represent an important input at this stage to provide a simple technique for predicting the vibration environment.

The vibration data available are assumed to be given for an unloaded local structure; that is, without the effect or presence of the mounted masses. The simple prediction technique attempts to give some insight into the

complex dynamic interaction of the mounted masses and the local structures, specifically to what extent the mounted mass affects the vibration input at its attach point and how the response characteristics are altered.

From Figure 92, it is clear that vibration spectra for unloaded structures are substantially changed because of the attachment of a component mass introducing the frequency shifts and attenuation of responses especially for higher modes. Information on frequency shifts may be obtained from Figures 82 through 87 and 93 through 97. Charts presented in the sections on "Transmissibility" may be used to predict the mass-loading attenuation of responses and higher modes.

A similar problem in acoustic cases can be seen in Figure 98. Assuming an acoustic spectrum is known from tests (wind tunnel tests, engine firing tests, or preliminary flight tests), the sonic-induced vibration spectrum for mass-loaded local structures may differ greatly from the unloaded structures. The difference may be predicted by employing information from Figures 59 and 60 for the frequency shift case and from Figures 61 through 77 for the response attenuation case.

The response relation between the unloaded and mass loaded structures is shown in Figure 99. The application of the mass-loading effects to environmental specifications such as MIL-STAN-810 and MIL-E-5272C, is illustrated in Figure 100.

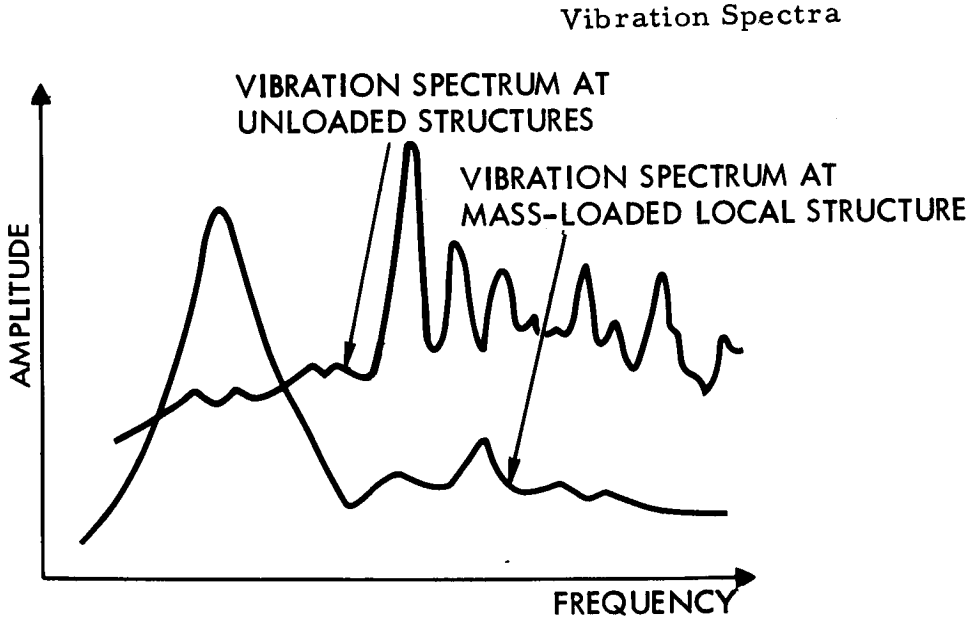

Figure 92. Typical Vibration Spectra

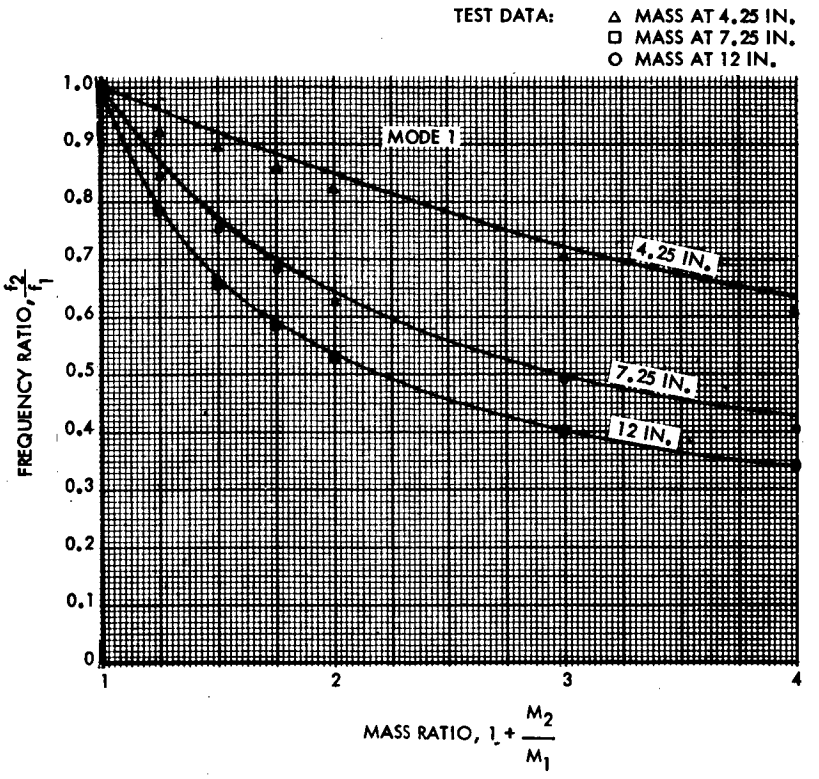

Figure 93. Mass-Loaded Beam, Frequency Comparison, Mode 1

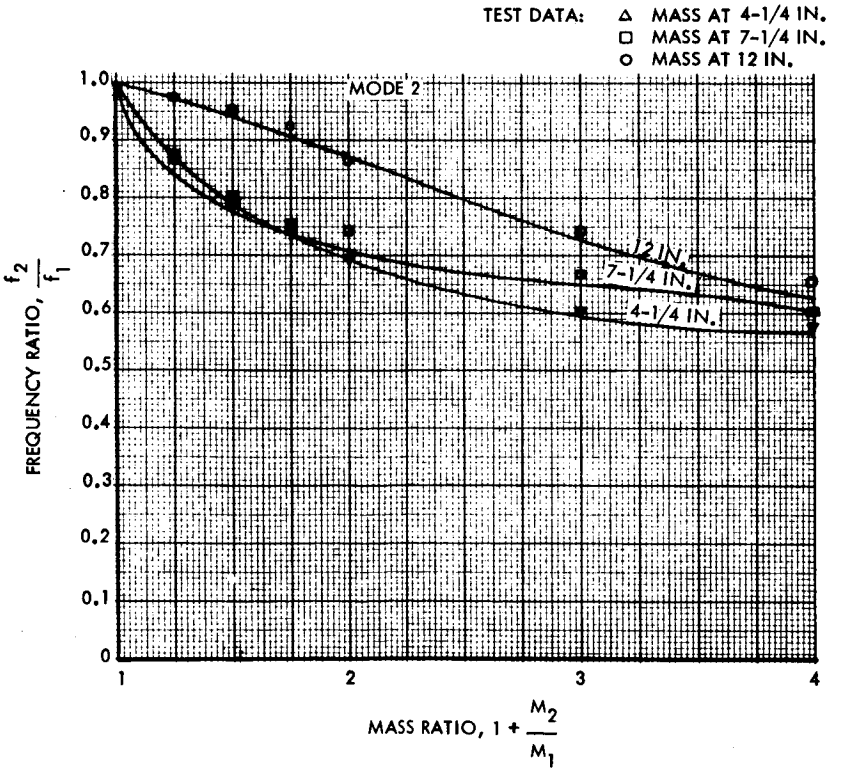

Figure 94. Mass-Loaded Beam, Frequency Comparison, Mode 2

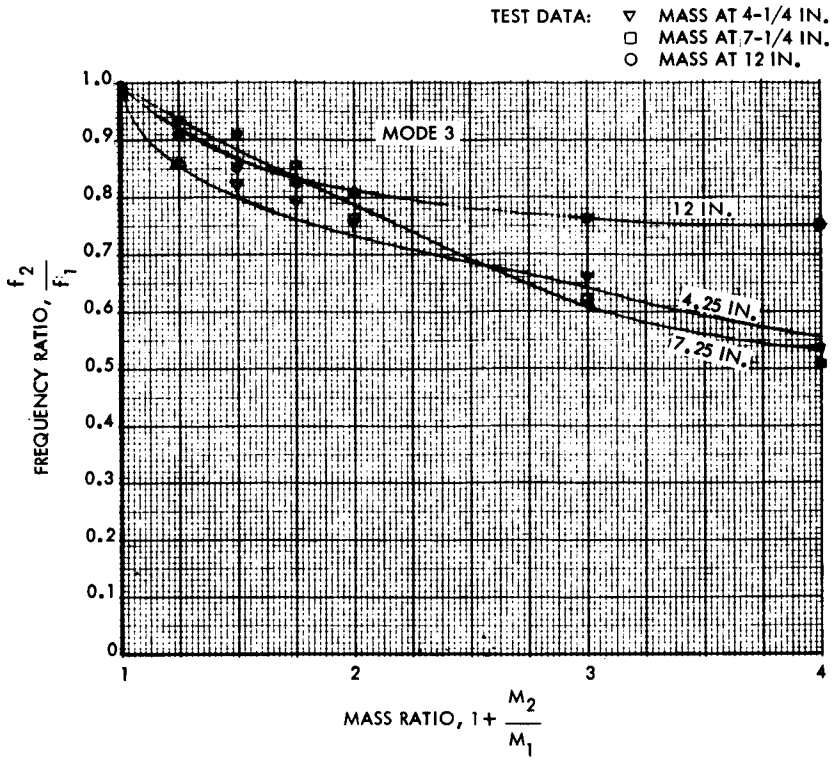

Figure 95. Mass-Loaded Beam, Frequency Comparison, Mode 3

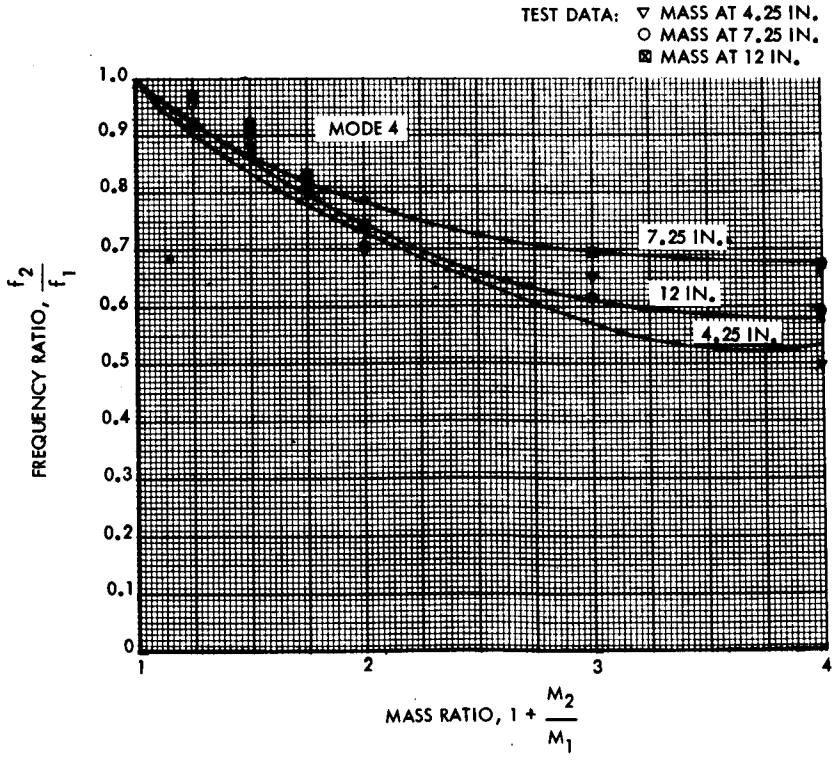

Figure 96. Mass-Loaded Beam, Frequency Comparison, Mode 4

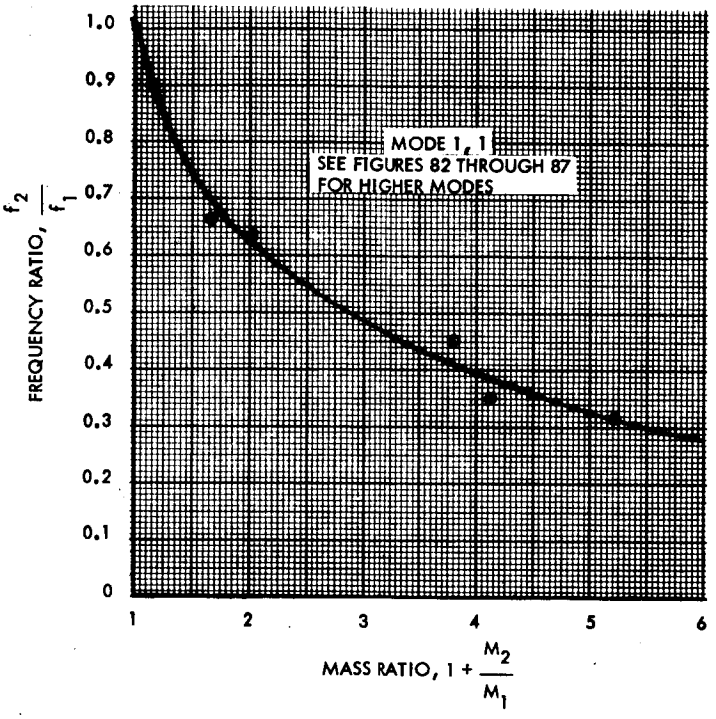

Figure 97. Mass-Loading Effects on Plate

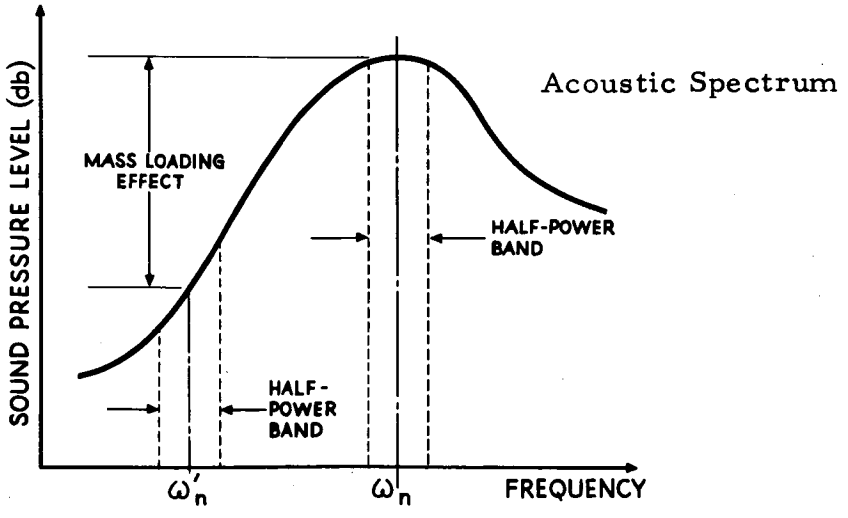

Figure 98. Typical Acoustic Spectrum

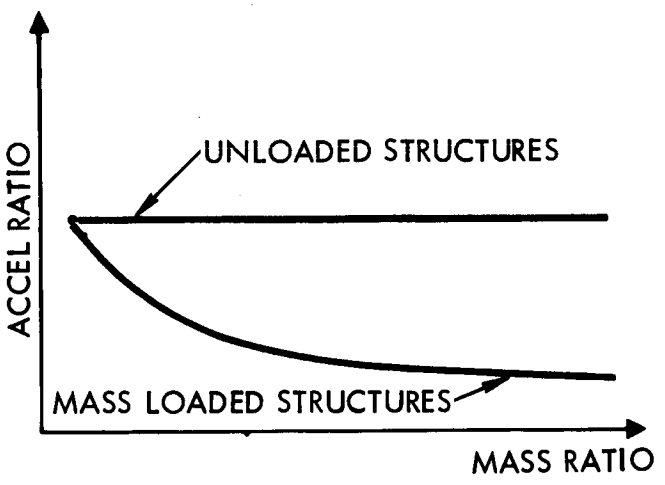

Figure 99. Prediction of Environment

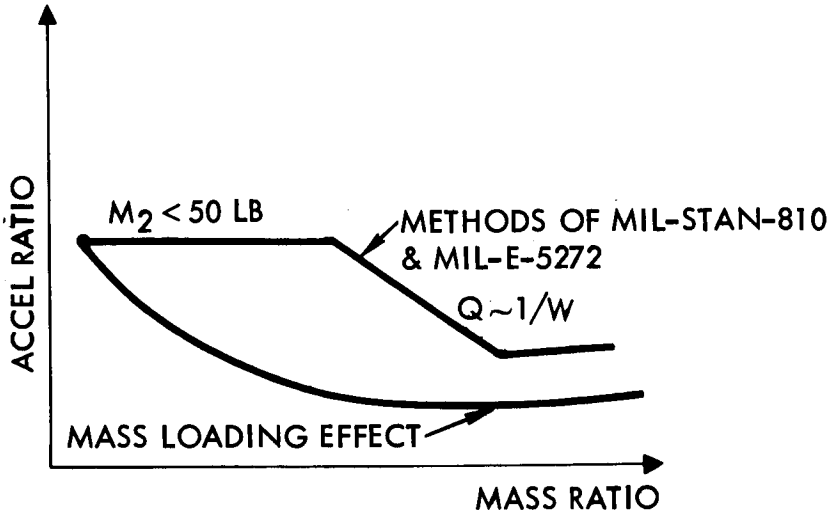

Figure 100. Environmental Specifications

For general application or direct solutions without giving a known environment for an unloaded structure, a thorough theoretical analysis using the presented methods instead of the figures is recommended.

DESIGN CRITERIA

After the shock and vibration environment is determined, it is a critical problem to define the design criteria and to develop an efficient method for designing an effective support structure as well as a component which can operate successfully under the dynamic environment. Design consideration involves many factors and is difficult to explain briefly; however, a detailed discussion is presented in the "Mass Coupling" Section, and the application of the mass-loading results have been described in their individual sections. Some important points that may be considered often in shock and vibration design are to be illustrated here.

Let the vibration environment be determined as in Figure 101, which shows an unconservative design that may result from the shift of the natural frequency; whereas, Figure 102 demonstrates a possible overconservative design. The difference between a design analysis accounting for the mass-loading effect and one assuming a constant damping coefficient, C, or a constant quality factor, Q, is shown in Figure 103. Figure 104 is a comparison of the mass-loading effect and the pseudo-static design concept, which assumes an attenuation factor inversely proportional to the weight of the mounted component.

TEST AND EVALUATION

Test and evaluation are important phases in the design, development, and reliability studies. Their success depends on an understanding of the mass-loading effect due to the mounted component.

The experimental phase of this report demonstrates the application of different concepts to test and evaluation. Consideration has been given to data analysis; design of test jigs; instrumentation; test set-ups; and methods of excitation including edge excitation, distributed force, point force, random, and sinusoidal. Three types of sources of excitation were used; they are mechanical, acoustical, and electromagnetic induction forces.

Environmental prediction techniques in conjunction with statistics constitute the most important factor to be considered in the definition of the requirement for test and evaluation. Design criteria and methods of analysis form the foundation of test-fixture design and the basis for interpretation of experimental results. From the analytical and experimental results, a certain type of test may be selected or substituted for test and evaluation of some special cases.

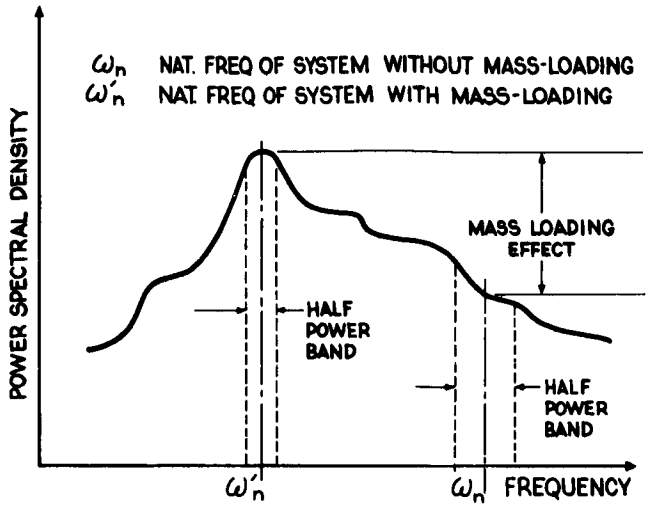

Figure 101. Power Spectrum for Random Vibration

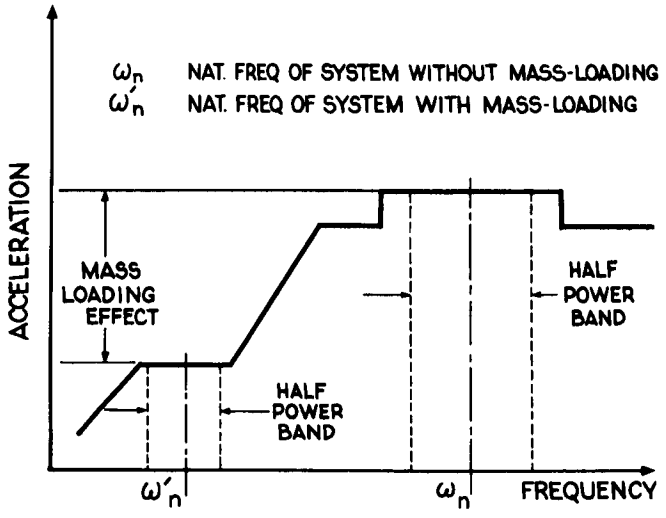

Figure 102. Acceleration Spectrum for Sinusoidal Forcing Function

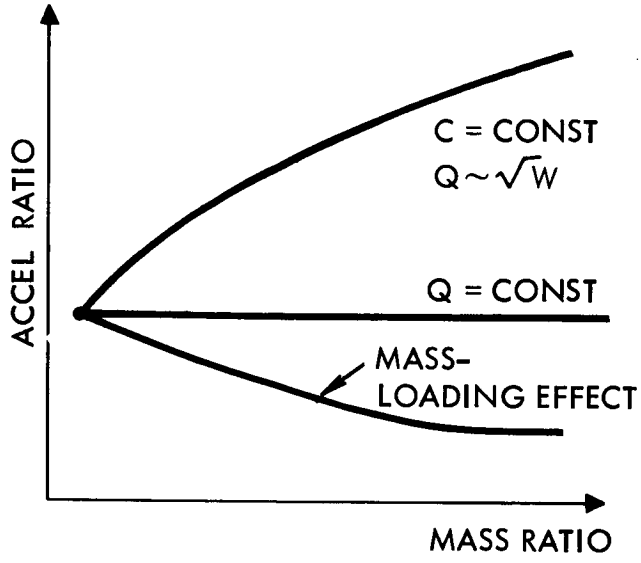

Figure 103. Vibration Analysis

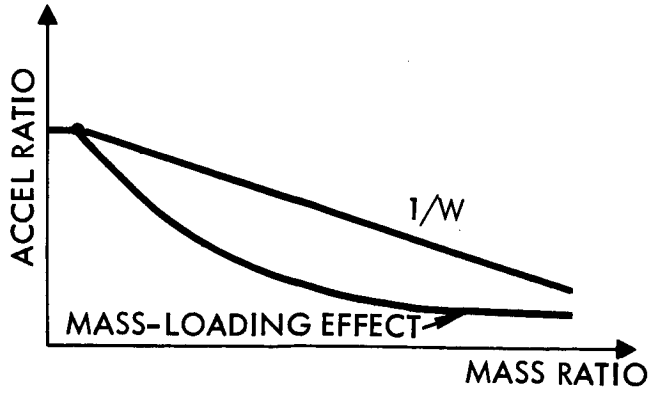

Figure 104. Pseudo-Static Design Concept

CONCLUSIONS AND RECOMMENDATIONS

The analytical and experimental studies of the program, which involved testing of 58 mass-loaded and unloaded structure models, can be concluded as follows:

1. Vibration response of mass-loaded structures differs significantly from that of unloaded structures. The vibration environment of components, defined as the response measured at the mounting point, is also greatly affected because of the phenomena of frequently shift and response attenuation due to the mass loading.

2. Analytical methods for computing natural frequencies and modes of the mass-loaded and unloaded structures have been developed through several approaches. The results agree closely with experimental data. In parallel with analytical methods, an empirical technique using charts or diagrams has been developed for prediction of frequency shift of the mass-loaded structures having similar material properties and geometry at the test specimens.

3. Vibration transmissibility and response characteristics of the mass-loaded structures can be predicted by a simple relation between the mass-loaded and unloaded structures. This relation is in the form

$$y = A + \frac{B}{x^n}$$

Detailed information is provided in the discussions on Mass-Loaded Beam and Mass-Loaded Plate Transmissibility Characteristics and in the Applications of the Mass-Loading Effects discussion.

4. Transmissibility characteristics of typical aerospace local structures is found dependent not only on damping but also on interaction among the component, local structure, bracketry, and damping. In fact, an increase of damping in a mass-coupled system may cause a higher response. This phenomenon is analyzed in detail in the Mass-Coupling discussion.

5. Experiments were accomplished through the use of a mechanical shaker, acoustic chamber, and electromagnetic-induction shaker representing edge excitation, uniformly distributed force, concentrated force, constant acceleration spectrum, constant force spectrum, sinusoidal excitation, and random excitations. Experiments were performed on 58 test models.

This program represents an exploratory investigation on mass-loading effects on localized vibratory environments of rocket vehicles. Although all the objectives have been successfully accomplished as planned, there remain several areas requiring further studies; i. e.:

1. Mass-Loading Effects on Structures of Different Geometry and Material Properties: For generalization of the empirical technique for prediction of vibratory environments; more studies on this area are needed.

2. Mass-Loading Effects on Shell Structures: Extend the basic approaches and methods of mass loading effects to investigate vibration response and transmissibility of shell structures mounted with components such as discrete masses, ring-frames, bulkheads, etc.

3. Mass-Loading Effects on Honeycomb Structures: This study would lead to more understanding of mass-loading problems as applied to aerospace vehicles since honeycomb construction are widely used in aerospace structures.

4. Mass-Loading Effects Under Shock: Because shock loads often produce ultimate stresses, it is important to investigate how the mass-loading and coupling effects alter the shock environment and response; this effort includes an investigation of the frequency shift and mass attenuation phenomena under shock loads instead of vibration loads.

5. Mass-Loading Effects Under Progressive Waves: Because of the imperfection in generating uniform sonic pressure over the test specimen in an acoustic reverberant chamber, it is recommended that the mass-loading effects under acoustic progressive waves be investigated to obtain more reliable data, from which a solution of an important acoustic mass-loading problem can be accomplished.

REFERENCES

1. Mahaffey, P. T. and Smith, K. W. "Methods for Predicting Environmental Vibration Levels in Jet Powered Vehicles," Noise Control (July-August 1960).

2. Franken, P. "Sound Induced Vibration of Cylindrical Vehicles," J. Acou. Soci. of America, Vol 34, No. 4 (April 1962).

3. MIL-STD-810 Dynamic Conference; USAF-ASD Wright-Patterson Air Force Base, Ohio (September 1960).

4. Schock, R. W. "Vibration, Acoustic, and Shock Environmental Specifications for Saturn Vehicles," NASA Internal Notes (1964-1966).

5. Barrett, R. E. "Statistical Techniques for Describing Localized Vibratory Environments of Rocket Vehicles," NASA TN D-2158, NASA/MSFC (July 1964).

6. Jewell, R. E. "A Technique for Predicting Localized Vibration Environments in Rocket Vehicles and Spacecraft," Shock and Vibration Bulletin No. 33, Part II (March 1964), pp. 26-33.

7. Lifer, C. E. "Design of Space Vehicle Structures for Vibration and Acoustic Environments," Shock and Vibration Bulletin No. 33, Part IV (March 1964), pp. 201-207.

8. Barrett, R. E. "Techniques for Predicting Localized Vibratory Environments of Rocket Vehicles," NASA TN D-1836 (Oct. 1963).

9. Lee, S. Y. "Shock and Vibration Analysis of Structures" Research Report ME590, Mechanical Engineering Department, University of Southern California (1959).

10. Lee, S. Y. "The Mass-Loading and Mass-Coupling Effects on Vibration Response," Research Reports AE590, Mechanical Engineering Department, University of Southern California (1959-1962).

11. Lee, S. Y. "Sonic Induced Vibration and Control for Advanced Spacecraft," Presented at the 65th Meeting of Acoustical Society of America, May 15-18, 1963, New York.

12. Lee, S.Y. "Vibration Environment and Design Development Program" SD 62-74, NAA-S&ID (May 1962).

13. Lee, S.Y. "Test Results of Mass-Loading and Mass-Coupling Investigation," Dynamic Sciences Internal Report, NAA-S&ID (June 1963).

14. Lee, S.Y. and M. Chapman, "Technical Proposal for a Study of Mass Loading Effects on Localized Vibratory Environments of Rocket Vehicles," NAA-S&ID, SID 64-2180-1 (December 1964).

15. Pan, H.H. "Transverse Vibration of an Euler Beam Carrying a System of Heavy Bodies," J. App. Mech., ASME (June 1965) pp. 434-437.

16. Myklestad, N.O. Vibration Analysis, p. 239.

17. McCue, G.A. and H.J. DuPrie. Improved FORTRAN IV Function Contouring Program. NAA S&ID, SID 65-672 (April 1, 1965).

18. Timoshenko, S. Vibration Problems in Engineering, D. Van Nostrand Co. (1928).

19. Den Hartog, J.P. Mechanical Vibrations, McGraw-Hill Book Co., New York (1934).

20. Curtis, A.J. and Boykin, T.R. "Response of Two-Degree-of-Freedom Systems to White Noise Base Excitation," J. Acoust. Soc. Am., 33:655-663, 1961.

21. Crandall, S.H., and W.D. Mark. Random Vibration in Mechanical Systems, Academic Press, New York, 1963.

22. Morrow, C.T. and R.B. Muchmore, J. Appl. Mech. 22, 367 (1955).

23. Lee, S.Y. "Vibration Environment and Design Development Program," SD 62-74, NAA (May 1962).

24. Lee, S.Y. "The Mass-Loading and Mass-Coupling Effects on Vibration Response," Research Report AE590, Univ. of Southern California (1959-1962).

25. Crede, C.E. and E.J. Lunney. WADC TR 56-503, ASTIA No. AD AD 118133 (December 1956).

26. McIntosh, V.C. WADC TN 59-193 (February 1960).

27. Graniek, N. and C.E. Thomas. WADC TN 56-514, ASTIA No. AD 110620 (December 1956).

28. Crandall, S. Random Vibration, The MIT Technical Press (1958).

29. Crandall, S. Random Vibration, Vol. 2, The MIT Technical Press (1963).

APPENDIX A

MODE SHAPES OF BEAM FROM COMPUTER PROGRAM

In the following pages the first four mode shapes of the unloaded and mass-loaded beams obtained from the computer program are presented. Table 12 designates the weight and location for each case.

Table 12. Mass-Loaded Beam Designation

Case No.	Additional Weight m^2 (Pounds)	Weight Location (Inches)	Mass Ratio (m_2/m_1*)
1	0.165	4.25	0.25
2	0.165	7.25	
3	0.165	12.00	
4	0.231	4.25	0.35
5	0.231	7.25	
6	0.231	12.00	
7	0.330	4.25	0.50
8	0.330	7.25	
9	0.330	12.00	
10	0.495	4.25	0.75
11	0.495	7.25	
12	0.495	12.00	
13	0.660	4.25	1.0
14	0.660	7.25	
15	0.660	12.00	
16	1.320	4.25	2.0
17	1.320	7.25	
18	1.320	12.00	
19	1.980	4.25	3.0
20	1.980	7.25	
21	1.980	12.00	

(*) m_1 = Weight of beam = 0.66 lb.

DECEMBER 13, 1965

2463-01
005 000

MASS LOADING EFFECTS ON BEAM VIBRATION-FIXED ENDS

FREQUENCY (1) = 4.1634613E 02 RAD./SEC., 6.6263544E 01 C.P.S.
STRUCTURAL MODE (1)
NORMALIZED TO TOTAL WEIGHT
TOTAL WEIGHT = 6.5999989E-01
DEFLECTION - IN./IN.

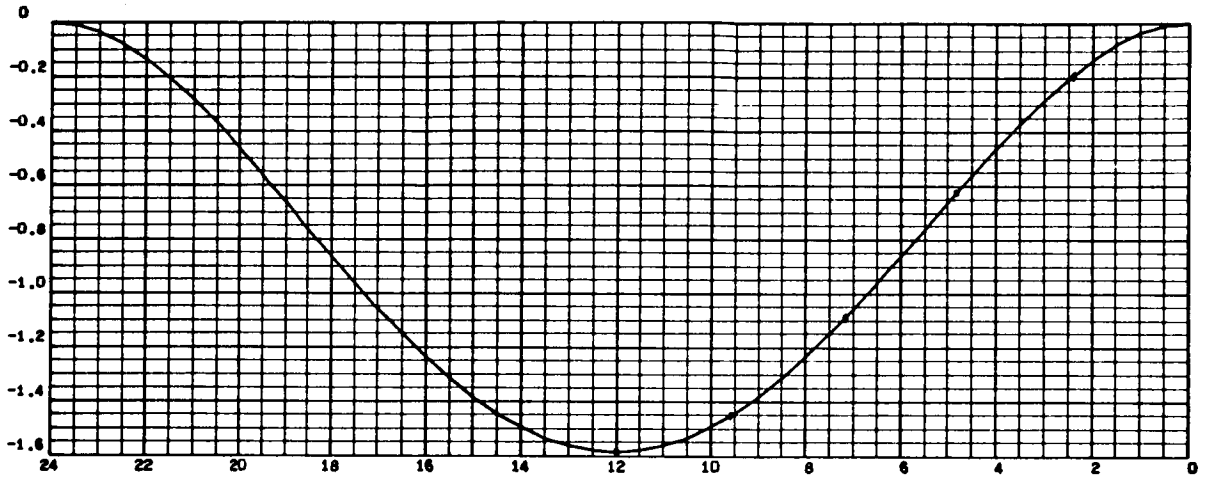

VEHICLE STATIONS - INCHES
SLOPE - RAD./IN.

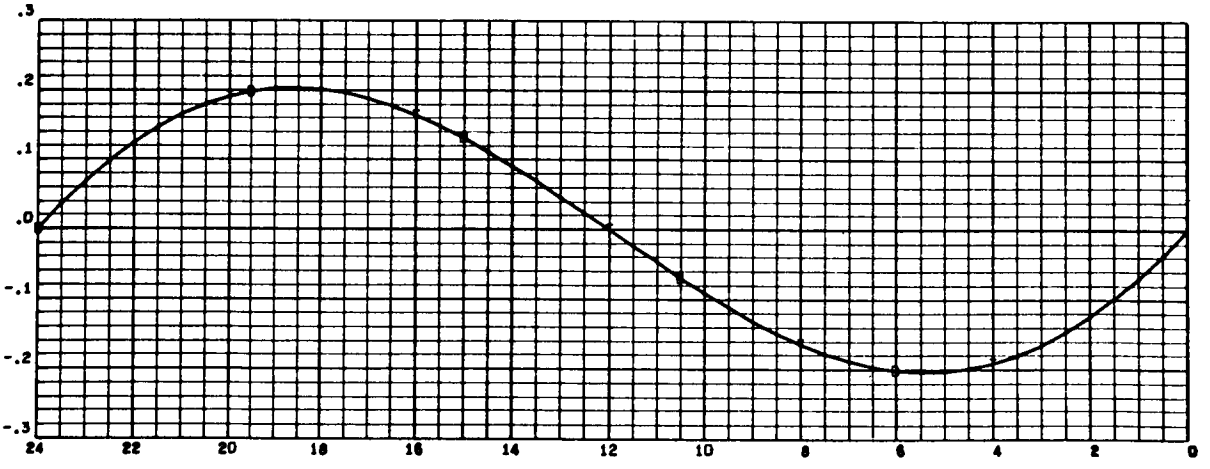

T = TOTAL SLOPE B = BENDING SLOPE
VEHICLE STATIONS - INCHES

DECEMBER 13, 1965

2463-01
007 000

MASS LOADING EFFECTS ON BEAM VIBRATION-FIXED ENDS

FREQUENCY (2) = 1.1471271E 03 RAD./SEC., 1.8257095E 02 C.P.S.
STRUCTURAL MODE (2)
NORMALIZED TO TOTAL WEIGHT
TOTAL WEIGHT = 6.5999989E-01
DEFLECTION - IN./IN.

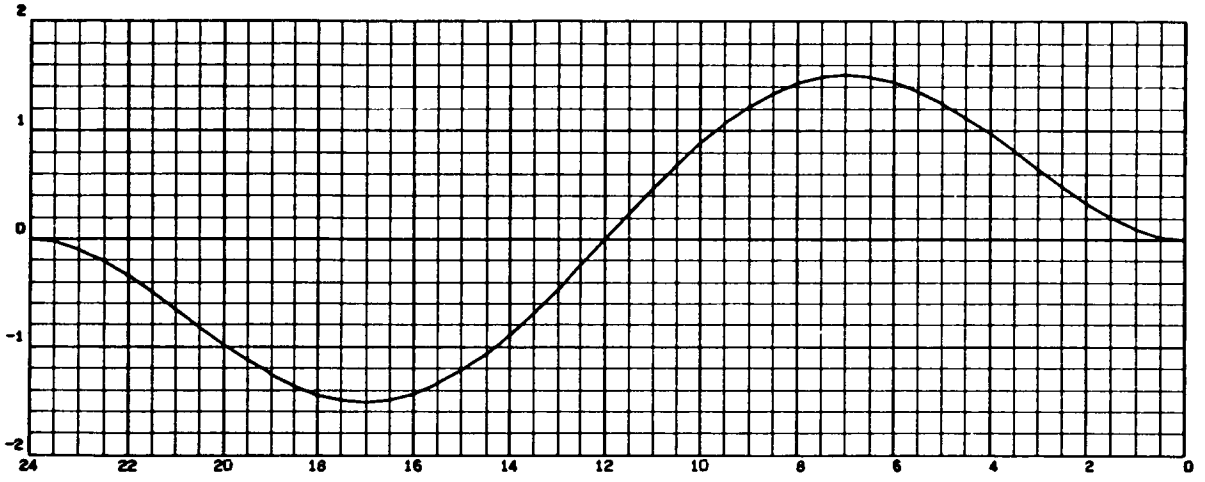

VEHICLE STATIONS - INCHES
SLOPE - RAD./IN.

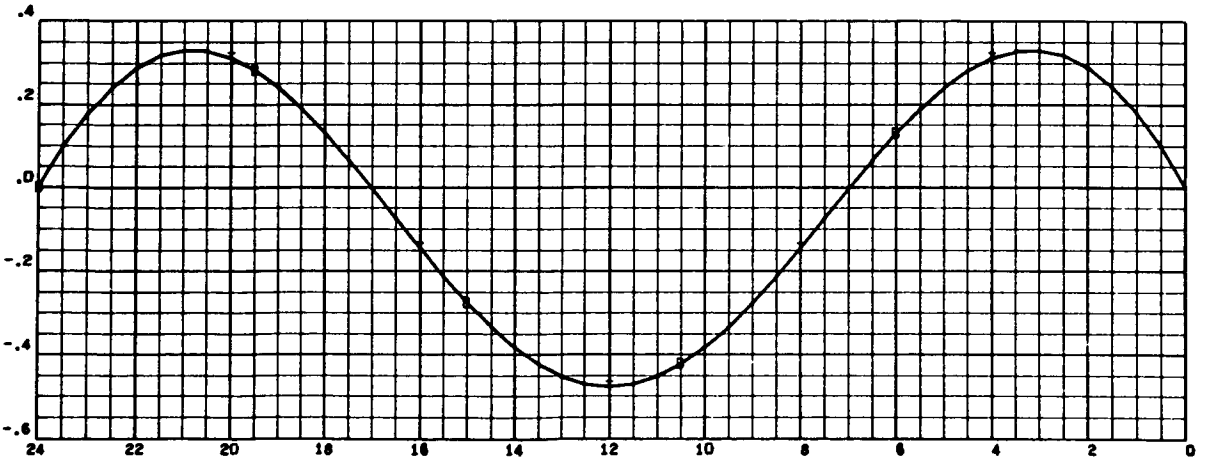

T = TOTAL SLOPE B = BENDING SLOPE
VEHICLE STATIONS - INCHES

DECEMBER 13, 1965

2463-01
009 000

MASS LOADING EFFECTS ON BEAM VIBRATION-FIXED ENDS

FREQUENCY (3) = 2.2474179E 03 RAD./SEC., 3.5768766E 02 C.P.S.
STRUCTURAL MODE (3)
NORMALIZED TO TOTAL WEIGHT
TOTAL WEIGHT = 6.5999989E-01
DEFLECTION - IN./IN.

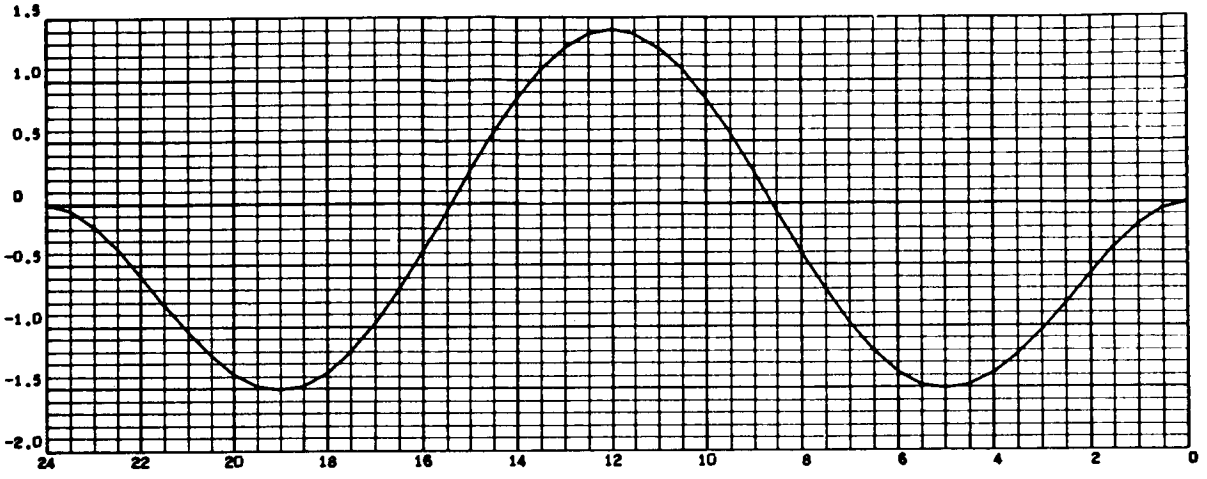

VEHICLE STATIONS - INCHES
SLOPE - RAD./IN.

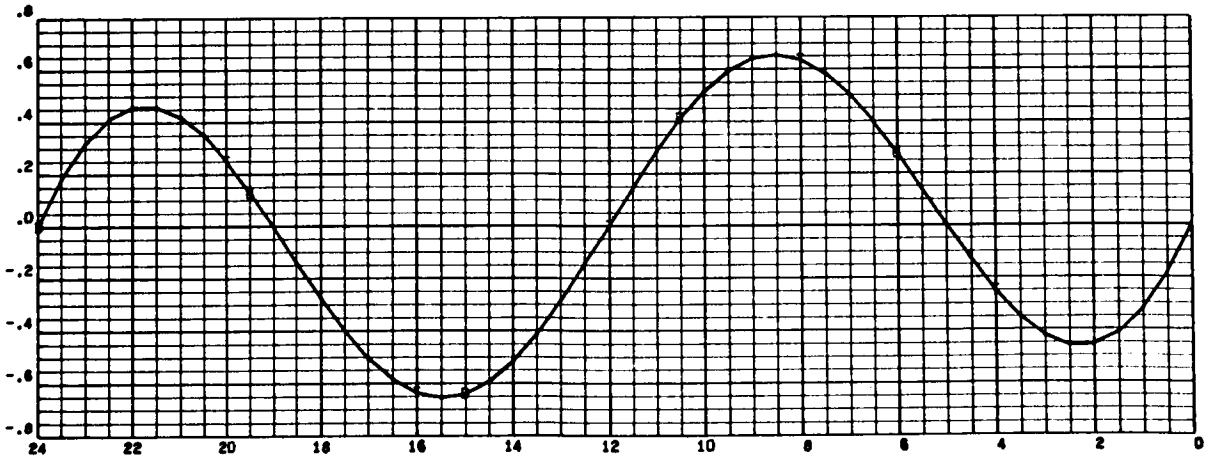

T = TOTAL SLOPE B = BENDING SLOPE
VEHICLE STATIONS - INCHES

DECEMBER 13, 1965

2463-01
011 000

MASS LOADING EFFECTS ON BEAM VIBRATION-FIXED ENDS

FREQUENCY (4) = 3.7121583E 03 RAD./SEC., 5.9080834E 02 C.P.S.
STRUCTURAL MODE (4)
NORMALIZED TO TOTAL WEIGHT
TOTAL WEIGHT = 6.5999989E-01
DEFLECTION - IN./IN.

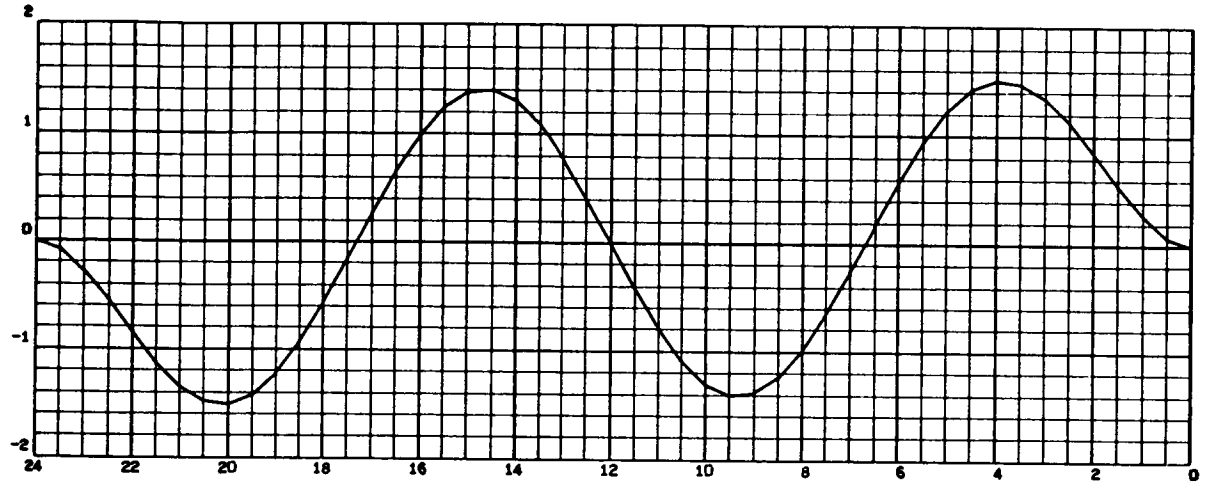

VEHICLE STATIONS - INCHES
SLOPE - RAD./IN.

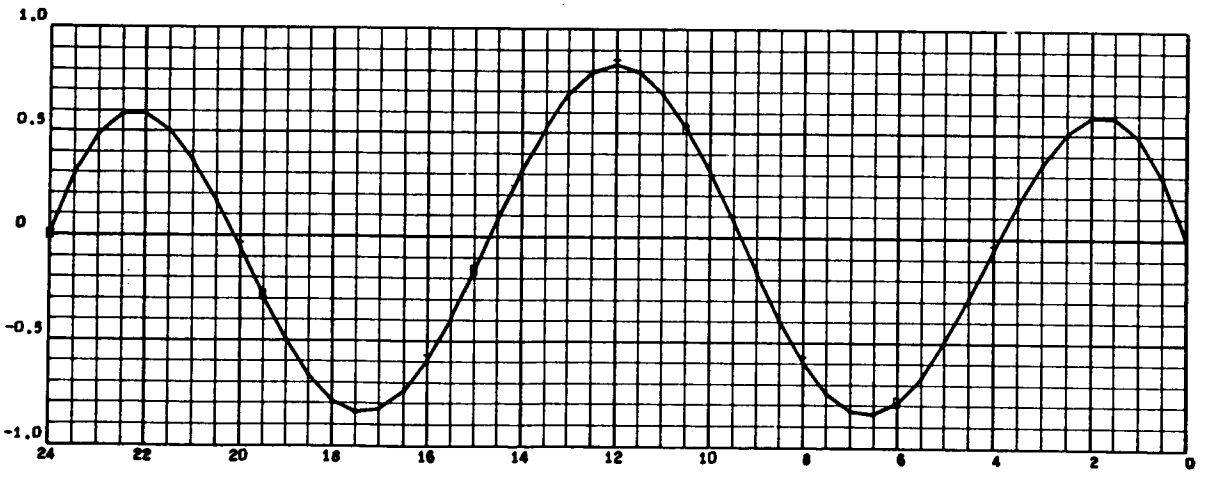

T = TOTAL SLOPE B = BENDING SLOPE
VEHICLE STATIONS - INCHES

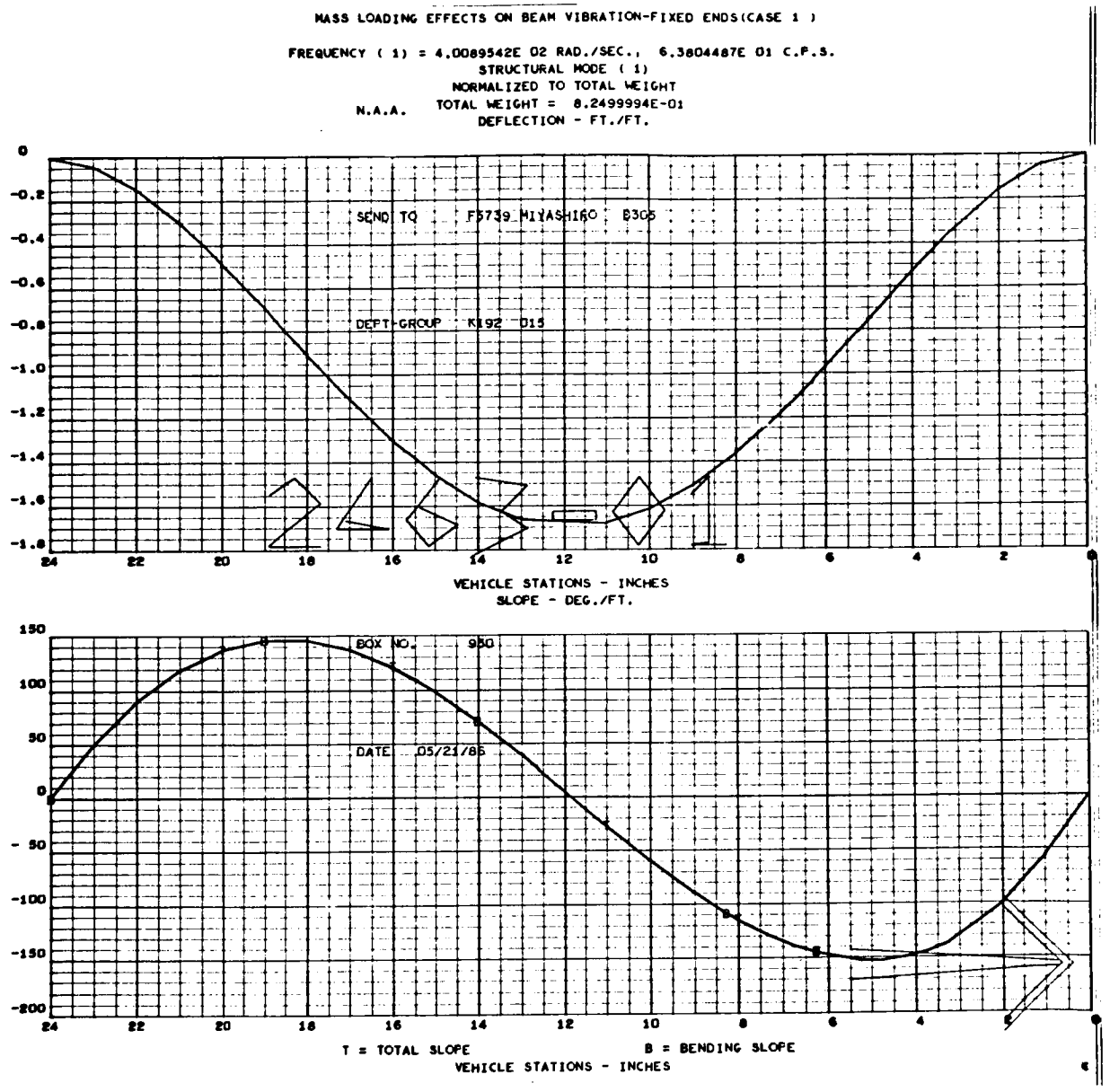
MASS LOADING EFFECTS ON BEAM VIBRATION-FIXED ENDS(CASE 1)
FREQUENCY (1) = 4.0089542E 02 RAD./SEC., 6.3804487E 01 C.P.S.
STRUCTURAL MODE (1)
NORMALIZED TO TOTAL WEIGHT
N.A.A. TOTAL WEIGHT = 8.2499994E-01
DEFLECTION - FT./FT.
SEND TO F5739 MIYASHIRO B305
DEPT-GROUP K192 D15
VEHICLE STATIONS - INCHES
SLOPE - DEG./FT.
BOX NO. 950
DATE 05/21/65
T = TOTAL SLOPE
B = BENDING SLOPE
VEHICLE STATIONS - INCHES

2463-01
002 000

MASS LOADING EFFECTS ON BEAM VIBRATION-FIXED ENDS(CASE 1)

FREQUENCY (2) = 9.9628259E 02 RAD./SEC., 1.5856330E 02 C.P.S.
STRUCTURAL MODE (2)
NORMALIZED TO TOTAL WEIGHT
TOTAL WEIGHT = 8.2499994E-0'
DEFLECTION - FT./FT.

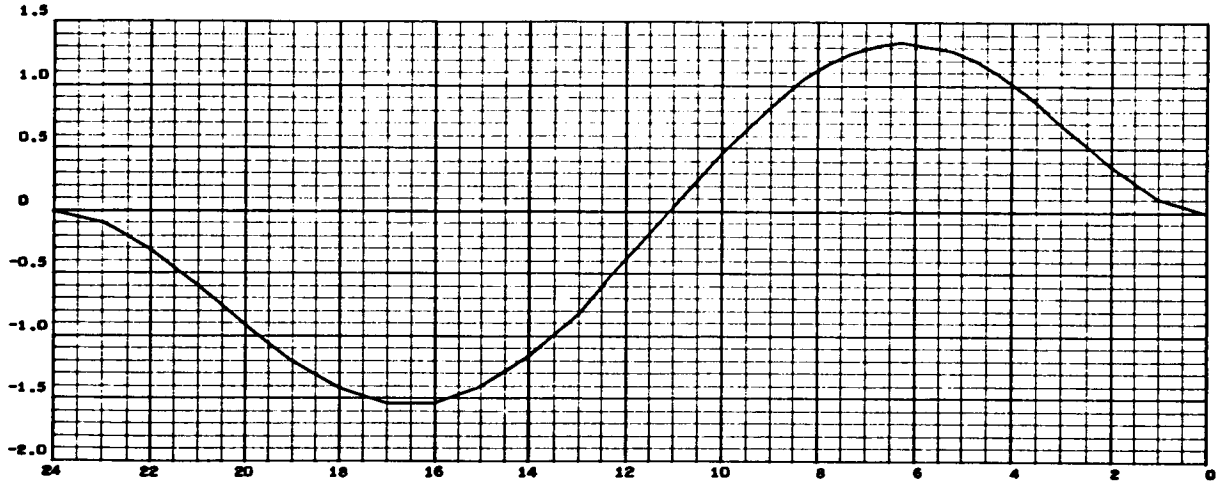

VEHICLE STATIONS - INCHES
SLOPE - DEG./FT.

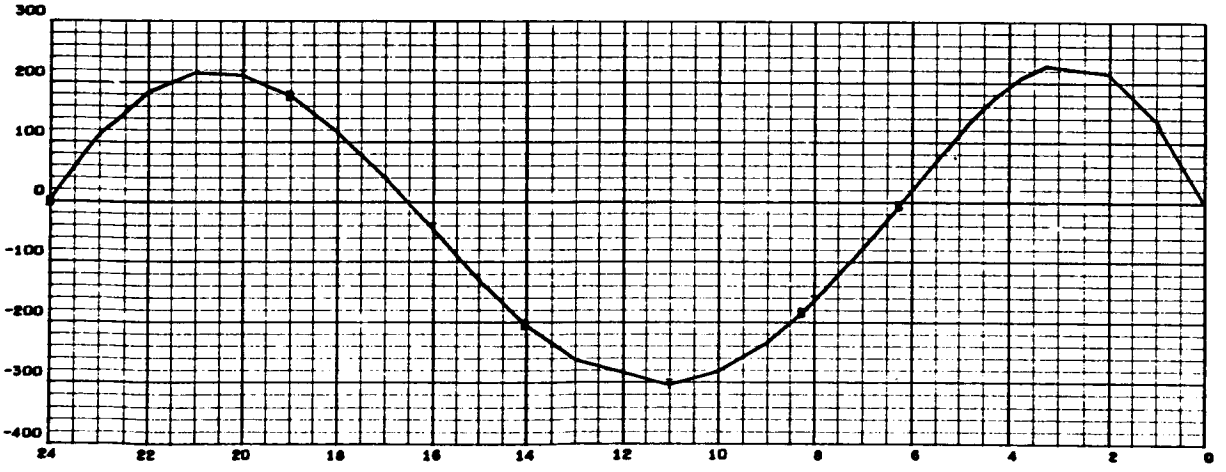

T = TOTAL SLOPE B = BENDING SLOPE
VEHICLE STATIONS - INCHES

MAY 21, 1966 2463-01
004 000

MASS LOADING EFFECTS ON BEAM VIBRATION-FIXED ENDS(CASE 1)

FREQUENCY (3) = 1.9203372E 03 RAD./SEC., 3.0563115E 02 C.P.S.
STRUCTURAL MODE (3)
NORMALIZED TO TOTAL WEIGHT
TOTAL WEIGHT = 8.2499994E-01
DEFLECTION - FT./FT.

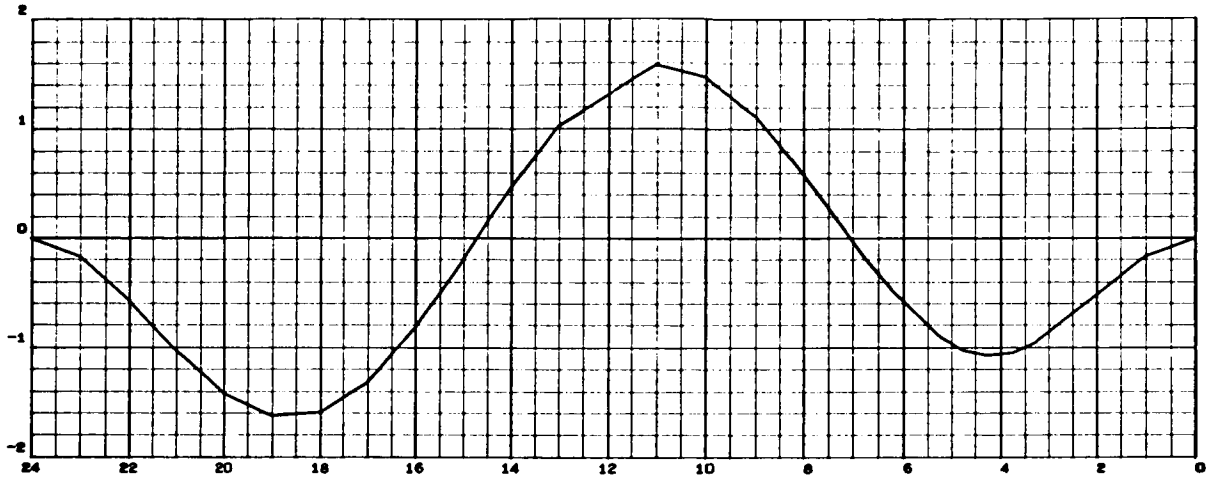

VEHICLE STATIONS - INCHES
SLOPE - DEG./FT.

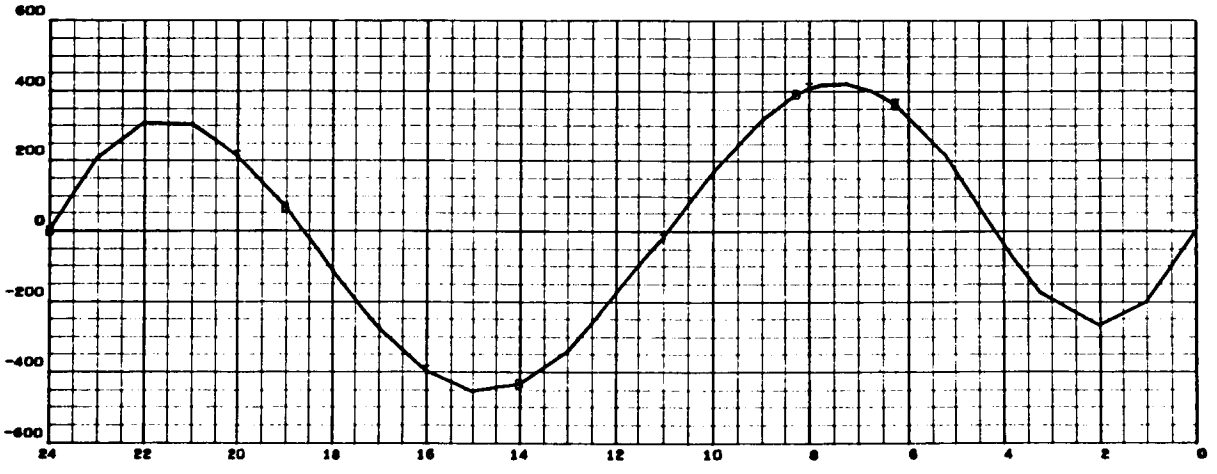

T = TOTAL SLOPE B = BENDING SLOPE
VEHICLE STATIONS - INCHES

MAY 21, 1966

2463-01
006 000

MASS LOADING EFFECTS ON BEAM VIBRATION-FIXED ENDS(CASE 1)

FREQUENCY (4) = 3.2392780E 03 RAD./SEC., 5.1554711E 02 C.P.S.
STRUCTURAL MODE (4)
NORMALIZED TO TOTAL WEIGHT
TOTAL WEIGHT = 8.2499994E-01
DEFLECTION - FT./FT.

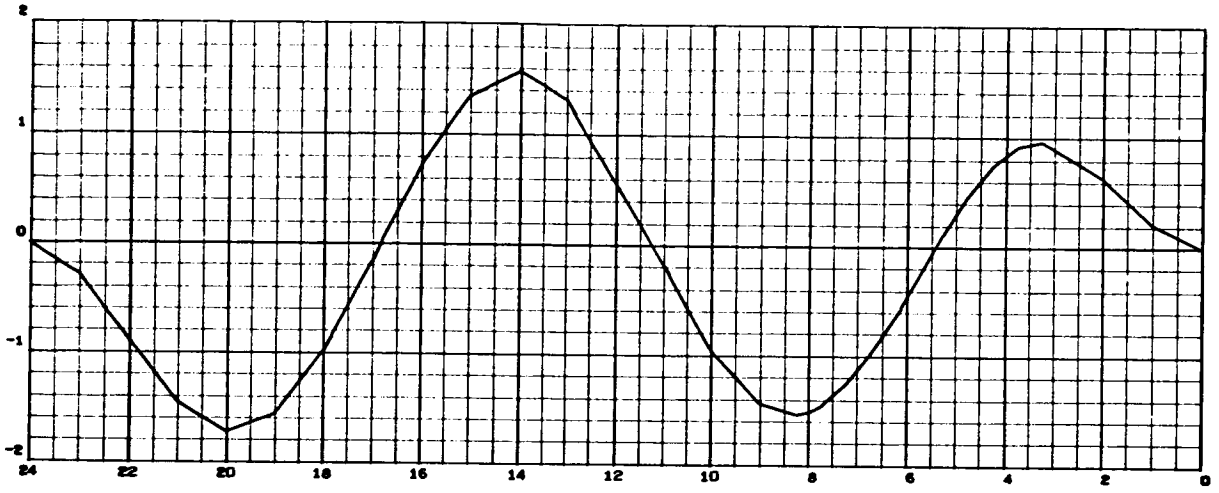

VEHICLE STATIONS - INCHES
SLOPE - DEG./FT.

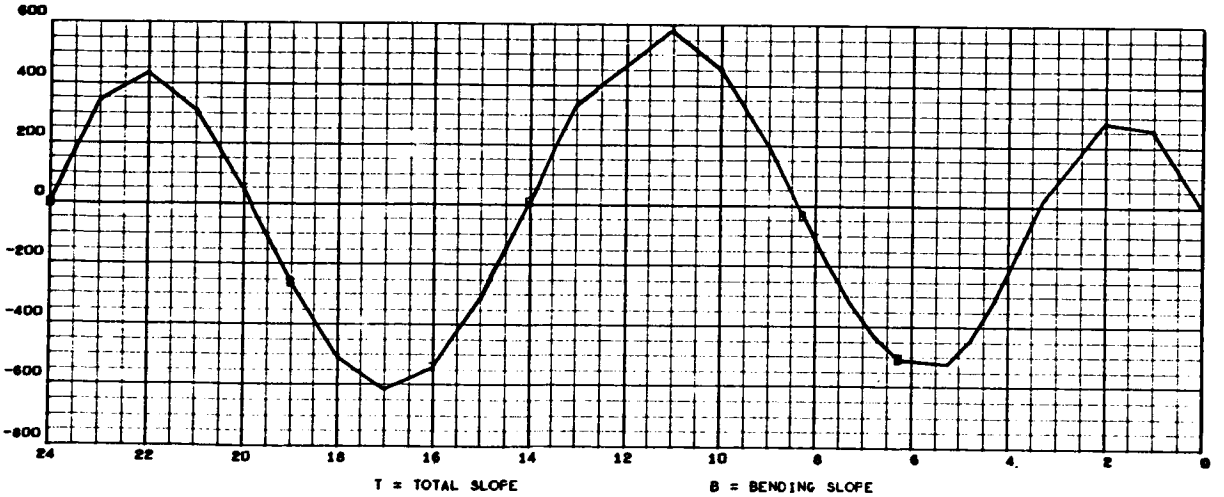

T = TOTAL SLOPE B = BENDING SLOPE
VEHICLE STATIONS - INCHES

MAY 21, 1966

2463-01
008 000

MASS LOADING EFFECTS ON BEAM VIBRATION-FIXED ENDS (CASE 2)

FREQUENCY (1) = 3.6102700E 02 RAD./SEC., 5.7459232E 01 C.P.S.
STRUCTURAL MODE (1)
NORMALIZED TO TOTAL WEIGHT
TOTAL WEIGHT = 8.2499993E-01
DEFLECTION - FT./FT.

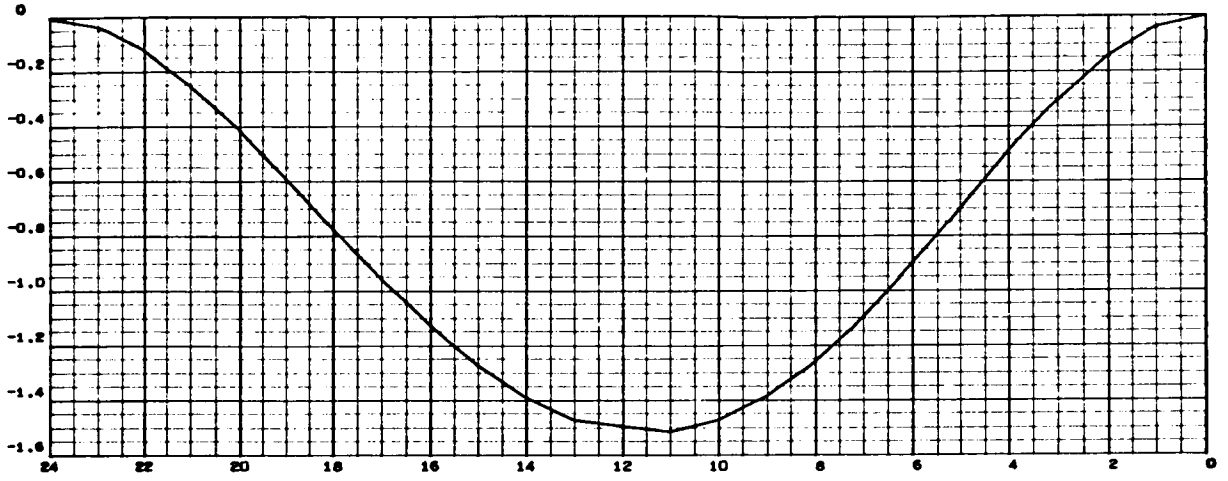

VEHICLE STATIONS - INCHES
SLOPE - DEG./FT.

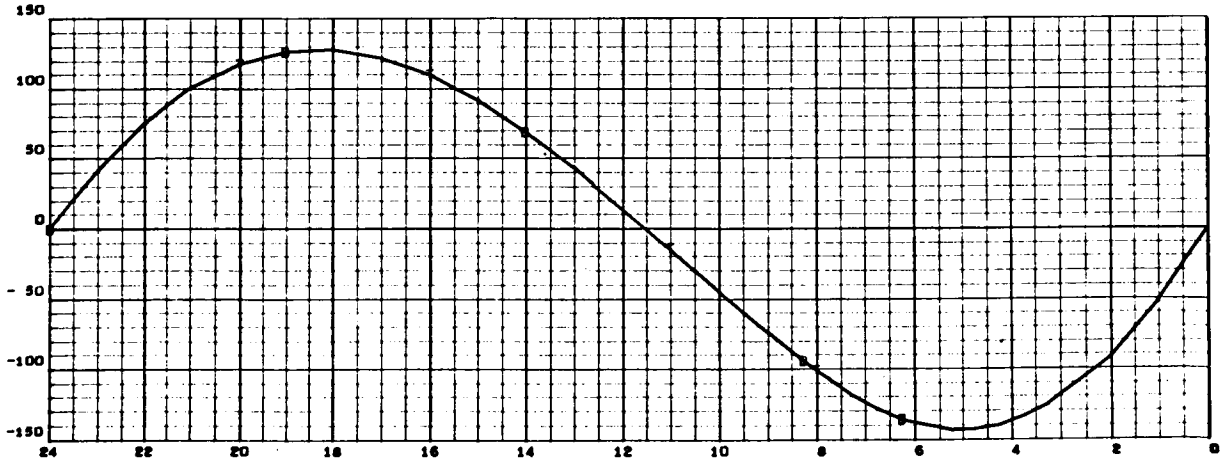

T = TOTAL SLOPE B = BENDING SLOPE
VEHICLE STATIONS - INCHES

MAY 21, 1966

2463-01
010 000

MASS LOADING EFFECTS ON BEAM VIBRATION-FIXED ENDS (CASE 2)

FREQUENCY (2) = 9.6047157E 02 RAD./SEC., 1.5286380E 02 C.P.S.
STRUCTURAL MODE (2)
NORMALIZED TO TOTAL WEIGHT
TOTAL WEIGHT = 8.2499993E-01
DEFLECTION - FT./FT.

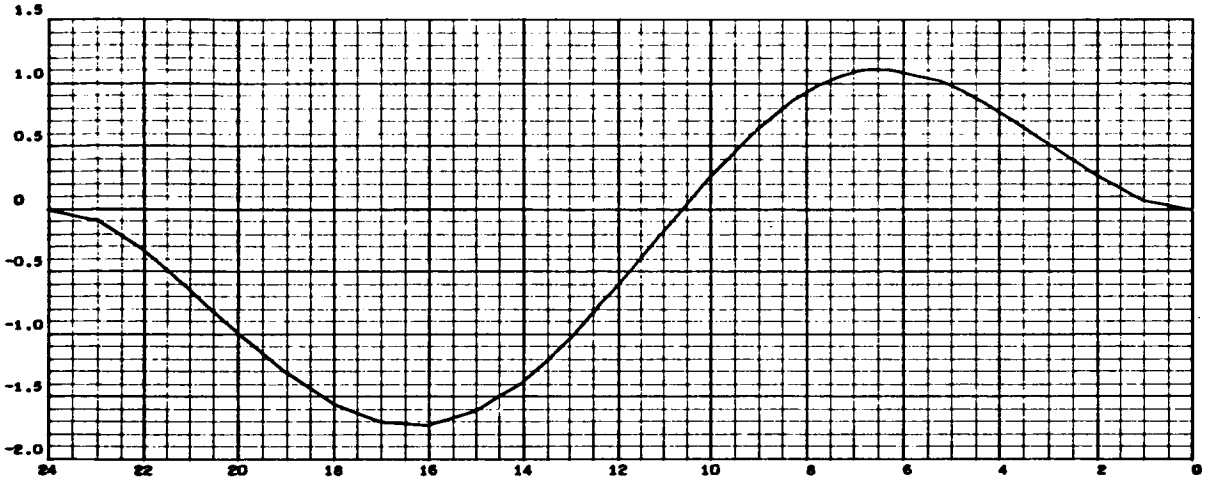

VEHICLE STATIONS - INCHES
SLOPE - DEG./FT.

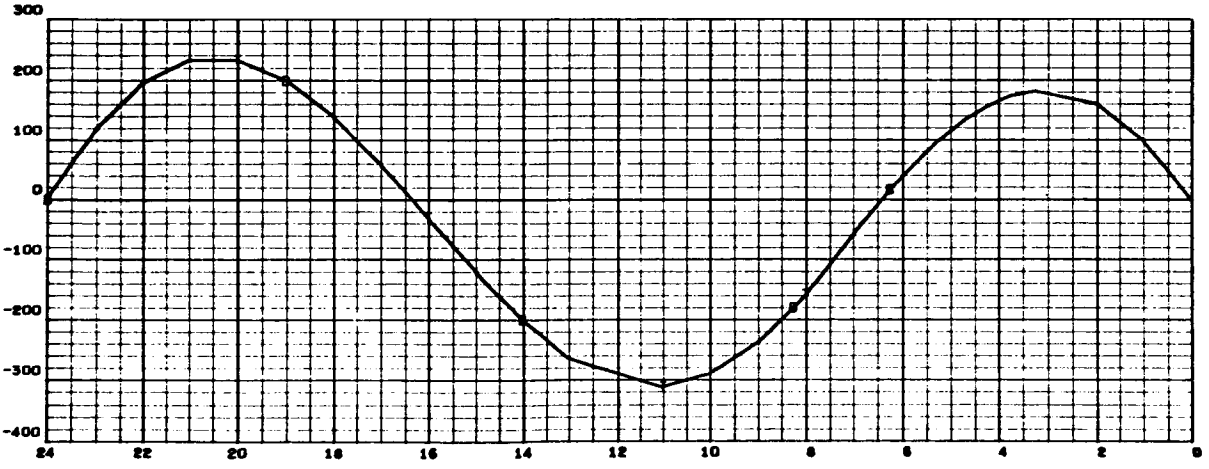

T = TOTAL SLOPE B = BENDING SLOPE
VEHICLE STATIONS - INCHES

MAY 21, 1966

2463-01 SL
012 000

MASS LOADING EFFECTS ON BEAM VIBRATION-FIXED ENDS (CASE 2)

FREQUENCY (3) = 2.0924209E 03 RAD./SEC., 3.3301913E 02 C.P.S.
STRUCTURAL MODE (3)
NORMALIZED TO TOTAL WEIGHT
TOTAL WEIGHT = 8.2499993E-01
DEFLECTION - FT./FT.

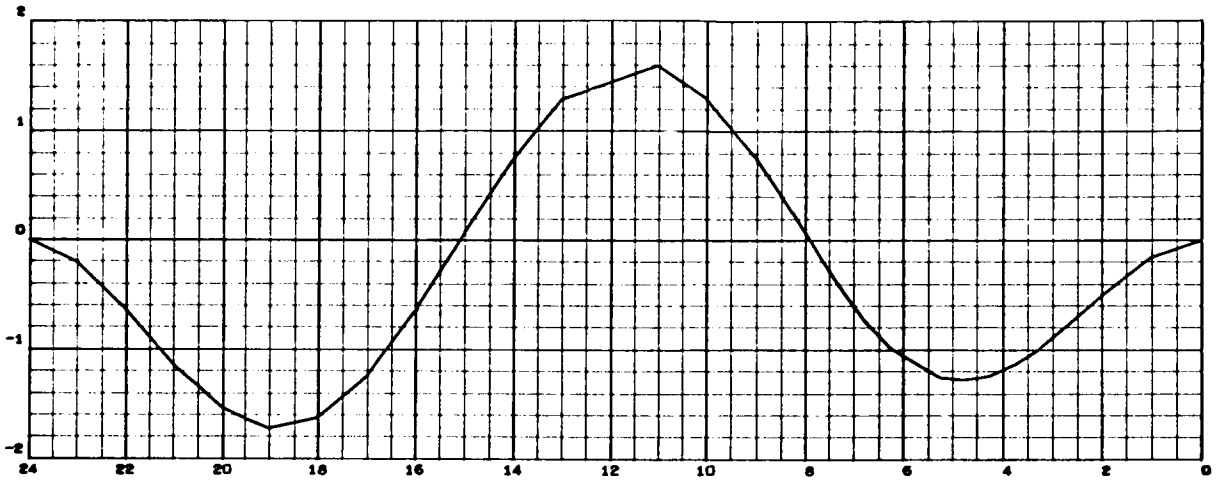

VEHICLE STATIONS - INCHES
SLOPE - DEG./FT.

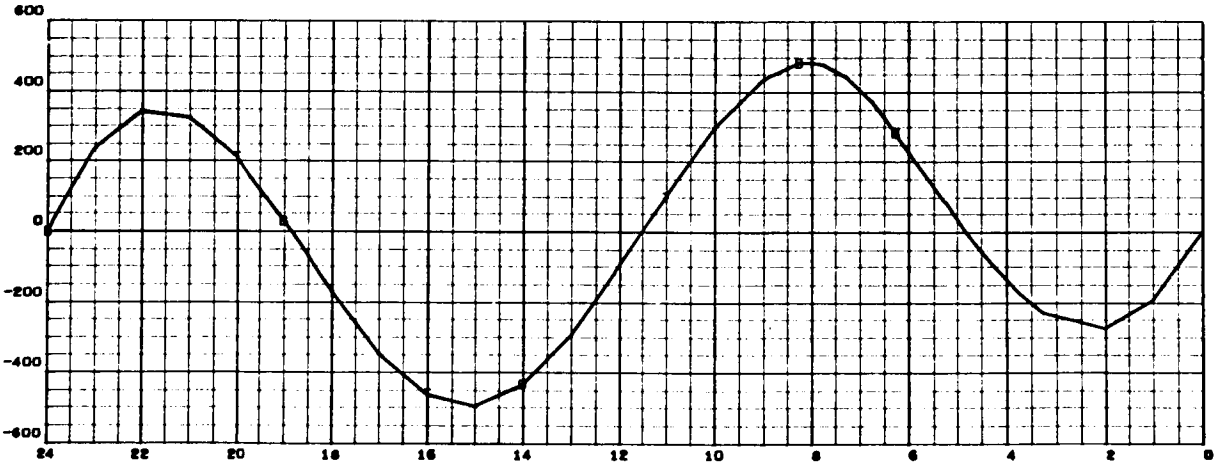

T = TOTAL SLOPE B = BENDING SLOPE
VEHICLE STATIONS - INCHES

MAY 21, 1966

2463-01
014 000

MASS LOADING EFFECTS ON BEAM VIBRATION-FIXED ENDS (CASE 2)

FREQUENCY (4) = 3.3570339E 03 RAD./SEC., 5.3428654E 02 C.P.S.
STRUCTURAL MODE (4)
NORMALIZED TO TOTAL WEIGHT
TOTAL WEIGHT = 8.2499993E-01
DEFLECTION - FT./FT.

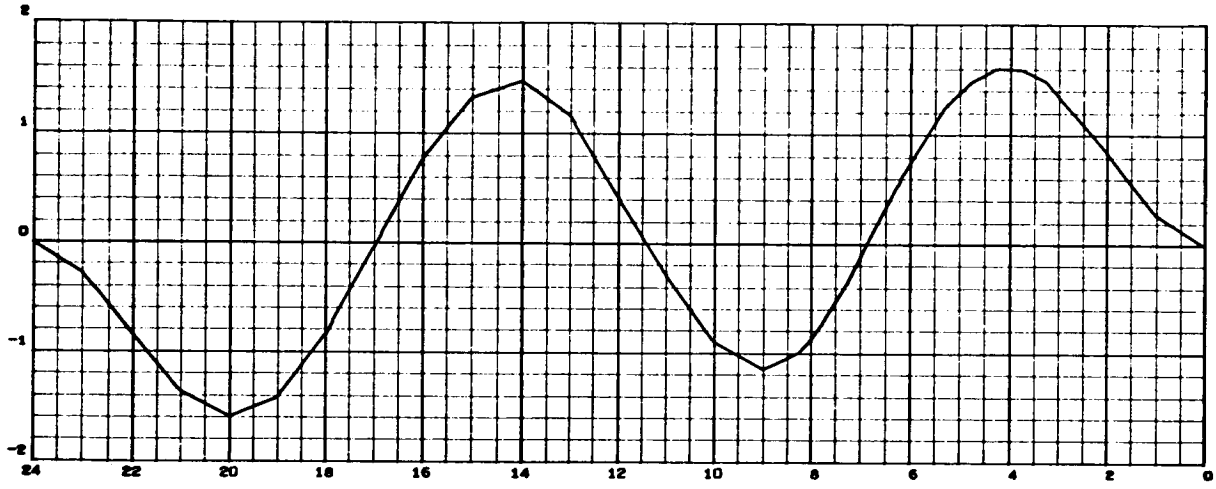

VEHICLE STATIONS - INCHES
SLOPE - DEG./FT.

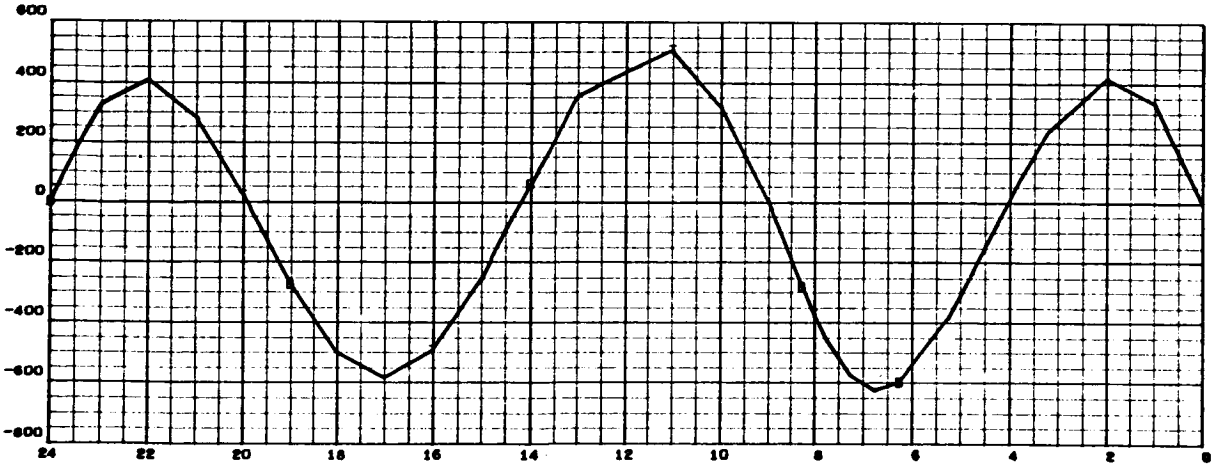

T = TOTAL SLOPE B = BENDING SLOPE
VEHICLE STATIONS - INCHES

MAY 21, 1966

2463-01 L
016 000

MASS LOADING EFFECTS ON BEAM VIBRATION-FIXED ENDS (CASE 3)

FREQUENCY (1) = 3.2621033E 02 RAD./SEC., 5.1917986E 01 C.F.S.
STRUCTURAL MODE (1)
NORMALIZED TO TOTAL WEIGHT
TOTAL WEIGHT = 8.2499991E-01
DEFLECTION - FT./FT.

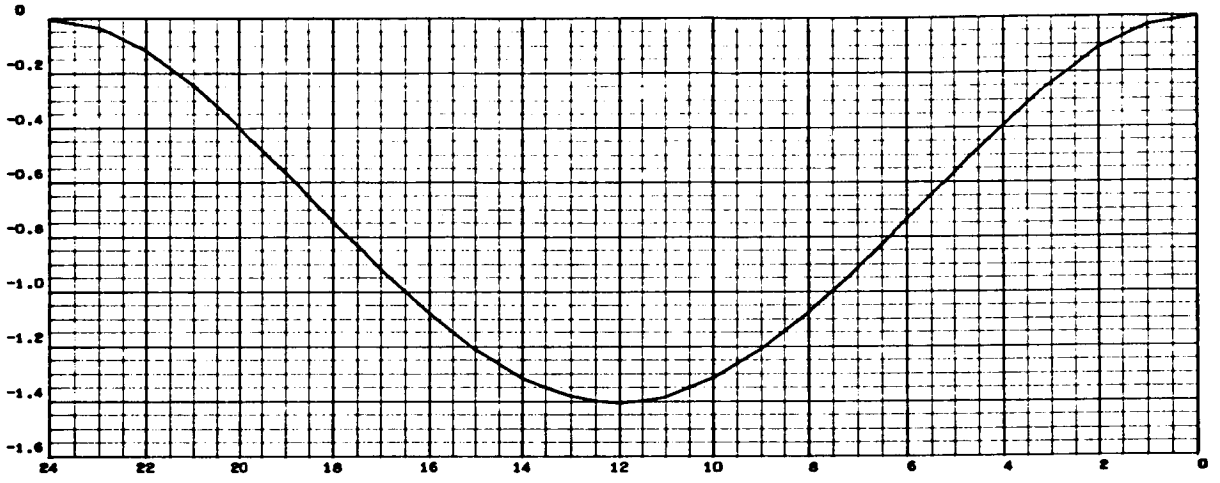

VEHICLE STATIONS - INCHES
SLOPE - DEG./FT.

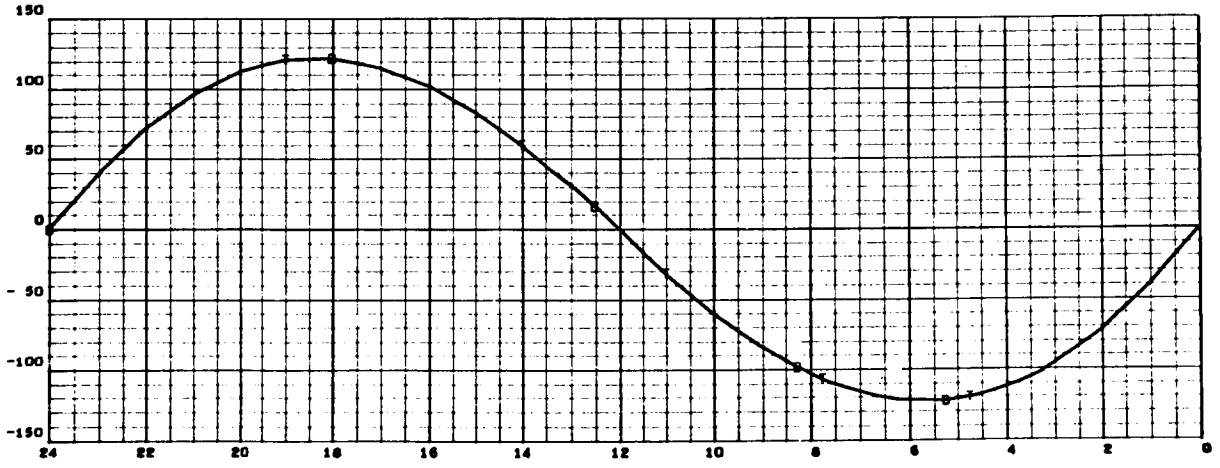

T = TOTAL SLOPE B = BENDING SLOPE
VEHICLE STATIONS - INCHES

MAY 21, 1966

2463-01 L
018 000

MASS LOADING EFFECTS ON BEAM VIBRATION-FIXED ENDS (CASE 3)

FREQUENCY (2) = 1.1115432E 03 RAD./SEC., 1.7690759E 02 C.F.S.
STRUCTURAL MODE (2)
NORMALIZED TO TOTAL WEIGHT
TOTAL WEIGHT = 8.2499991E-01
DEFLECTION - FT./FT.

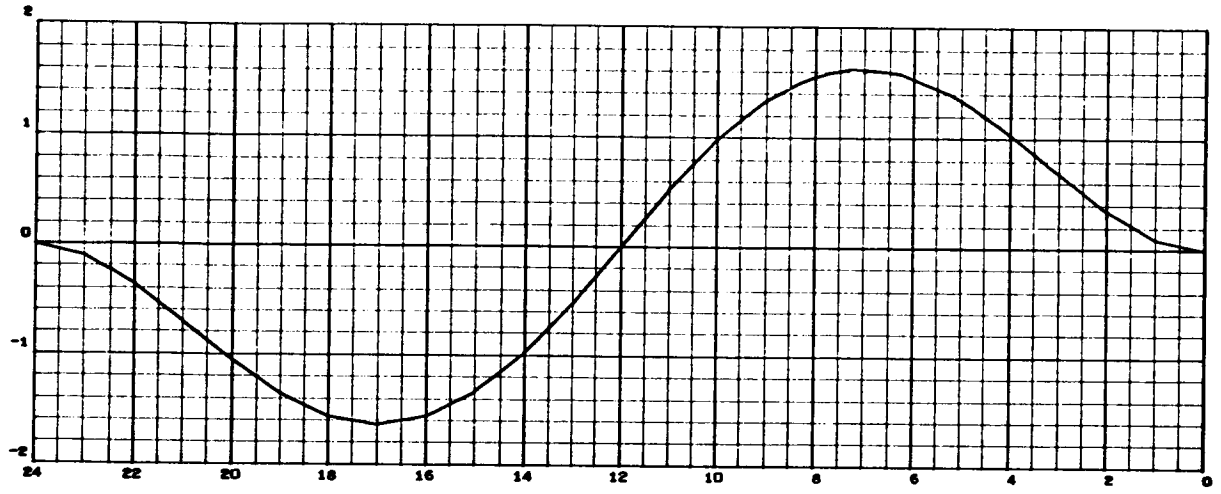

VEHICLE STATIONS - INCHES
SLOPE - DEG./FT.

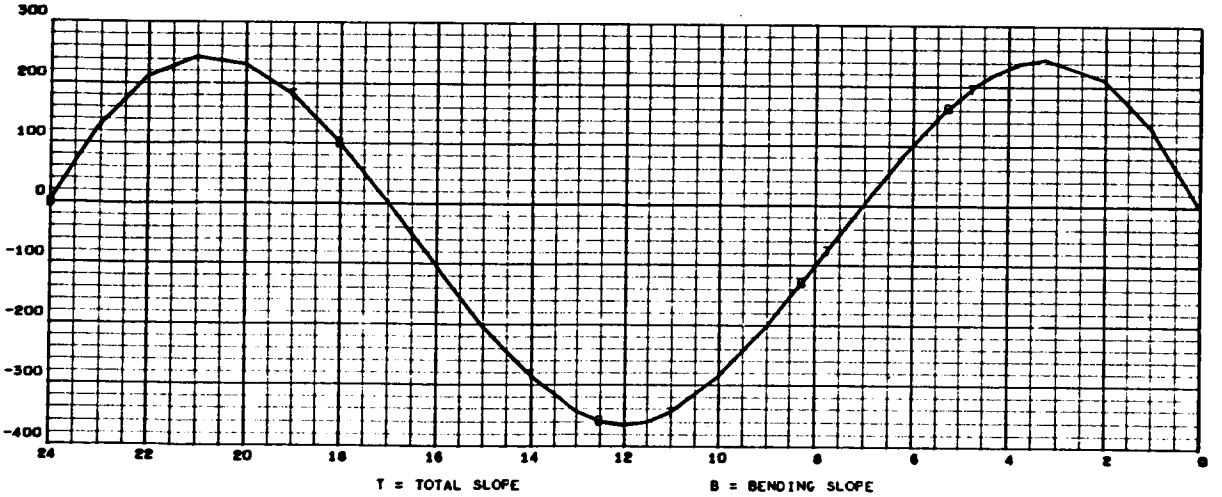

T = TOTAL SLOPE B = BENDING SLOPE
VEHICLE STATIONS - INCHES

MAY 21, 1966

2463-01
020 000

MASS LOADING EFFECTS ON BEAM VIBRATION-FIXED ENDS (CASE 3)

FREQUENCY (3) = 1.9738871E 03 RAD./SEC., 3.1415389E 02 C.P.S.
STRUCTURAL MODE (3)
NORMALIZED TO TOTAL WEIGHT
TOTAL WEIGHT = 8.2499991E-01
DEFLECTION - FT./FT.

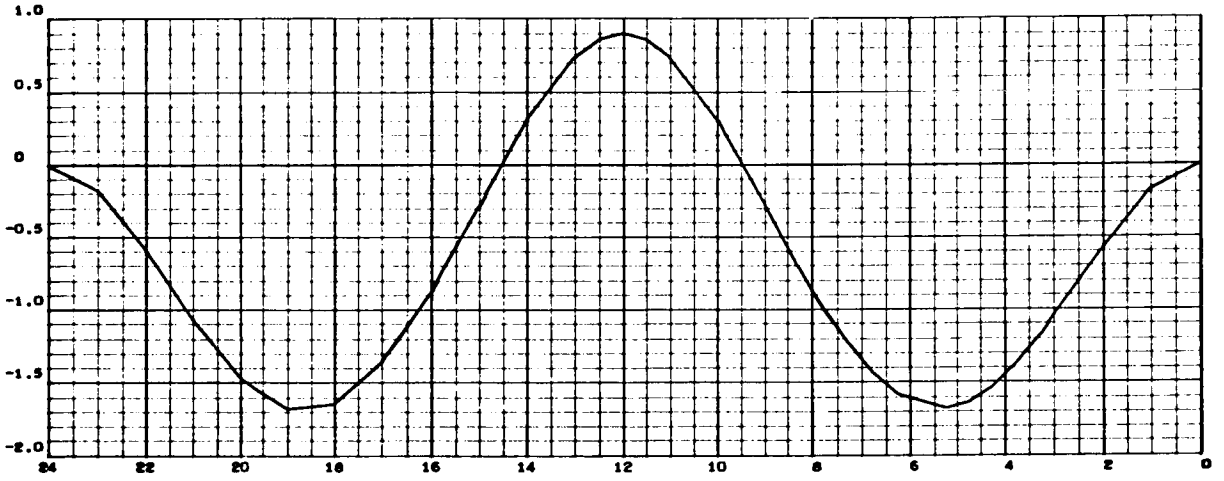

VEHICLE STATIONS - INCHES
SLOPE - DEG./FT.

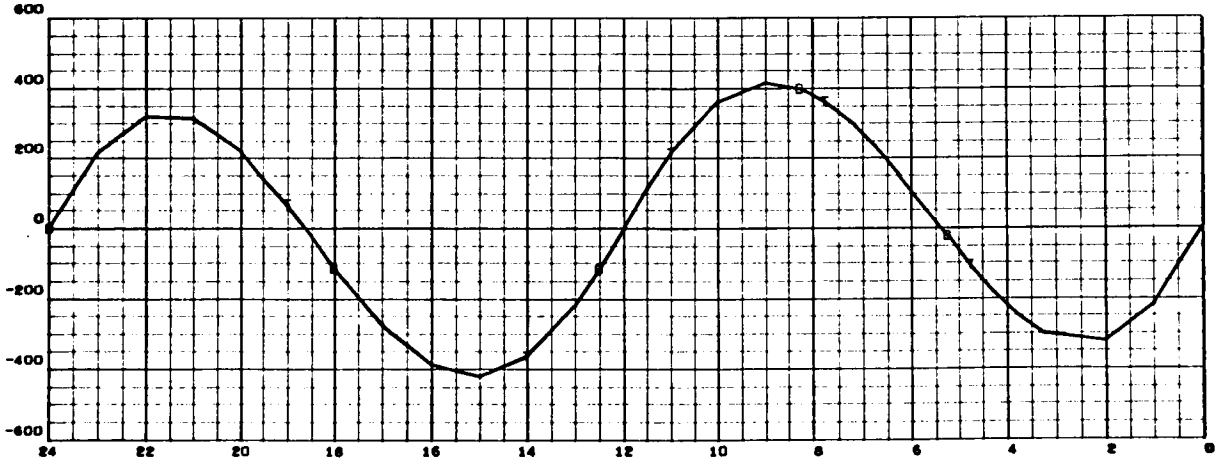

T = TOTAL SLOPE B = BENDING SLOPE
VEHICLE STATIONS - INCHES

MAY 21, 1966

2463-01
022 000

MASS LOADING EFFECTS ON BEAM VIBRATION-FIXED ENDS (CASE 3)

FREQUENCY (4) = 3.4171212E 03 RAD./SEC., 5.4385173E 02 C.P.S.
STRUCTURAL MODE (4)
NORMALIZED TO TOTAL WEIGHT
TOTAL WEIGHT = 8.2499991E-01
DEFLECTION - FT./FT.

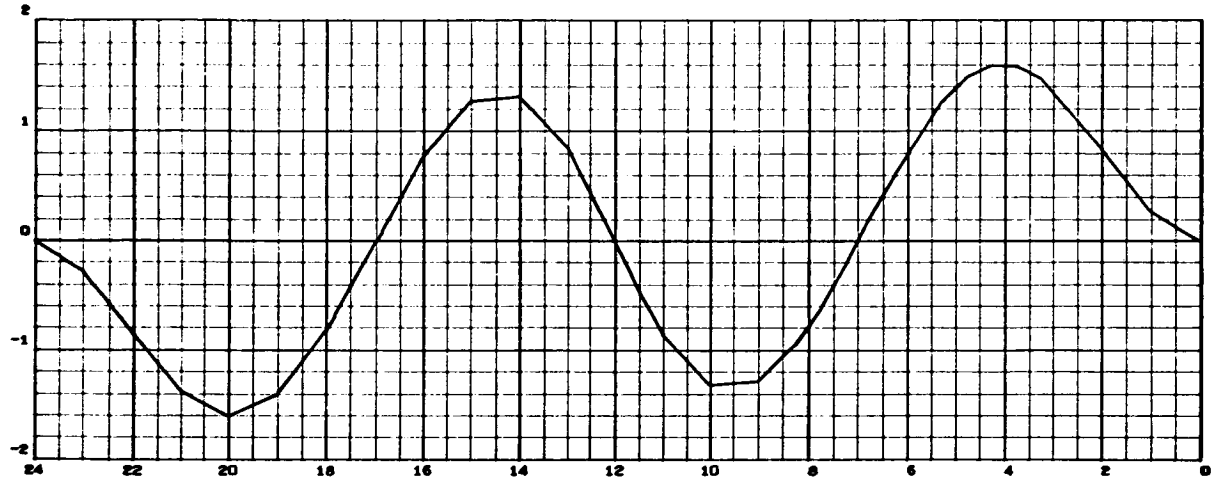

VEHICLE STATIONS - INCHES
SLOPE - DEG./FT.

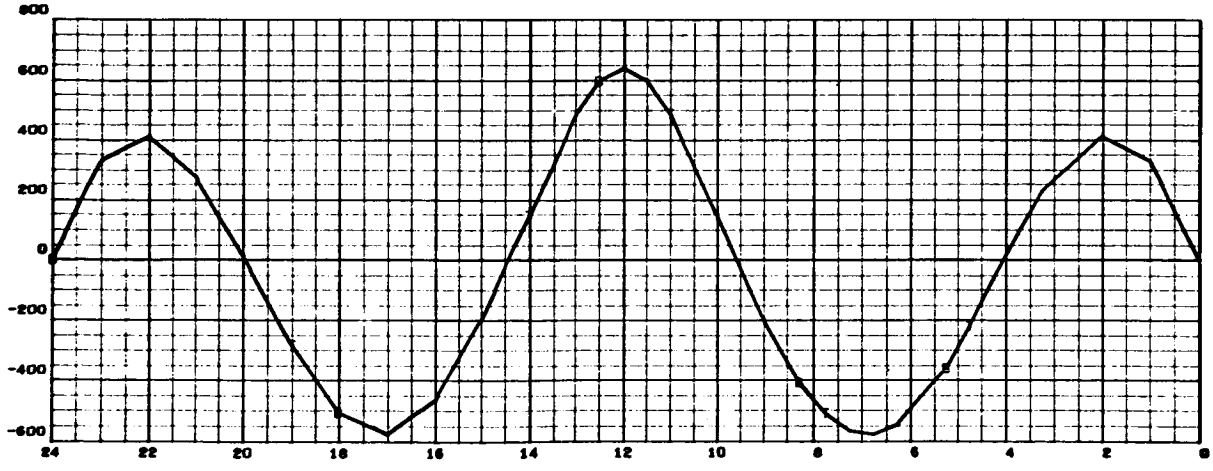

T = TOTAL SLOPE B = BENDING SLOPE
VEHICLE STATIONS - INCHES

MAY 24, 1966

2463-01
005 000

MASS LOADING EFFECTS ON BEAM VIBRATION - FIXED ENDS (CASE 4)

FREQUENCY (1) = 3.946344DE 02 RAD./SEC., 6.2808016E 01 C.P.S.
STRUCTURAL MODE (1)
NORMALIZED TO TOTAL WEIGHT
TOTAL WEIGHT = 8.9099994E-01
DEFLECTION - FT./FT.

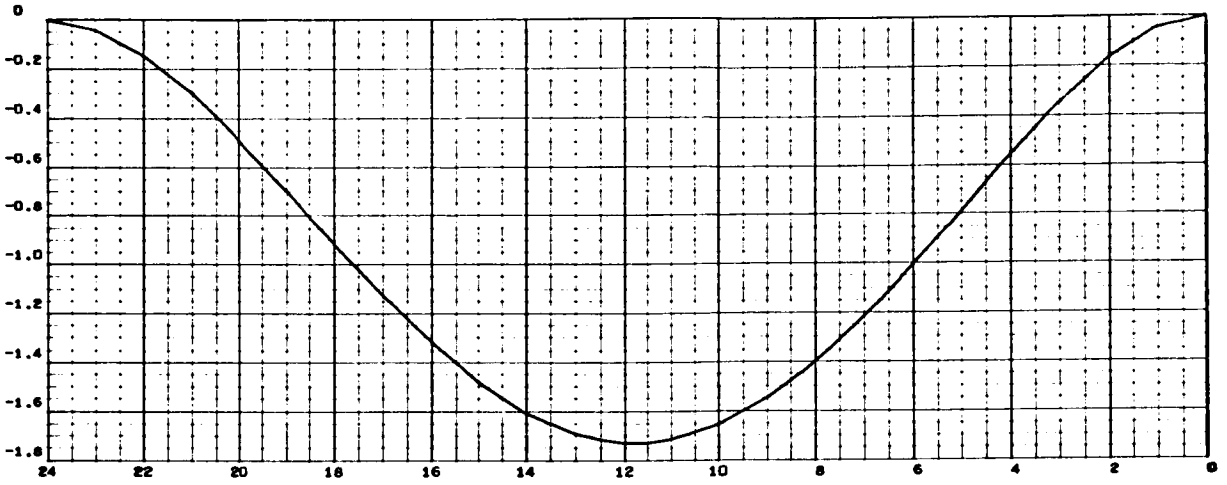

VEHICLE STATIONS - INCHES
SLOPE - DEG./FT.

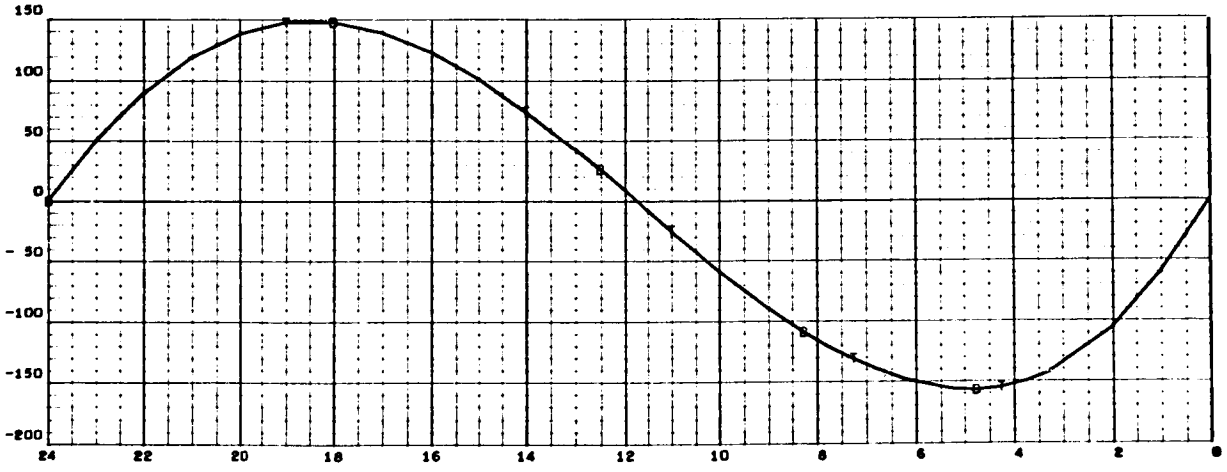

T = TOTAL SLOPE B = BENDING SLOPE
VEHICLE STATIONS - INCHES

MAY 24, 1966

2463-01
007 000

MASS LOADING EFFECTS ON BEAM VIBRATION - FIXED ENDS (CASE 4)

FREQUENCY (2) = 9.5692471E 02 RAD./SEC., 1.5229930E 02 C.P.S.
STRUCTURAL MODE (2)
NORMALIZED TO TOTAL WEIGHT
TOTAL WEIGHT = 8.9099994E-01
DEFLECTION - FT./FT.

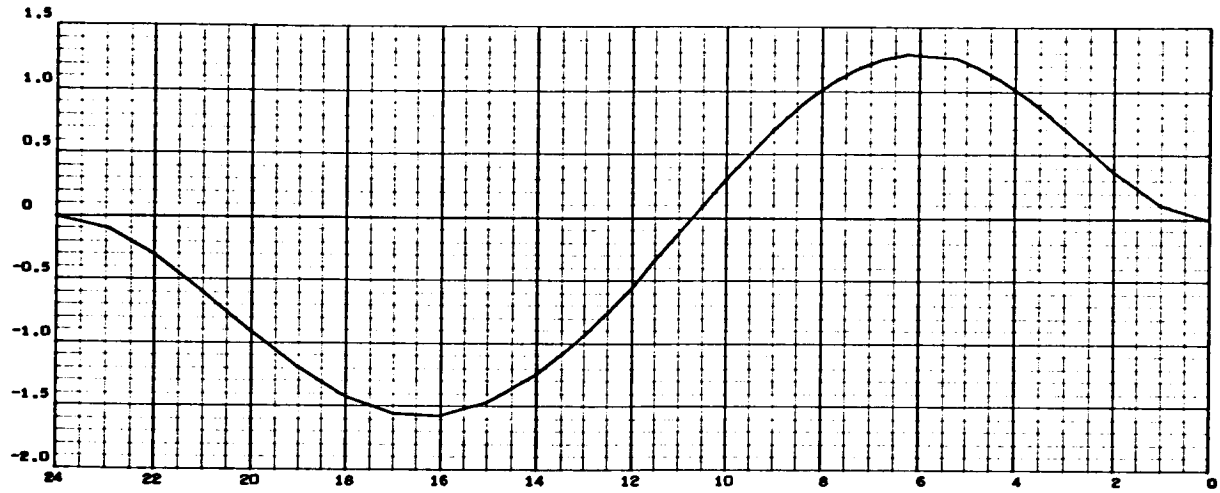

VEHICLE STATIONS - INCHES
SLOPE - DEG./FT.

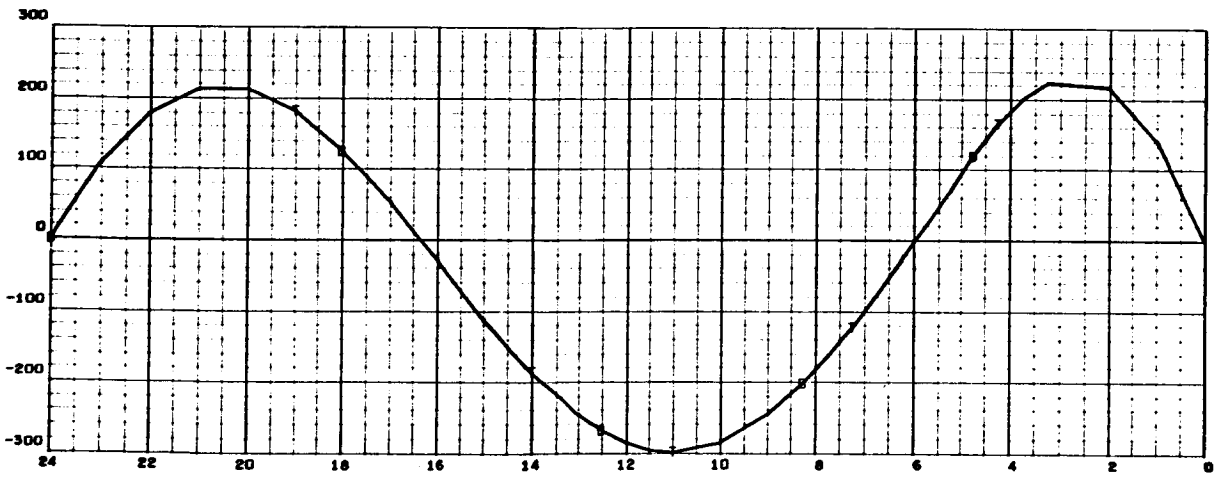

T = TOTAL SLOPE B = BENDING SLOPE
VEHICLE STATIONS - INCHES

MAY 24, 1966

2463-01 L
009 000

MASS LOADING EFFECTS ON BEAM VIBRATION - FIXED ENDS (CASE 4)

FREQUENCY (3) = 1.8502983E 03 RAD./SEC., 2.9448412E 02 C.P.S.
STRUCTURAL MODE (3)
NORMALIZED TO TOTAL WEIGHT
TOTAL WEIGHT = 8.9099994E-01
DEFLECTION - FT./FT.

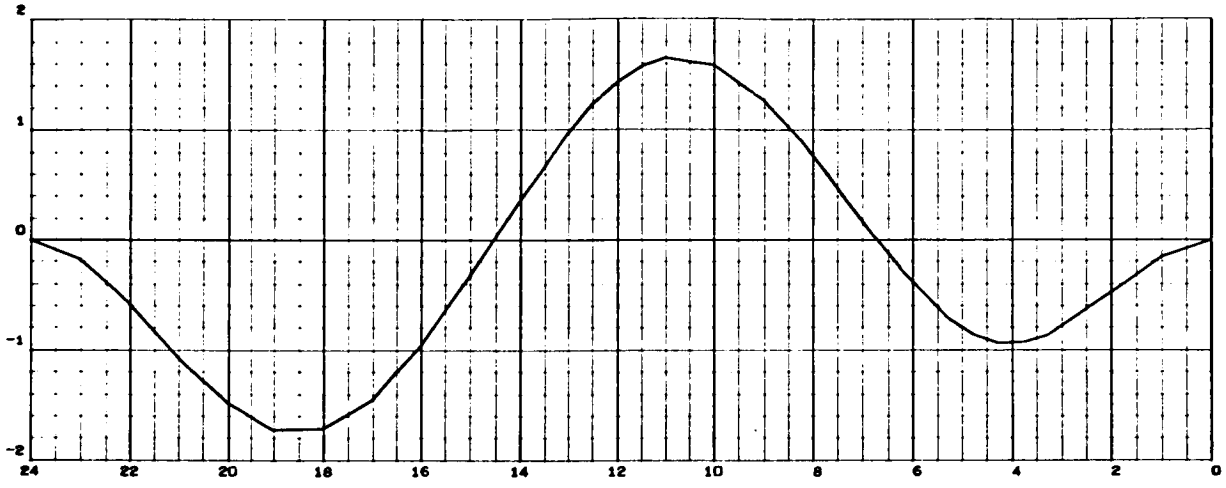

VEHICLE STATIONS - INCHES
SLOPE - DEG./FT.

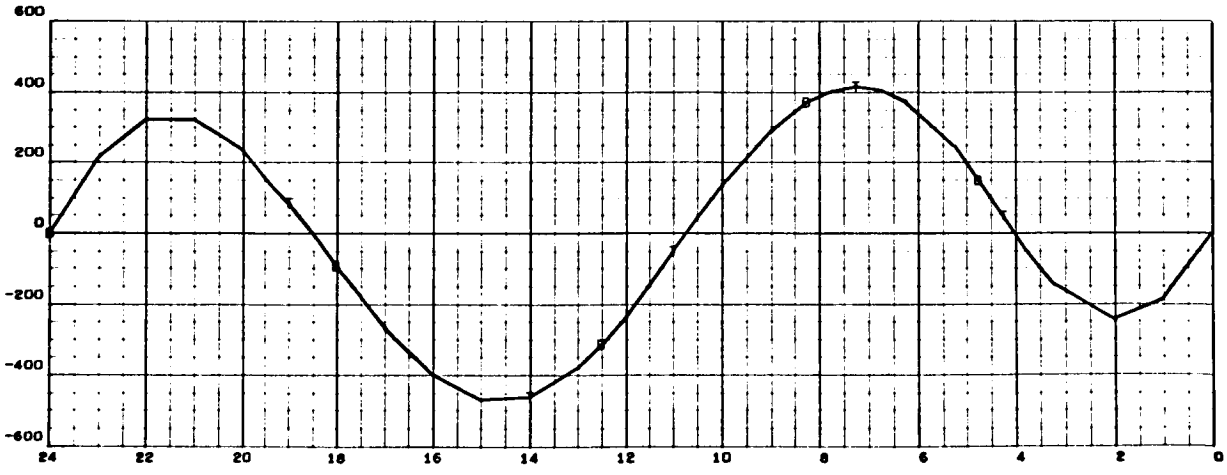

T = TOTAL SLOPE B = BENDING SLOPE
VEHICLE STATIONS - INCHES

MAY 24, 1966

2463-01 L
011 000

MASS LOADING EFFECTS ON BEAM VIBRATION - FIXED ENDS (CASE 4)

FREQUENCY (4) = 3.2247923E 03 RAD./SEC., 5.1324162E 02 C.P.S.
STRUCTURAL MODE (4)
NORMALIZED TO TOTAL WEIGHT
TOTAL WEIGHT = 8.9099994E-01
DEFLECTION - FT./FT.

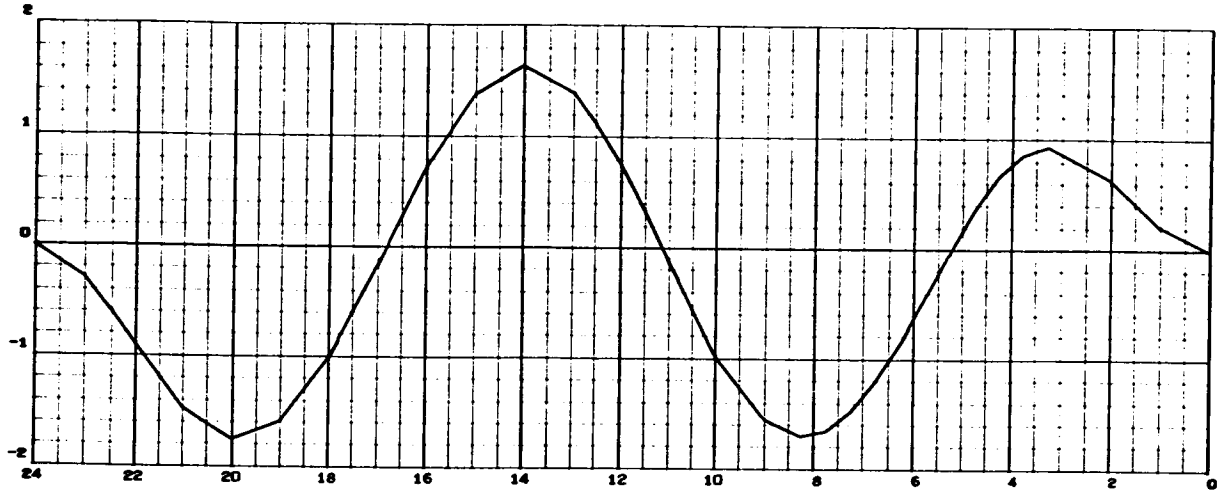

VEHICLE STATIONS - INCHES
SLOPE - DEG./FT.

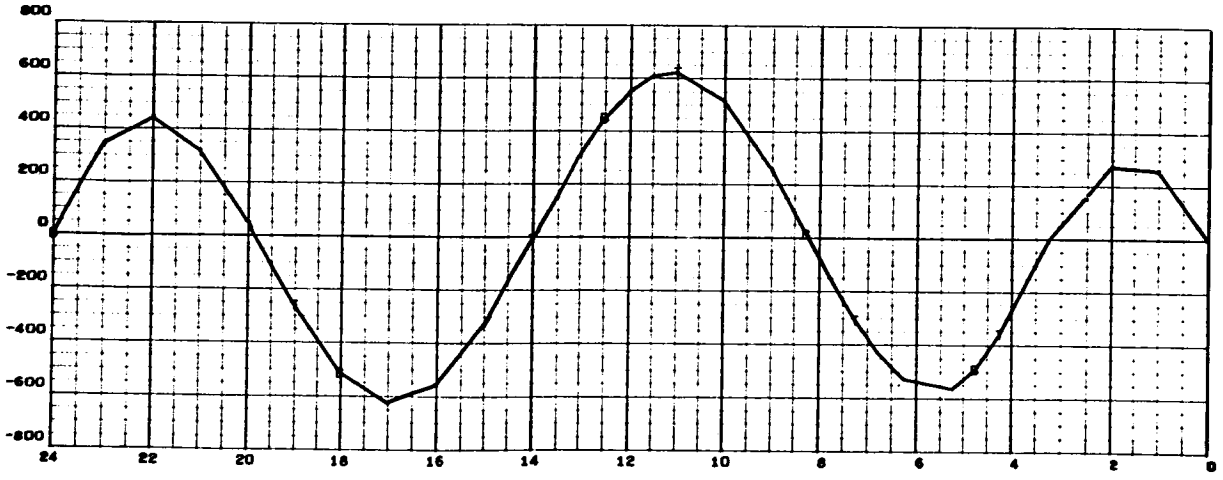

T = TOTAL SLOPE B = BENDING SLOPE
VEHICLE STATIONS - INCHES

MAY 24, 1966

2463-01
013 000

MASS LOADING EFFECTS ON BEAM VIBRATION - FIXED ENDS (CASE 5)

FREQUENCY (1) = 3.4324341E 02 RAD./SEC., 5.4628885E 01 C.P.S.
STRUCTURAL MODE (1)
NORMALIZED TO TOTAL WEIGHT
TOTAL WEIGHT = 8.9099993E-01
DEFLECTION - FT./FT.

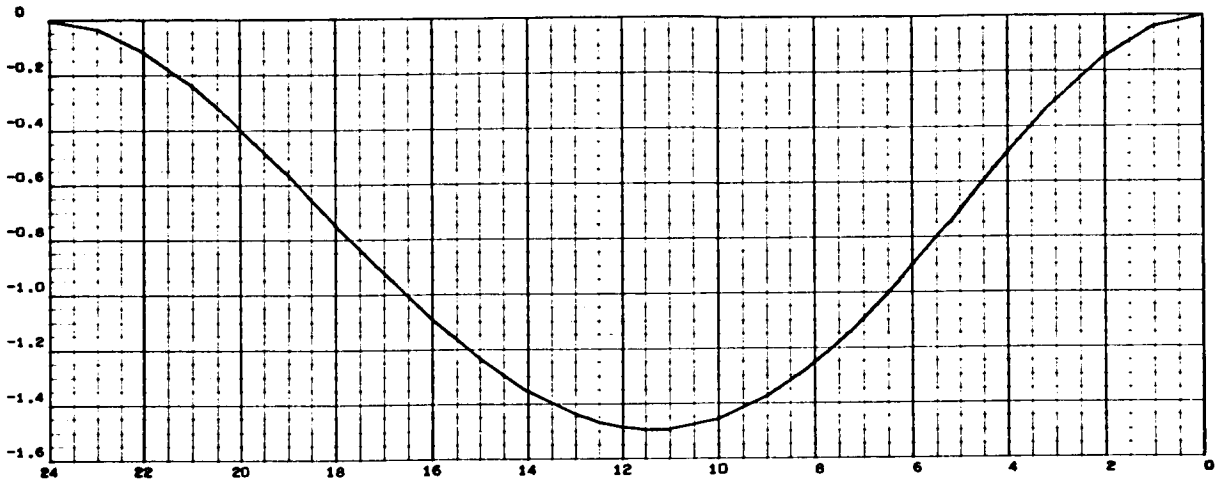

VEHICLE STATIONS - INCHES
SLOPE - DEG./FT.

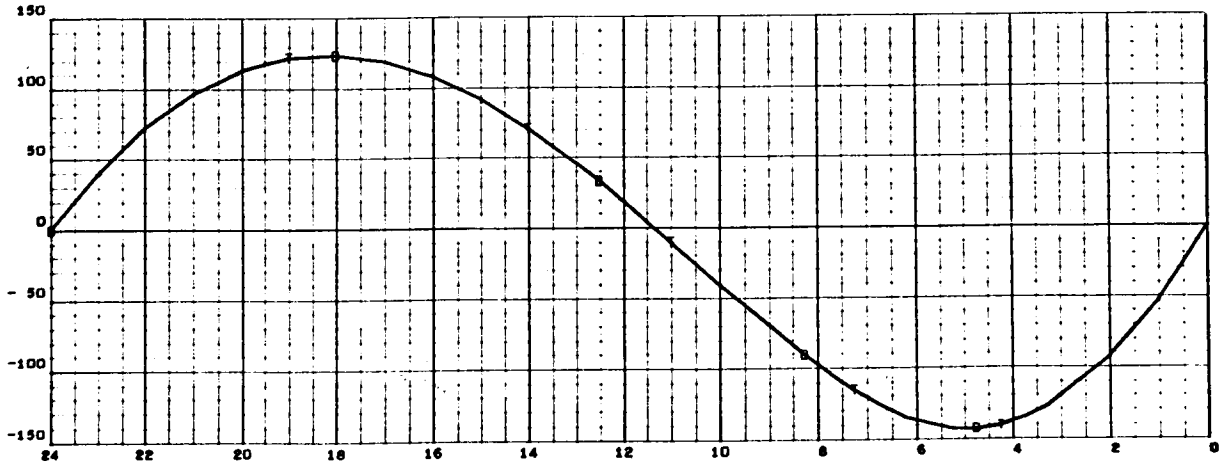

T = TOTAL SLOPE B = BENDING SLOPE
VEHICLE STATIONS - INCHES

MAY 24, 1966

2463-01 L
015 000

MASS LOADING EFFECTS ON BEAM VIBRATION - FIXED ENDS (CASE 5)

FREQUENCY (2) = 9.2862366E 02 RAD./SEC., 1.4779504E 02 C.P.S.
STRUCTURAL MODE (2)
NORMALIZED TO TOTAL WEIGHT
TOTAL WEIGHT = 8.9099993E-01
DEFLECTION - FT./FT.

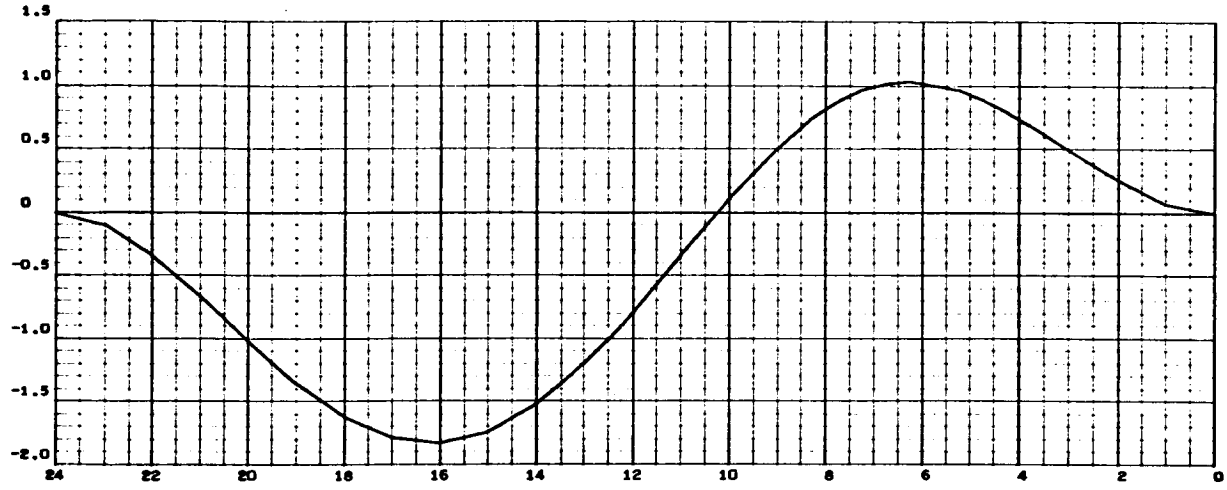

VEHICLE STATIONS - INCHES
SLOPE - DEG./FT.

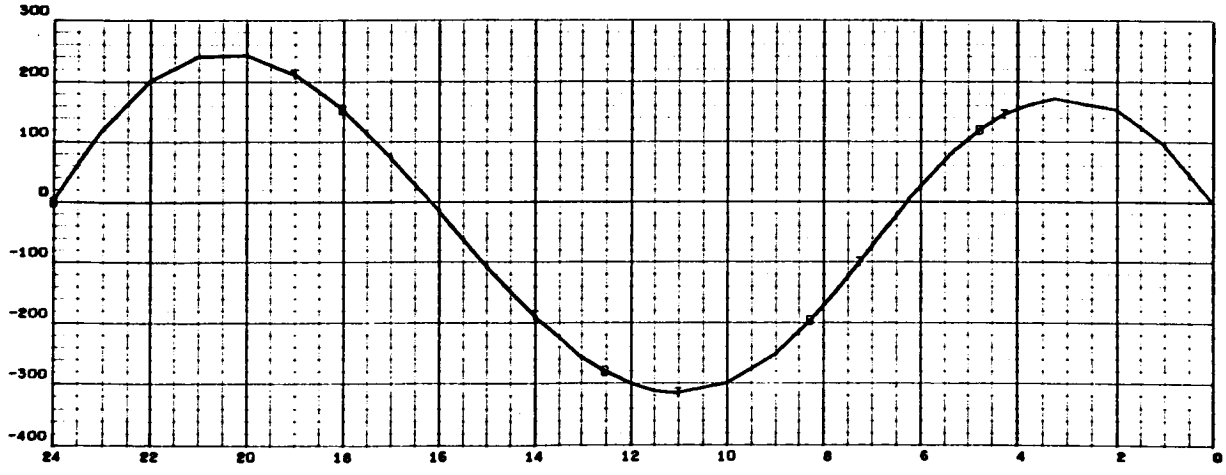

T = TOTAL SLOPE B = BENDING SLOPE
VEHICLE STATIONS - INCHES

MAY 24, 1966

2463-01
017 000

MASS LOADING EFFECTS ON BEAM VIBRATION - FIXED ENDS (CASE 5)

FREQUENCY (3) = 2.0615551E 03 RAD./SEC., 3.2810667E 02 C.P.S.
STRUCTURAL MODE (3)
NORMALIZED TO TOTAL WEIGHT
TOTAL WEIGHT = 8.9099993E-01
DEFLECTION - FT./FT.

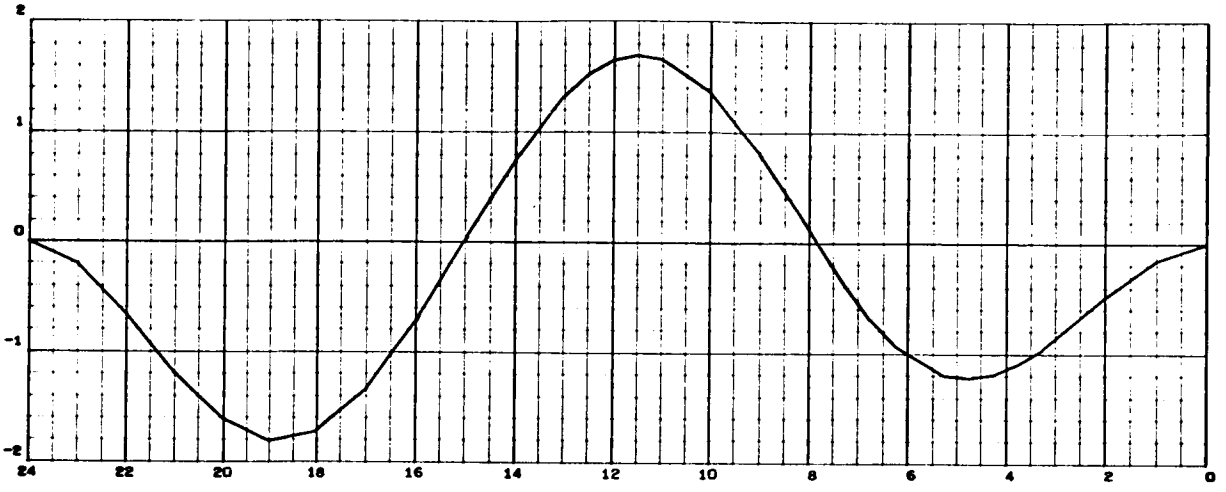

VEHICLE STATIONS - INCHES
SLOPE - DEG./FT.

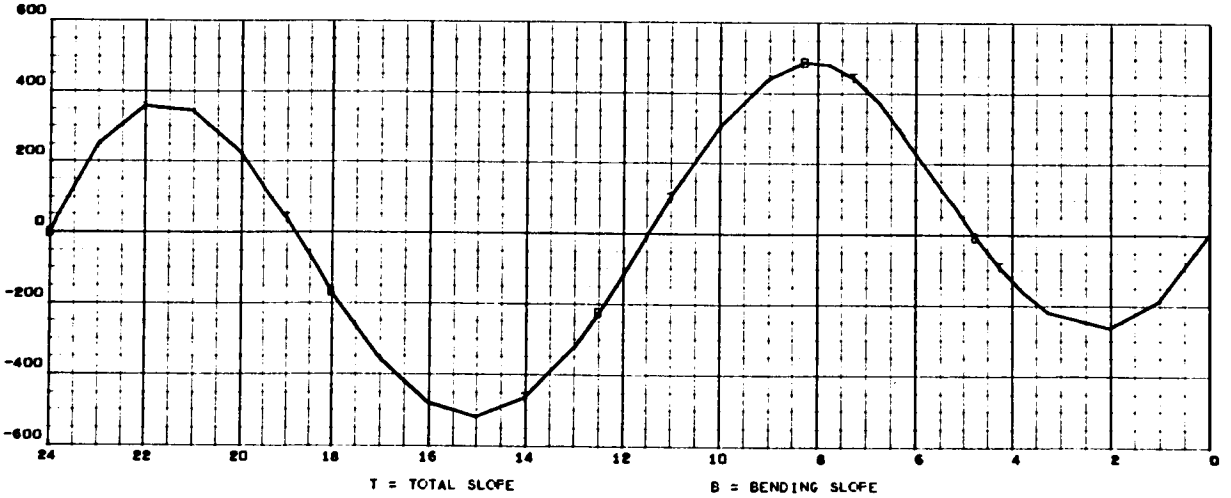

T = TOTAL SLOPE B = BENDING SLOPE
VEHICLE STATIONS - INCHES

MAY 24, 1966

2463-01 L
019 000

MASS LOADING EFFECTS ON BEAM VIBRATION - FIXED ENDS (CASE 5)

FREQUENCY (4) = 3.3727836E 03 RAD./SEC., 5.3679518E 02 C.F.S.
STRUCTURAL MODE (4)
NORMALIZED TO TOTAL WEIGHT
TOTAL WEIGHT = 8.9099993E-01
DEFLECTION - FT./FT.

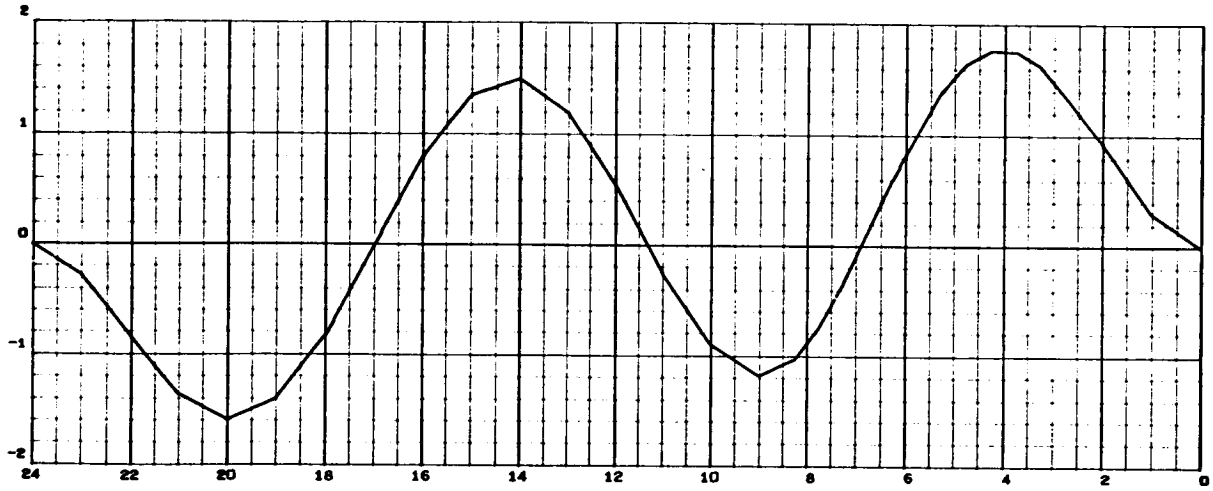

VEHICLE STATIONS - INCHES
SLOPE - DEG./FT.

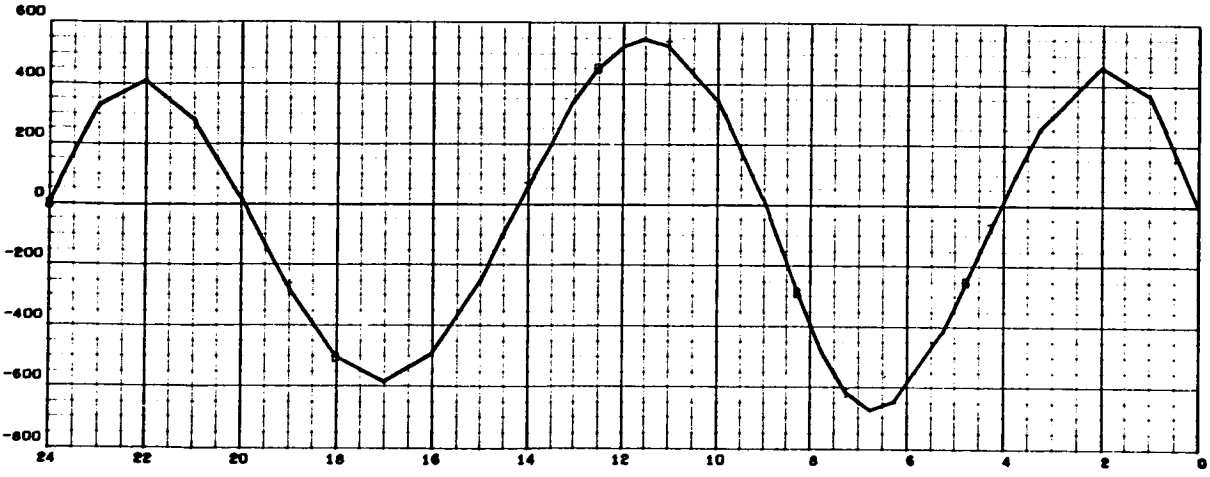

T = TOTAL SLOPE B = BENDING SLOPE
VEHICLE STATIONS - INCHES

MAY 24, 1966

2463-01 L
021 000

MASS LOADING EFFECTS ON BEAM VIBRATION FIXED ENDS (CASE 6)

FREQUENCY (1) = 3.0346289E 02 RAD./SEC., 4.8297619E 01 C.P.S.
STRUCTURAL MODE (1)
NORMALIZED TO TOTAL WEIGHT
TOTAL WEIGHT = 8.9099991E-01
DEFLECTION - FT./FT.

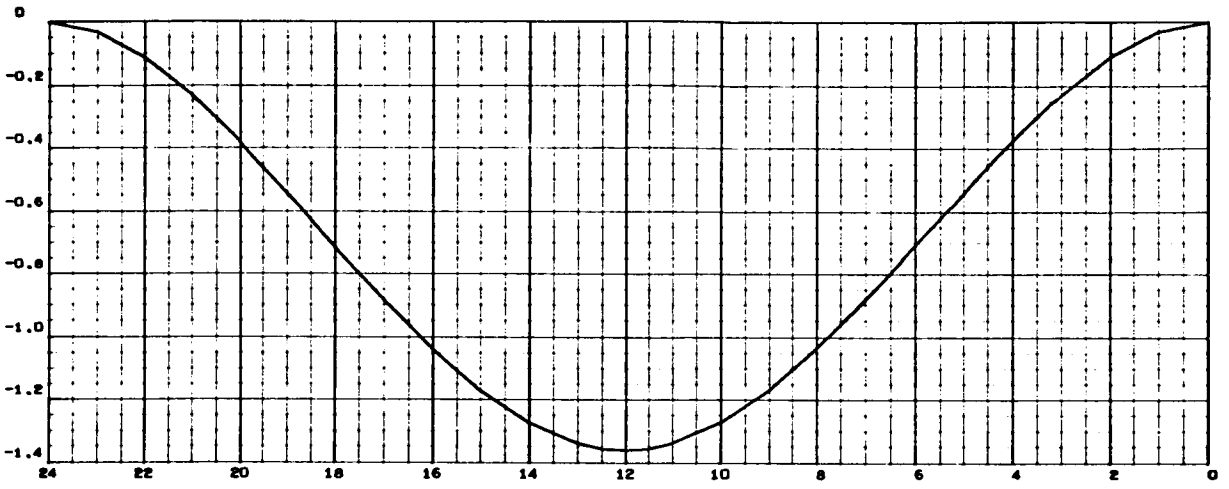

VEHICLE STATIONS - INCHES
SLOPE - DEG./FT.

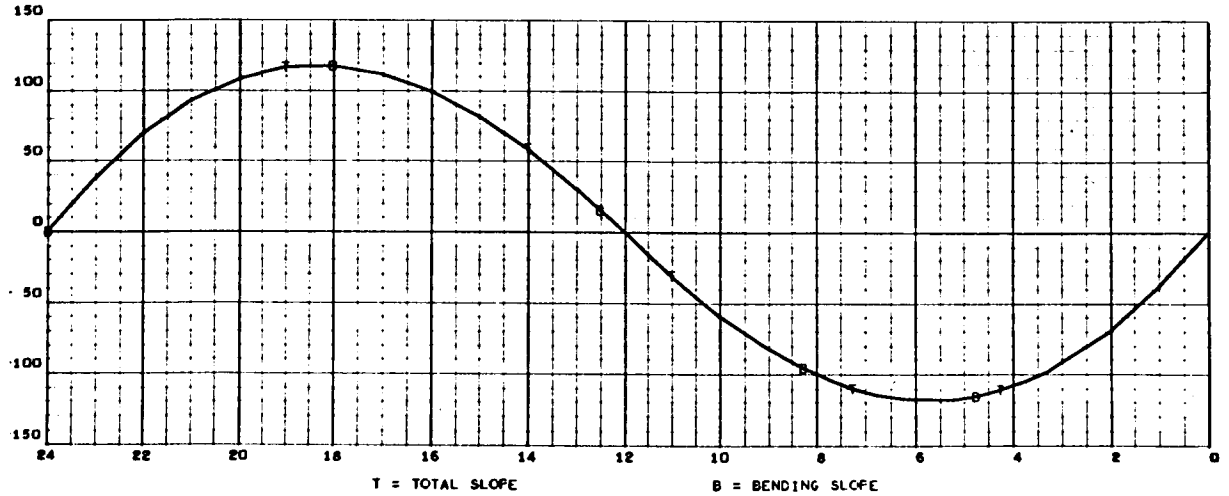

T = TOTAL SLOPE B = BENDING SLOPE
VEHICLE STATIONS - INCHES

MAY 24, 1966

2463-01
023 000

MASS LOADING EFFECTS ON BEAM VIBRATION FIXED ENDS (CASE 6)

FREQUENCY (2) = 1.1111296E 03 RAD./SEC., 1.7684176E 02 C.F.S.
STRUCTURAL MODE (2)
NORMALIZED TO TOTAL WEIGHT
TOTAL WEIGHT = 8.9099991E-01
DEFLECTION - FT./FT.

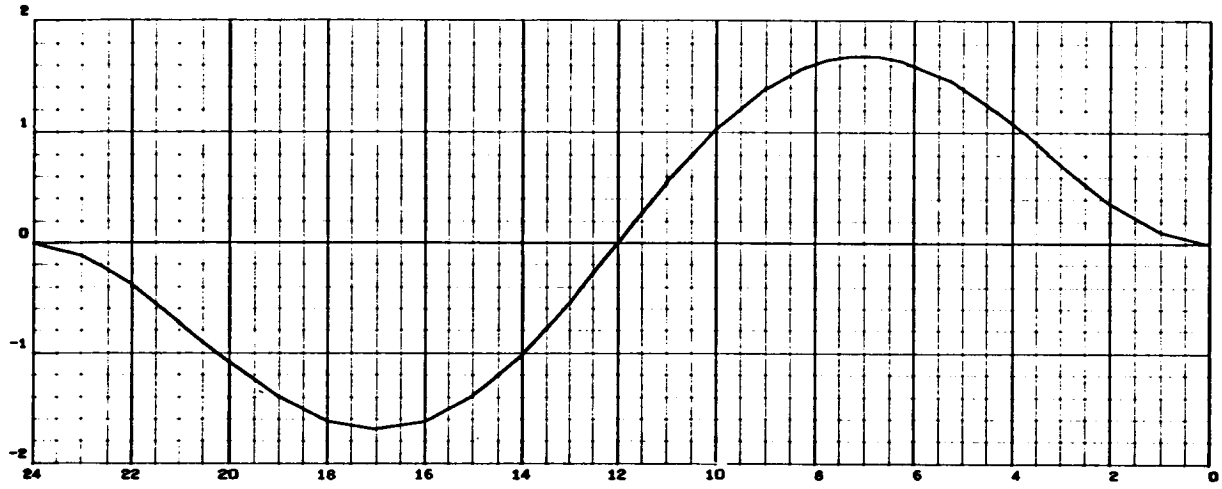

VEHICLE STATIONS - INCHES
SLOPE - DEG./FT.

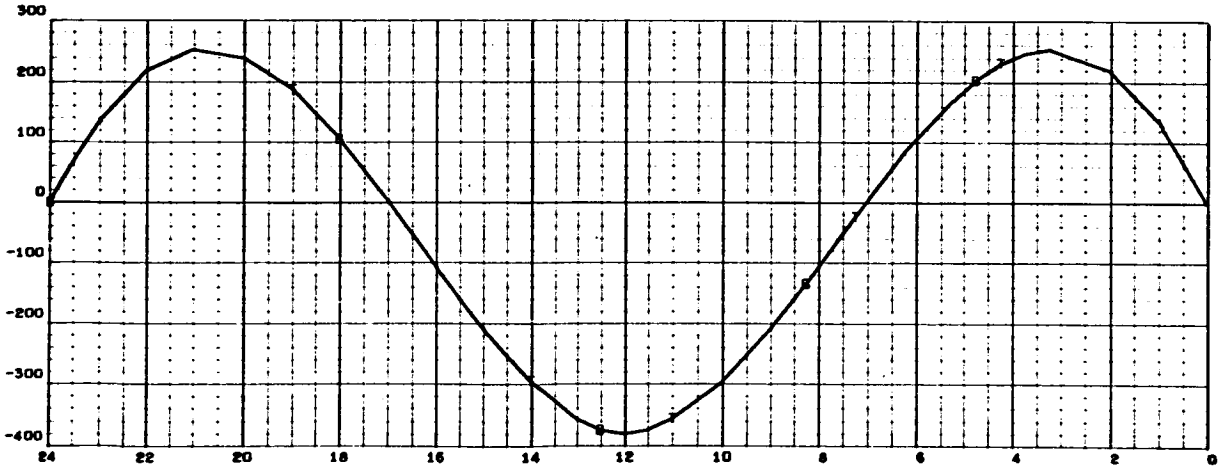

T = TOTAL SLOPE B = BENDING SLOPE
VEHICLE STATIONS - INCHES

MAY 24, 1966

2463-01 L
025 000

MASS LOADING EFFECTS ON BEAM VIBRATION FIXED ENDS (CASE 6)

FREQUENCY (3) = 1.9303416E 03 RAD./SEC., 3.0722341E 02 C.F.S.
STRUCTURAL MODE (3)
NORMALIZED TO TOTAL WEIGHT
TOTAL WEIGHT = 8.9099991E-01
DEFLECTION - FT./FT.

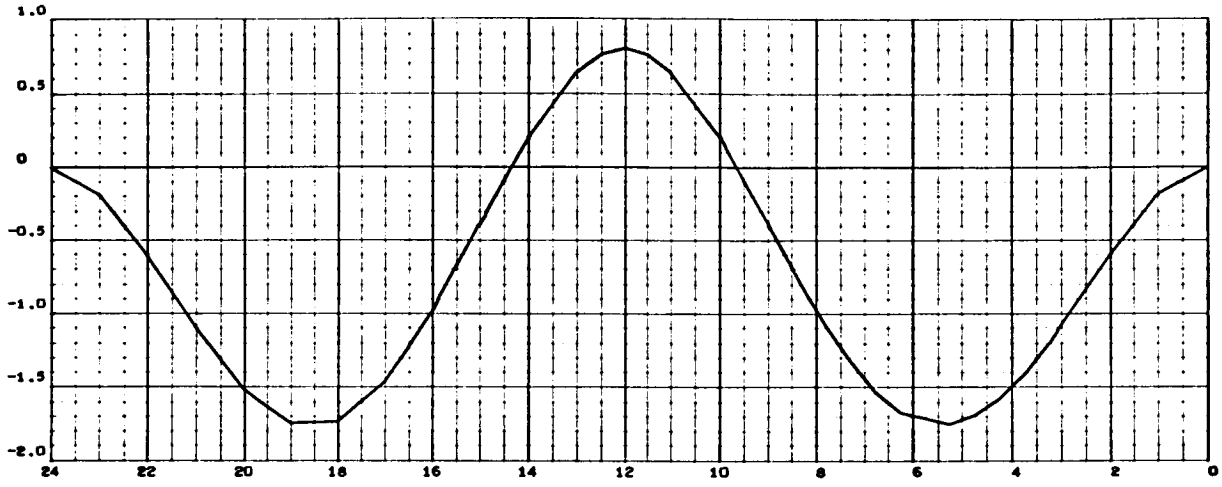

VEHICLE STATIONS - INCHES
SLOPE - DEG./FT.

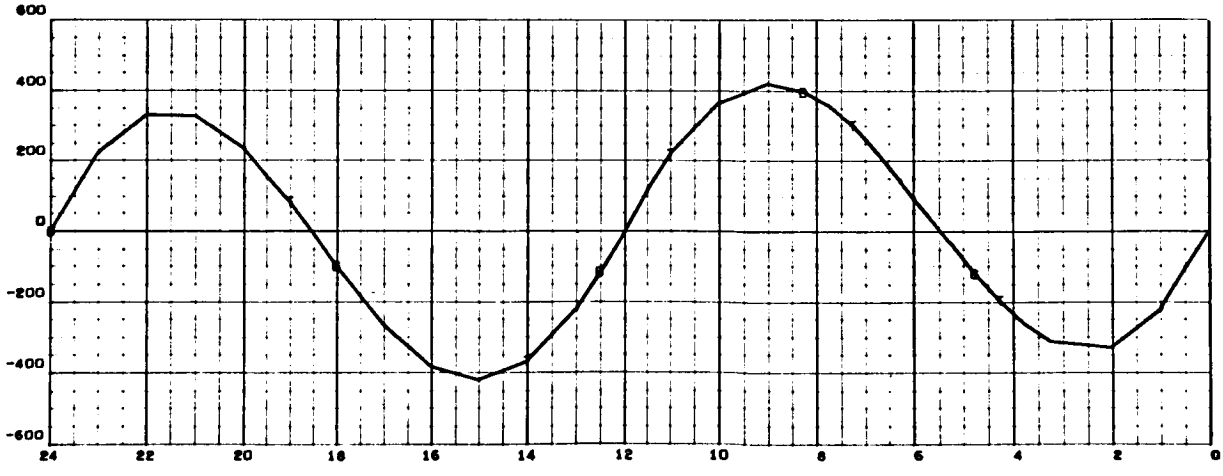

T = TOTAL SLOPE B = BENDING SLOPE

VEHICLE STATIONS - INCHES

MAY 24, 1966

2463-01 L
027 000

MASS LOADING EFFECTS ON BEAM VIBRATION FIXED ENDS (CASE 6)

FREQUENCY (4) = 3.4094323E 03 RAD./SEC., 5.4262800E 02 C.P.S.
STRUCTURAL MODE (4)
NORMALIZED TO TOTAL WEIGHT
TOTAL WEIGHT = 8.9099991E-01
DEFLECTION - FT./FT.

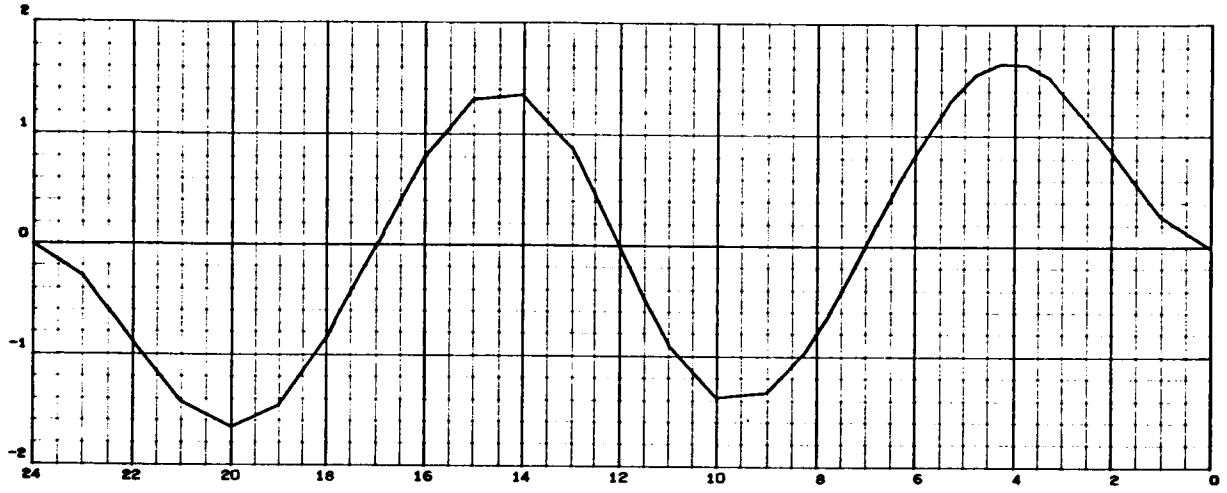

VEHICLE STATIONS - INCHES
SLOPE - DEG./FT.

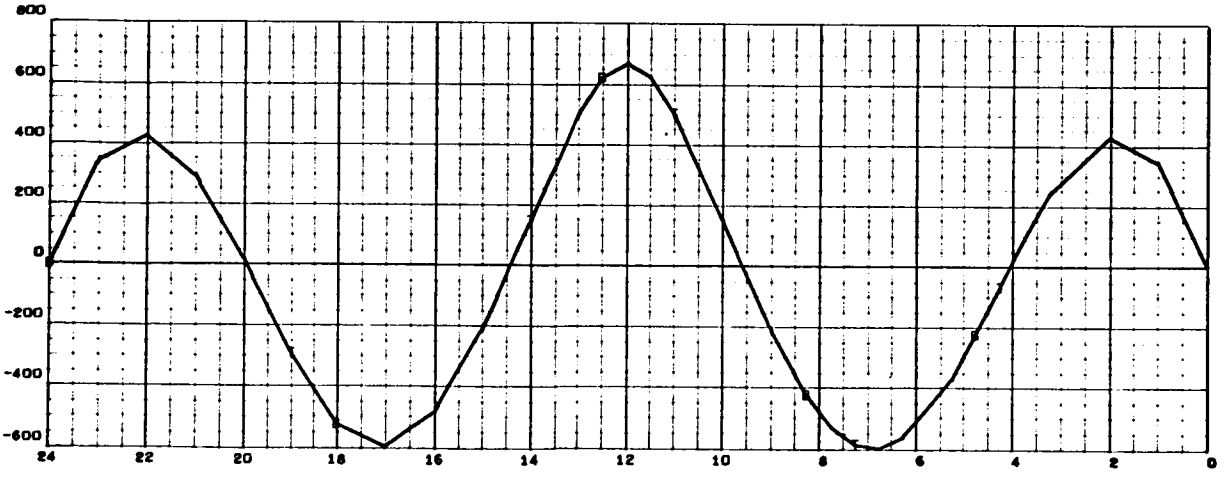

T = TOTAL SLOPE B = BENDING SLOPE
VEHICLE STATIONS - INCHES

MAY 24, 1966

2463-01 L
029 000

MASS LOADING EFFECTS ON BEAM VIBRATION-FIXED ENDS(CASE 7)

FREQUENCY (1) = 3.8499570E 02 RAD./SEC., 6.1273969E 01 C.P.S.
STRUCTURAL MODE (1)
NORMALIZED TO TOTAL WEIGHT
TOTAL WEIGHT = 9.8999994E-01
DEFLECTION - FT./FT.

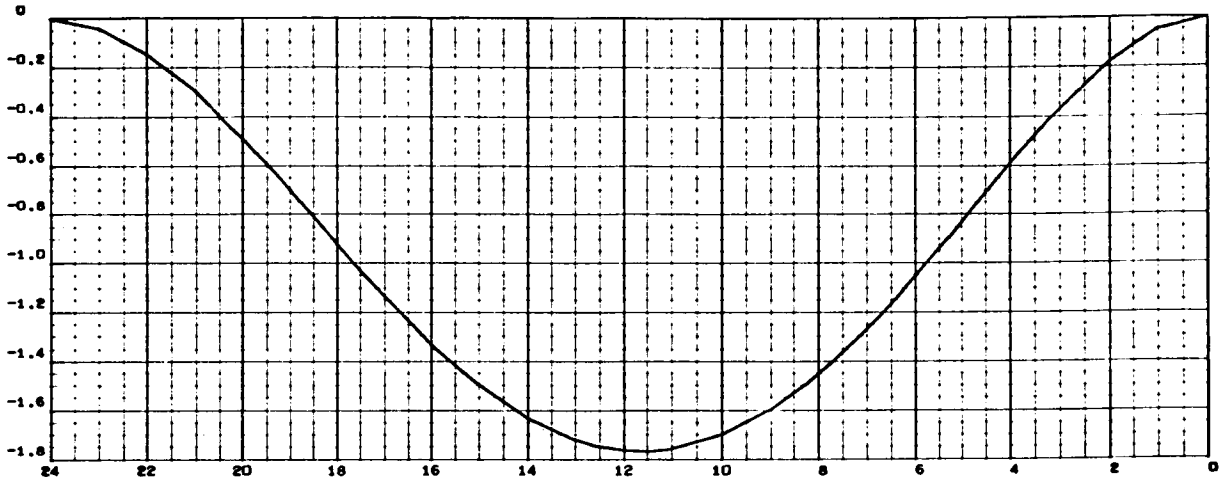

VEHICLE STATIONS - INCHES
SLOPE - DEG./FT.

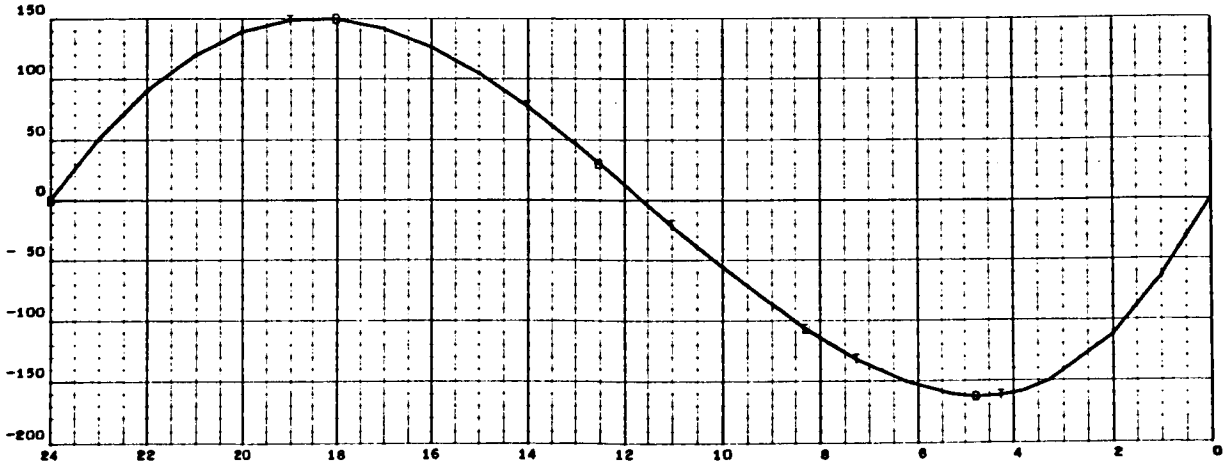

T = TOTAL SLOPE B = BENDING SLOPE
VEHICLE STATIONS - INCHES

MAY 24, 1966

2463-01 L
031 000

MASS LOADING EFFECTS ON BEAM VIBRATION-FIXED ENDS(CASE 7)

FREQUENCY (2) = 9.0077065E 02 RAD./SEC., 1.4336210E 02 C.P.S.
STRUCTURAL MODE (2)
NORMALIZED TO TOTAL WEIGHT
TOTAL WEIGHT = 9.8999994E-01
DEFLECTION - FT./FT.

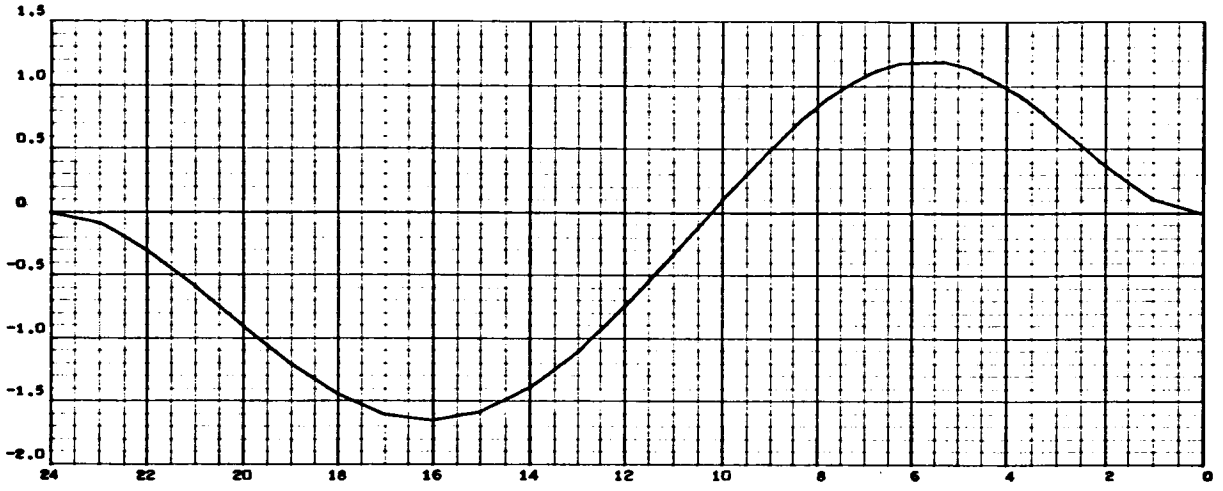

VEHICLE STATIONS - INCHES
SLOPE - DEG./FT.

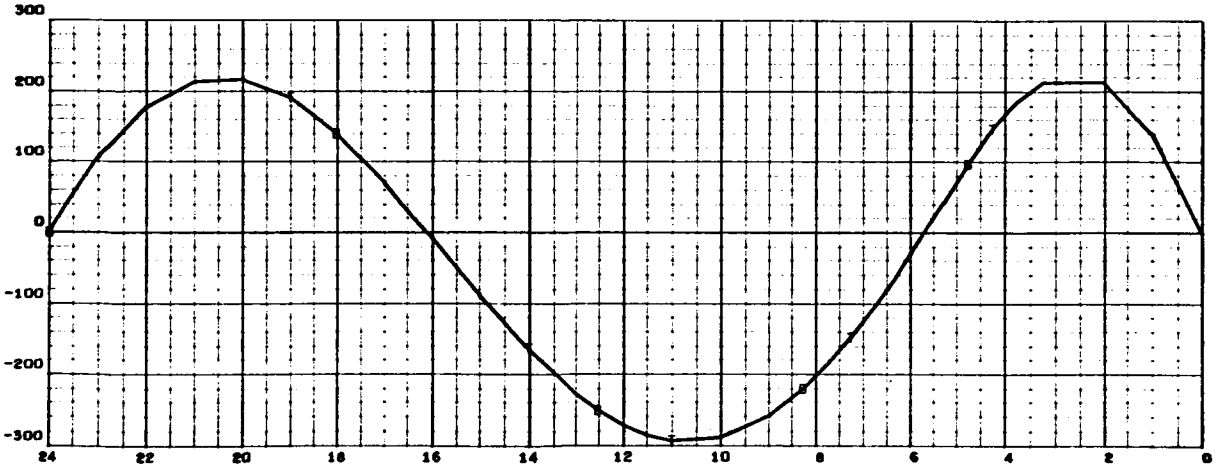

T = TOTAL SLOPE B = BENDING SLOPE
VEHICLE STATIONS - INCHES

MAY 24, 1966

2463-01 L
033 000

MASS LOADING EFFECTS ON BEAM VIBRATION-FIXED ENDS(CASE 7)

FREQUENCY (3) = 1.7849466E 03 RAD./SEC., 2.8408307E 02 C.P.S.
STRUCTURAL MODE (3)
NORMALIZED TO TOTAL WEIGHT
TOTAL WEIGHT = 9.8999994E-01
DEFLECTION - FT./FT.

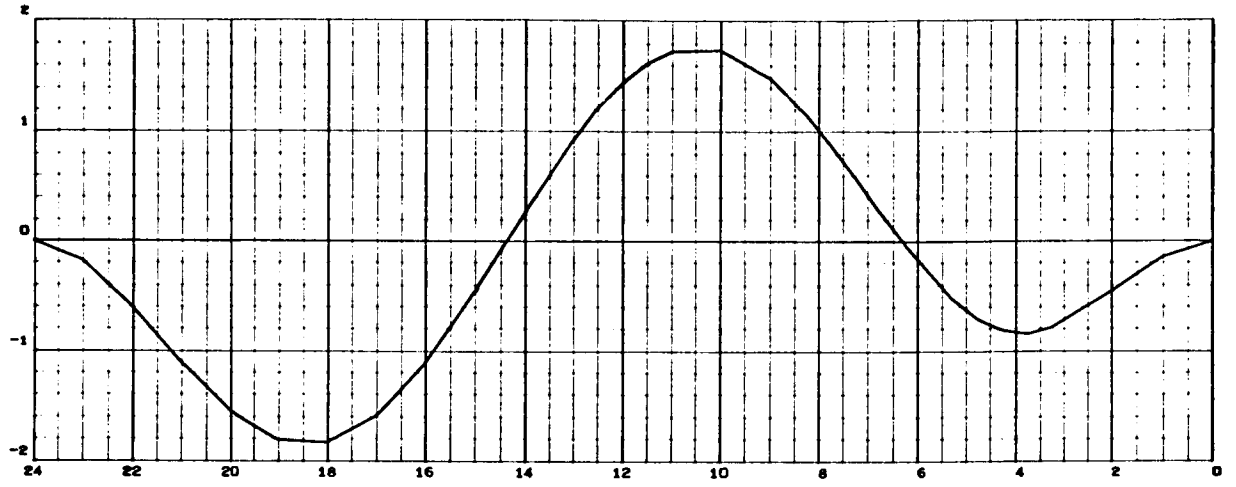

VEHICLE STATIONS - INCHES
SLOPE - DEG./FT.

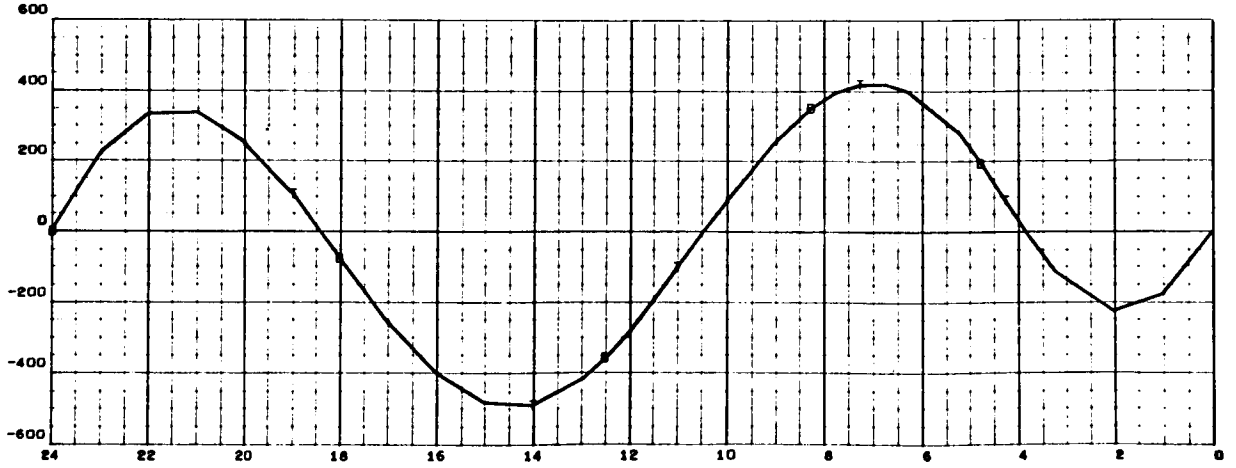

T = TOTAL SLOPE B = BENDING SLOPE
VEHICLE STATIONS - INCHES

MAY 24, 1966

2463-01
035 000

MASS LOADING EFFECTS ON BEAM VIBRATION-FIXED ENDS(CASE 7)

FREQUENCY (4) = 3.1110792E 03 RAD./SEC., 4.9514363E 02 C.F.S.
STRUCTURAL MODE (4)
NORMALIZED TO TOTAL WEIGHT
TOTAL WEIGHT = 9.8999994E-01
DEFLECTION - FT./FT.

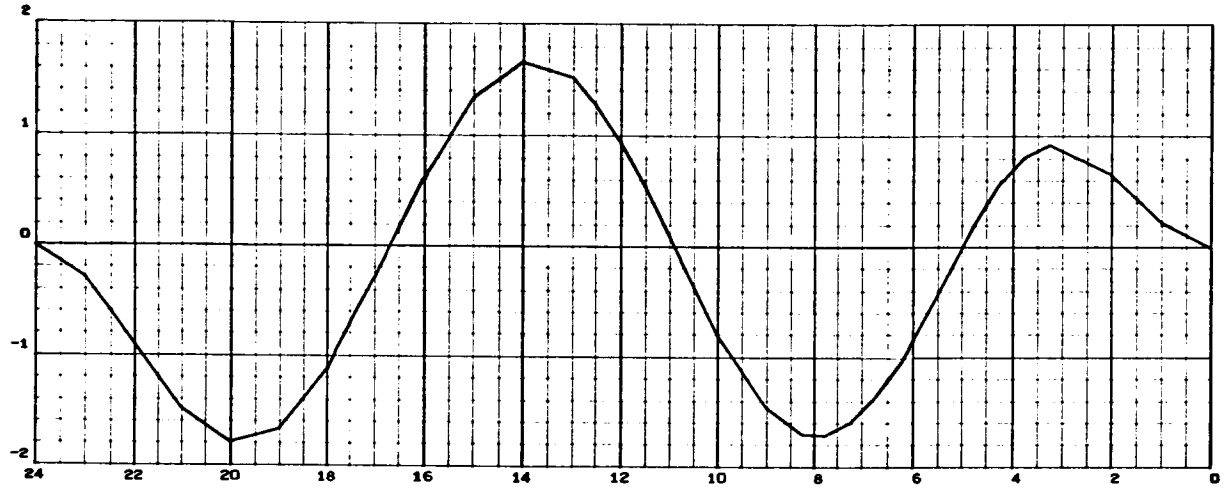

VEHICLE STATIONS - INCHES
SLOPE - DEG./FT.

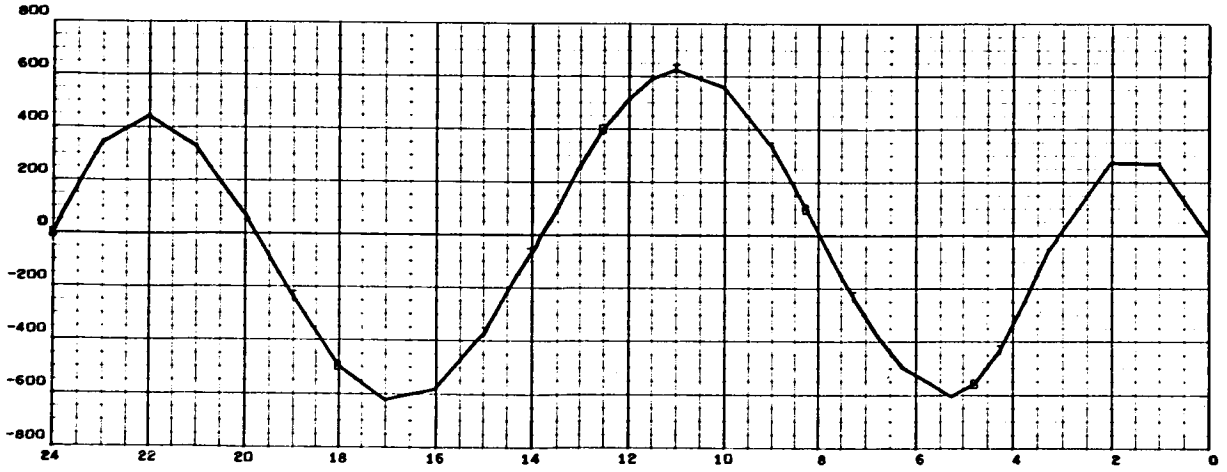

T = TOTAL SLOPE B = BENDING SLOPE
VEHICLE STATIONS - INCHES

MAY 24, 1966

2463-01
037 000

MASS LOADING EFFECTS ON BEAM VIBRATION-FIXED ENDS (CASE 8)

FREQUENCY (1) = 3.2035380E 02 RAD./SEC., 5.0985891E 01 C.P.S.
STRUCTURAL MODE (1)
NORMALIZED TO TOTAL WEIGHT
TOTAL WEIGHT = 9.8999992E-01
DEFLECTION - FT./FT.

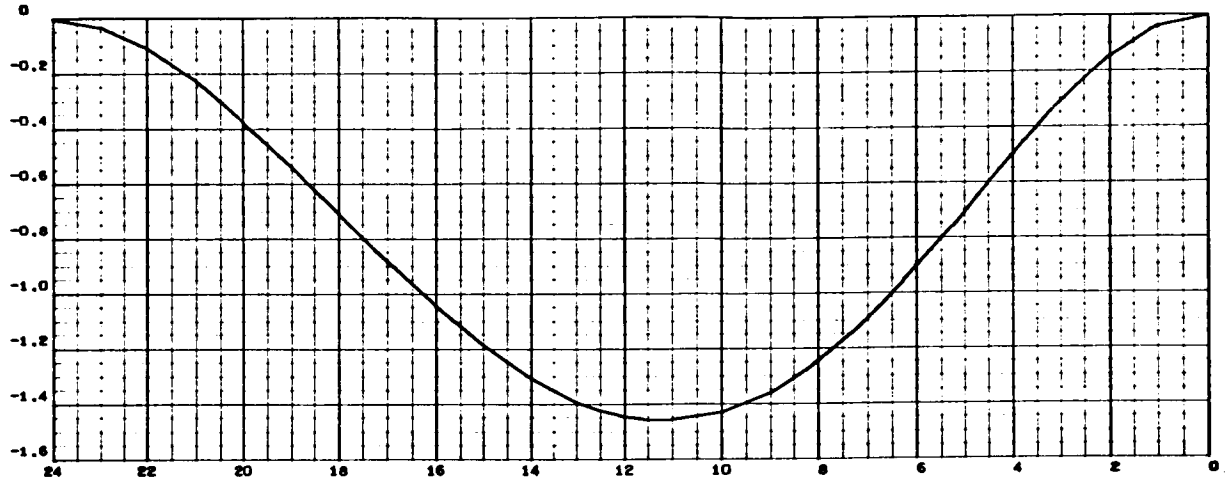

VEHICLE STATIONS - INCHES
SLOPE - DEG./FT.

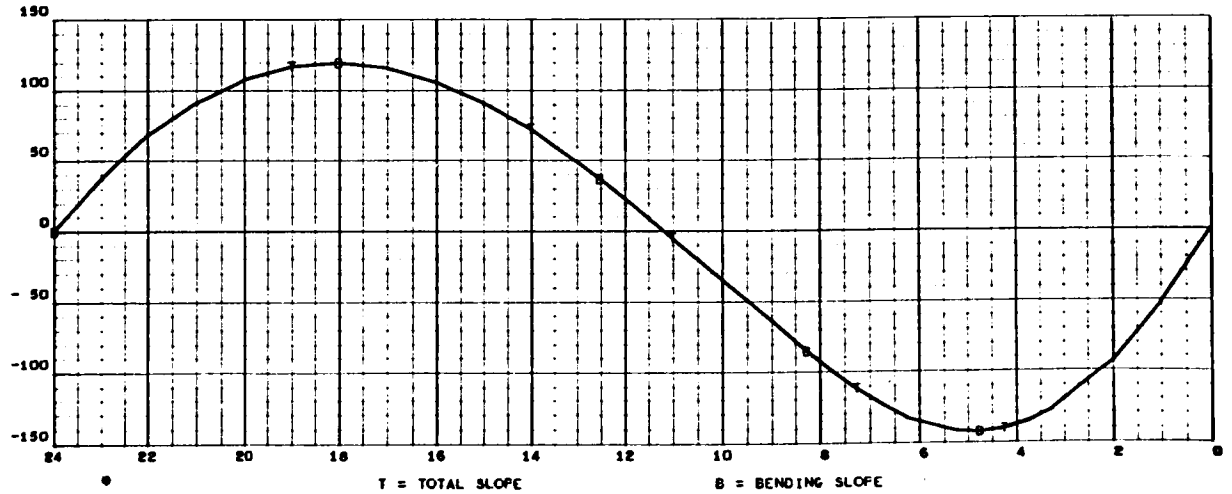

T = TOTAL SLOPE B = BENDING SLOPE
VEHICLE STATIONS - INCHES

MAY 24, 1966

2463-01 L
039 000

MASS LOADING EFFECTS ON BEAM VIBRATION-FIXED ENDS (CASE 8)

FREQUENCY (2) = 8.9026649E 02 RAD./SEC., 1.4169031E 02 C.P.S.
STRUCTURAL MODE (2)
NORMALIZED TO TOTAL WEIGHT
TOTAL WEIGHT = 9.8999992E-01
DEFLECTION - FT./FT.

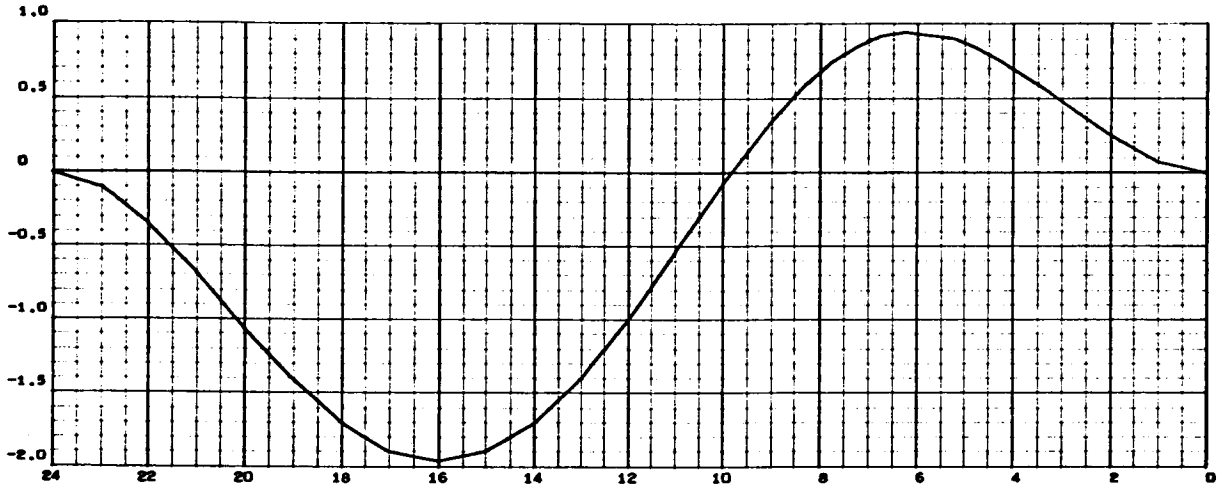

VEHICLE STATIONS - INCHES
SLOPE - DEG./FT.

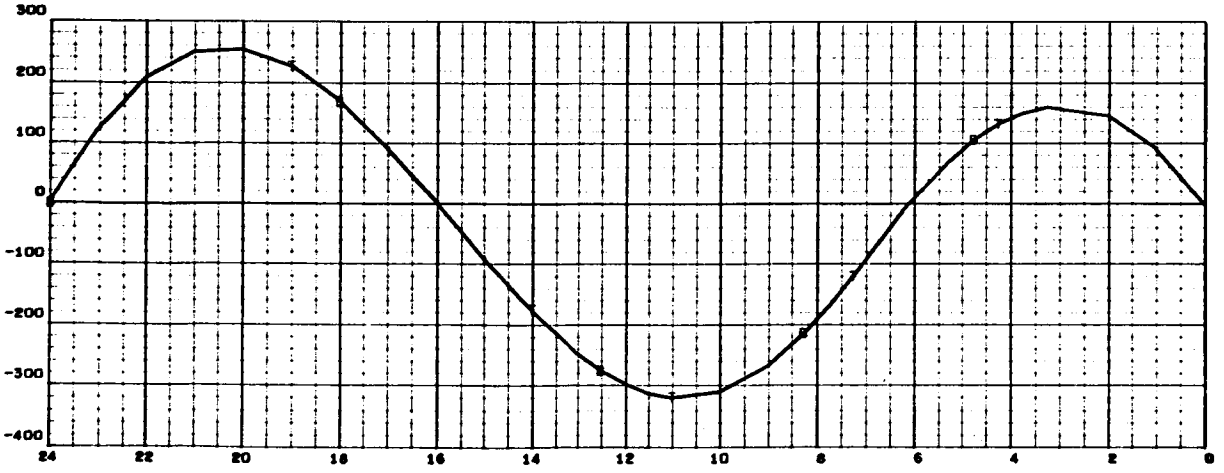

T = TOTAL SLOPE B = BENDING SLOPE
VEHICLE STATIONS - INCHES

MAY 24, 1966

2463-01 L
041 000

MASS LOADING EFFECTS ON BEAM VIBRATION-FIXED ENDS (CASE 8)

FREQUENCY (3) = 1.9950764E 03 RAD./SEC., 3.1752628E 02 C.P.S.
STRUCTURAL MODE (3)
NORMALIZED TO TOTAL WEIGHT
TOTAL WEIGHT = 9.8999992E-01
DEFLECTION - FT./FT.

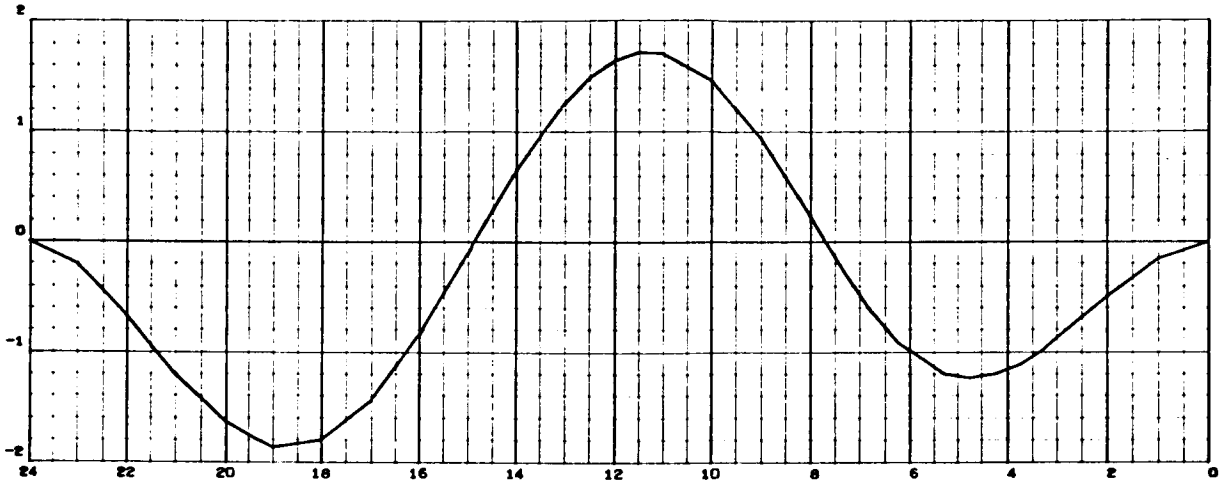

VEHICLE STATIONS - INCHES
SLOPE - DEG./FT.

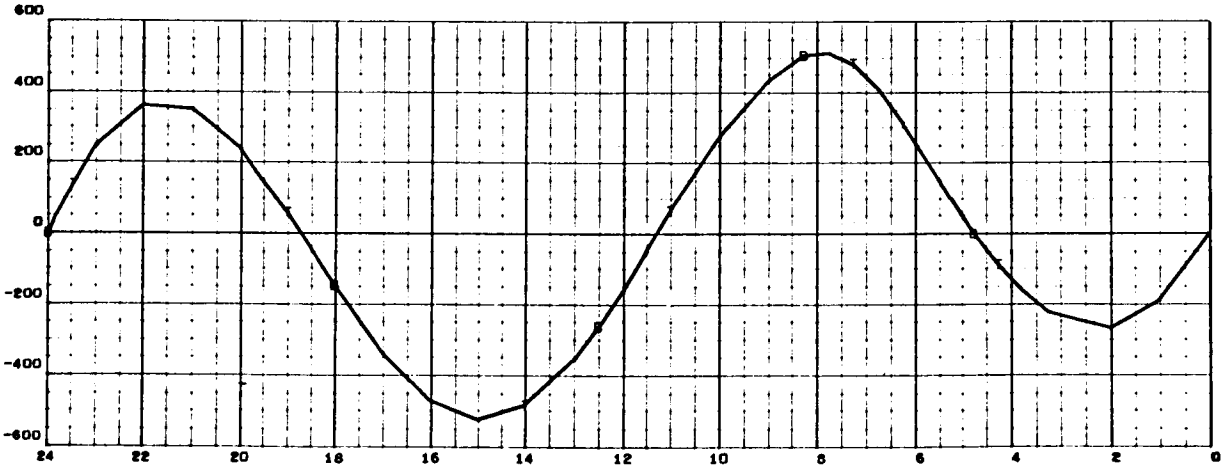

T = TOTAL SLOPE B = BENDING SLOPE
VEHICLE STATIONS - INCHES

MAY 24, 1966

2463-01 L
043 000

MASS LOADING EFFECTS ON BEAM VIBRATION-FIXED ENDS (CASE 8)

FREQUENCY (4) = 3.2140961E 03 RAD./SEC., 5.1153928E 02 C.P.S.
STRUCTURAL MODE (4)
NORMALIZED TO TOTAL WEIGHT
TOTAL WEIGHT = 9.8999992E-01
DEFLECTION - FT./FT.

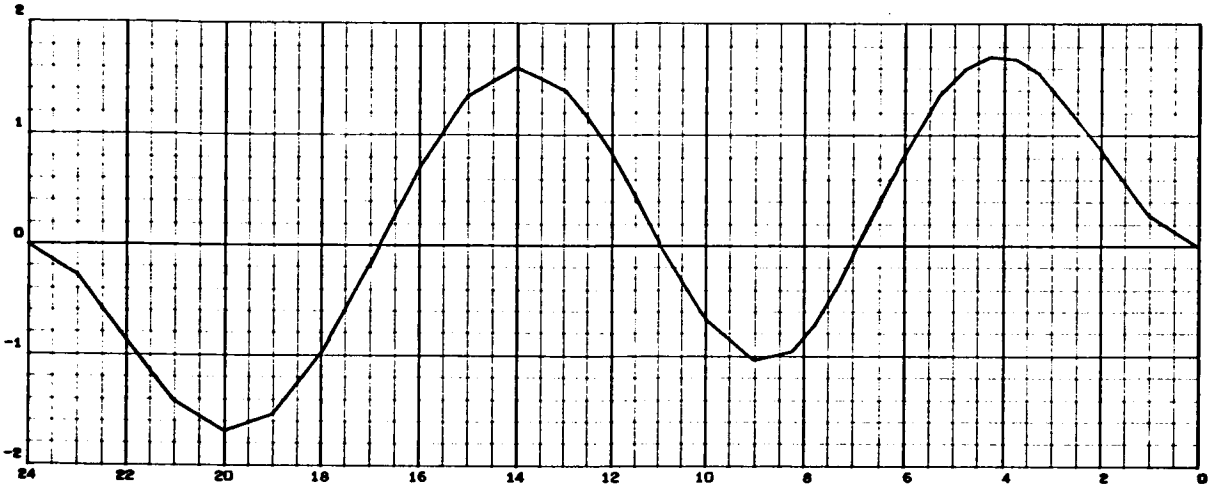

VEHICLE STATIONS - INCHES
SLOPE - DEG./FT.

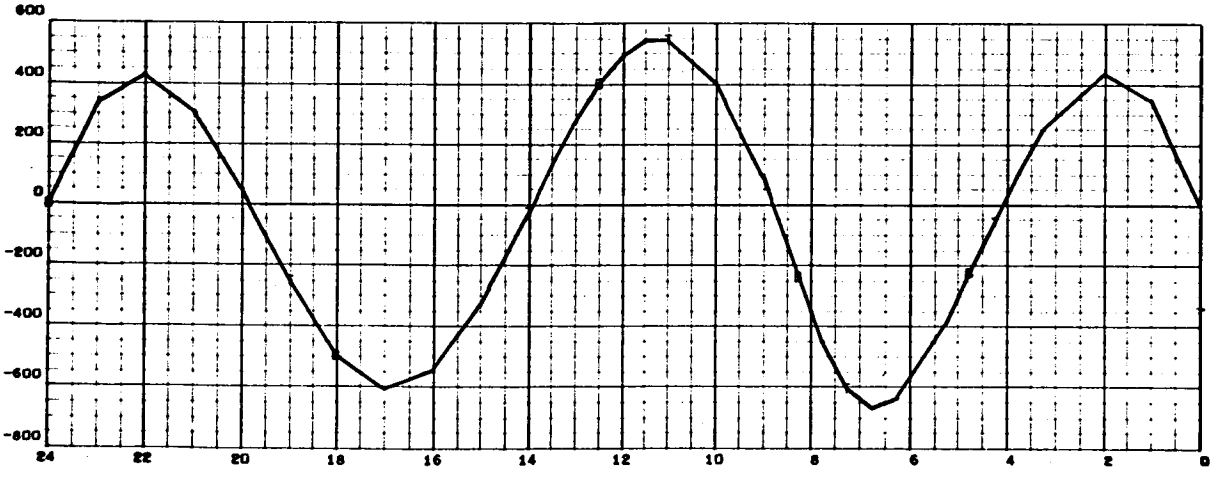

T = TOTAL SLOPE B = BENDING SLOPE
VEHICLE STATIONS - INCHES

MAY 24, 1966

2463-01 L
045 000

MASS LOADING EFFECTS ON BEAM VIBRATION-FIXED ENDS (CASE 9)

FREQUENCY (1) = 2.7672644E 02 RAD./SEC., 4.4042380E 01 C.P.S.
STRUCTURAL MODE (1)
NORMALIZED TO TOTAL WEIGHT
TOTAL WEIGHT = 9.8999991E-01
DEFLECTION - FT./FT.

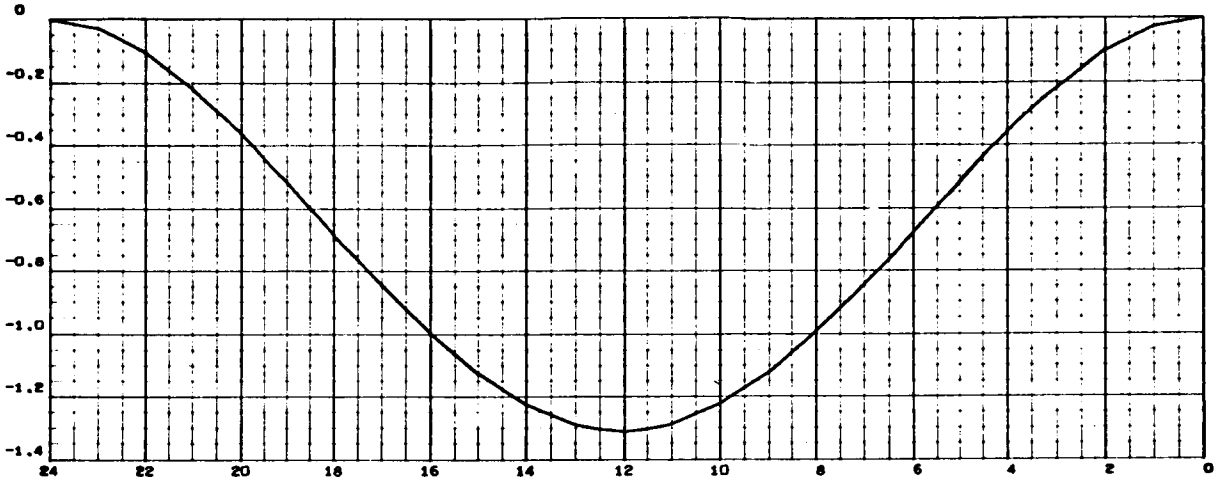

VEHICLE STATIONS - INCHES
SLOPE - DEG./FT.

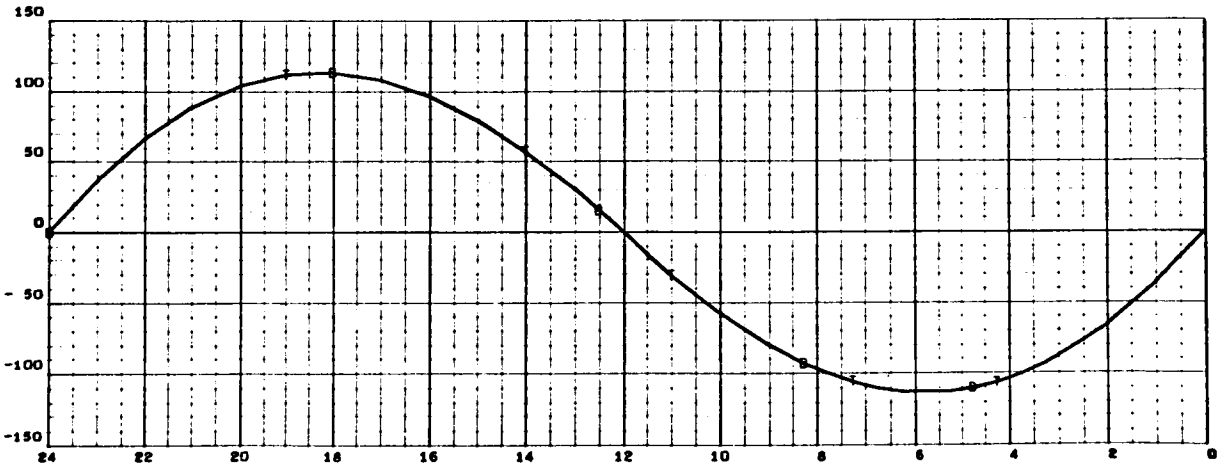

T = TOTAL SLOPE B = BENDING SLOPE
VEHICLE STATIONS - INCHES

MAY 24, 1966

2463-01 L
047 000

MASS LOADING EFFECTS ON BEAM VIBRATION-FIXED ENDS (CASE 9)

FREQUENCY (2) = 1.0863240E 03 RAD./SEC., 1.7321214E 02 C.P.S.
STRUCTURAL MODE (2)
NORMALIZED TO TOTAL WEIGHT
TOTAL WEIGHT = 9.8999991E-01
DEFLECTION - FT./FT.

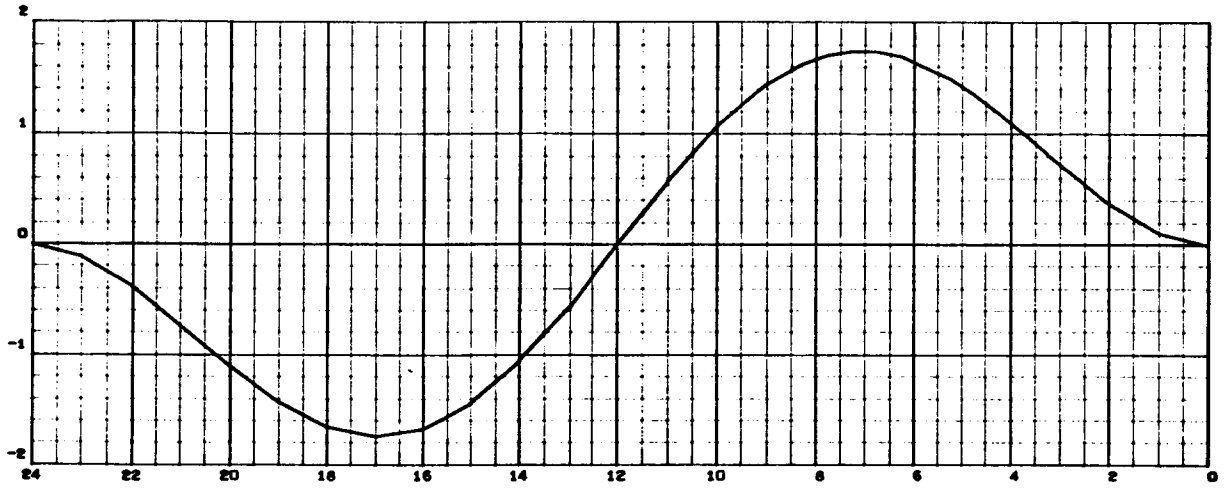

VEHICLE STATIONS - INCHES
SLOPE - DEG./FT.

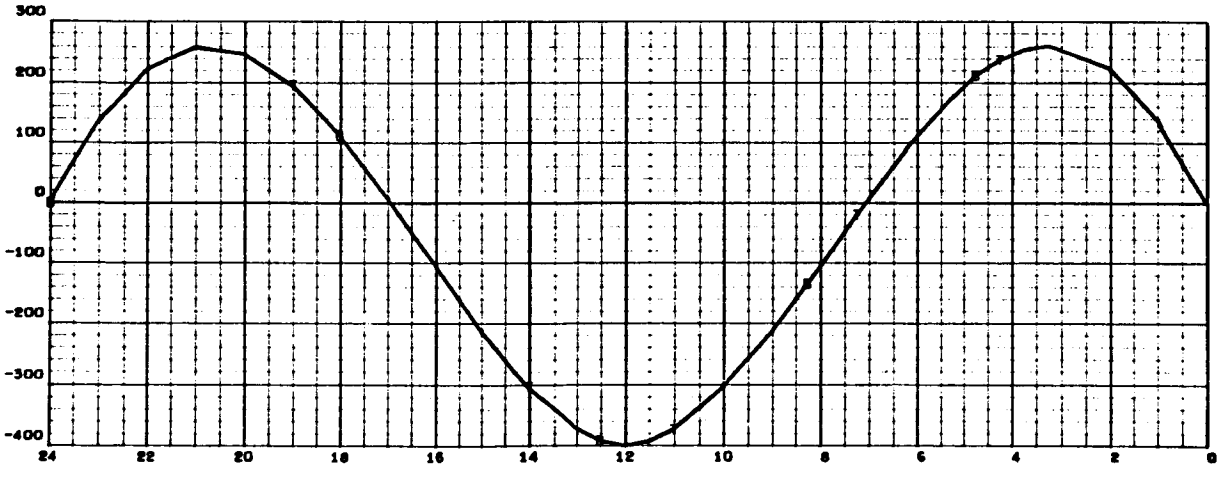

T = TOTAL SLOPE B = BENDING SLOPE
VEHICLE STATIONS - INCHES

MAY 24, 1966

2463-01
049 000

MASS LOADING EFFECTS ON BEAM VIBRATION-FIXED ENDS (CASE 9)

FREQUENCY (3) = 1.8803277E 03 RAD./SEC., 2.9926344E 02 C.P.S.
STRUCTURAL MODE (3)
NORMALIZED TO TOTAL WEIGHT
TOTAL WEIGHT = 9.8999991E-01
DEFLECTION - FT./FT.

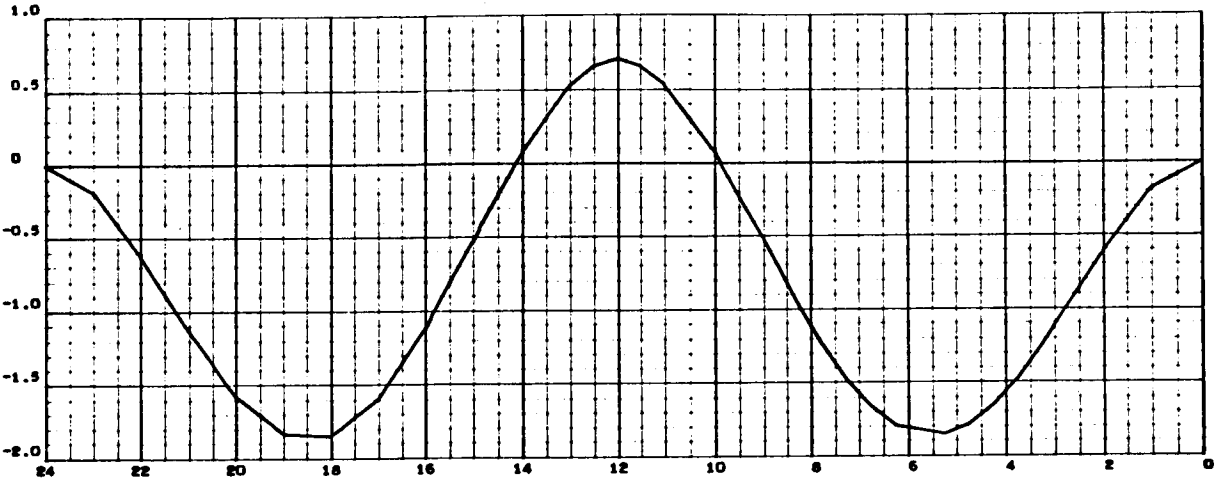

VEHICLE STATIONS - INCHES
SLOPE - DEG./FT.

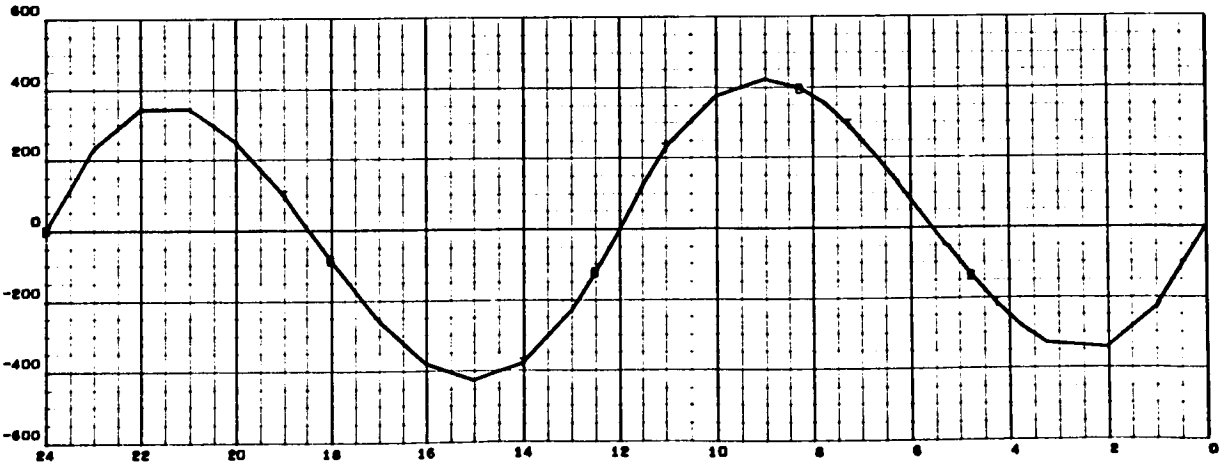

T = TOTAL SLOPE B = BENDING SLOPE
VEHICLE STATIONS - INCHES

MAY 24, 1966

2463-01
051 000

MASS LOADING EFFECTS ON BEAM VIBRATION-FIXED ENDS (CASE 9)

FREQUENCY (4) = 3.2370315E 03 RAD./SEC., 5.1518955E 02 C.P.S.
STRUCTURAL MODE (4)
NORMALIZED TO TOTAL WEIGHT
TOTAL WEIGHT = 9.8999991E-01
DEFLECTION - FT./FT.

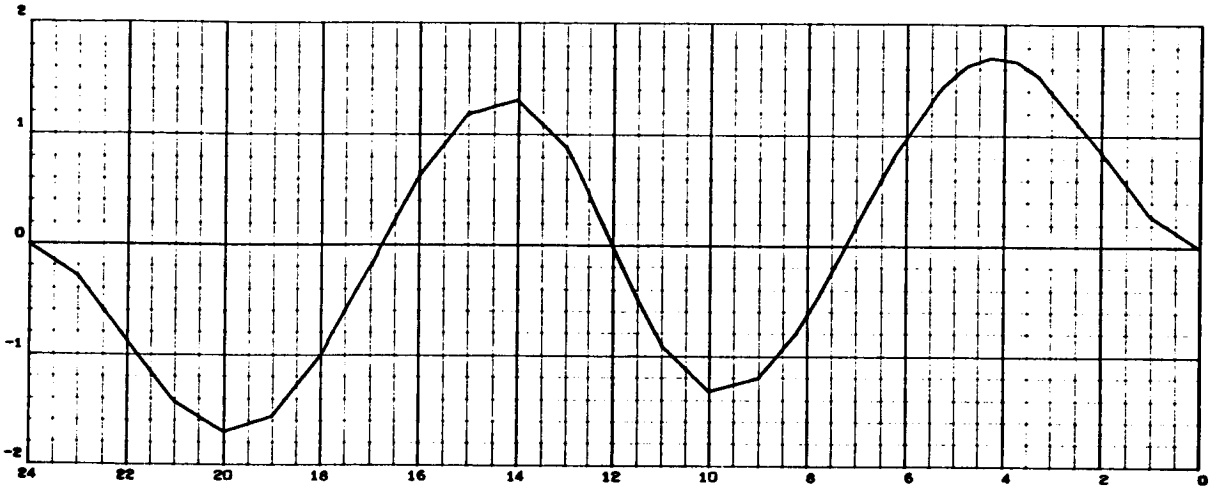

VEHICLE STATIONS - INCHES
SLOPE - DEG./FT.

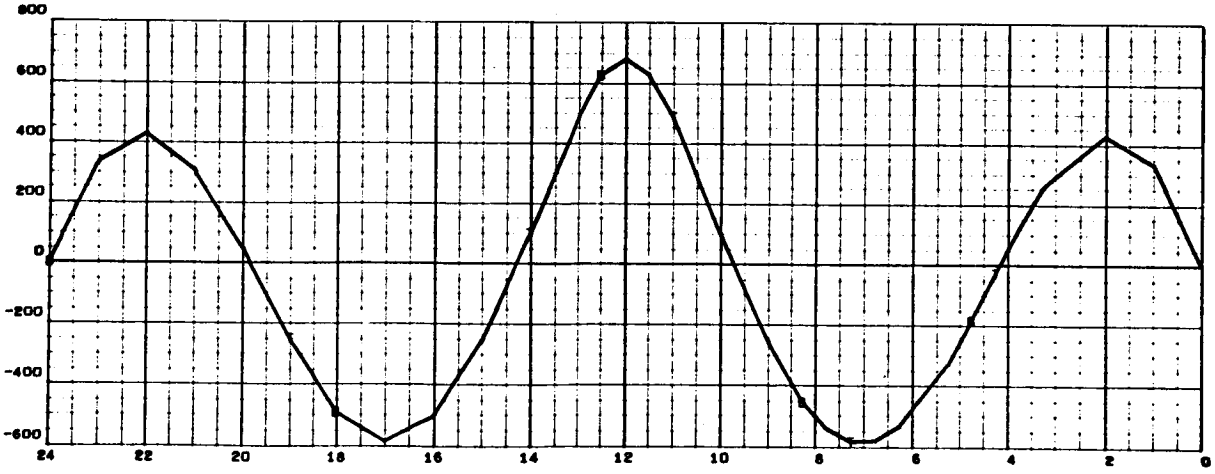

T = TOTAL SLOPE B = BENDING SLOPE
VEHICLE STATIONS - INCHES

MAY 24, 1966

2463-01 L
053 000

MASS LOADING EFFECTS ON BEAM VIBRATION FIXED ENDS (CASE 10)

FREQUENCY (1) = 3.6881385E 02 RAD./SEC., 5.8698548E 01 C.P.S.
STRUCTURAL MODE (1)
NORMALIZED TO TOTAL WEIGHT
TOTAL WEIGHT = 1.1549999E 00
DEFLECTION - FT./FT.

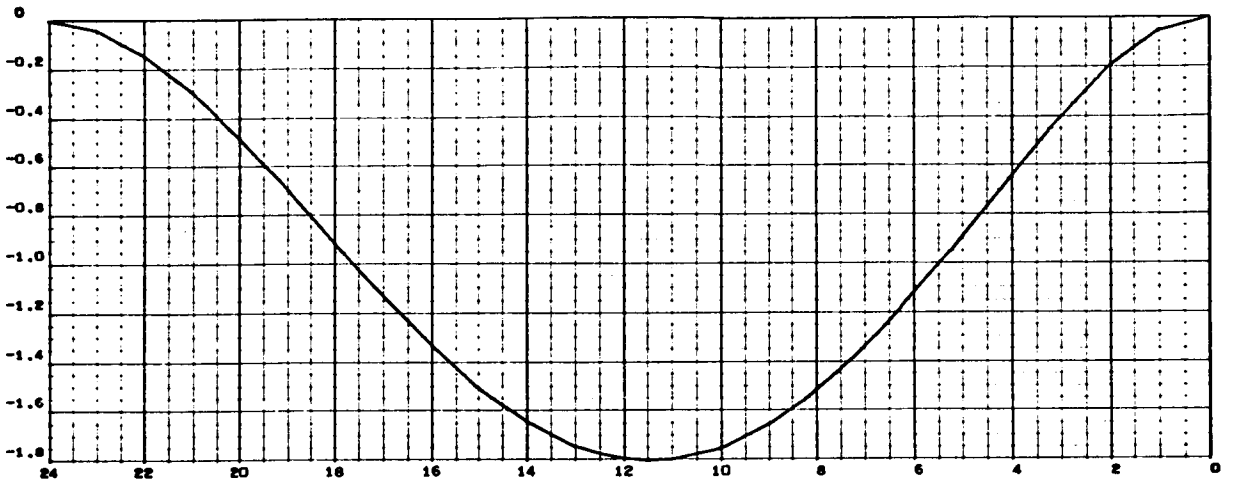

VEHICLE STATIONS - INCHES
SLOPE - DEG./FT.

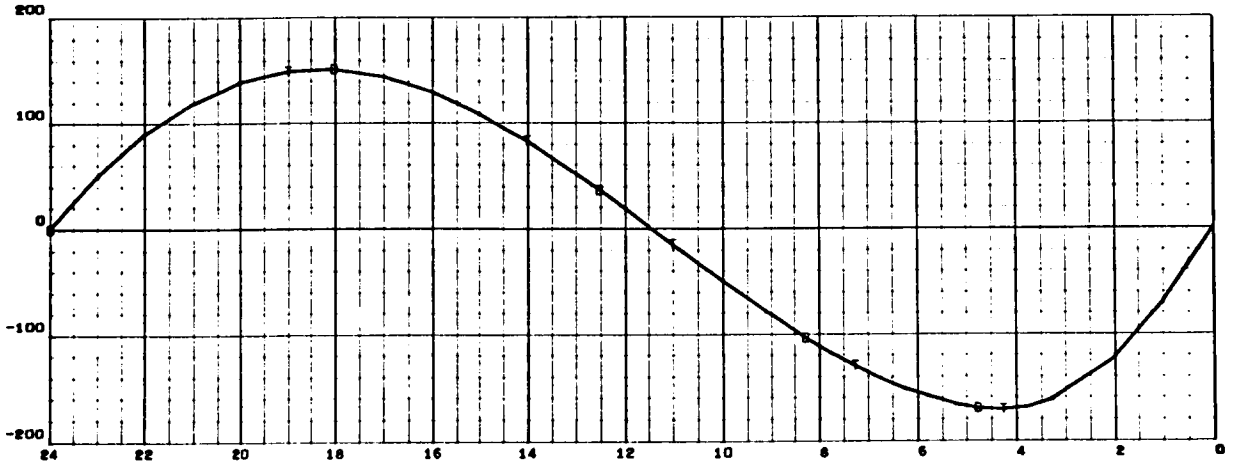

T = TOTAL SLOPE B = BENDING SLOPE
VEHICLE STATIONS - INCHES

MAY 24, 1966

2463-01
055 000

MASS LOADING EFFECTS ON BEAM VIBRATION FIXED ENDS (CASE 10)

FREQUENCY (2) = 8.3194969E 02 RAD./SEC., 1.3240747E 02 C.P.S.
STRUCTURAL MODE (2)
NORMALIZED TO TOTAL WEIGHT
TOTAL WEIGHT = 1.1549999E 00
DEFLECTION - FT./FT.

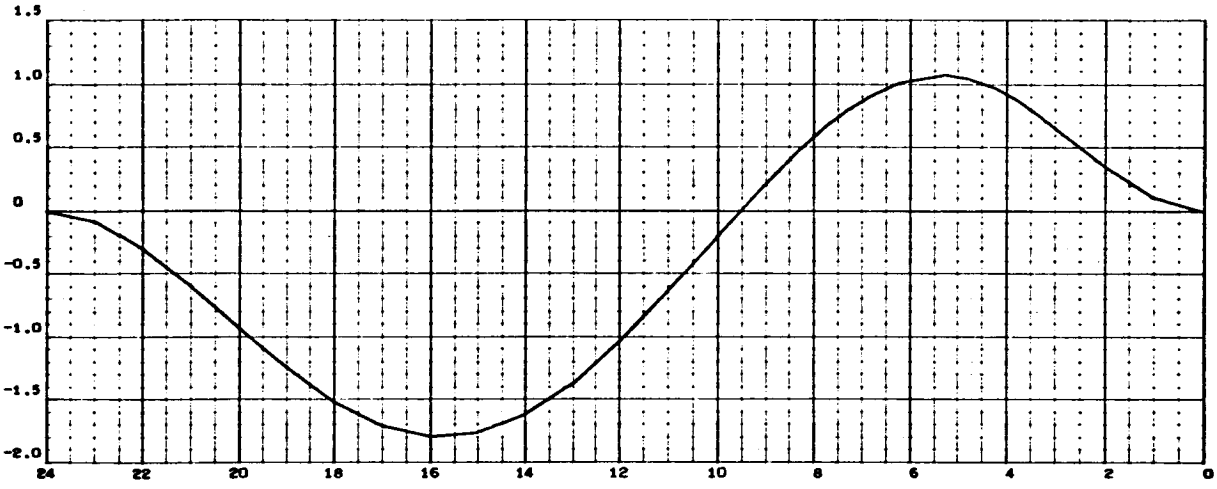

VEHICLE STATIONS - INCHES
SLOPE - DEG./FT.

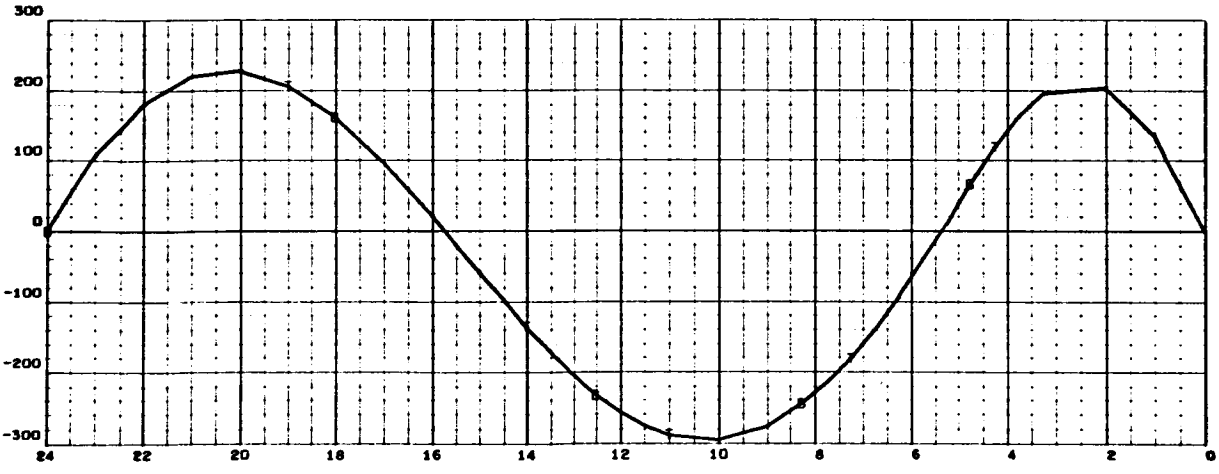

T = TOTAL SLOPE B = BENDING SLOPE
VEHICLE STATIONS - INCHES

MAY 24, 1966

2463-01 L
057 000

MASS LOADING EFFECTS ON BEAM VIBRATION FIXED ENDS (CASE 10)

FREQUENCY (3) = 1.7107233E 02 RAD./SEC., 2.7227006E 02 C.P.S.
STRUCTURAL MODE (3)
NORMALIZED TO TOTAL WEIGHT
TOTAL WEIGHT = 1.1549999E 00
DEFLECTION - FT./FT.

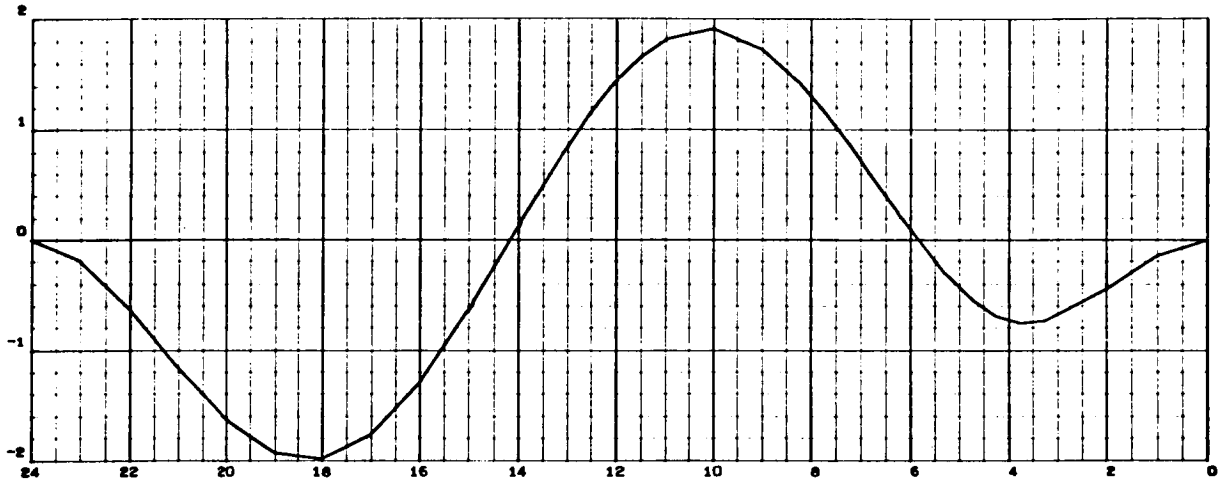

VEHICLE STATIONS - INCHES
SLOPE - DEG./FT.

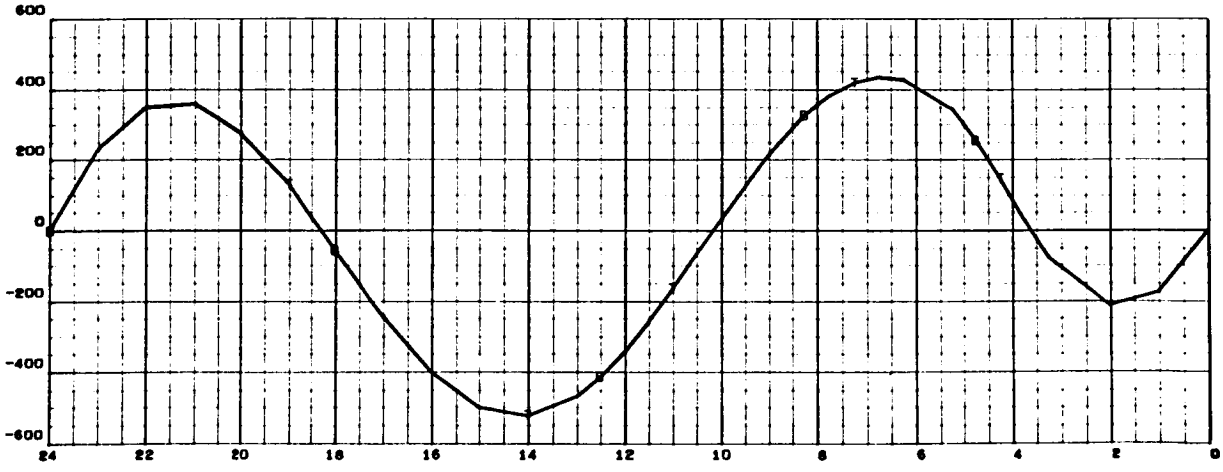

T = TOTAL SLOPE B = BENDING SLOPE
VEHICLE STATIONS - INCHES

MAY 24, 1966

2463-01 L
059 000

MASS LOADING EFFECTS ON BEAM VIBRATION FIXED ENDS (CASE 10)

FREQUENCY (4) = 2.8943498E 03 RAD./SEC., 4.6065007E 02 C.P.S.
STRUCTURAL MODE (4)
NORMALIZED TO TOTAL WEIGHT
TOTAL WEIGHT = 1.1549999E 00
DEFLECTION - FT./FT.

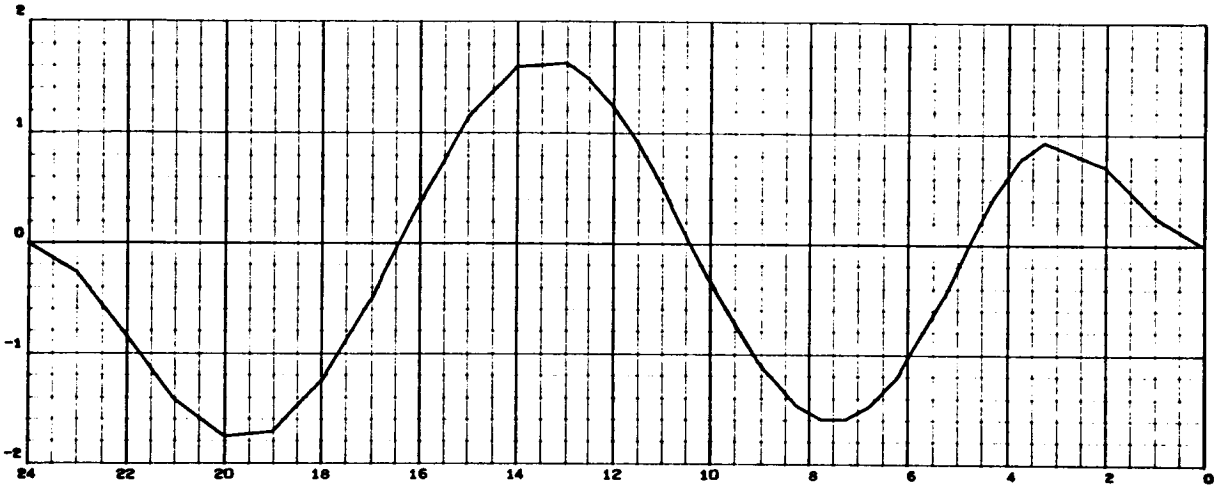

VEHICLE STATIONS - INCHES
SLOPE - DEG./FT.

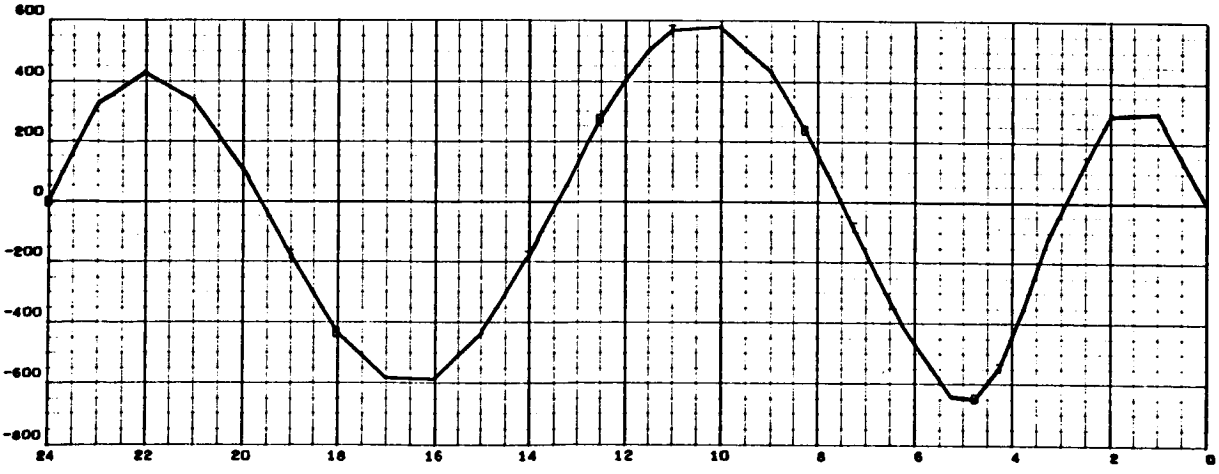

T = TOTAL SLOPE B = BENDING SLOPE
VEHICLE STATIONS - INCHES

MAY 24, 1966

2463-01 L
061 000

MASS LOADING EFFECTS ON BEAM VIBRATION - FIXED ENDS (CASE 11)

FREQUENCY (1) = 2.8984338E 02 RAD./SEC., 4.6130006E 01 C.P.S.
STRUCTURAL MODE (1)
NORMALIZED TO TOTAL WEIGHT
TOTAL WEIGHT = 1.1549999E 00
DEFLECTION - FT./FT.

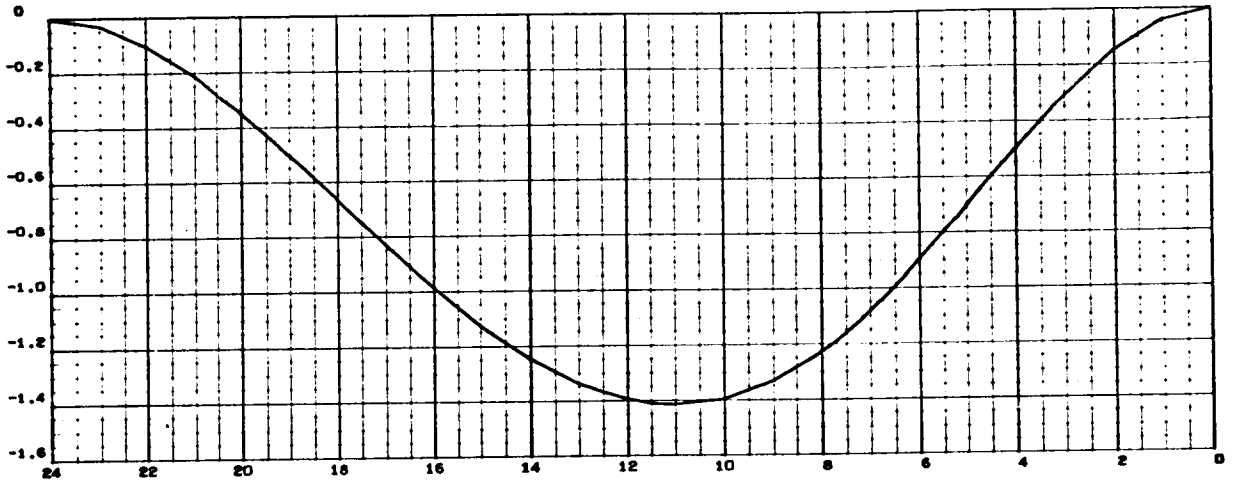

VEHICLE STATIONS - INCHES
SLOPE - DEG./FT.

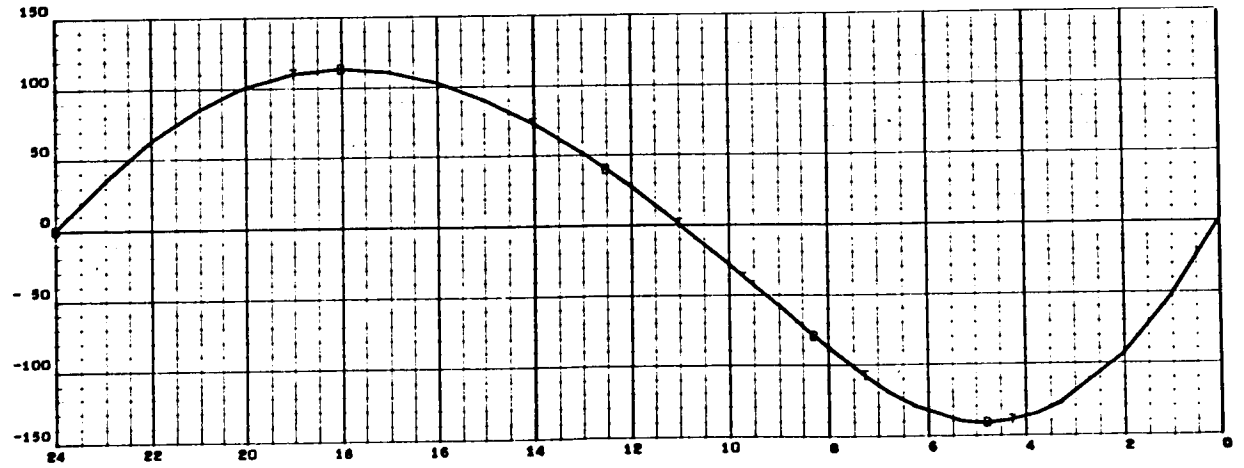

T = TOTAL SLOPE B = BENDING SLOPE
VEHICLE STATIONS - INCHES

MAY 24, 1966

2463-01 L
063 000

MASS LOADING EFFECTS ON BEAM VIBRATION - FIXED ENDS (CASE 11)

FREQUENCY (2) = 8.4786705E 02 RAD./SEC., 1.3494223E 02 C.P.S.
STRUCTURAL MODE (2)
NORMALIZED TO TOTAL WEIGHT
TOTAL WEIGHT = 1.1549999E 00
DEFLECTION - FT./FT.

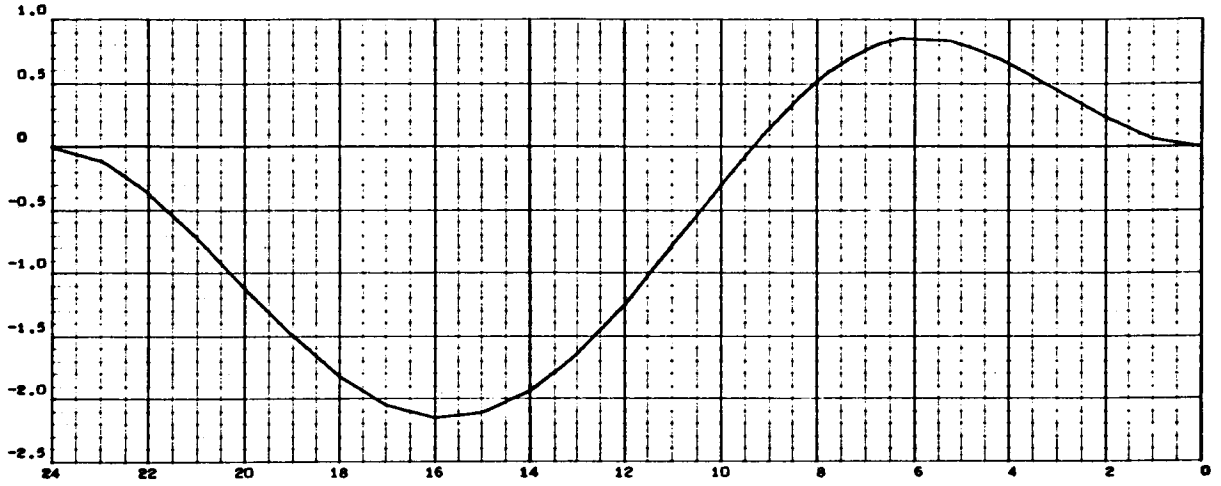

VEHICLE STATIONS - INCHES
SLOPE - DEG./FT.

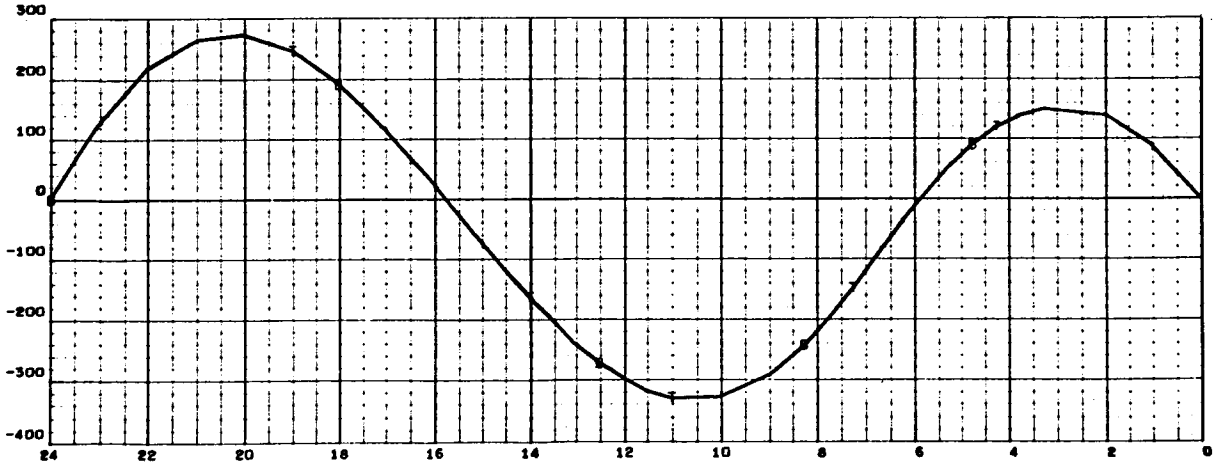

T = TOTAL SLOPE B = BENDING SLOPE
VEHICLE STATIONS - INCHES

MAY 24, 1966

8463-01
065 000

MASS LOADING EFFECTS ON BEAM VIBRATION - FIXED ENDS (CASE 11)

FREQUENCY (3) = 1.8671238E 03 RAD./SEC., 2.9716198E 02 C.P.S.
STRUCTURAL MODE (3)
NORMALIZED TO TOTAL WEIGHT
TOTAL WEIGHT = 1.1549999E 00
DEFLECTION - FT./FT.

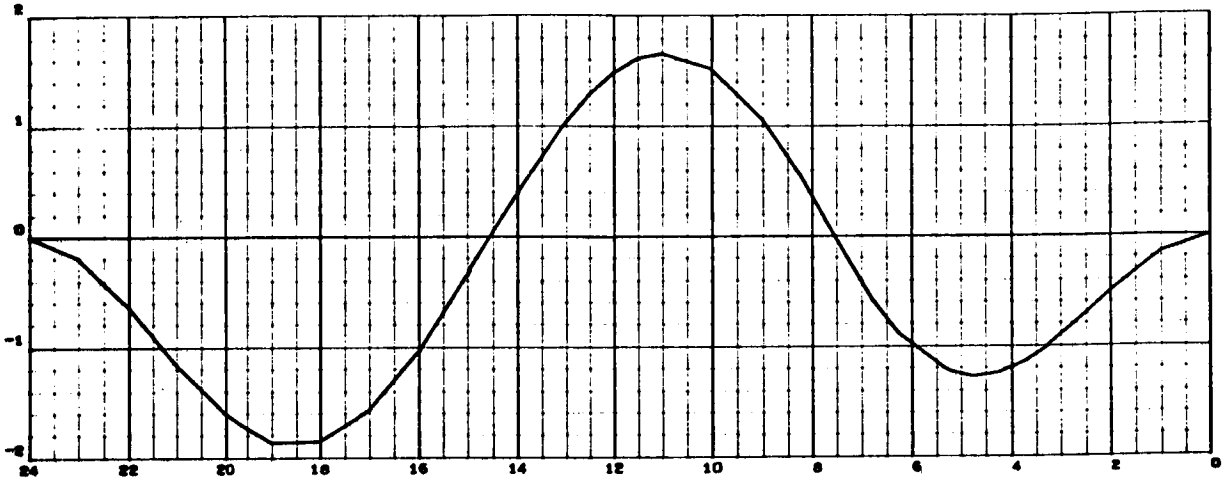

VEHICLE STATIONS - INCHES
SLOPE - DEG./FT.

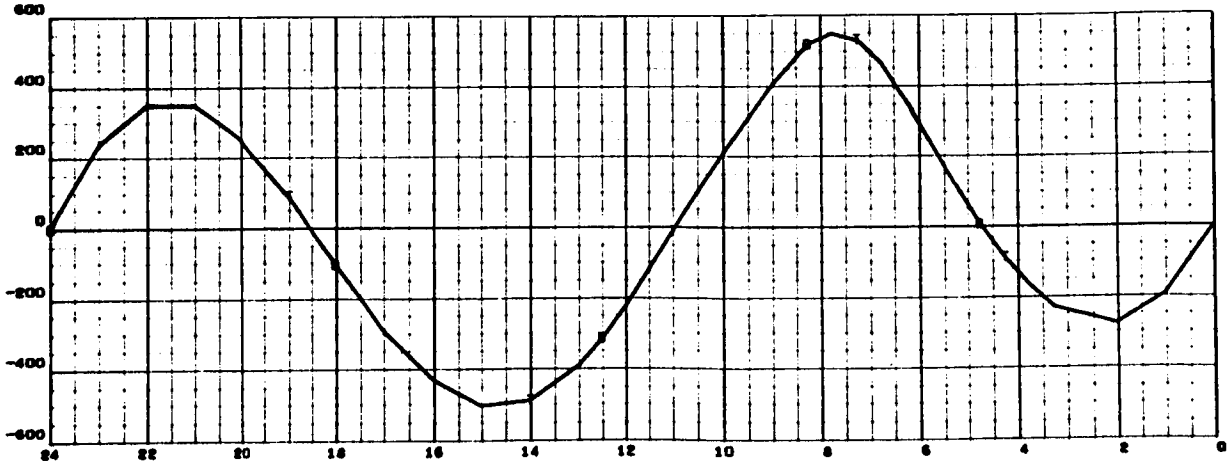

T = TOTAL SLOPE B = BENDING SLOPE
VEHICLE STATIONS - INCHES

MAY 24, 1966

2463-01
067 000

MASS LOADING EFFECTS ON BEAM VIBRATION - FIXED ENDS (CASE 11)

FREQUENCY (4) = 2.9751783E 03 RAD./SEC., 4.7351432E 02 C.P.S.
STRUCTURAL MODE (4)
NORMALIZED TO TOTAL WEIGHT
TOTAL WEIGHT = 1.1549999E 00
DEFLECTION - FT./FT.

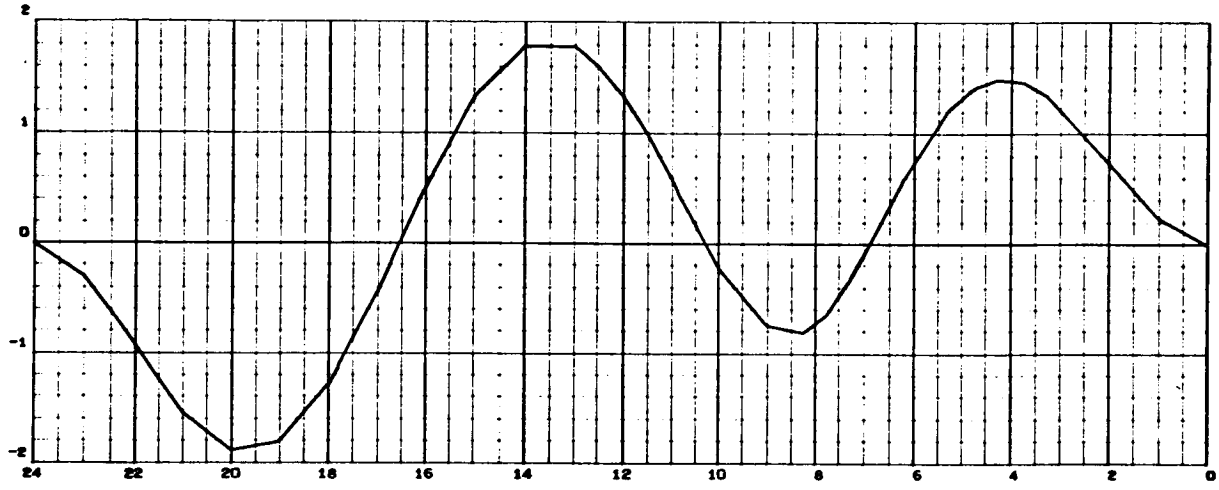

VEHICLE STATIONS - INCHES
SLOPE - DEG./FT.

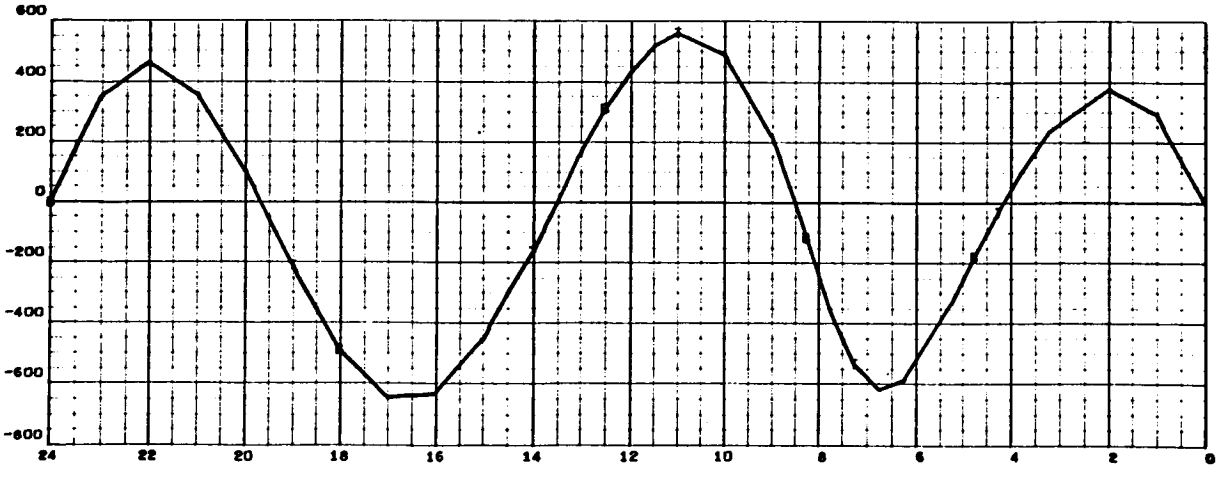

T = TOTAL SLOPE B = BENDING SLOPE
VEHICLE STATIONS - INCHES

MAY 24, 1966

2463-01 L
069 000

MASS LOADING EFFECTS ON BEAM VIBRATION - FIXED ENDS (CASE 12)

FREQUENCY (1) = 2.4445425E 02 RAD./SEC., 3.8906102E 01 C.P.S.
STRUCTURAL MODE (1)
NORMALIZED TO TOTAL WEIGHT
TOTAL WEIGHT = 1.1549999E 00
DEFLECTION - FT./FT.

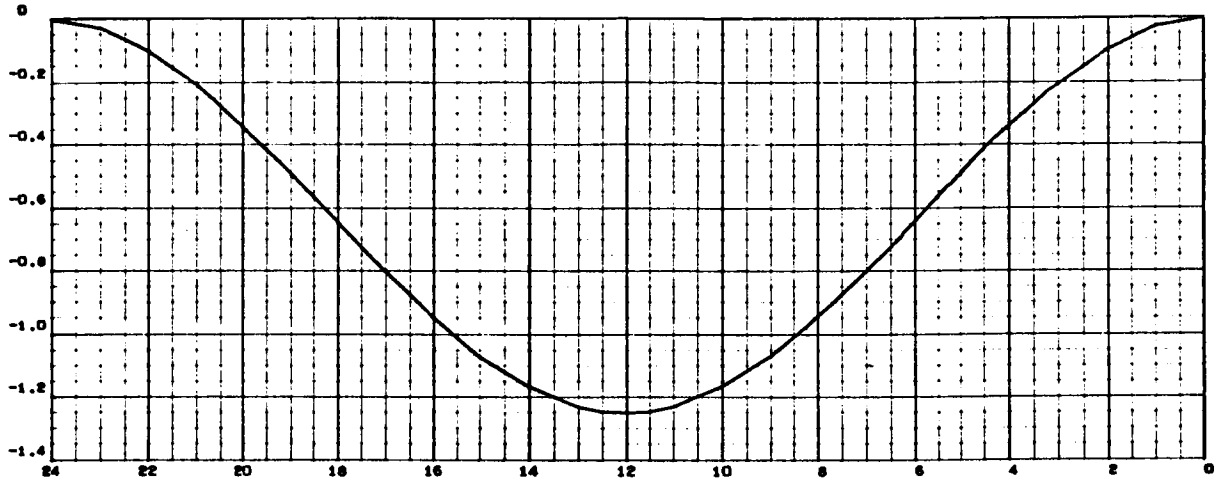

VEHICLE STATIONS - INCHES
SLOPE - DEG./FT.

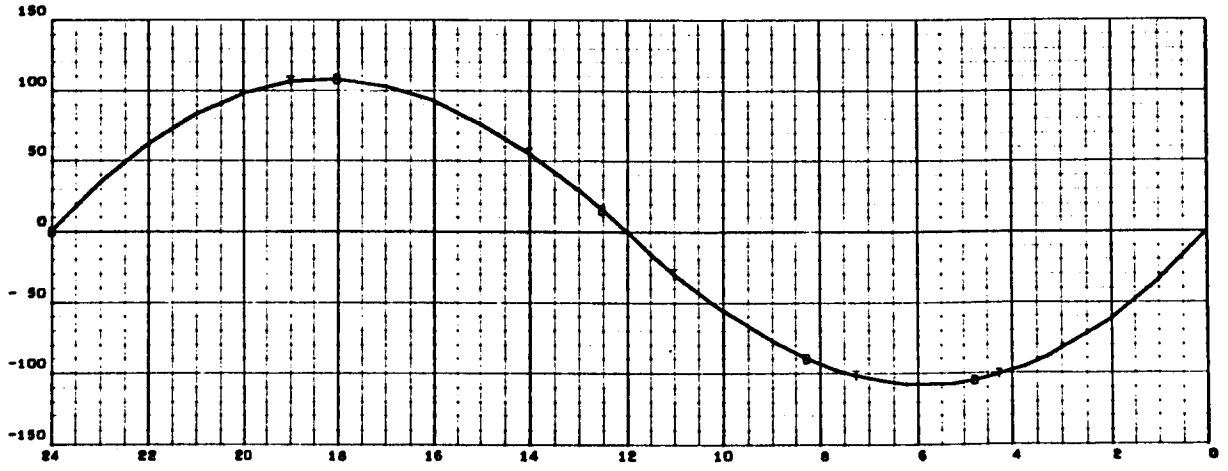

T = TOTAL SLOPE B = BENDING SLOPE
VEHICLE STATIONS - INCHES

MAY 24, 1966

2463-01
071 000

MASS LOADING EFFECTS ON BEAM VIBRATION - FIXED ENDS (CASE 12)

FREQUENCY (2) = 1.0410465E 03 RAD./SEC., 1.6568769E 02 C.P.S.
STRUCTURAL MODE (2)
NORMALIZED TO TOTAL WEIGHT
TOTAL WEIGHT = 1.1549999E 00
DEFLECTION - FT./FT.

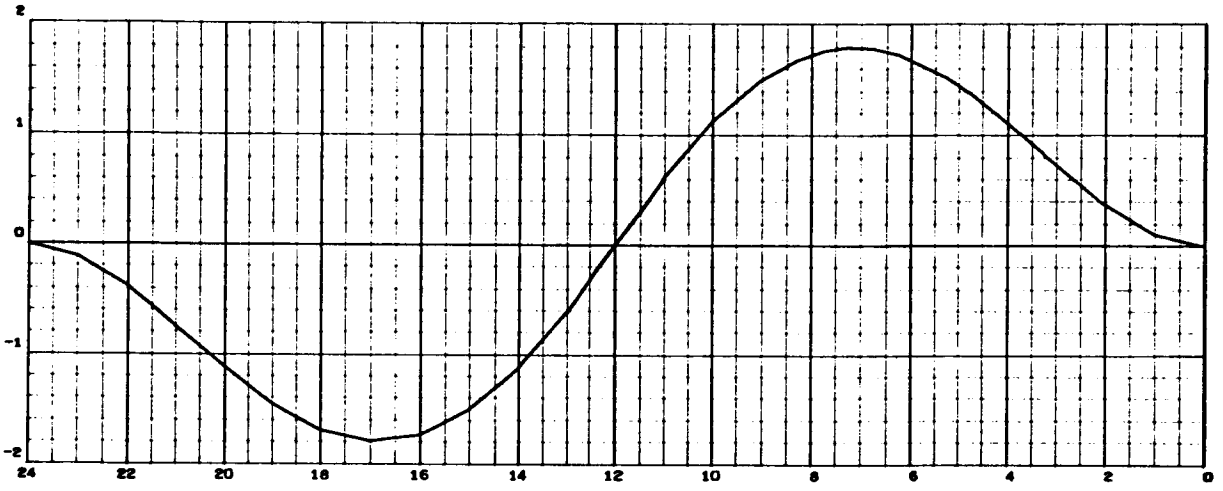

VEHICLE STATIONS - INCHES
SLOPE - DEG./FT.

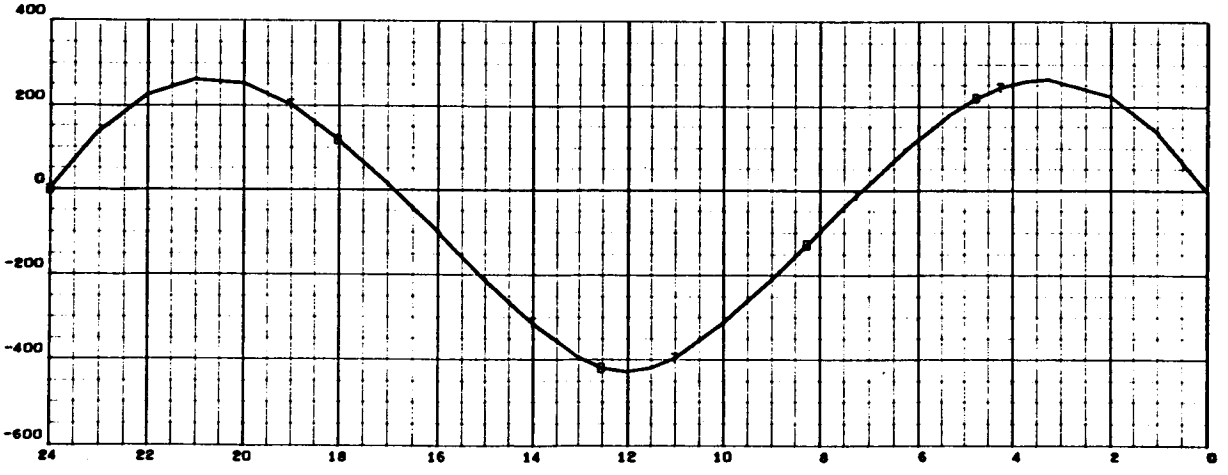

T = TOTAL SLOPE B = BENDING SLOPE
VEHICLE STATIONS - INCHES

MAY 24, 1966

2463-01
073 000

MASS LOADING EFFECTS ON BEAM VIBRAT - FIXED ENDS (CASE 12)

FREQUENCY (3) = 1.8240082E 03 RAD./SEC., 2.9029993E 02 C.P.S.
STRUCTURAL MODE (3)
NORMALIZED TO TOTAL WEIGHT
TOTAL WEIGHT = 1.1549999E 00
DEFLECTION - FT./FT.

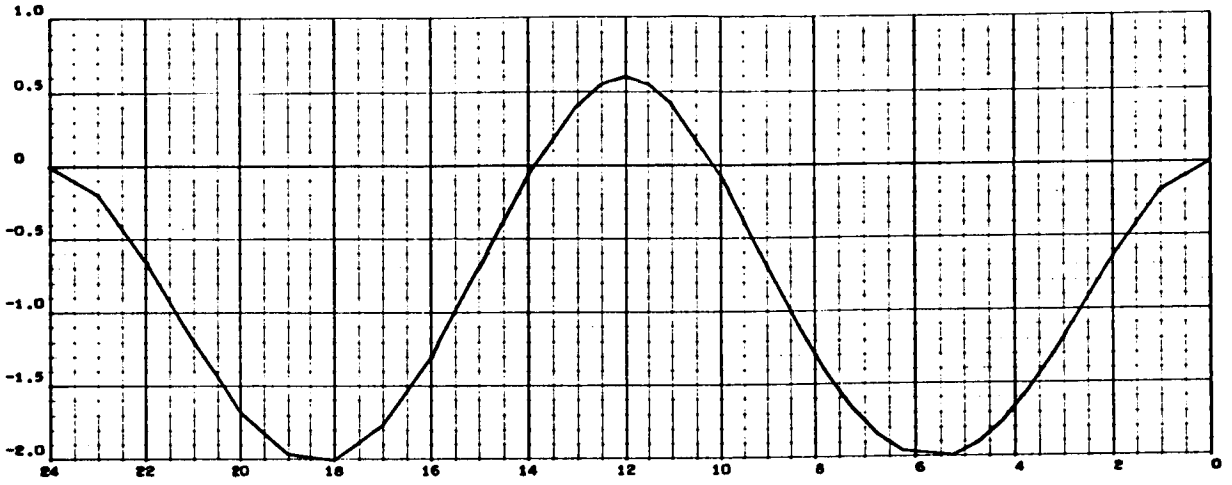

VEHICLE STATIONS - INCHES
SLOPE - DEG./FT.

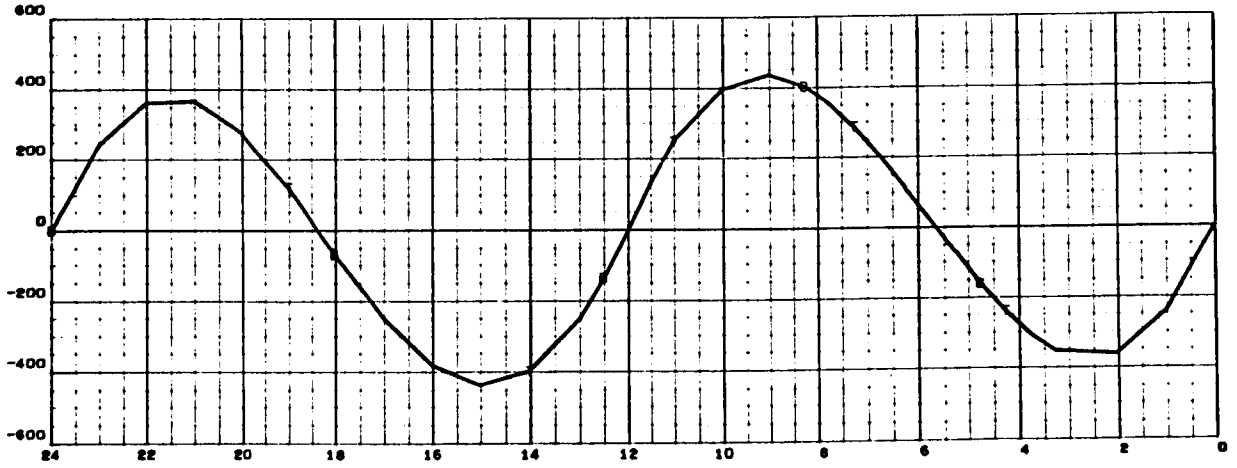

T = TOTAL SLOPE B = BENDING SLOPE
VEHICLE STATIONS - INCHES

MAY 24, 1966

2463-01 L
075 000

MASS LOADING EFFECTS ON BEAM VIBRATION - FIXED ENDS (CASE 12)

FREQUENCY (4) = 2.9487684E 03 RAD./SEC., 4.6931107E 02 C.P.S.
STRUCTURAL MODE (4)
NORMALIZED TO TOTAL WEIGHT
TOTAL WEIGHT = 1.1549999E 00
DEFLECTION - FT./FT.

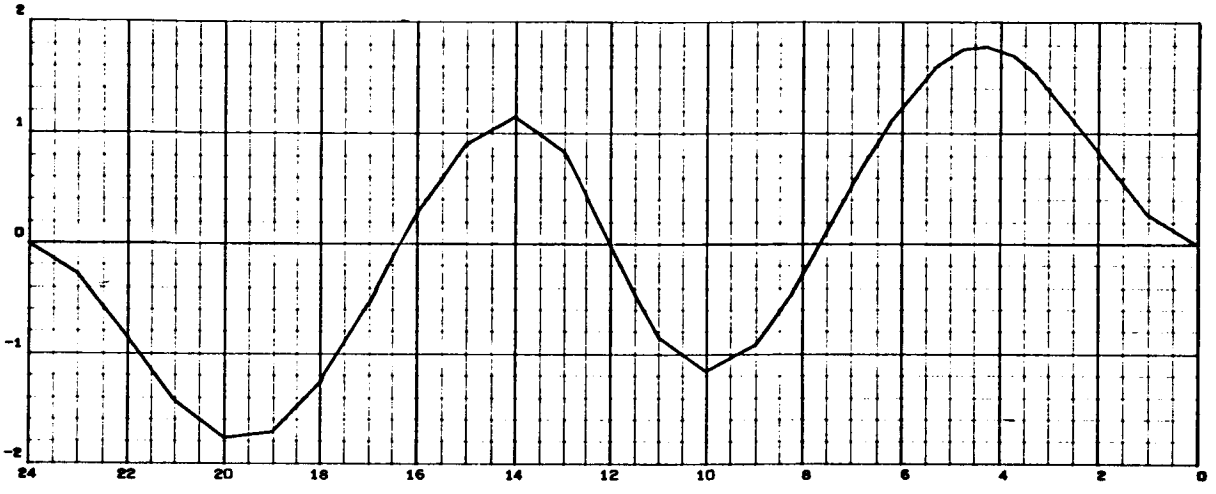

VEHICLE STATIONS - INCHES
SLOPE - DEG./FT.

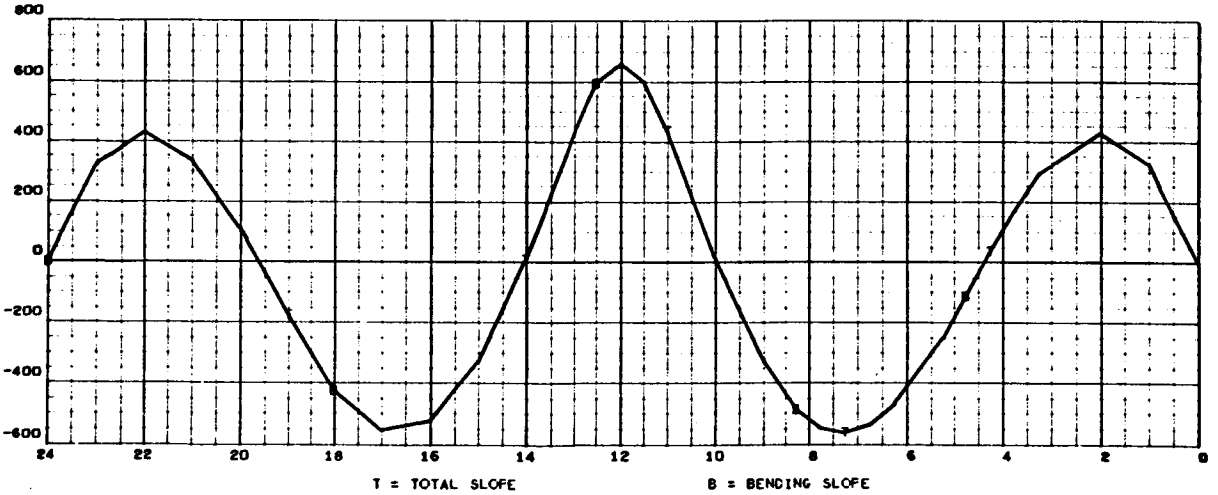

T = TOTAL SLOPE B = BENDING SLOPE
VEHICLE STATIONS - INCHES

MAY 24, 1966

2463-01
077 000

MASS LOADING EFFECTS ON BEAM VIBRATIONS - FIXED ENDS (CASE 13)

FREQUENCY (1) = 3.5388567E 02 RAD./SEC., 5.6322653E 01 C.P.S.
STRUCTURAL MODE (1)
NORMALIZED TO TOTAL WEIGHT
TOTAL WEIGHT = 1.3199999E 00
DEFLECTION - FT./FT.

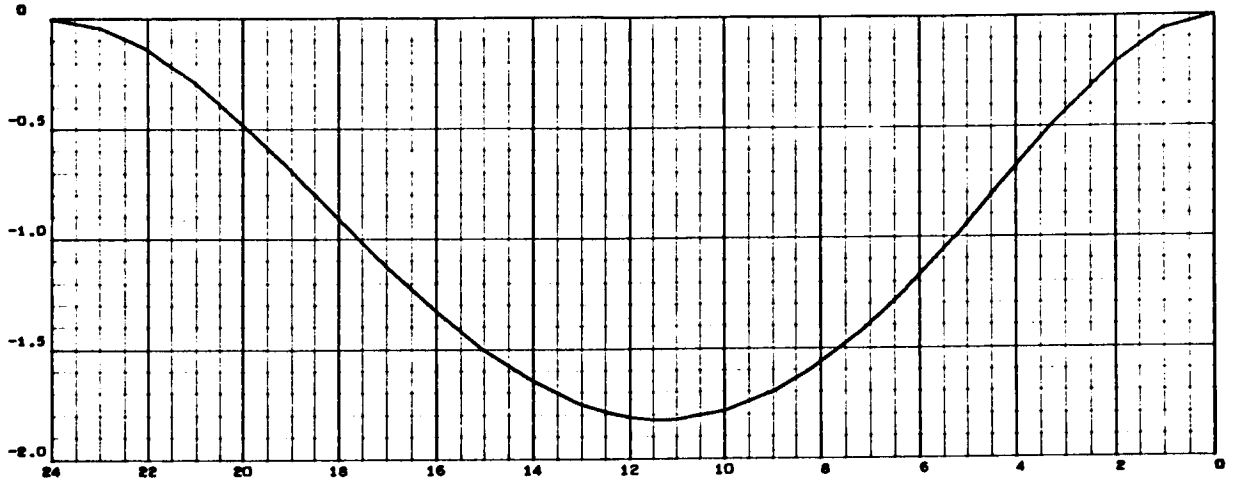

VEHICLE STATIONS - INCHES
SLOPE - DEG./FT.

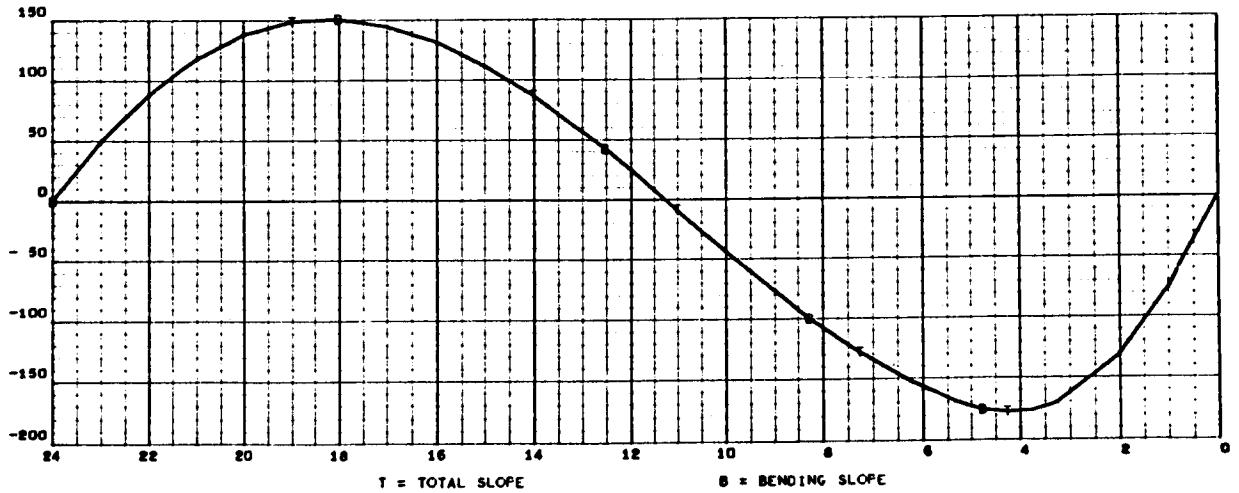

T = TOTAL SLOPE B = BENDING SLOPE
VEHICLE STATIONS - INCHES

MAY 24, 1966

2463-01 L
079 000

MASS LOADING EFFECTS ON BEAM VIBRATIONS - FIXED ENDS (CASE 13)

FREQUENCY (2) = 7.8497063E 02 RAD./SEC., 1.2493196E 02 C.P.S.
STRUCTURAL MODE (2)
NORMALIZED TO TOTAL WEIGHT
TOTAL WEIGHT = 1.3199999E 00
DEFLECTION - FT./FT.

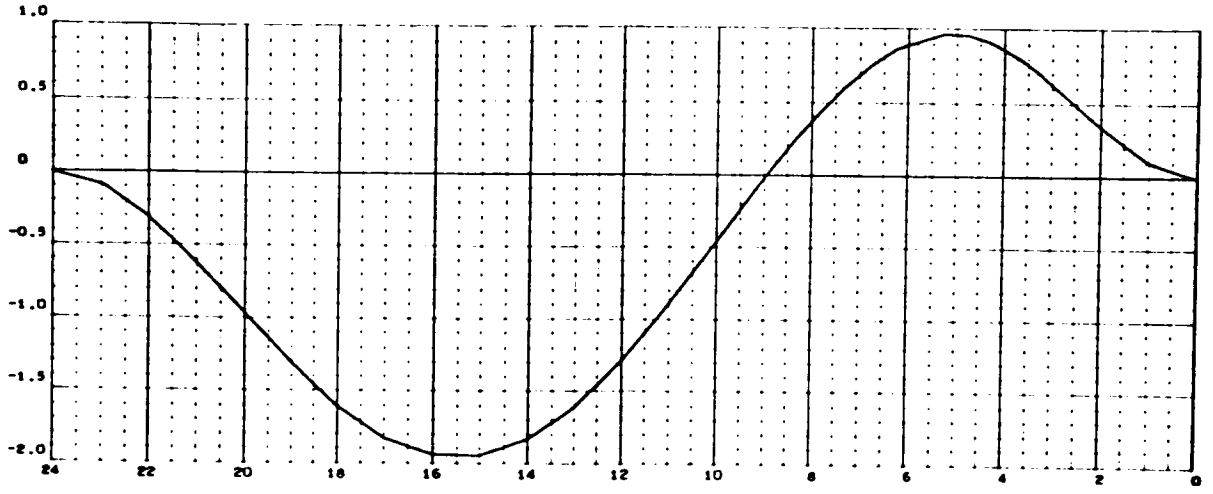

VEHICLE STATIONS - INCHES
SLOPE - DEG./FT.

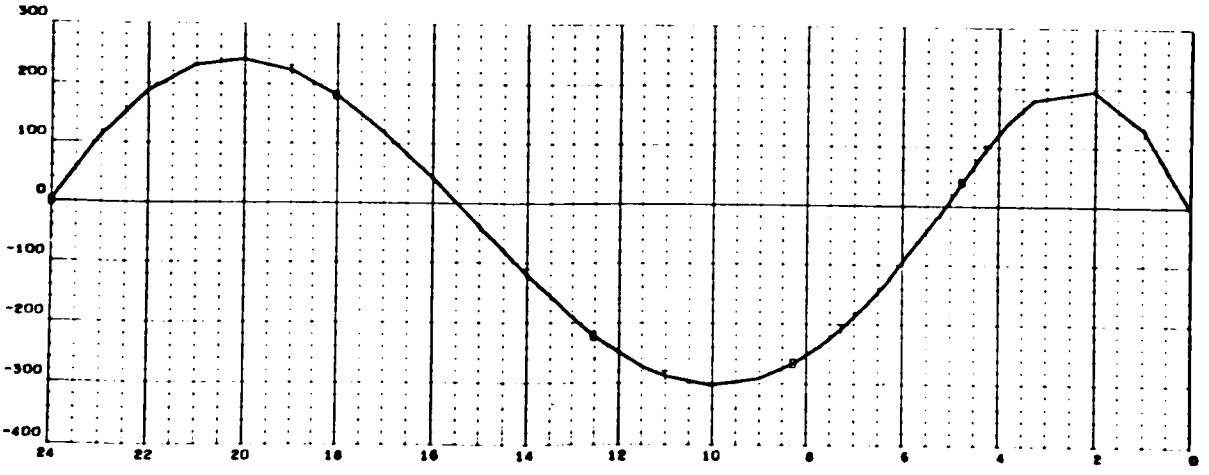

T = TOTAL SLOPE B = BENDING SLOPE
VEHICLE STATIONS - INCHES

MAY 24, 1966

2463-01 L
081 000

MASS LOADING EFFECTS ON BEAM VIBRATIONS - FIXED ENDS (CASE 13)

FREQUENCY (3) = 1.6590789E 03 RAD./SEC., 2.6405061E 02 C.P.S.
STRUCTURAL MODE (3)
NORMALIZED TO TOTAL WEIGHT
TOTAL WEIGHT = 1.3199999E 00
DEFLECTION - FT./FT.

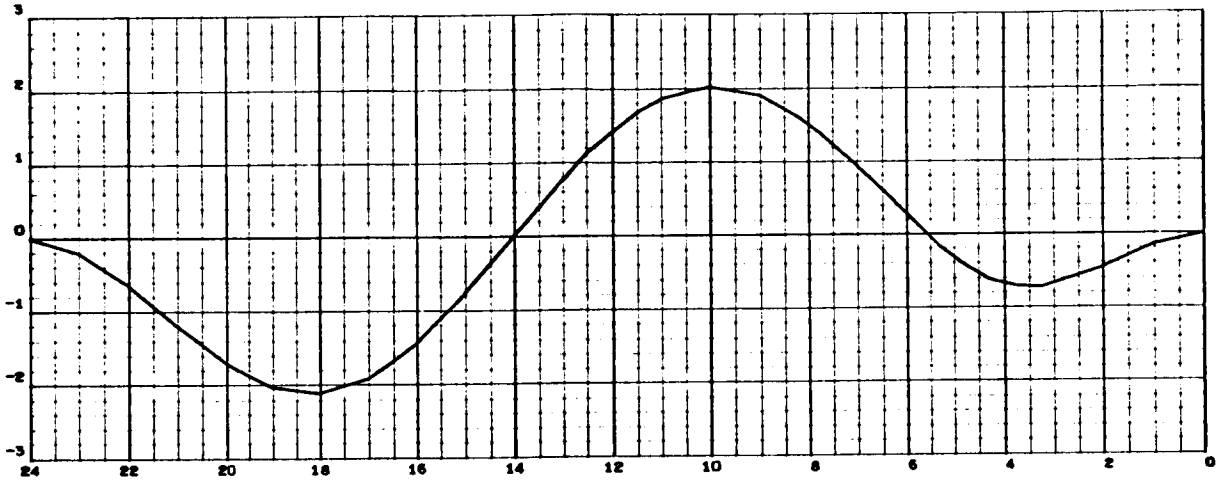

VEHICLE STATIONS - INCHES
SLOPE - DEG./FT.

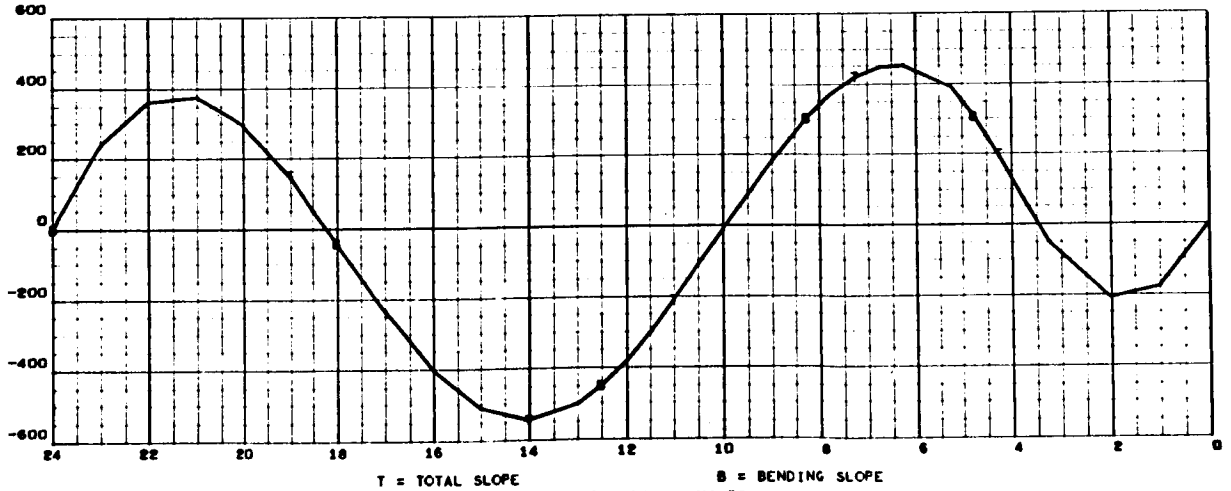

T = TOTAL SLOPE B = BENDING SLOPE
VEHICLE STATIONS - INCHES

MAY 24, 1966

2463-01
083 000

MASS LOADING EFFECTS ON BEAM VIBRATIONS - FIXED ENDS (CASE 13)

FREQUENCY (4) = 2.7181244E 03 RAD./SEC., 4.3260294E 02 C.P.S.
STRUCTURAL MODE (4)
NORMALIZED TO TOTAL WEIGHT
TOTAL WEIGHT = 1.3199999E 00
DEFLECTION - FT./FT.

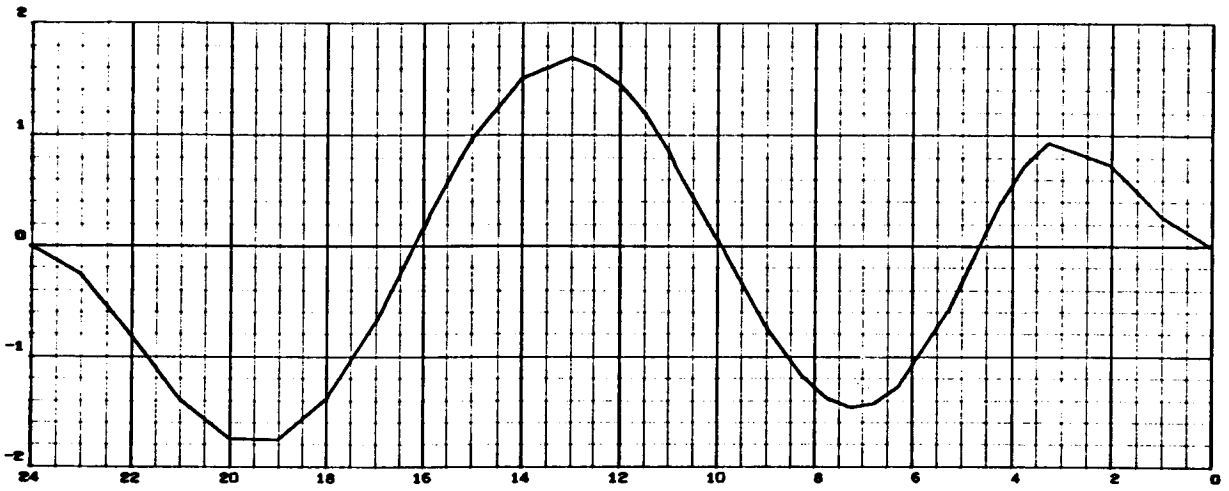

VEHICLE STATIONS - INCHES
SLOPE - DEG./FT.

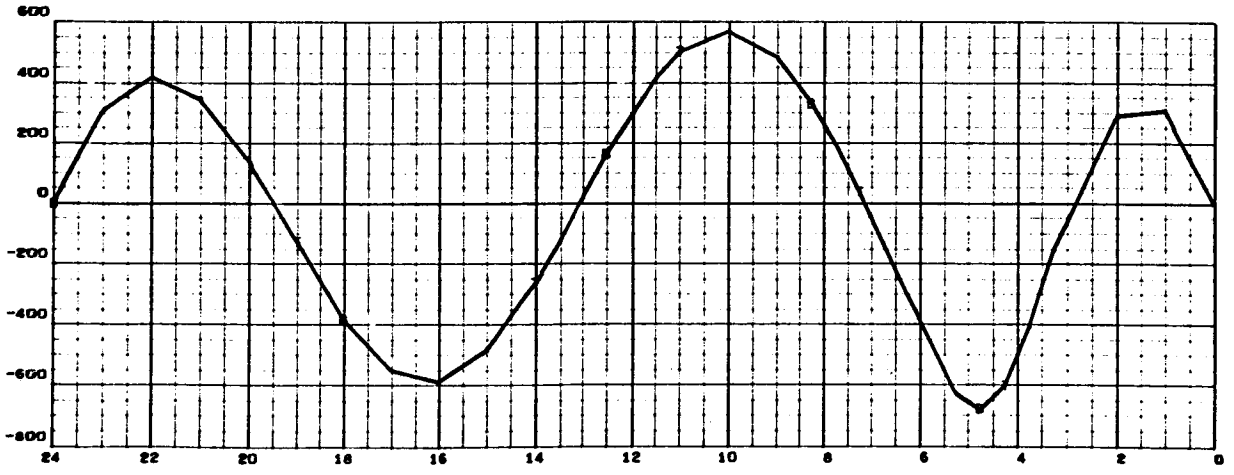

T = TOTAL SLOPE B = BENDING SLOPE
VEHICLE STATIONS - INCHES

MAY 24, 1966

2463-01
085 000

MASS LOADING EFFECTS ON BEAM VIBRATION - FIXED ENDS (CASE 14)

FREQUENCY (1) = 2.6641163E 02 RAD./SEC., 4.2400728E 01 C.P.S.
STRUCTURAL MODE (1)
NORMALIZED TO TOTAL WEIGHT
TOTAL WEIGHT = 1.3199999E 00
DEFLECTION - FT./FT.

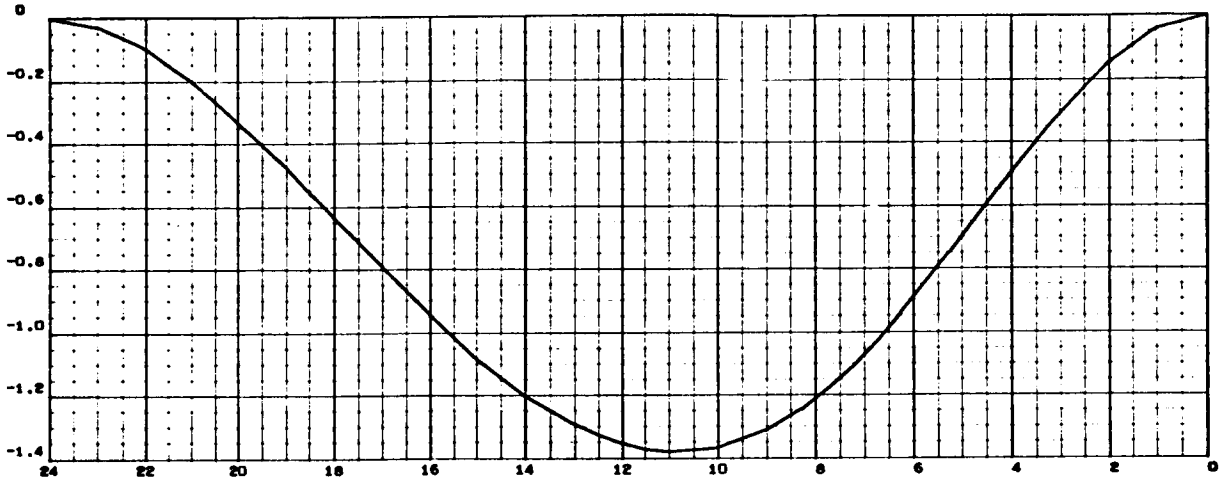

VEHICLE STATIONS - INCHES
SLOPE - DEG./FT.

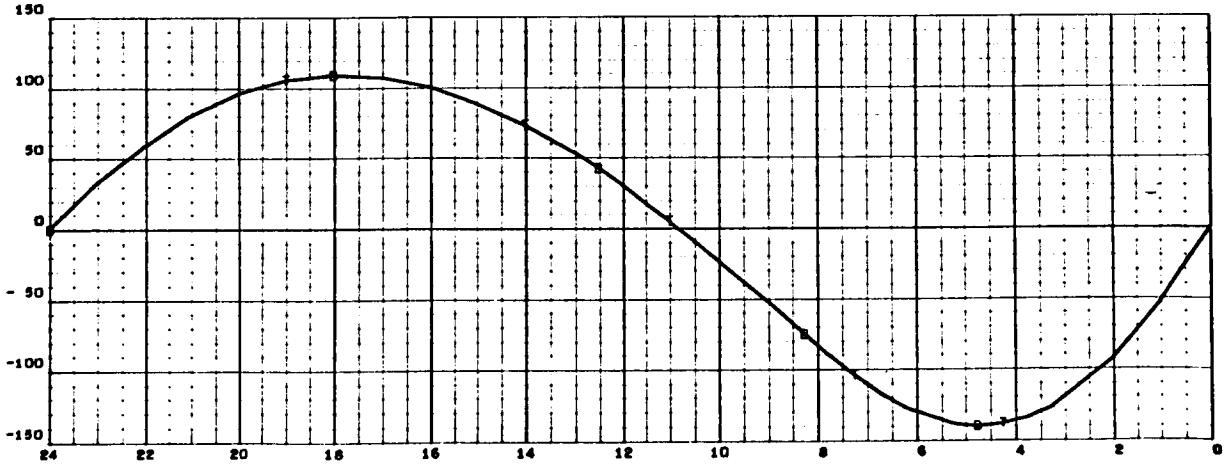

T = TOTAL SLOPE B = BENDING SLOPE
VEHICLE STATIONS - INCHES

MAY 24, 1966

2463-01
087 000

MASS LOADING EFFECTS ON BEAM VIBRATION - FIXED ENDS (CASE 14)

FREQUENCY (2) = 8.2015427E 02 RAD./SEC., 1.3053160E 02 C.P.S.
STRUCTURAL MODE (2)
NORMALIZED TO TOTAL WEIGHT
TOTAL WEIGHT = 1.3199999E 00
DEFLECTION - FT./FT.

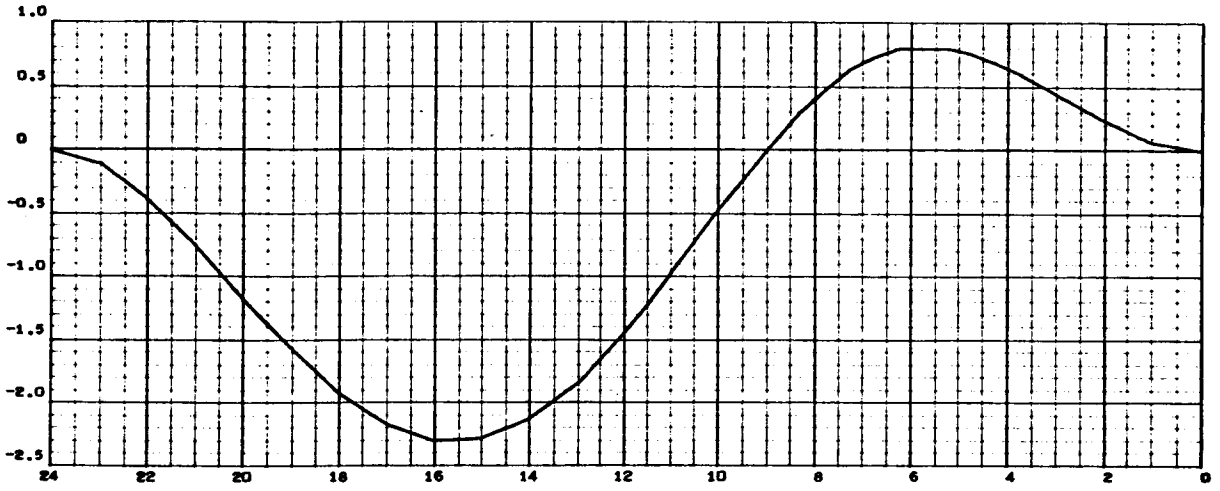

VEHICLE STATIONS - INCHES
SLOPE - DEG./FT.

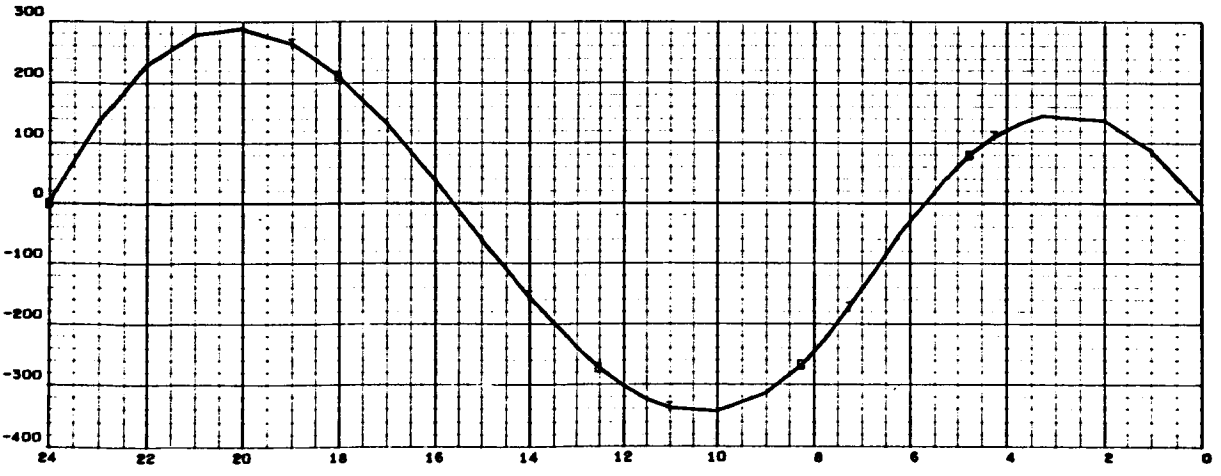

T = TOTAL SLOPE B = BENDING SLOPE
VEHICLE STATIONS - INCHES

MAY 24, 1966

2463-01
089 000

MASS LOADING EFFECTS ON BEAM VIBRATION - FIXED ENDS (CASE 14)

FREQUENCY (3) = 1.7661506E 03 RAD./SEC., 2.8109160E 02 C.P.S.
STRUCTURAL MODE (3)
NORMALIZED TO TOTAL WEIGHT
TOTAL WEIGHT = 1.3199999E 00
DEFLECTION - FT./FT.

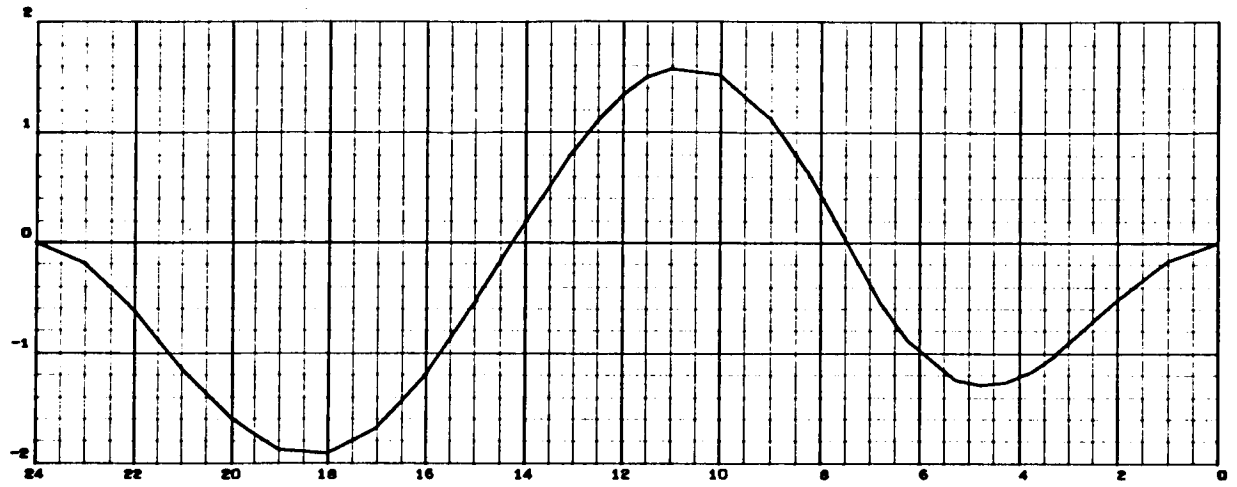

VEHICLE STATIONS - INCHES
SLOPE - DEG./FT.

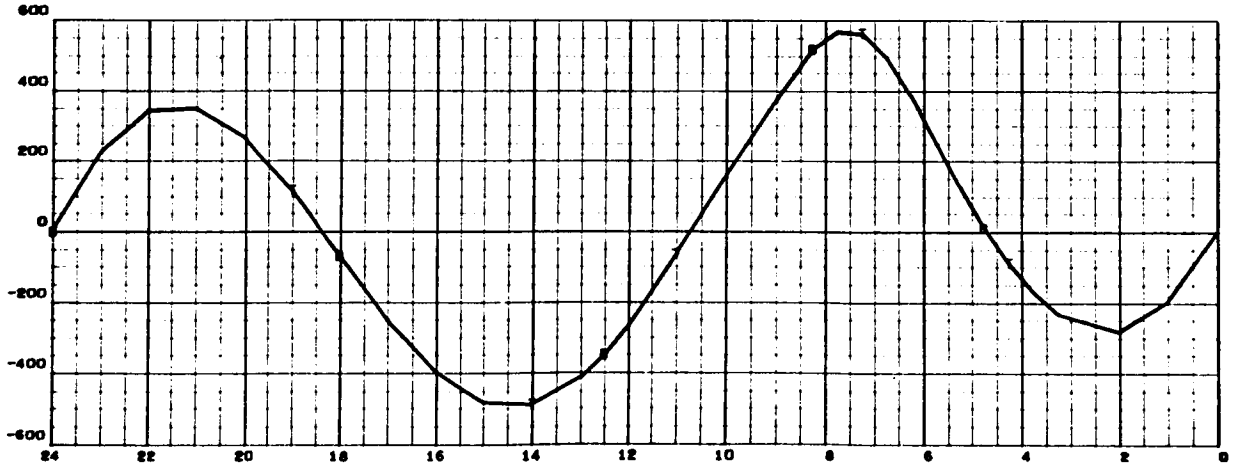

T = TOTAL SLOPE B = BENDING SLOPE
VEHICLE STATIONS - INCHES

MAY 24, 1966

2463-01 L
091 000

MASS LOADING EFFECTS ON BEAM VIBRATION - FIXED ENDS (CASE 14)

FREQUENCY (4) = 2.8391363E 03 RAD./SEC., 4.5186258E 02 C.P.S.
STRUCTURAL MODE (4)
NORMALIZED TO TOTAL WEIGHT
TOTAL WEIGHT = 1.3199999E 00
DEFLECTION - FT./FT.

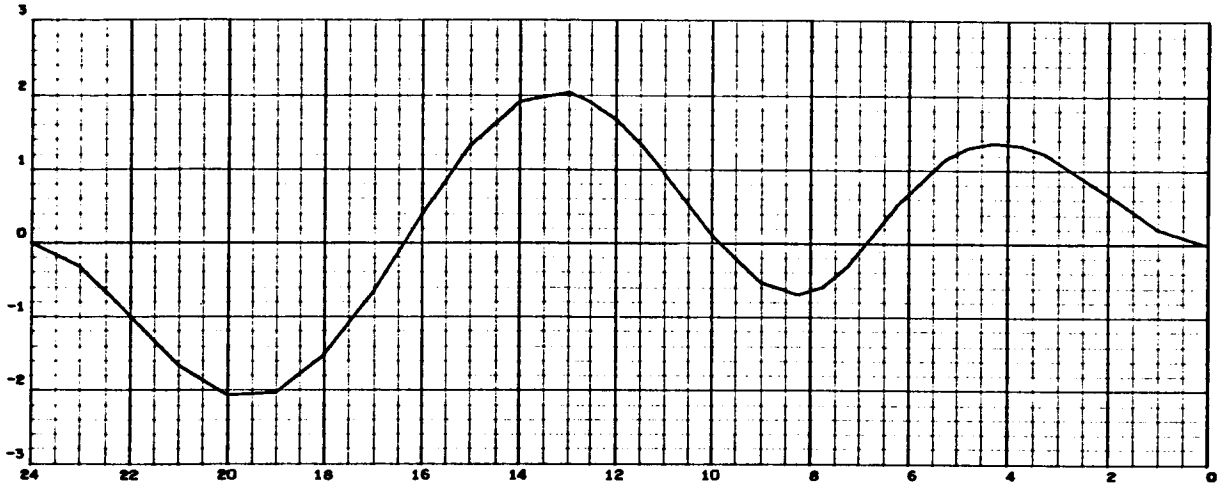

VEHICLE STATIONS - INCHES
SLOPE - DEG./FT.

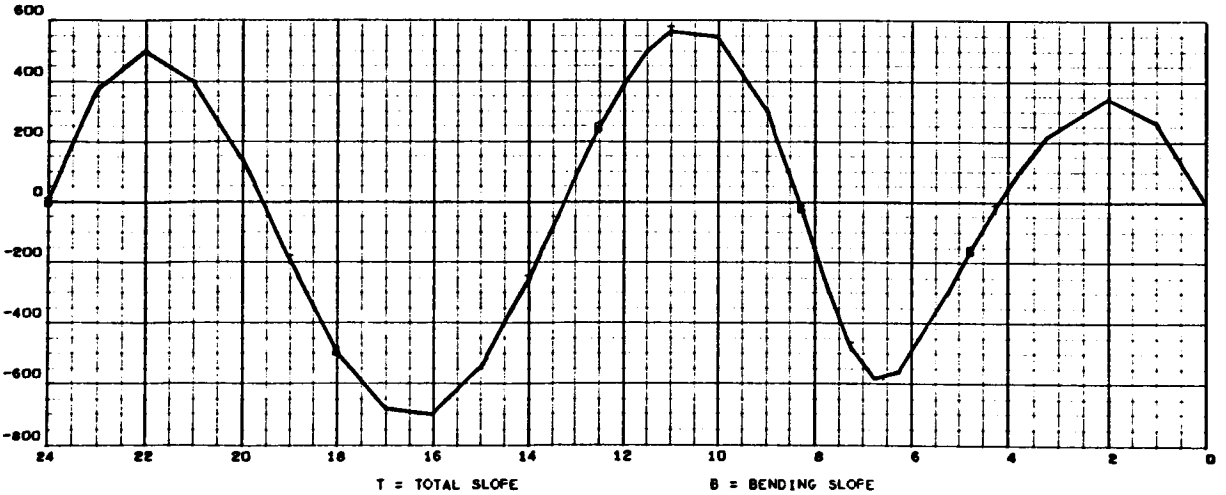

T = TOTAL SLOPE B = BENDING SLOPE
VEHICLE STATIONS - INCHES

MAY 24, 1966

2463-01 L
093 000

MASS LOADING EFFECTS ON BEAM VIBRATION - FIXED ENDS (CASE 15)

FREQUENCY (1) = 2.2132291E 02 RAD./SEC., 3.5224635E 01 C.P.S.
STRUCTURAL MODE (1)
NORMALIZED TO TOTAL WEIGHT
TOTAL WEIGHT = 1.3199998E 00
DEFLECTION - FT./FT.

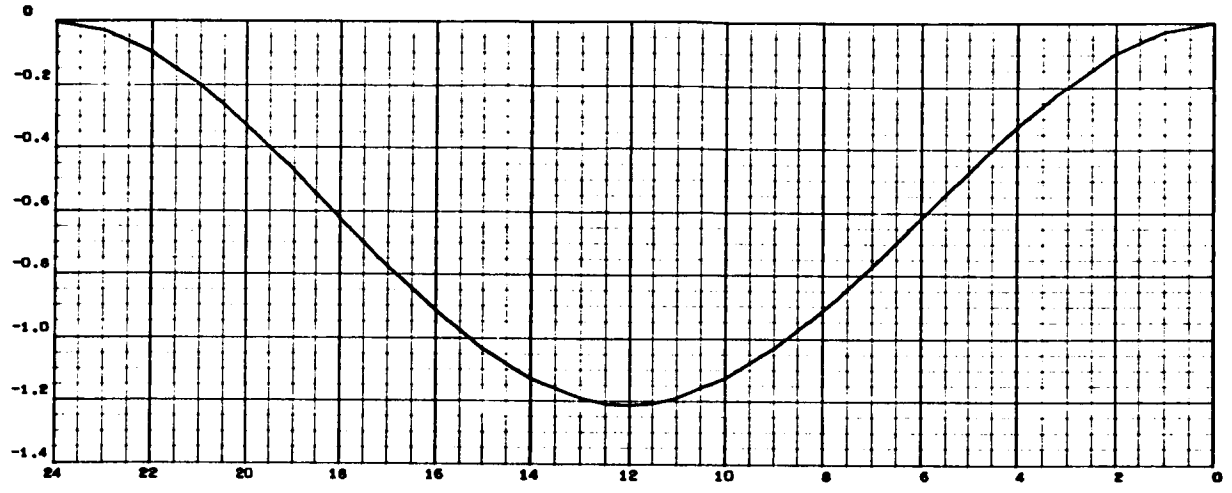

VEHICLE STATIONS - INCHES
SLOPE - DEG./FT.

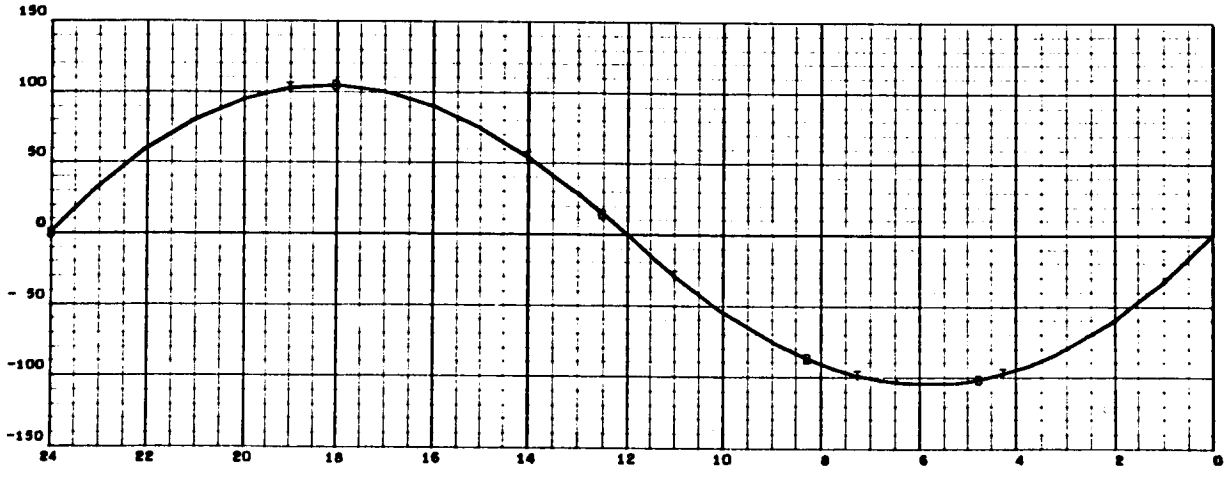

T = TOTAL SLOPE B = BENDING SLOPE
VEHICLE STATIONS - INCHES

MAY 24, 1966

2463-01 L
095 000

MASS LOADING EFFECTS ON BEAM VIBRATION - FIXED ENDS (CASE 15)

FREQUENCY (2) = 1.0023860E 03 RAD./SEC., 1.5953468E 02 C.P.S.
STRUCTURAL MODE (2)
NORMALIZED TO TOTAL WEIGHT
TOTAL WEIGHT = 1.3199998E 00
DEFLECTION - FT./FT.

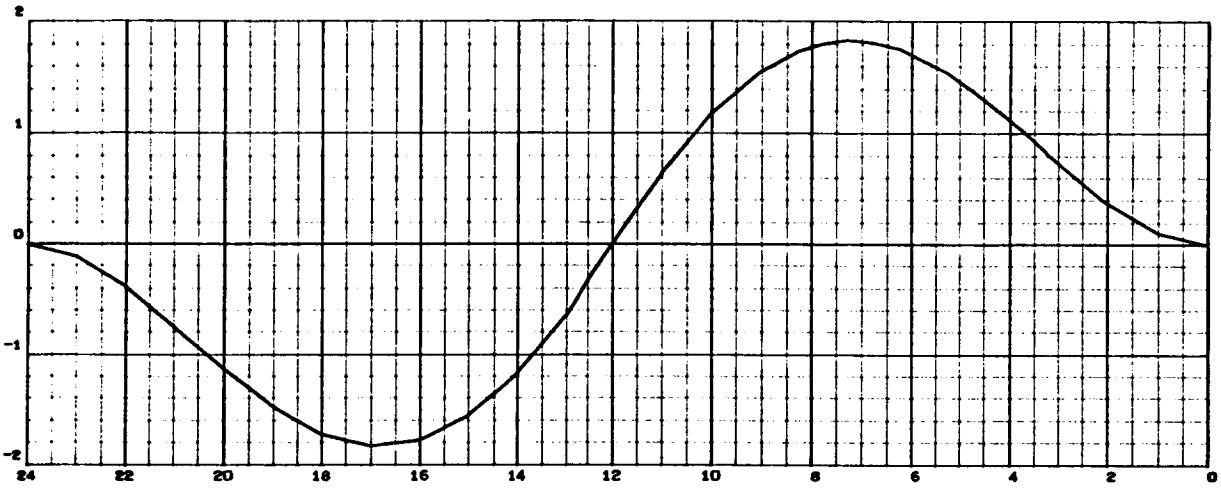

VEHICLE STATIONS - INCHES
SLOPE - DEG./FT.

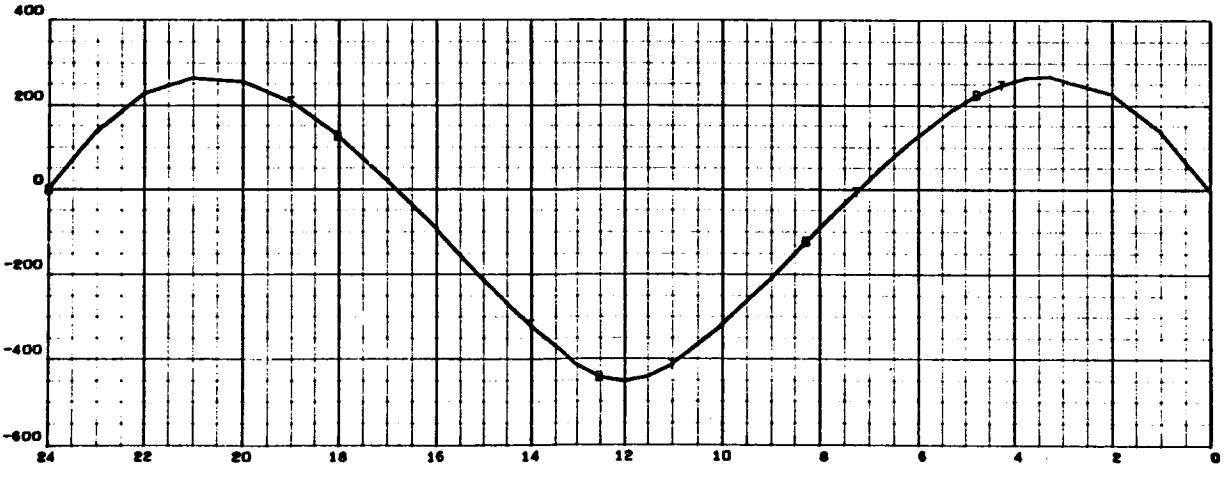

T = TOTAL SLOPE B = BENDING SLOPE
VEHICLE STATIONS - INCHES

MAY 24, 1966

2463-01 L
097 000

MASS LOADING EFFECTS ON BEAM VIBRATION - FIXED ENDS (CASE 15)

FREQUENCY (3) = 1.7879779E 03 RAD./SEC., 2.8456546E 02 C.P.S.
STRUCTURAL MODE (3)
NORMALIZED TO TOTAL WEIGHT
TOTAL WEIGHT = 1.3199998E 00
DEFLECTION - FT./FT.

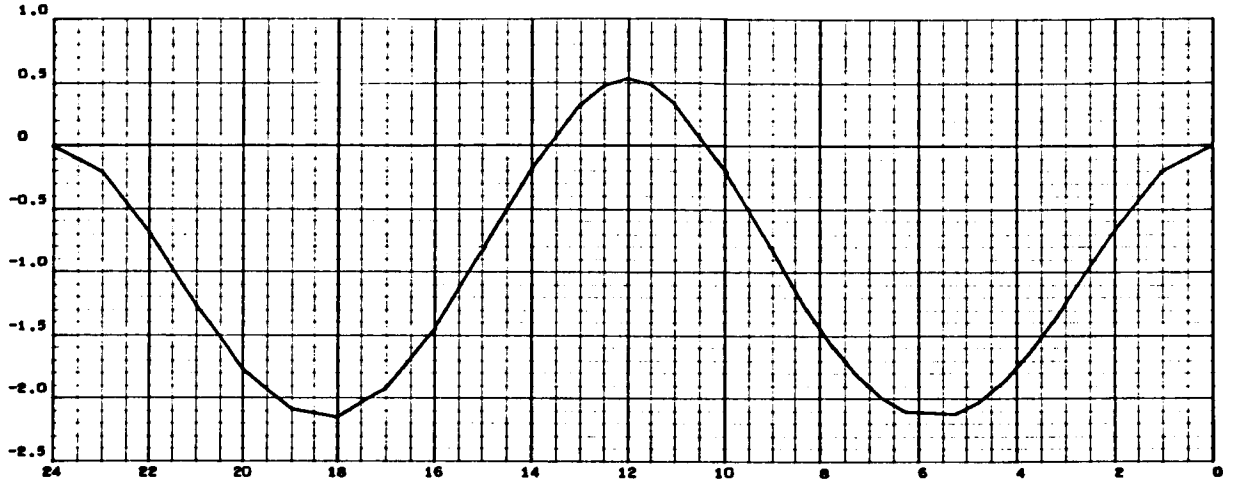

VEHICLE STATIONS - INCHES
SLOPE - DEG./FT.

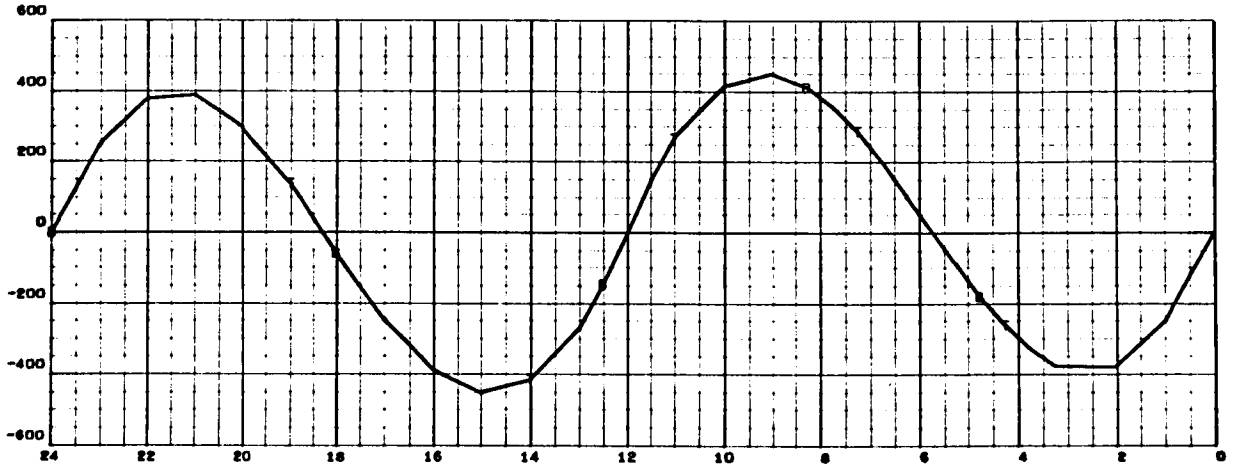

T = TOTAL SLOPE B = BENDING SLOPE
VEHICLE STATIONS - INCHES

MAY 24, 1966

2463-01
099 000

MASS LOADING EFFECTS ON BEAM VIBRATION - FIXED ENDS (CASE 15)

FREQUENCY (4) = 2.7683829E 03 R../SEC., 4.4060175E 02 C.P.S.
STRUCTURAL MODE (4)
NORMALIZED TO TOTAL WEIGHT
TOTAL WEIGHT = 1.3199998E 00
DEFLECTION - FT./FT.

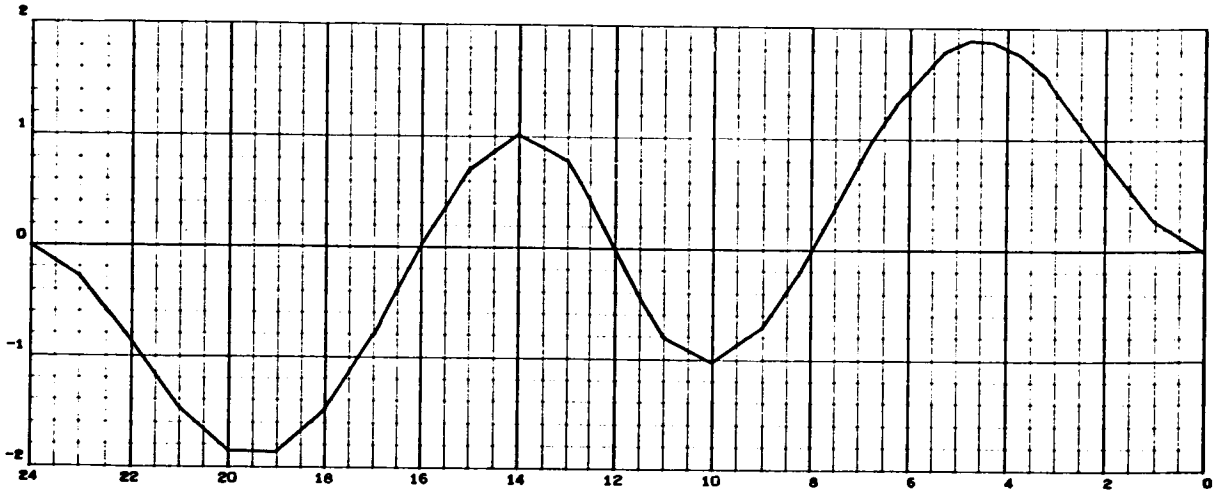

VEHICLE STATIONS - INCHES
SLOPE - DEG./FT.

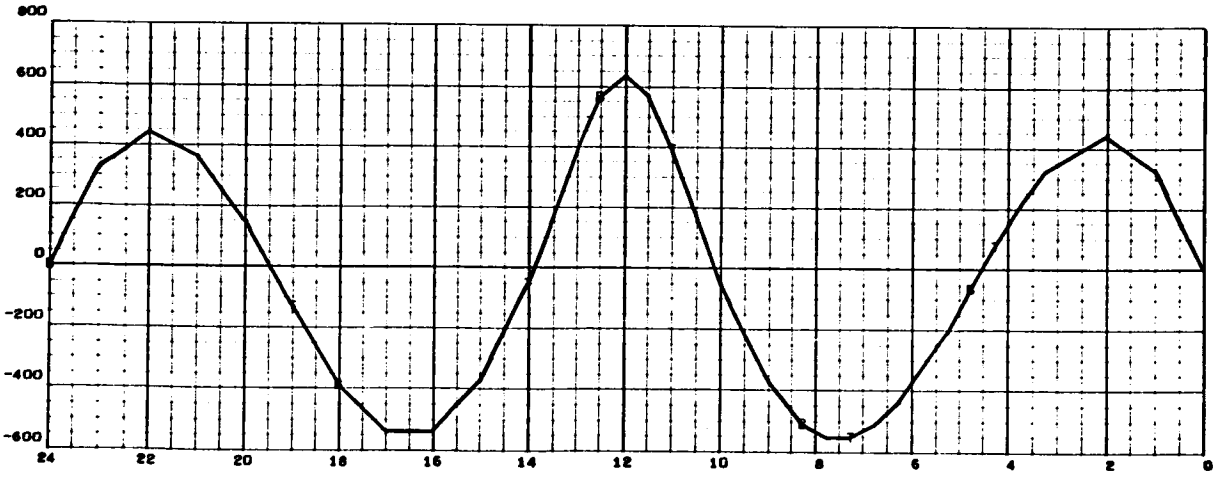

T = TOTAL SLOPE B = BENDING SLOPE

VEHICLE STATIONS - INCHES

MAY 24, 1966

2463-01
101 000

MASS LOADING EFFECTS ON BEAM VIBRATION - FIXED (CASE 16)

FREQUENCY (1) = 3.0113483E 02 RAD./SEC., 4.7927097E 01 C.P.S.
STRUCTURAL MODE (1)
NORMALIZED TO TOTAL WEIGHT
TOTAL WEIGHT = 1.9799999E 00
DEFLECTION - FT./FT.

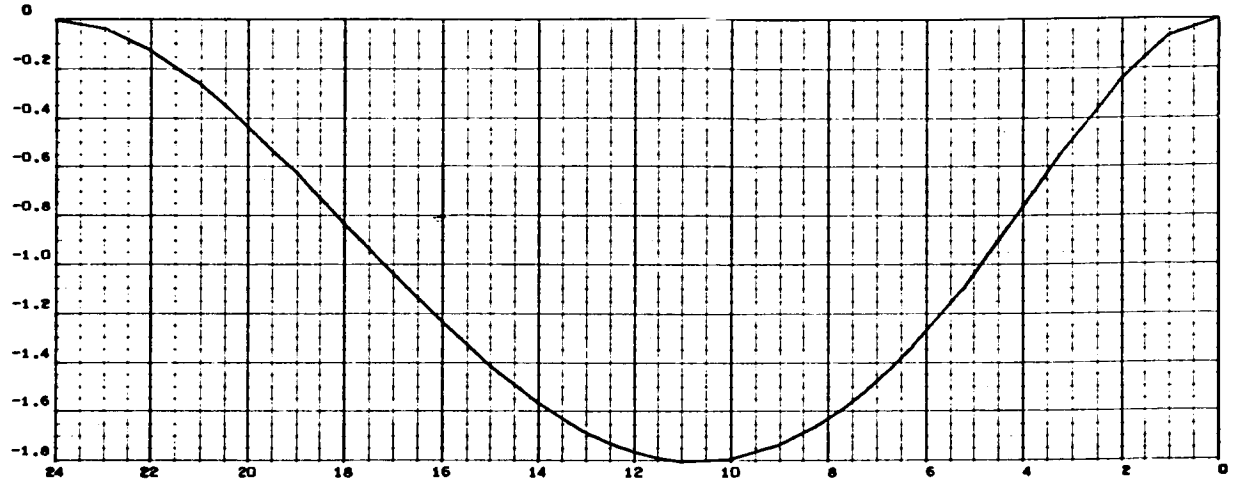

VEHICLE STATIONS - INCHES
SLOPE - DEG./FT.

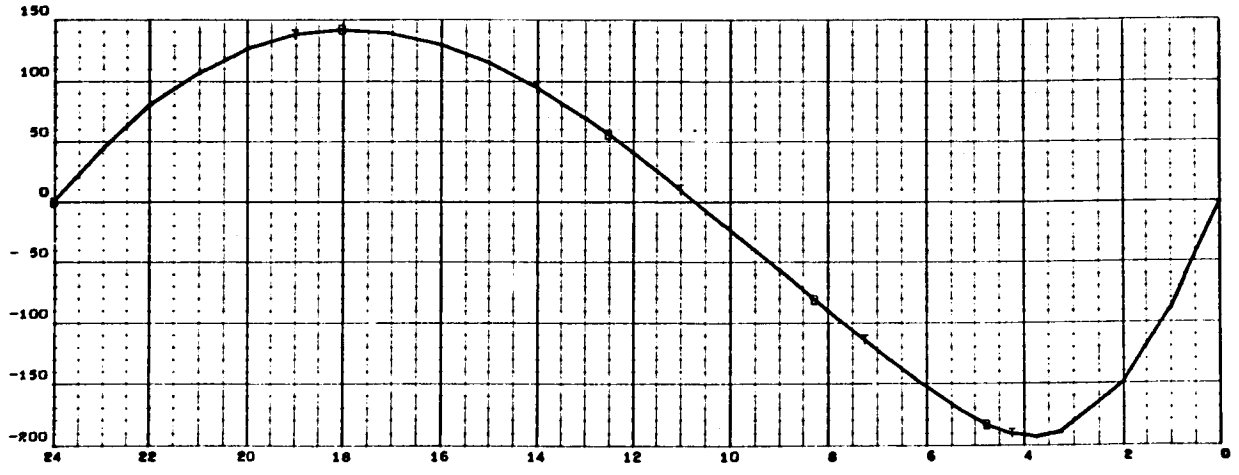

T = TOTAL SLOPE B = BENDING SLOPE
VEHICLE STATIONS - INCHES

MAY 24, 1966

2463-01 L
103 000

MASS LOADING EFFECTS ON BEAM VIBRATION - FIXED (CASE 16)

FREQUENCY (2) = 6.887565E 02 RAD./SEC., 1.0961900E 02 C.P.S.
STRUCTURAL MODE (2)
NORMALIZED TO TOTAL WEIGHT
TOTAL WEIGHT = 1.9799999E 00
DEFLECTION - FT./FT.

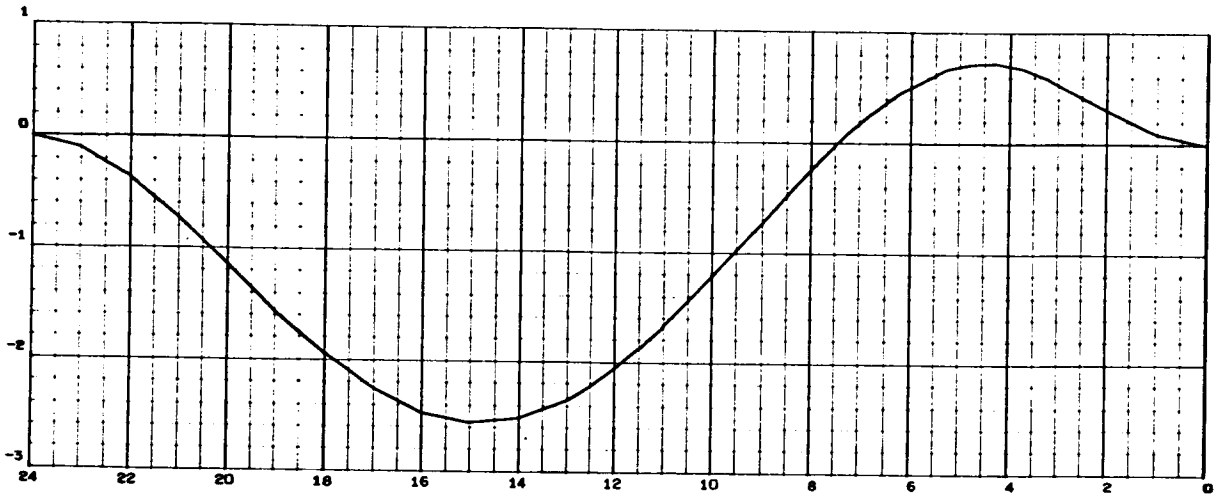

VEHICLE STATIONS - INCHES
SLOPE - DEG./FT.

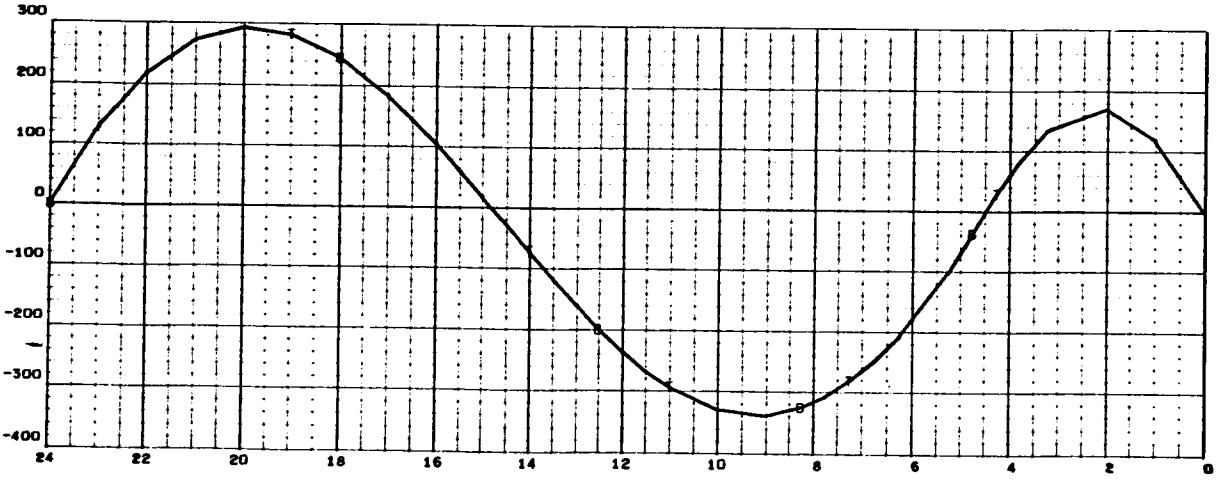

T = TOTAL SLOPE B = BENDING SLOPE
VEHICLE STATIONS - INCHES

MAY 24, 1966

2463-01
105 000

MASS LOADING EFFECTS ON BEAM VIBRATION - FIXED (CASE 16)

FREQUENCY (3) = 1.4380566E 00 RAD./SEC., 2.2887382E 02 C.P.S.
STRUCTURAL MODE (3)
NORMALIZED TO TOTAL WEIGHT
TOTAL WEIGHT = 1.9799999E 00
DEFLECTION - FT./FT.

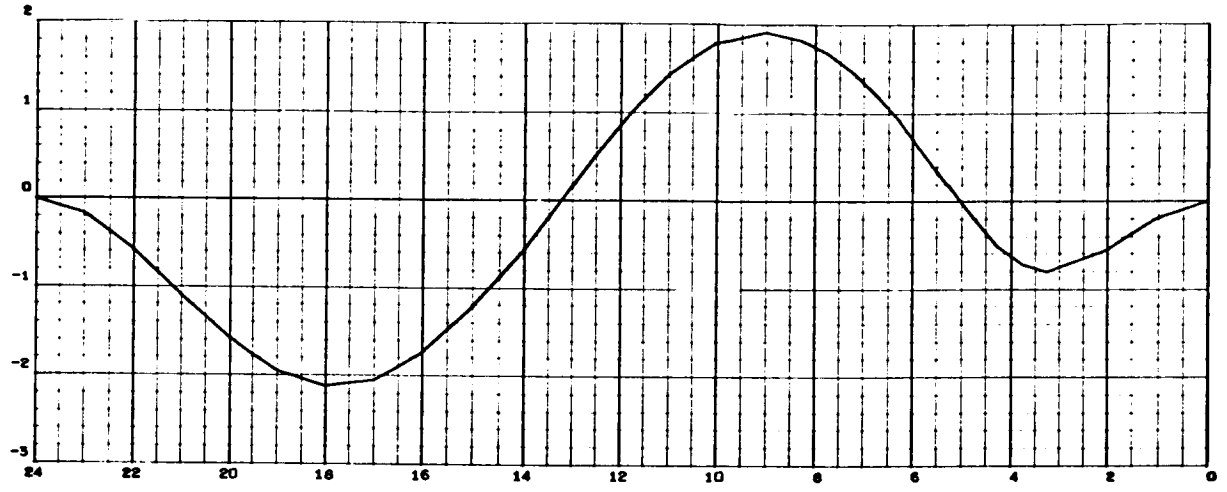

VEHICLE STATIONS - INCHES
SLOPE - DEG./FT.

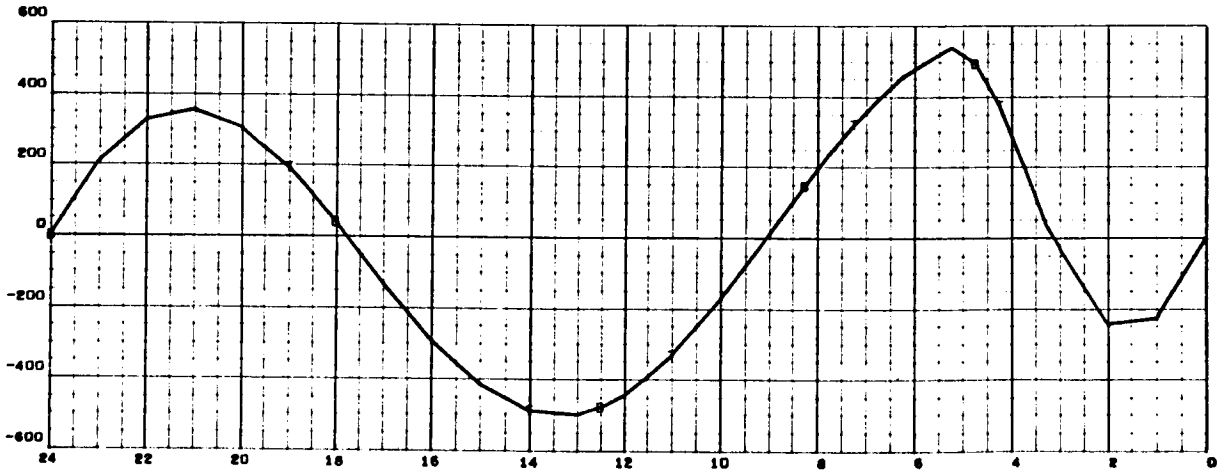

T = TOTAL SLOPE B = BENDING SLOPE
VEHICLE STATIONS - INCHES

MAY 24, 1966

2463-01 L
107 000

MASS LOADING EFFECTS ON BEAM VIBRATION - FIXED (CASE 16)

FREQUENCY (4) = 2.1291424E 03 RAD./ C., 3.3886354E 02 C.P.S.
STRUCTURAL MODE (4)
NORMALIZED TO TOTAL WEIGHT
TOTAL WEIGHT = 1.9799999E 00
DEFLECTION - FT./FT.

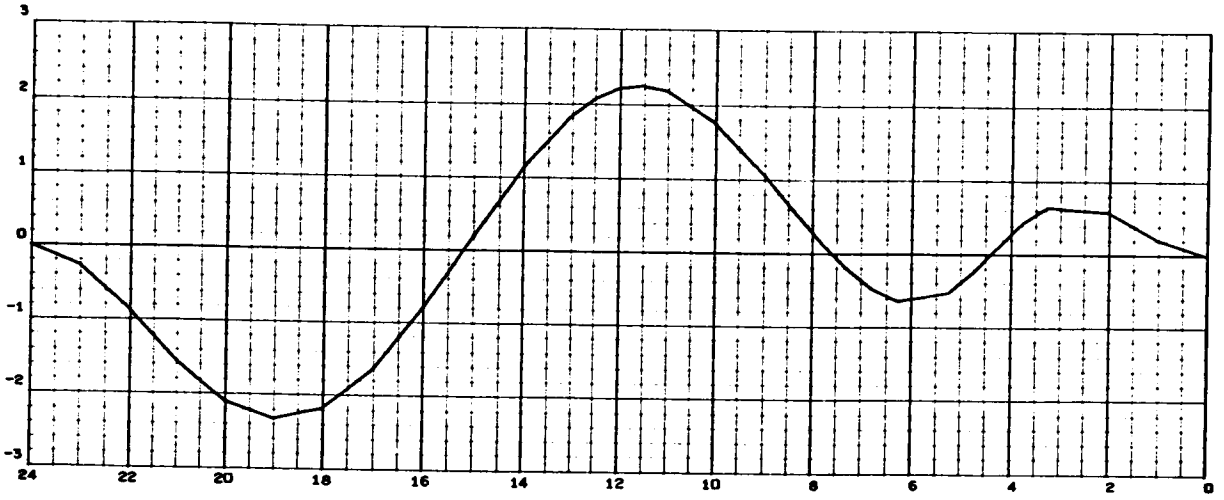

VEHICLE STATIONS - INCHES
SLOPE - DEG./FT.

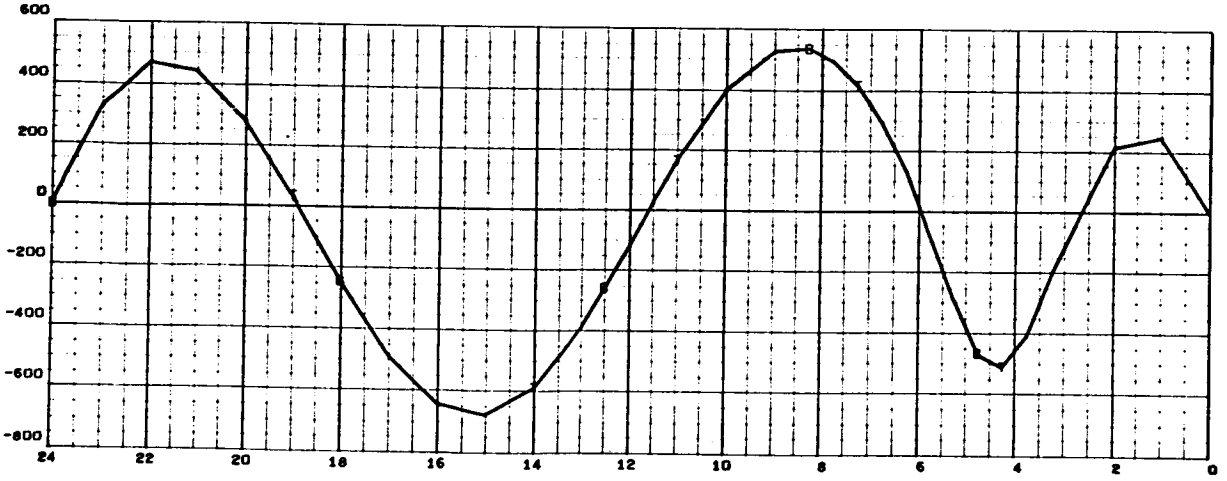

T = TOTAL SLOPE B = BENDING SLOPE
VEHICLE STATIONS - INCHES

MAY 24, 1966

2463-01
109 000

MASS LOADING EFFECTS ON BEAM VIBRATION - FIXED ENDS (CASE 17)

FREQUENCY (1) = 2.0799564E 02 RAD./SEC., 3.3103534E 01 C.P.S.
STRUCTURAL MODE (1)
NORMALIZED TO TOTAL WEIGHT
TOTAL WEIGHT = 1.9799999E 00
DEFLECTION - FT./FT.

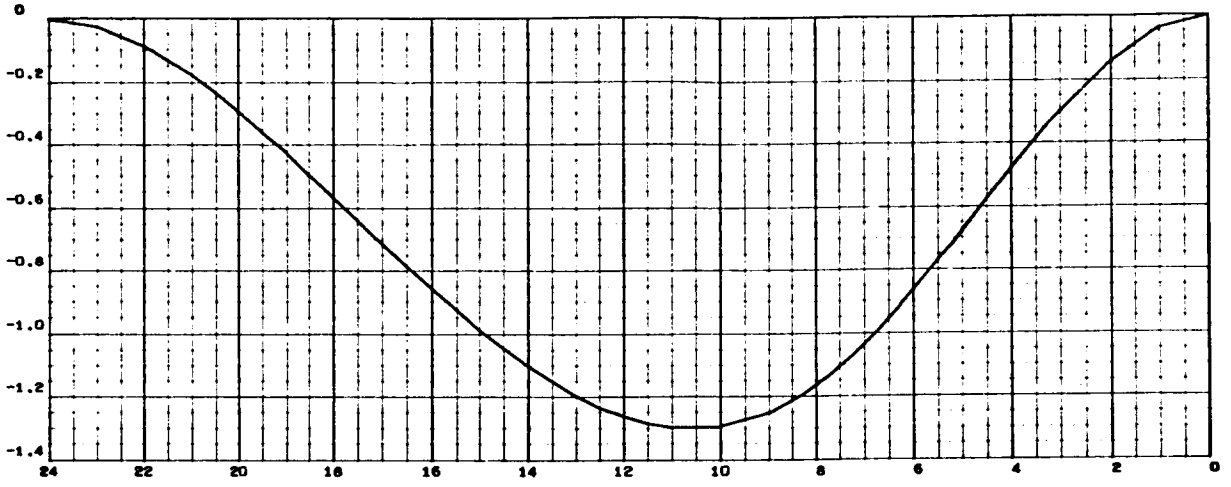

VEHICLE STATIONS - INCHES
SLOPE - DEG./FT.

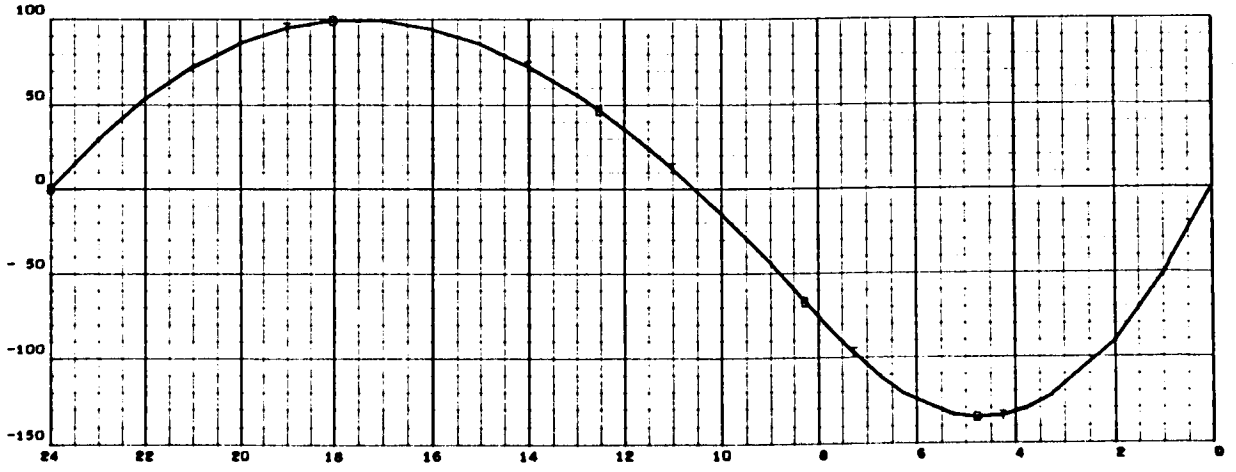

T = TOTAL SLOPE B = BENDING SLOPE
VEHICLE STATIONS - INCHES

MAY 24, 1966

2463-01
111 000

MASS LOADING EFFECTS ON BEAM VIBRATION - FIXED ENDS (CASE 17)

FREQUENCY (2) = 7.4029861E 02 RAD./SEC., 1.1782218E 02 C.P.S.
STRUCTURAL MODE (2)
NORMALIZED TO TOTAL WEIGHT
TOTAL WEIGHT = 1.9799999E 00
DEFLECTION - FT./FT.

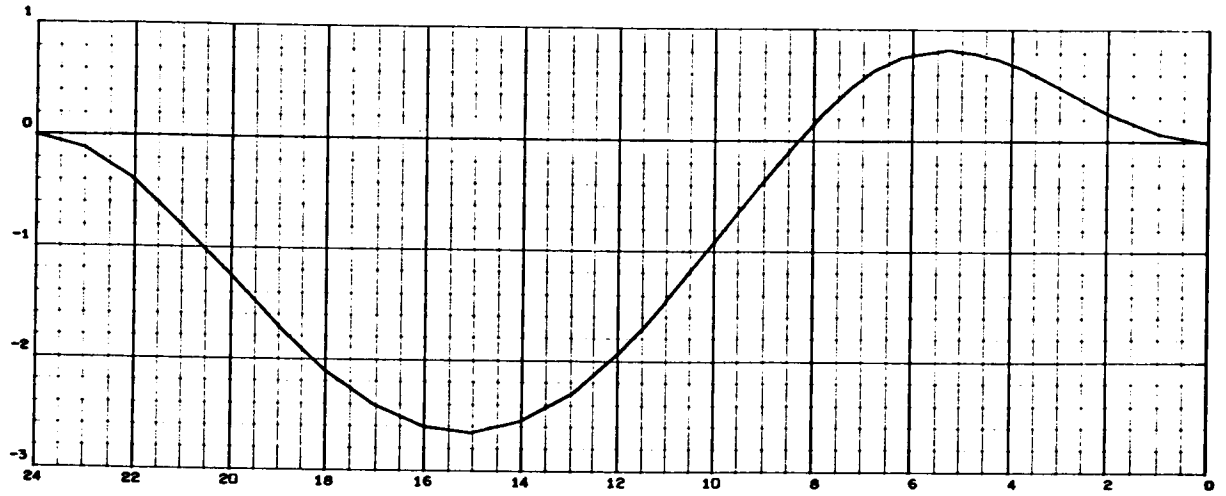

VEHICLE STATIONS - INCHES
SLOPE - DEG./FT.

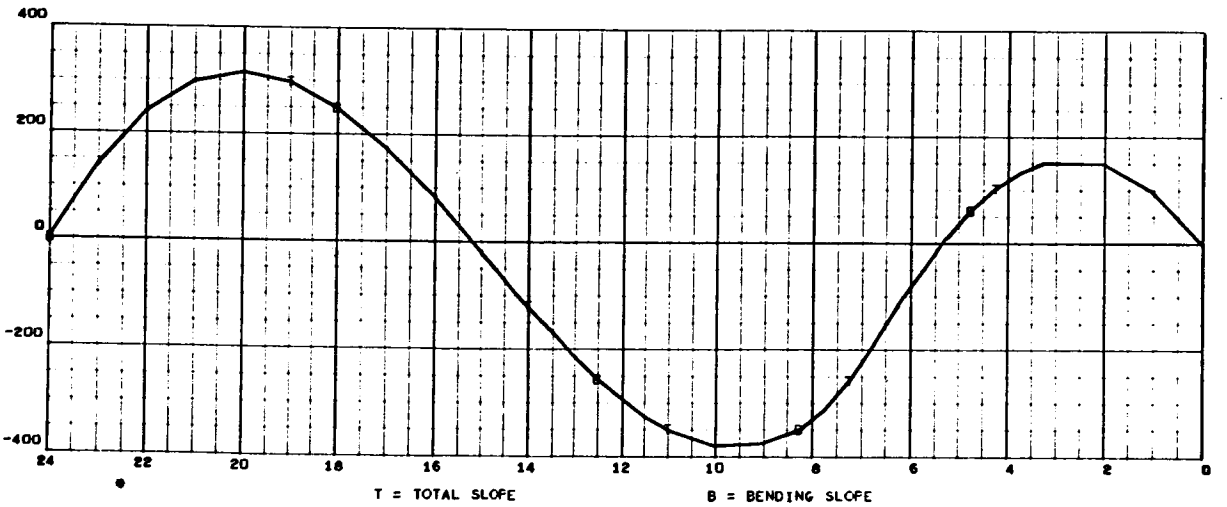

T = TOTAL SLOPE B = BENDING SLOPE
VEHICLE STATIONS - INCHES

MAY 24, 1966

2463-01
113 000

MASS LOADING EFFECTS ON BEAM VIBRATION - FIXED ENDS (CASE 17)

FREQUENCY (3) = 1.3673195E 03 RAD./SEC., 2.1761566E 02 C.P.S.
STRUCTURAL MODE (3)
NORMALIZED TO TOTAL WEIGHT
TOTAL WEIGHT = 1.9799999E 00
DEFLECTION - FT./FT.

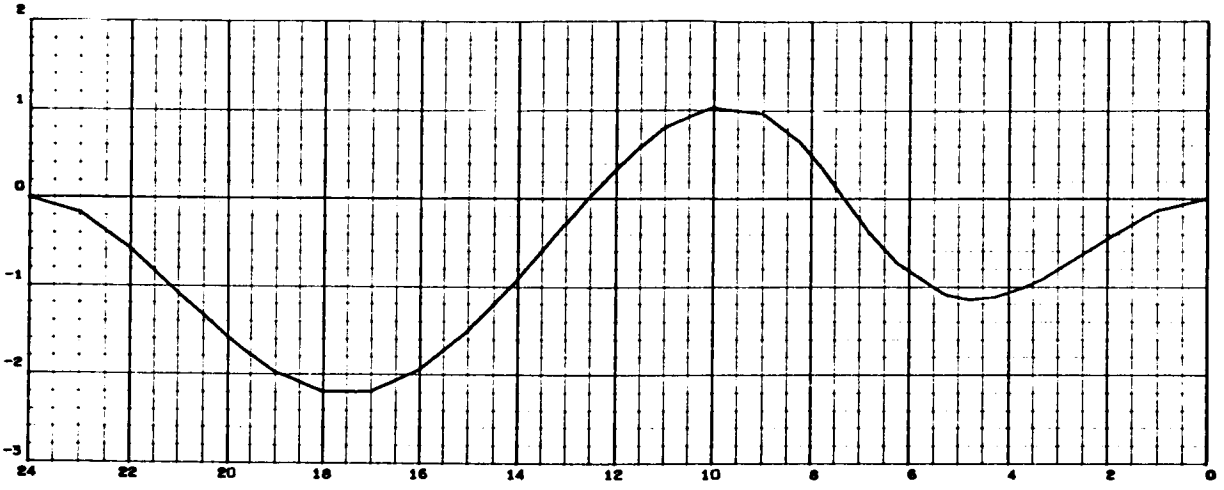

VEHICLE STATIONS - INCHES
SLOPE - DEG./FT.

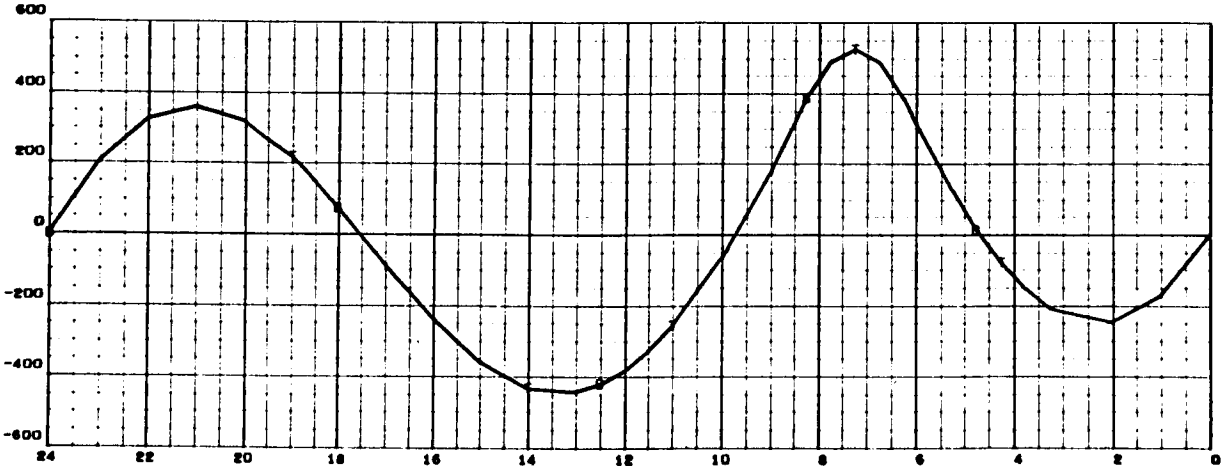

T = TOTAL SLOPE B = BENDING SLOPE
VEHICLE STATIONS - INCHES

MAY 24, 1966

2463-01
115 000

MASS LOADING EFFECTS ON BEAM VIBRATION - FIXED ENDS (CASE 17)

FREQUENCY (4) = 2.4415676E 03 RAD./SEC., 3.8858755E 02 C.P.S.
STRUCTURAL MODE (4)
NORMALIZED TO TOTAL WEIGHT
TOTAL WEIGHT = 1.9799999E 00
DEFLECTION - FT./FT.

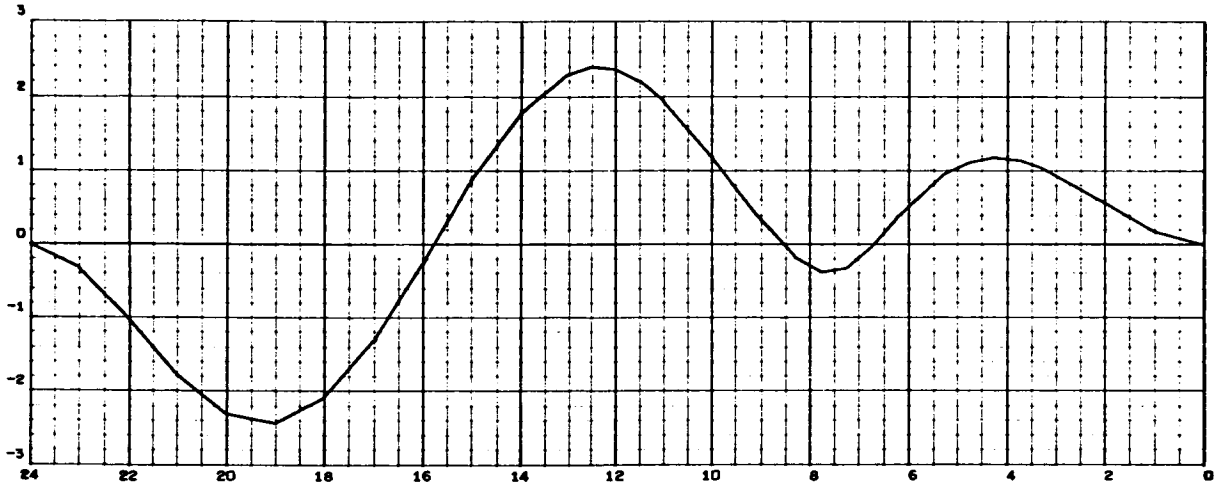

VEHICLE STATIONS - INCHES
SLOPE - DEG./FT.

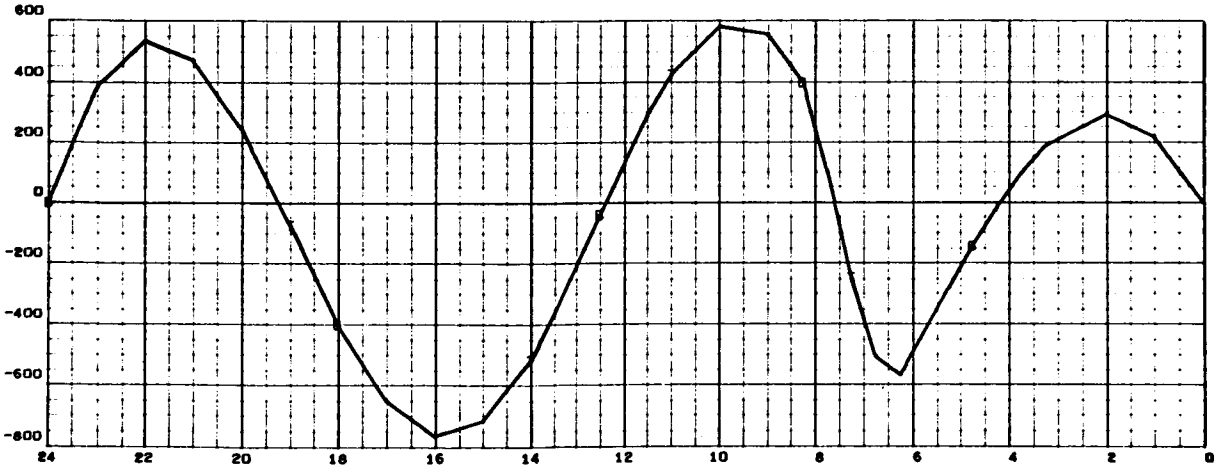

T = TOTAL SLOPE B = BENDING SLOPE
VEHICLE STATIONS - INCHES

MAY 24, 1966

2463-01 L
117 000

MASS LOADING EFFECTS ON BEAM VIBRAT[illegible] - FIXED ENDS (CASE 18)

FREQUENCY (1) = 1.6862862E 02 RAD./SEC., 2.6838078E 01 C.P.S.
STRUCTURAL MODE (1)
NORMALIZED TO TOTAL WEIGHT
TOTAL WEIGHT = 1.9799998E 00
DEFLECTION - FT./FT.

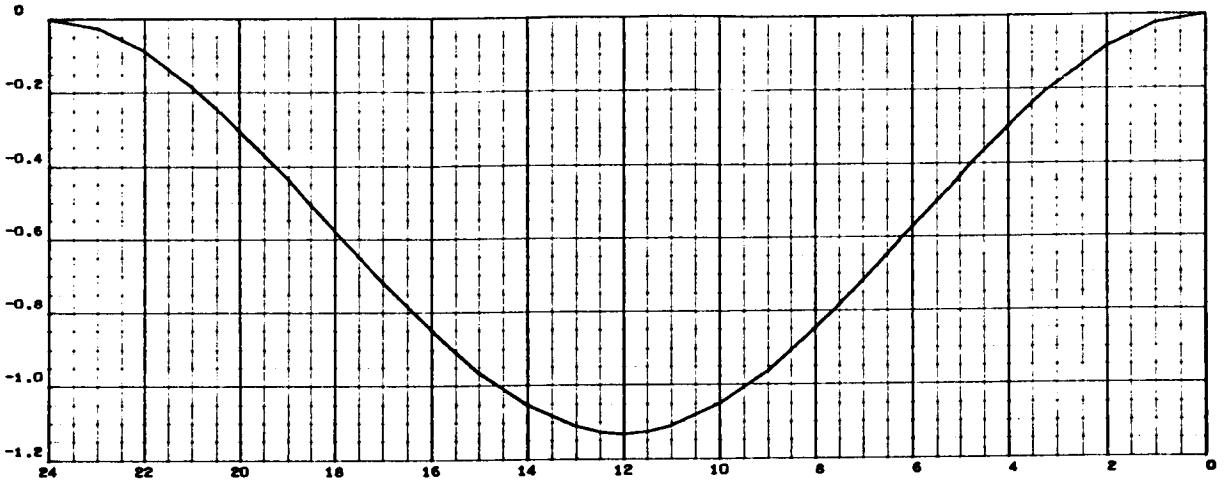

VEHICLE STATIONS - INCHES
SLOPE - DEG./FT.

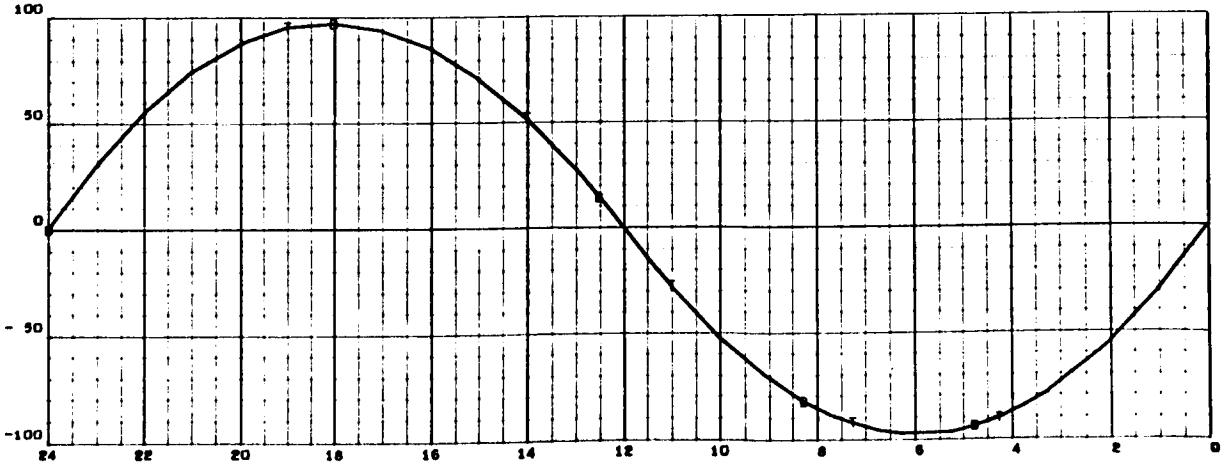

T = TOTAL SLOPE B = BENDING SLOPE
VEHICLE STATIONS - INCHES

MAY 24, 1966

2463-01 L
119 000

MASS LOADING EFFECTS ON BEAM VIBRATION - FIXED ENDS (CASE 18)

FREQUENCY (2) = 8.1467471E 02 RAD./SEC., 1.2965951E 02 C.P.S.
STRUCTURAL MODE (2)
NORMALIZED TO TOTAL WEIGHT
TOTAL WEIGHT = 1.9799998E 00
DEFLECTION - FT./FT.

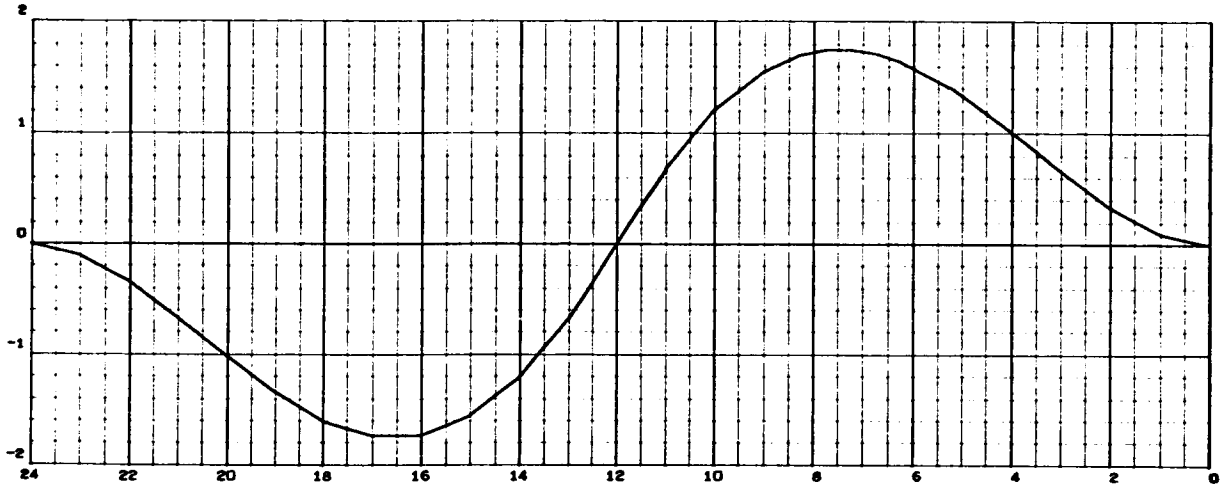

VEHICLE STATIONS - INCHES
SLOPE - DEG./FT.

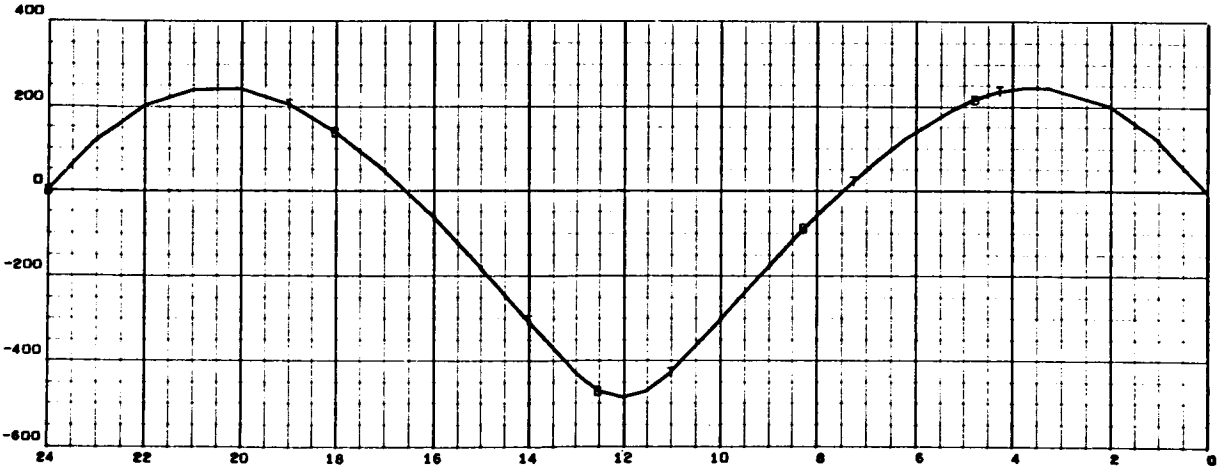

T = TOTAL SLOPE B = BENDING SLOPE
VEHICLE STATIONS - INCHES

MAY 24, 1966

2463-01 L
121 000

MASS LOADING EFFECTS ON BEAM VIBRATION - FIXED ENDS (CASE 18)

FREQUENCY (3) = 1.6683712E 03 RAD./SEC., 2.6552951E 02 C.P.S.
STRUCTURAL MODE (3)
NORMALIZED TO TOTAL WEIGHT
TOTAL WEIGHT = 1.9799998E 00
DEFLECTION - FT./FT.

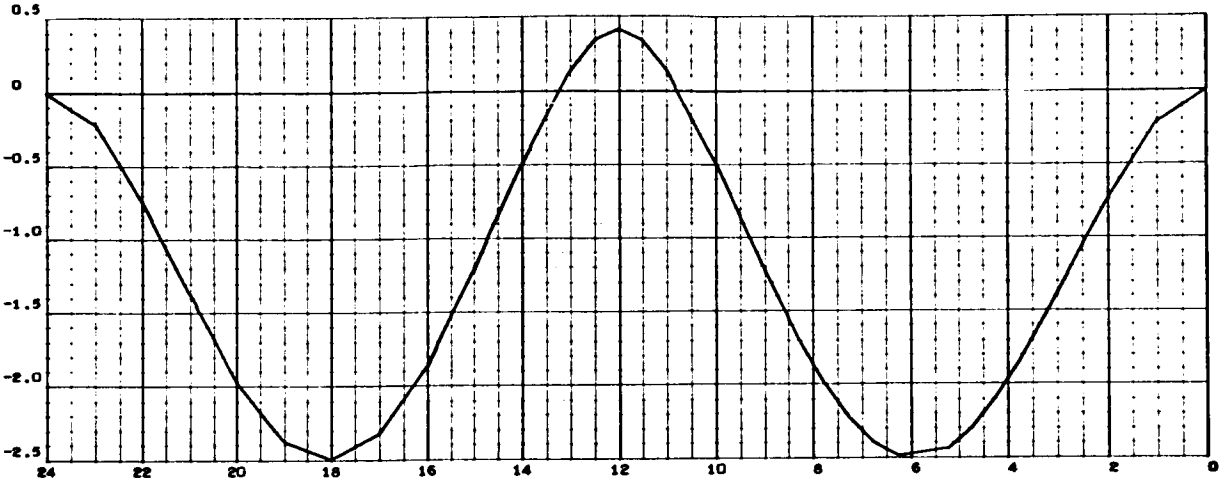

VEHICLE STATIONS - INCHES
SLOPE - DEG./FT.

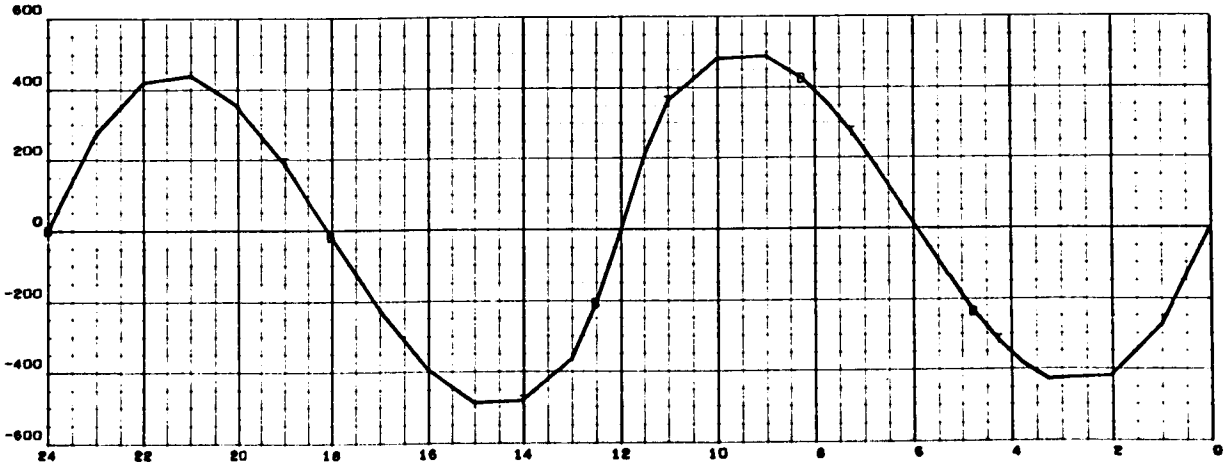

T = TOTAL SLOPE B = BENDING SLOPE
VEHICLE STATIONS - INCHES

MAY 24, 1966

2463-01
123 000

MASS LOADING EFFECTS ON BEAM VIBRATION - FIXED ENDS (CASE 18)

FREQUENCY (4) = 2.2826626E 03 RAD./SEC., 3.6329703E 02 C.P.S.
STRUCTURAL MODE (4)
NORMALIZED TO TOTAL WEIGHT
TOTAL WEIGHT = 1.9799998E 00
DEFLECTION - FT./FT.

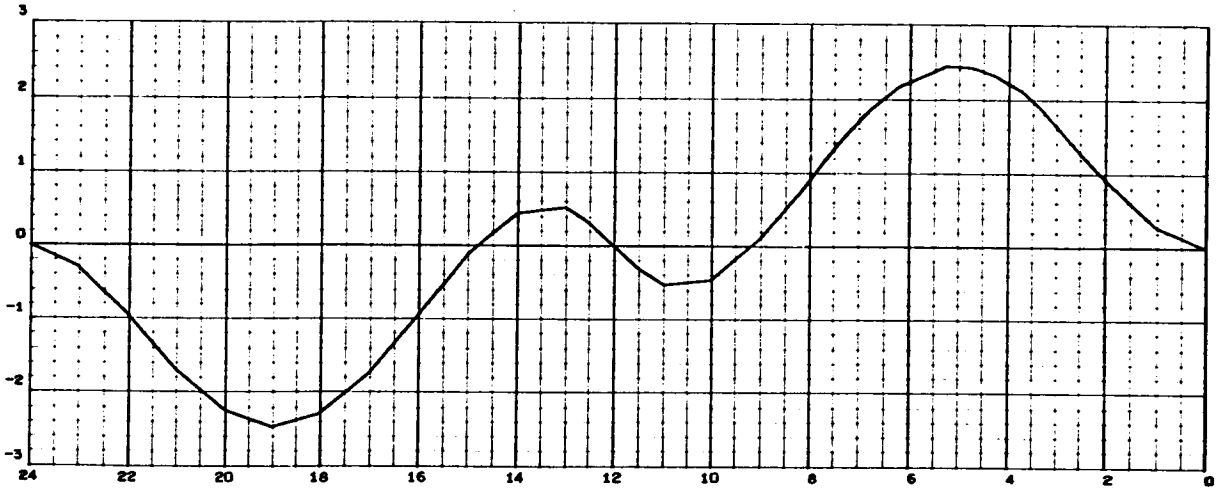

VEHICLE STATIONS - INCHES
SLOPE - DEG./FT.

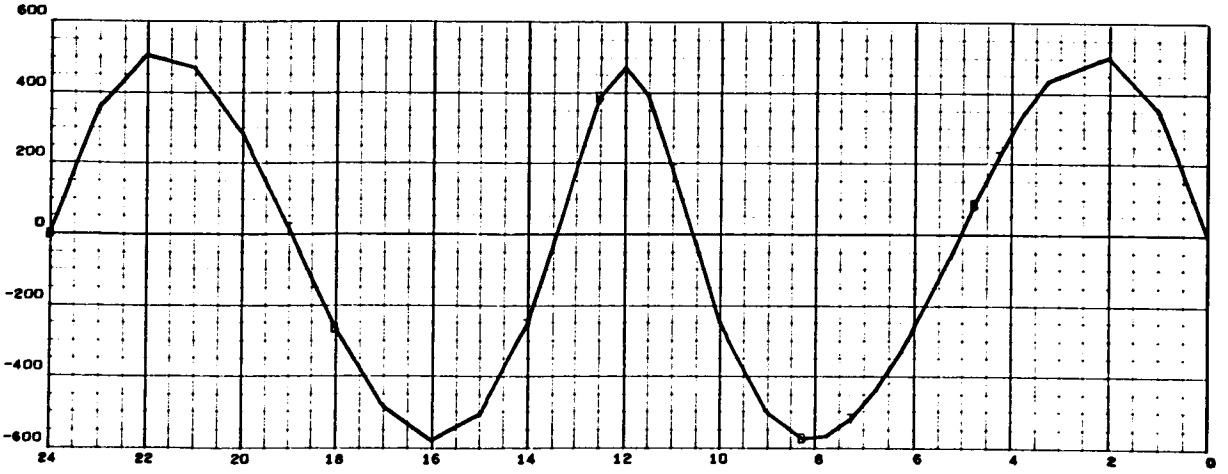

T = TOTAL SLOPE B = BENDING SLOPE
VEHICLE STATIONS - INCHES

MAY 24, 1966

2463-01 L
125 000

MASS LOADING EFFECTS ON BEAM VIBRATION - FIXED ENDS (CASE 19)

FREQUENCY (1) = 2.6554251E 02 RAD./SEC., 4.2262403E 01 C.P.S.
STRUCTURAL MODE (1)
NORMALIZED TO TOTAL WEIGHT
TOTAL WEIGHT = 2.6399999E 00
DEFLECTION - FT./FT.

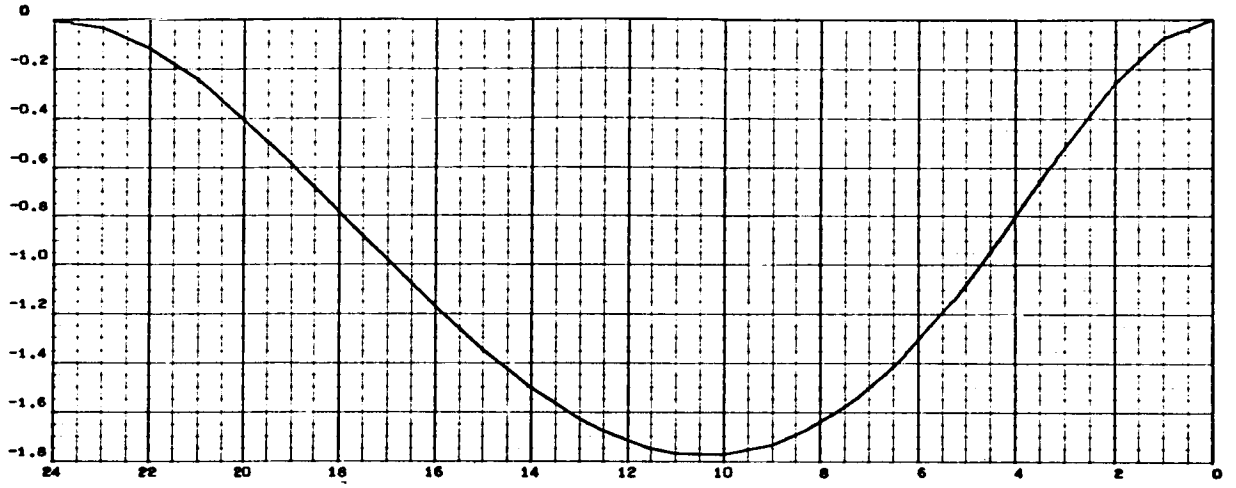

VEHICLE STATIONS - INCHES
SLOPE - DEG./FT.

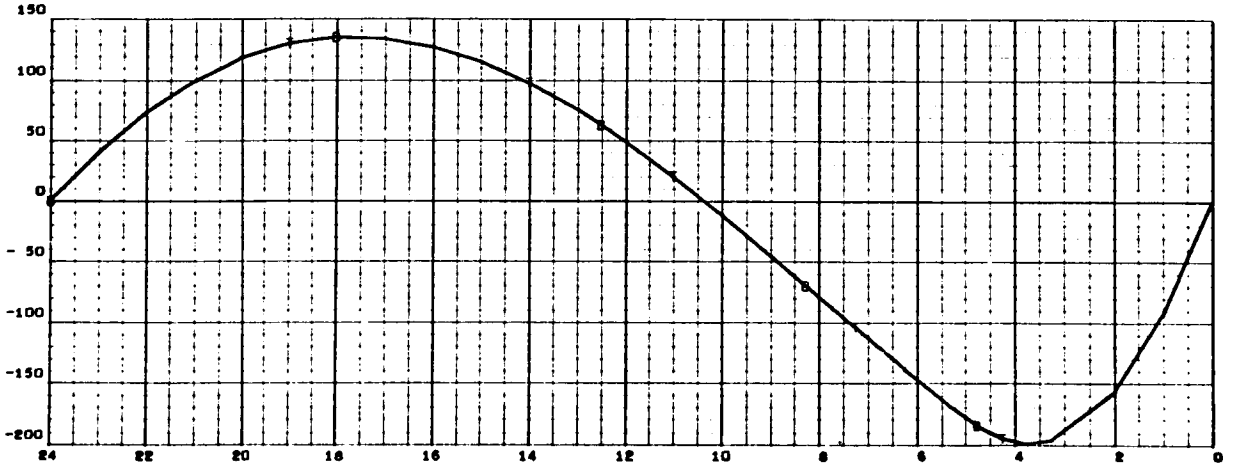

T = TOTAL SLOPE B = BENDING SLOPE
VEHICLE STATIONS - INCHES

MAY 24, 1966

2463-01
127 000

MASS LOADING EFFECTS ON BEAM VIBRATION - FIXED ENDS (CASE 19)

FREQUENCY (2) = 6.4780406E 02 RAD./SEC., 1.0310122E 02 C.P.S.
STRUCTURAL MODE (2)
NORMALIZED TO TOTAL WEIGHT
TOTAL WEIGHT = 2.6399999E 00
DEFLECTION - FT./FT.

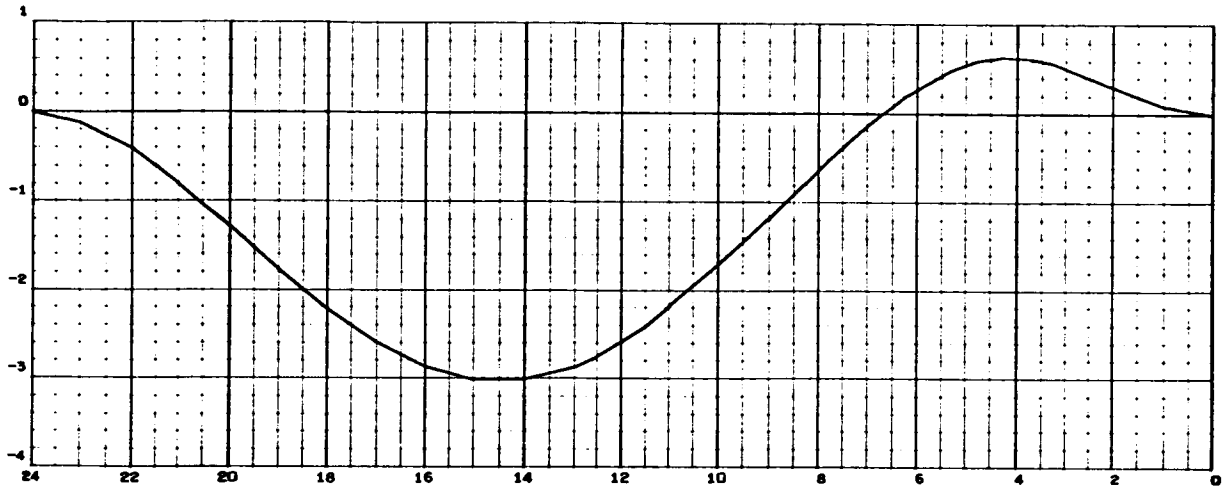

VEHICLE STATIONS - INCHES
SLOPE - DEG./FT.

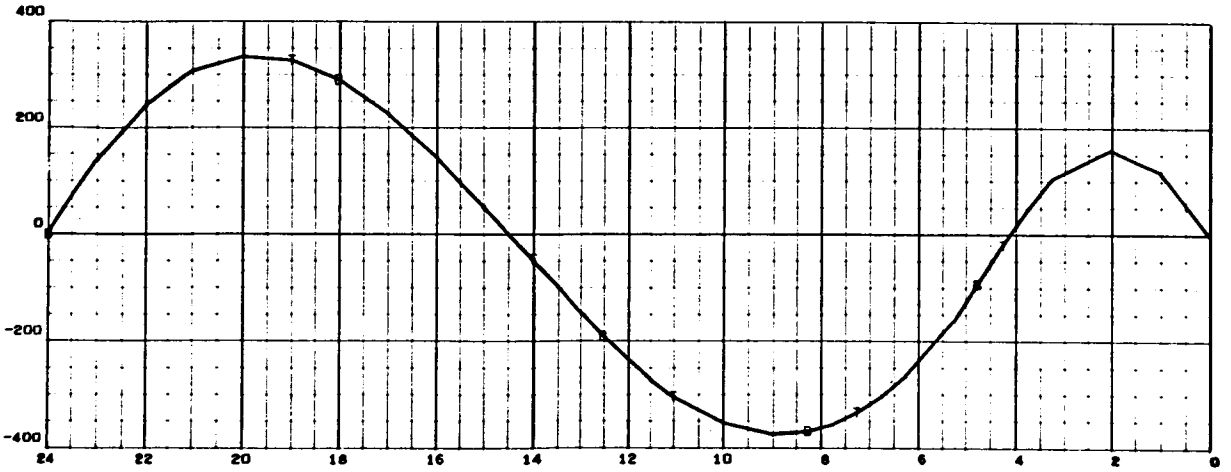

T = TOTAL SLOPE B = BENDING SLOPE
VEHICLE STATIONS - INCHES

MAY 24, 1966

2463-01
129 000

MASS LOADING EFFECTS ON BEAM VIBRATION - FIXED ENDS (CASE 19)

FREQUENCY (3) = 1.2778556E 03 RAD./S C., 2.0337703E 02 C.P.S.
STRUCTURAL MODE (3)
NORMALIZED TO TOTAL WEIGHT
TOTAL WEIGHT = 2.6399999E 00
DEFLECTION - FT./FT.

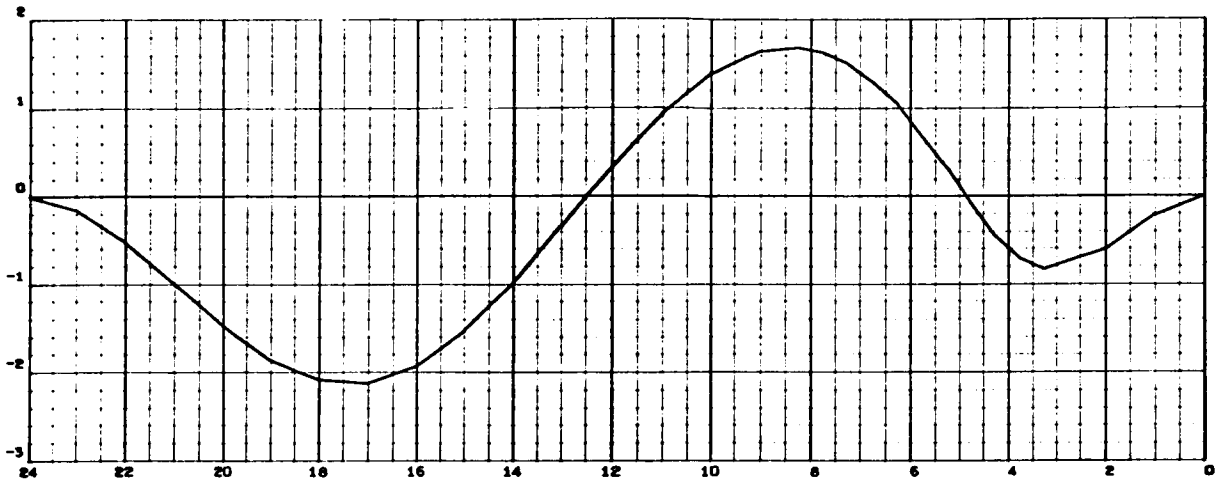

VEHICLE STATIONS - INCHES
SLOPE - DEG./FT.

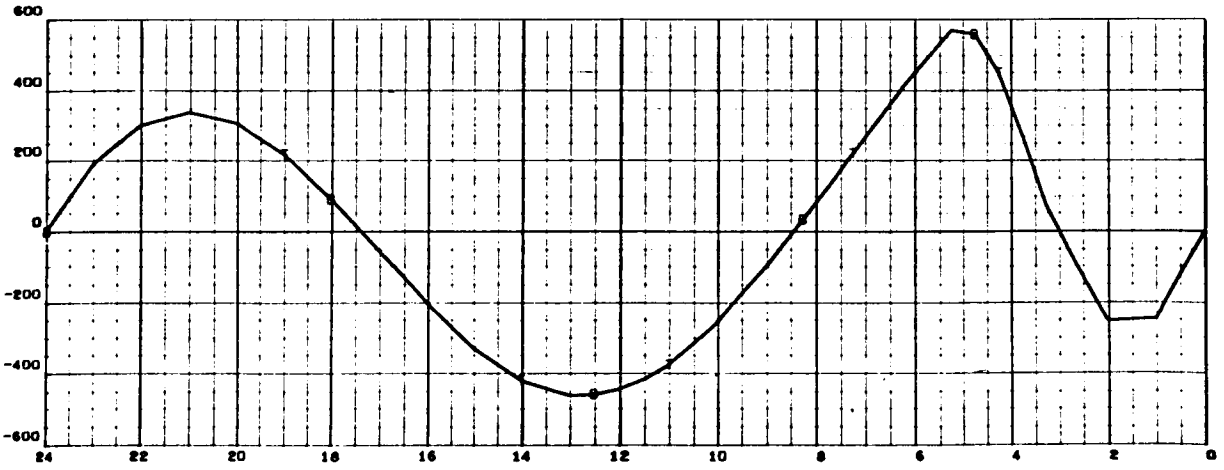

T = TOTAL SLOPE B = BENDING SLOPE
VEHICLE STATIONS - INCHES

MAY 24, 1966

2463-01 L
131 000

MASS LOADING EFFECTS ON BEAM VIBRATION - FIXED ENDS (CASE 19)

FREQUENCY (4) = 1.9680090E 03 RAD./SEC., 3.1321835E 02 C.P.S.
STRUCTURAL MODE (4)
NORMALIZED TO TOTAL WEIGHT
TOTAL WEIGHT = 2.6399999E 00
DEFLECTION - FT./FT.

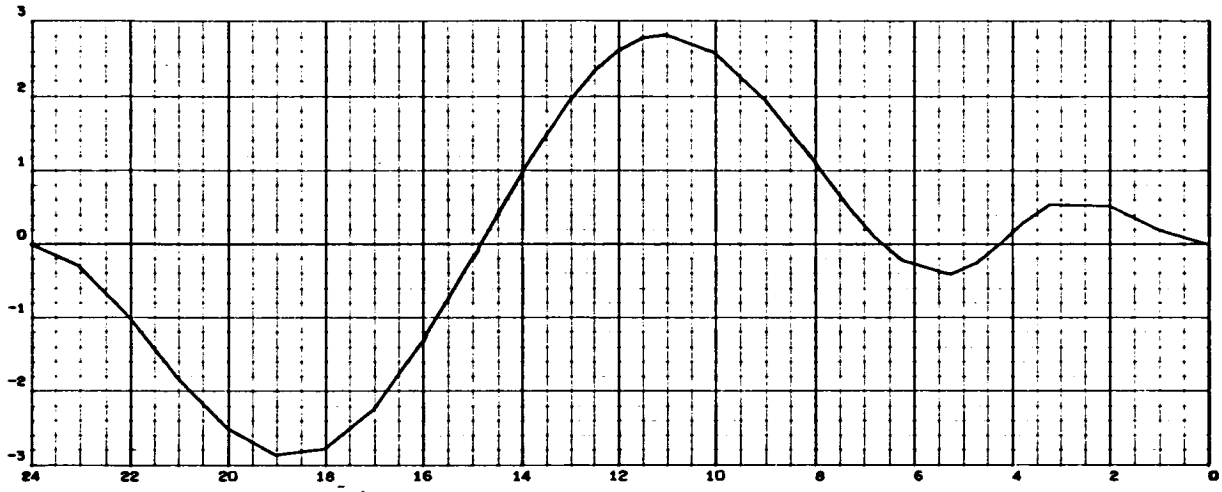

VEHICLE STATIONS - INCHES
SLOPE - DEG./FT.

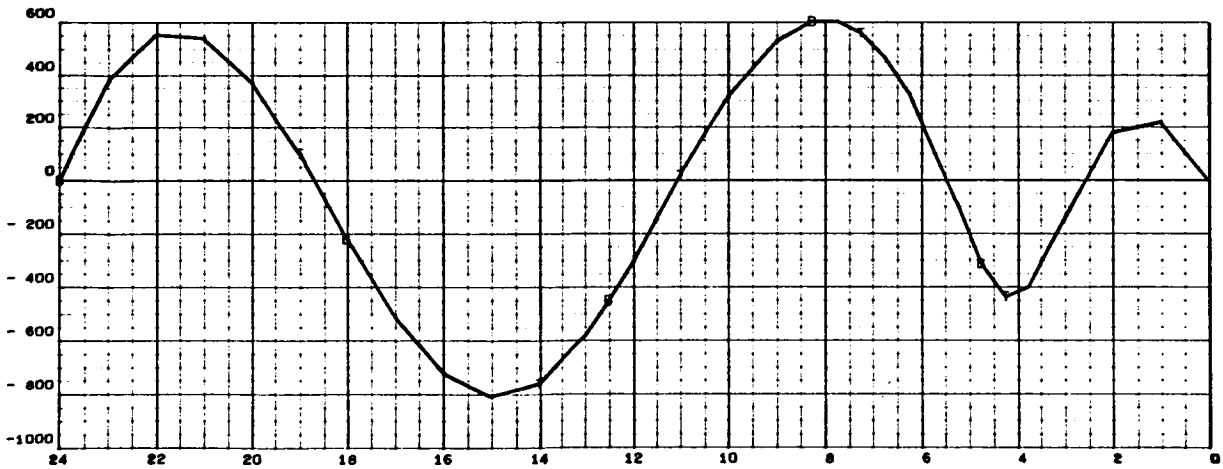

T = TOTAL SLOPE B = BENDING SLOPE
VEHICLE STATIONS - INCHES

MAY 24, 1966

2463-01 L
133 000

MASS LOADING EFFECTS ON BEAM VIBRATION - FIXED ENDS (CASE 20)

FREQUENCY (1) = 1.7636660E 02 RAD./SEC., 2.8069616E 01 C.P.S.
STRUCTURAL MODE (1)
NORMALIZED TO TOTAL WEIGHT
TOTAL WEIGHT = 2.6399998E 00
DEFLECTION - FT./FT.

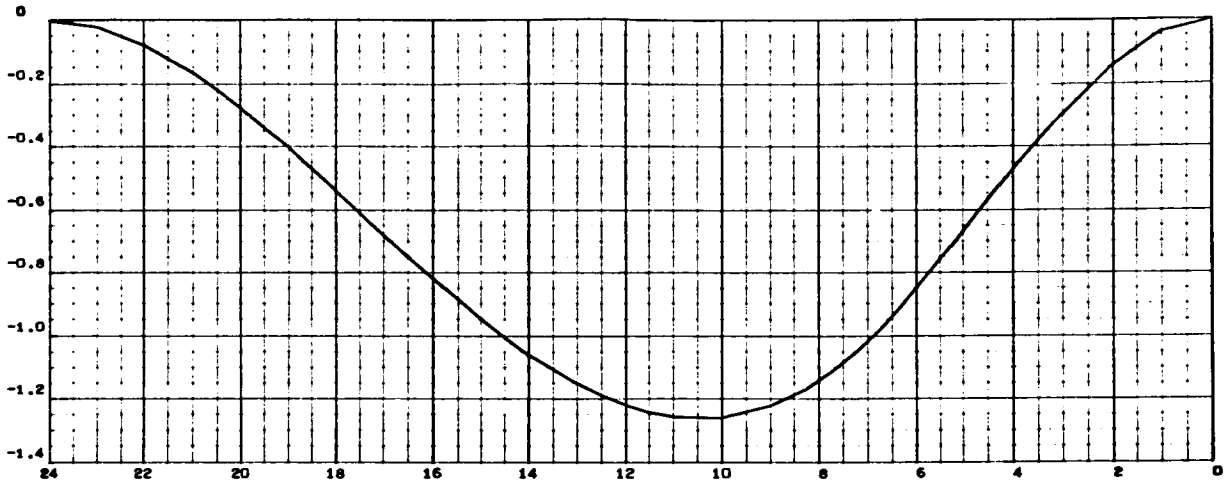

VEHICLE STATIONS - INCHES
SLOPE - DEG./FT.-

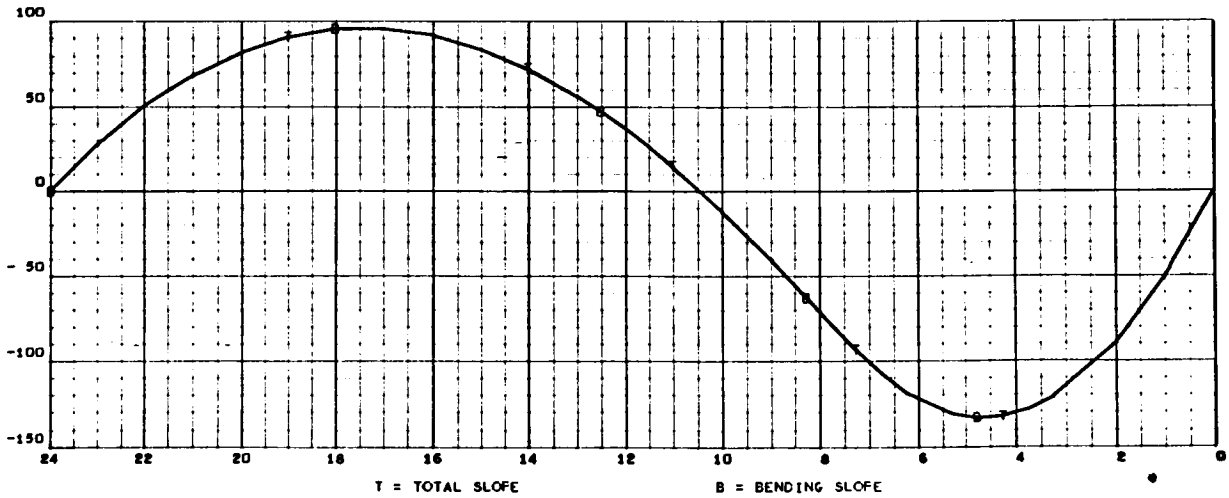

T = TOTAL SLOPE B = BENDING SLOPE
VEHICLE STATIONS - INCHES

MAY 24, 1966

2463-01
135 000

MASS LOADING EFFECTS ON BEAM VIBRATION - FIXED ENDS (CASE 20)

FREQUENCY (2) = 6.8852826E 02 RAD./SEC., 1.0958268E 02 C.P.S.
STRUCTURAL MODE (2)
NORMALIZED TO TOTAL WEIGHT
TOTAL WEIGHT = 2.6399998E 00
DEFLECTION - FT./FT.

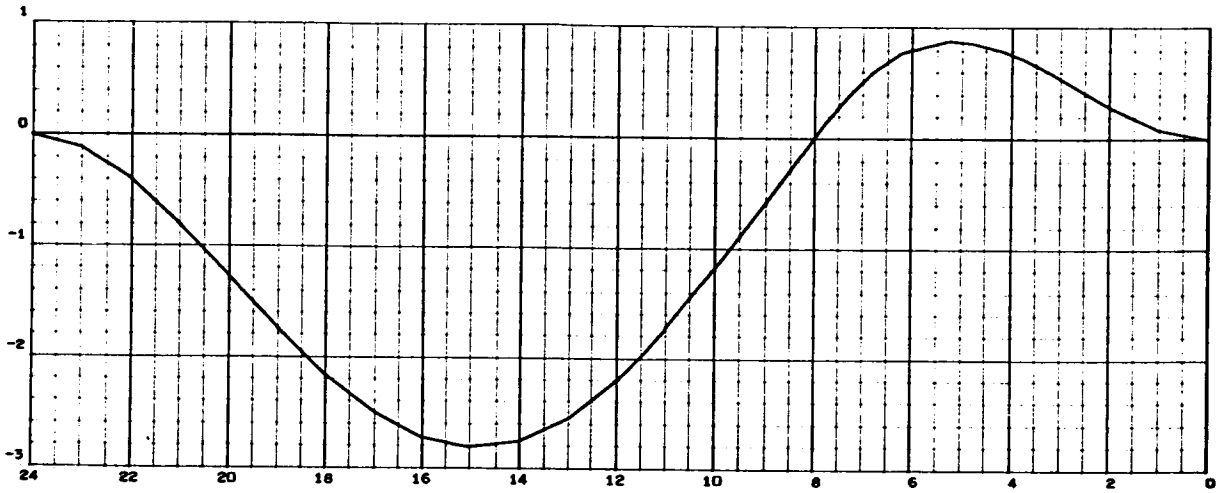

VEHICLE STATIONS - INCHES
SLOPE - DEG./FT.

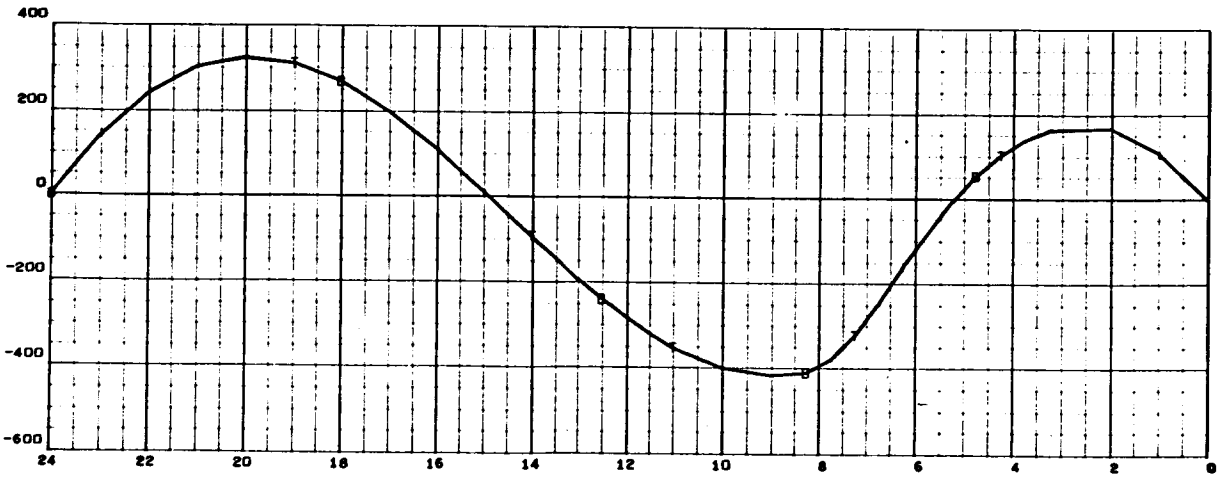

T = TOTAL SLOPE B = BENDING SLOPE
VEHICLE STATIONS - INCHES

MAY 24, 1966

2463-01
137 000

MASS LOADING EFFECTS ON BEAM VIBRATION - FIXED ENDS (CASE 20)

FREQUENCY (3) = 1.2144574E 03 RAD./SEC., 1.9328689E 02 C.P.S.
STRUCTURAL MODE (3)
NORMALIZED TO TOTAL WEIGHT
TOTAL WEIGHT = 2.6399998E 00
DEFLECTION - FT./FT.

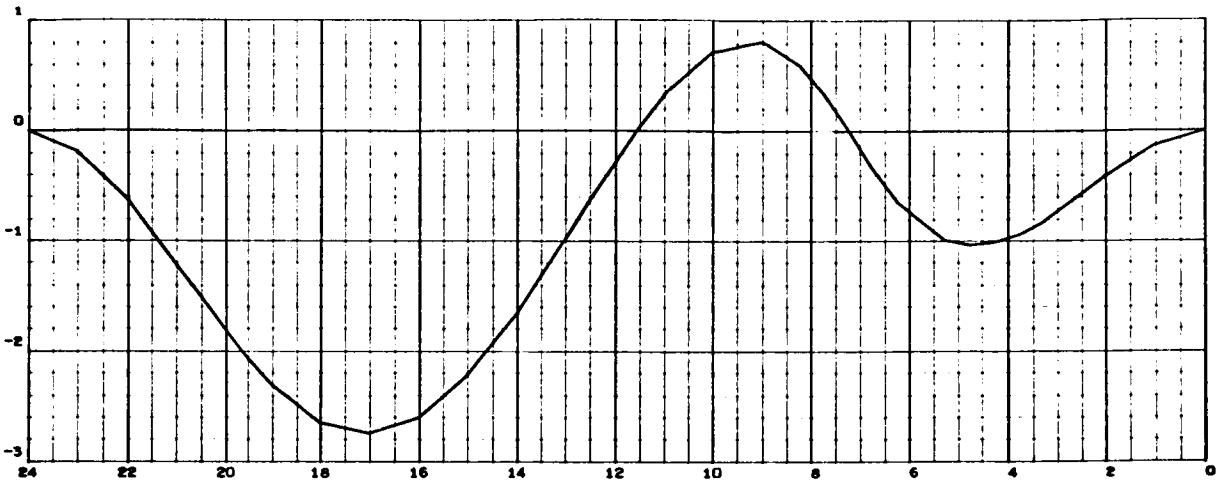

VEHICLE STATIONS - INCHES
SLOPE - DEG./FT.

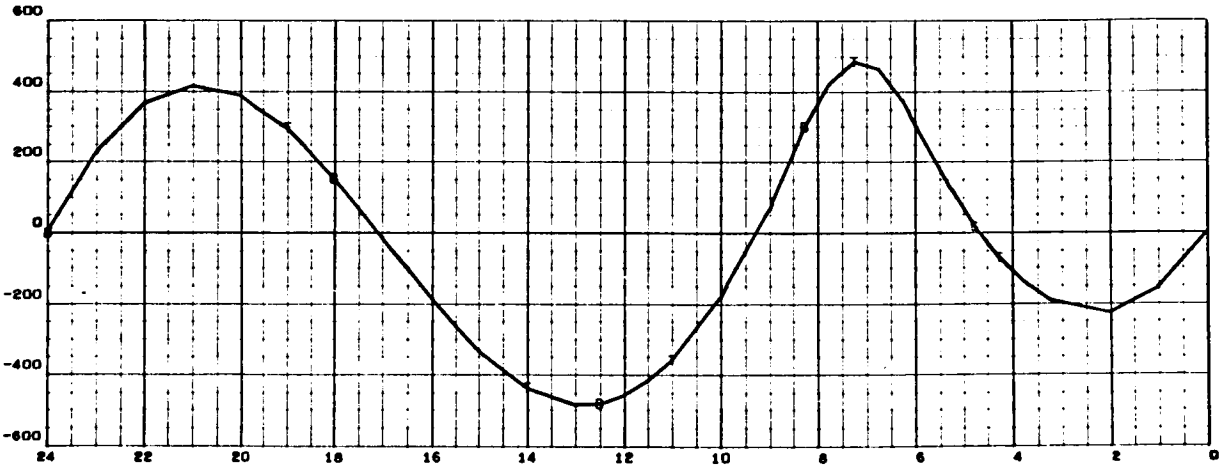

T = TOTAL SLOPE B = BENDING SLOPE
VEHICLE STATIONS - INCHES

MAY 24, 1966

2463-01
139 000

MASS LOADING EFFECTS ON BEAM VIBRATION - FIXED ENDS (CASE 20)

FREQUENCY (4) = 2.2130212E 03 RAD./SEC., 3.5221327E 02 C.P.S.
STRUCTURAL MODE (4)
NORMALIZED TO TOTAL WEIGHT
TOTAL WEIGHT = 2.6399998E 00
DEFLECTION - FT./FT.

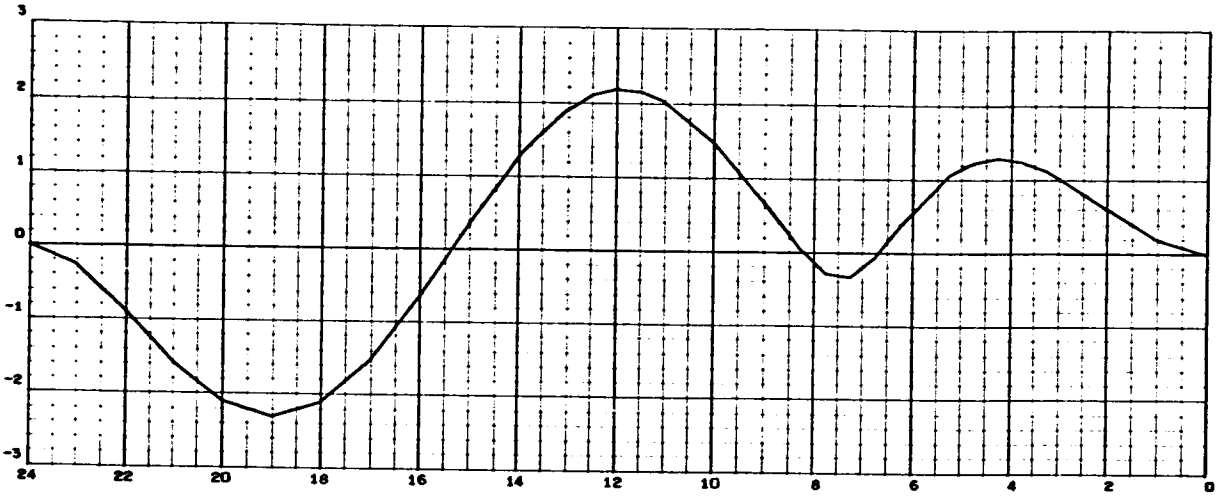

VEHICLE STATIONS - INCHES
SLOPE - DEG./FT.

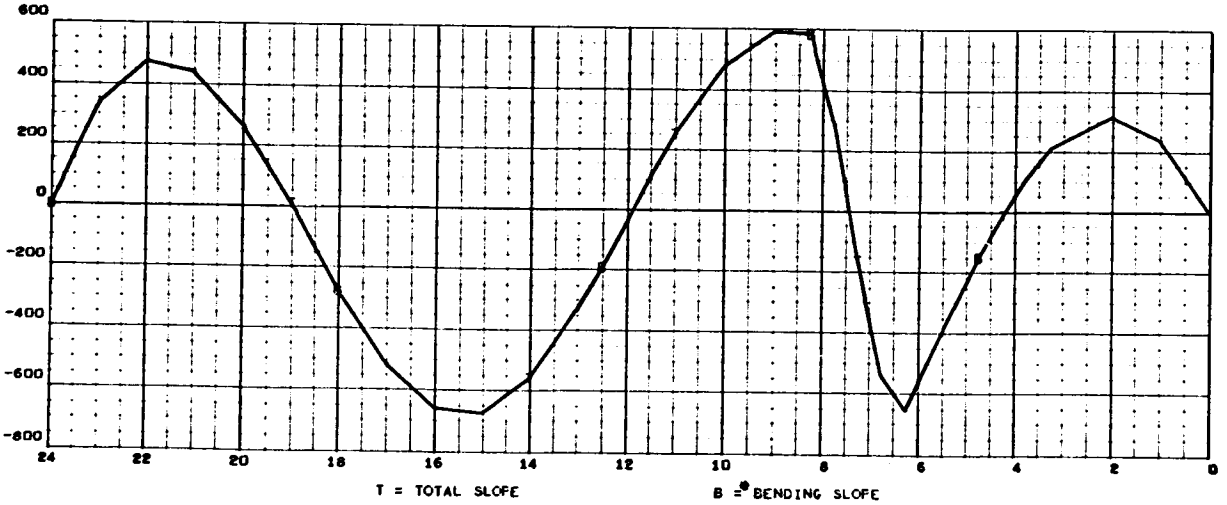

T = TOTAL SLOPE B = BENDING SLOPE
VEHICLE STATIONS - INCHES

MAY 24, 1966

2463-01
141 000

MASS LOADING EFFECTS ON BEAM VIBRATION - FIXED ENDS (CASE 21)

FREQUENCY (1) = 1.4152537E 02 RAD./SEC., 2.2524462E 01 C.P.S.
STRUCTURAL MODE (1)
NORMALIZED TO TOTAL WEIGHT
TOTAL WEIGHT = 2.6399997E 00
DEFLECTION - FT./FT.

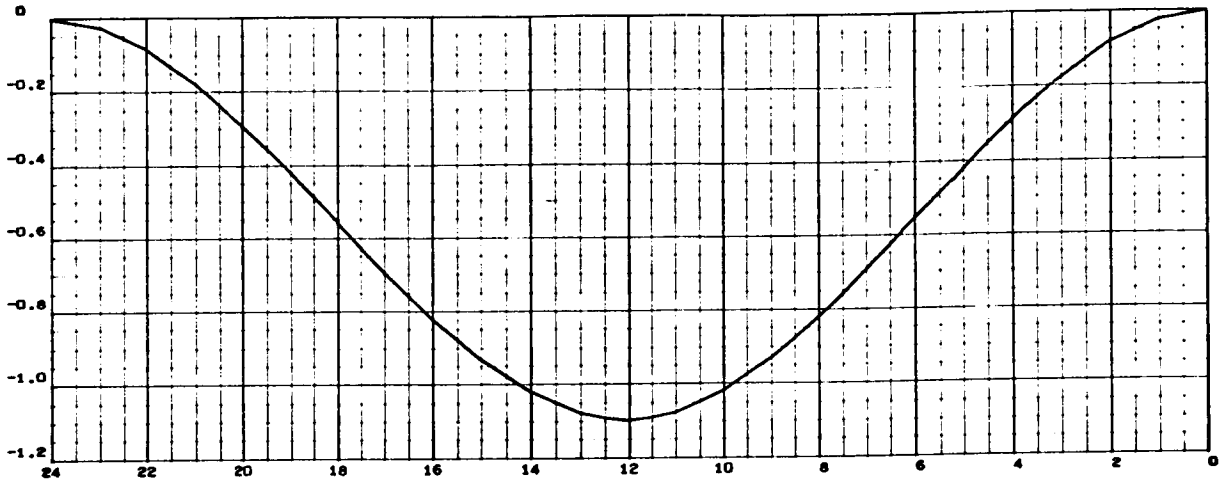

VEHICLE STATIONS - INCHES
SLOPE - DEG./FT.

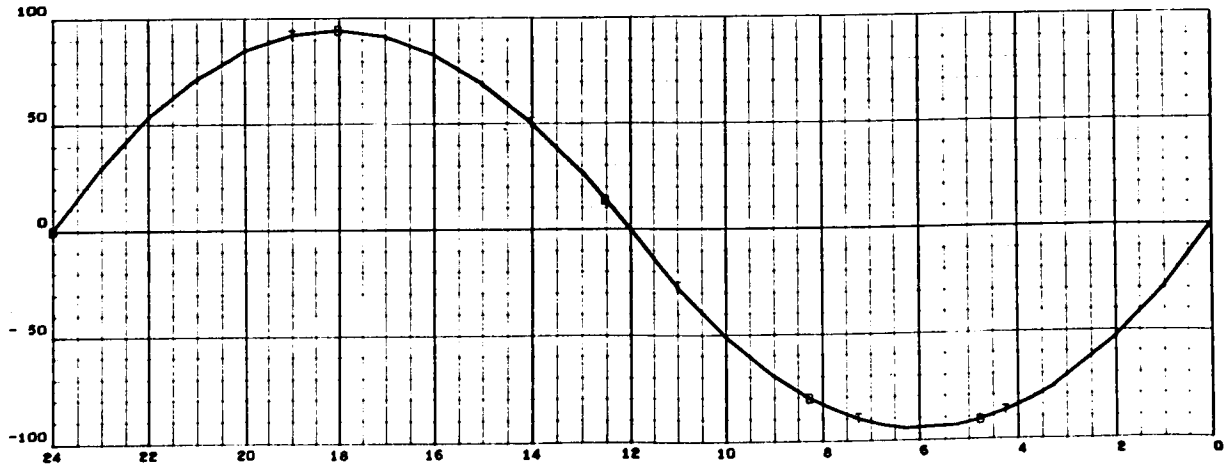

T = TOTAL SLOPE B = BENDING SLOPE
VEHICLE STATIONS - INCHES

MAY 24, 1966

2463-01 L
143 000

MASS LOADING EFFECTS ON BEAM VIBRATION - FIXED ENDS (CASE 21)

FREQUENCY (2) = 7.1488448E 02 RAD./SEC., 1.1377740E 02 C.F.S.
STRUCTURAL MODE (2)
NORMALIZED TO TOTAL WEIGHT
TOTAL WEIGHT = 2.6399997E 00
DEFLECTION - FT./FT.

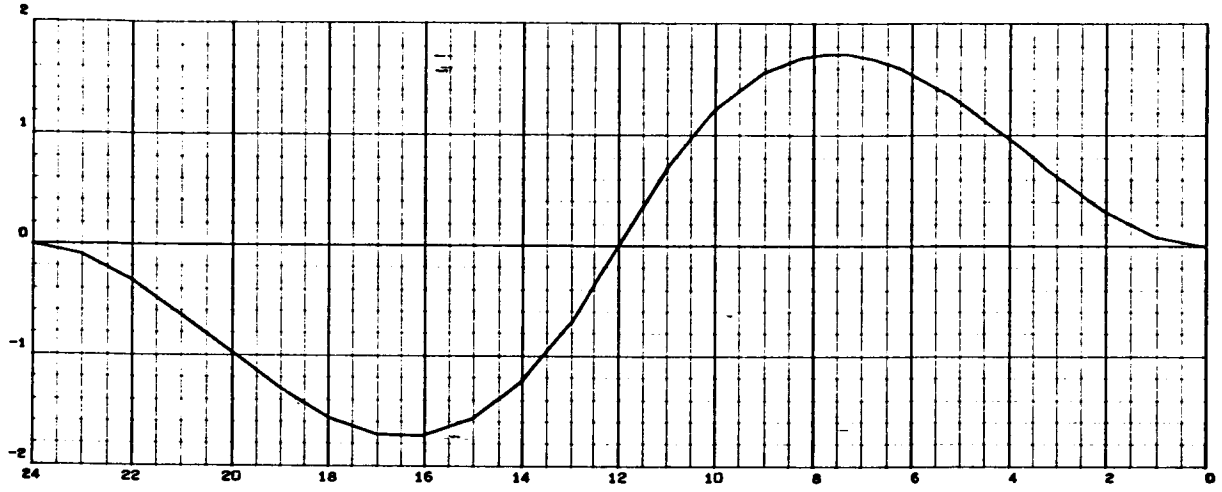

VEHICLE STATIONS - INCHES
SLOPE - DEG./FT.

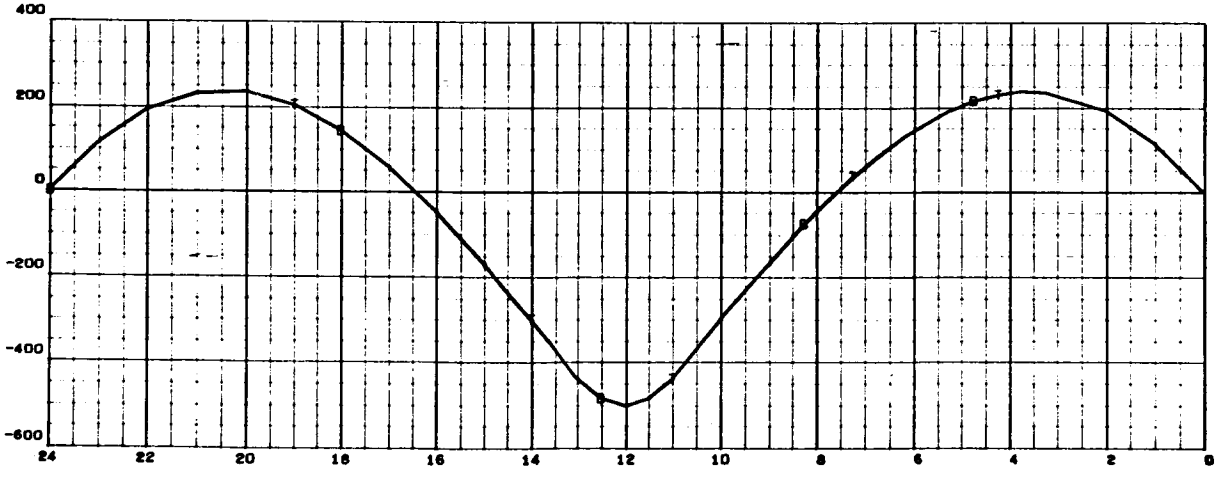

T = TOTAL SLOPE B = BENDING SLOPE
VEHICLE STATIONS - INCHES

MAY 24, 1966

2463-01
145 000

MASS LOADING EFFECTS ON BEAM VIBRATION - FIXED ENDS (CASE 21)

FREQUENCY (3) = 1.5877605E 03 RAD./SEC., 2.5269993E 02 C.P.S.
STRUCTURAL MODE (3)
NORMALIZED TO TOTAL WEIGHT
TOTAL WEIGHT = 2.6399997E 00
DEFLECTION - FT./FT.

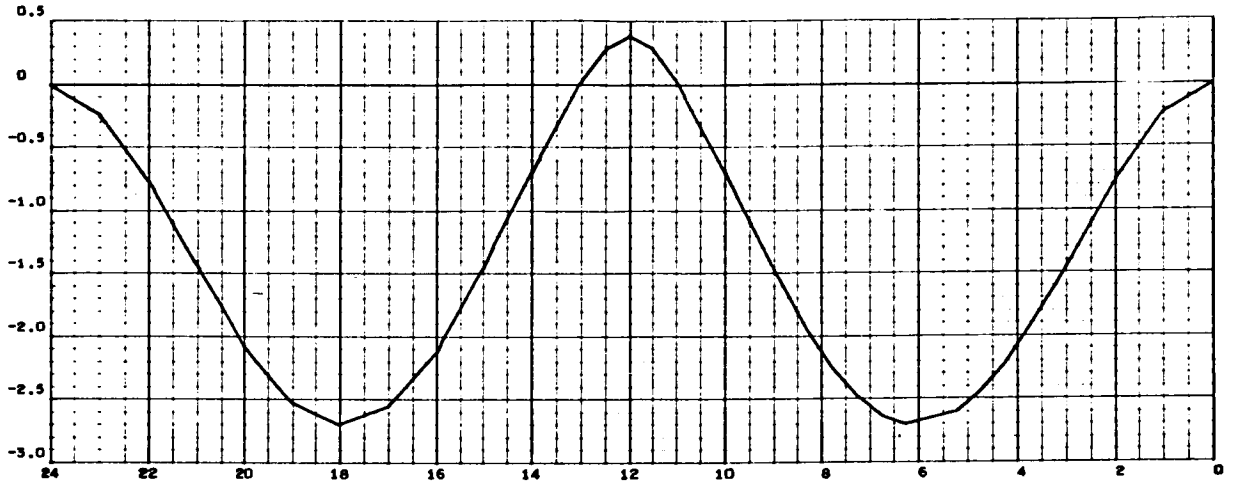

VEHICLE STATIONS - INCHES
SLOPE - DEG./FT.

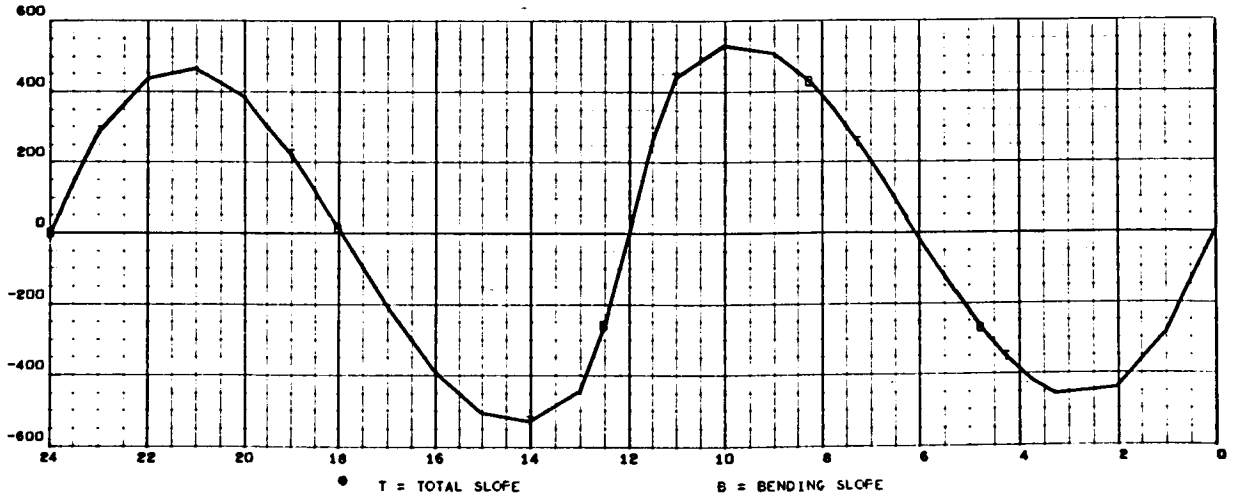

T = TOTAL SLOPE B = BENDING SLOPE
VEHICLE STATIONS - INCHES

MAY 24, 1966

2463-01
147 000

MASS LOADING EFFECTS ON BEAM VIBRATION - FIXED ENDS (CASE 21)

FREQUENCY (4) = 2.1440160E 03 RAD./SEC., 3.4123075E 02 C.P.S.
STRUCTURAL MODE (4)
NORMALIZED TO TOTAL WEIGHT
TOTAL WEIGHT = 2.6399997E 00
DEFLECTION - FT./FT.

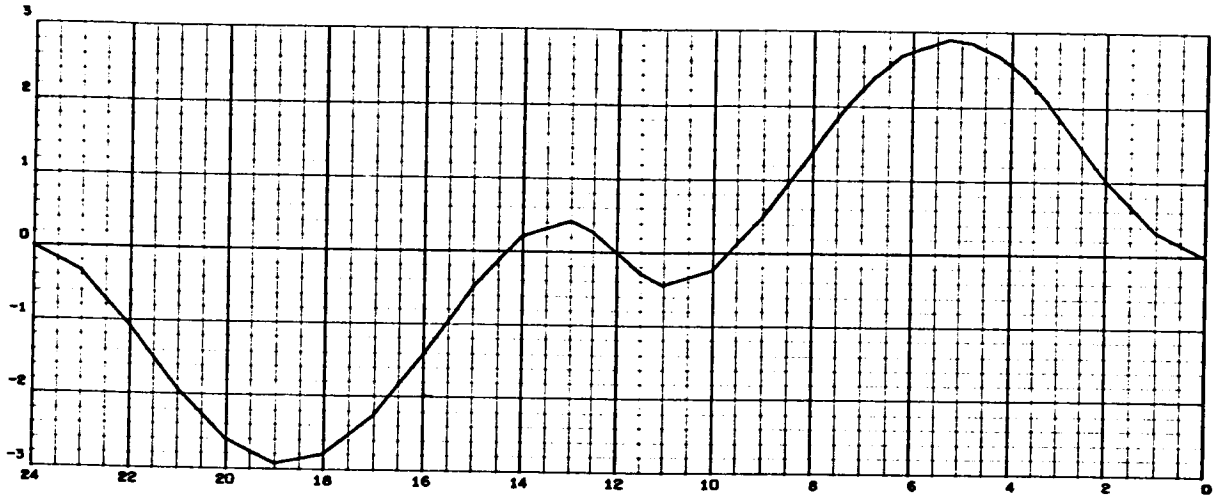

VEHICLE STATIONS - INCHES
SLOPE - DEG./FT.

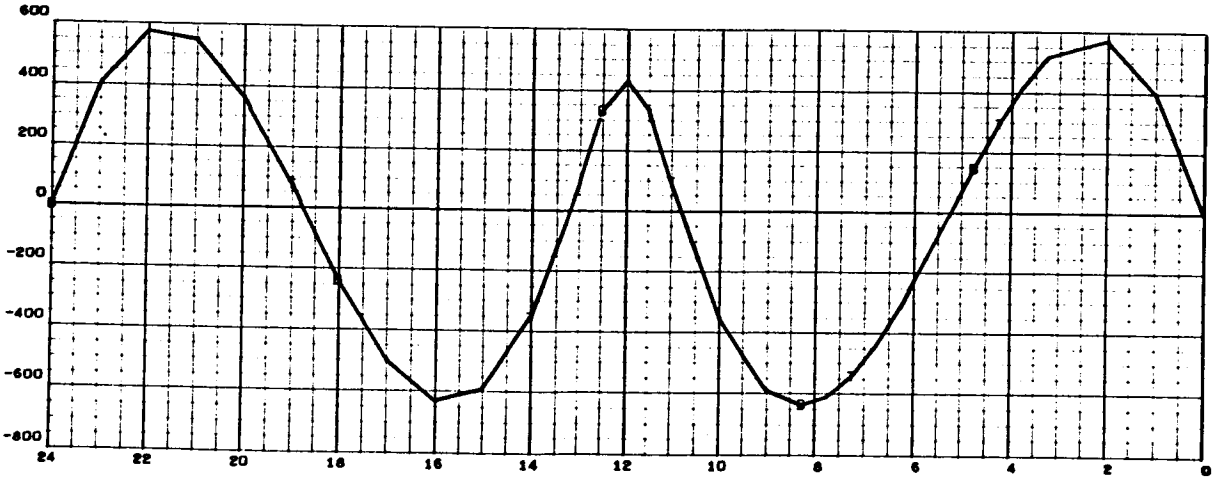

T = TOTAL SLOPE B = BENDING SLOPE
VEHICLE STATIONS - INCHES

APPENDIX B

ACCELERATION SPECTRAL DENSITY OF MASS-LOADED PLATES

The acceleration spectral density of the mass-loaded plates are presented in the following nine diagrams. The first one is the constant white-noise input for all random vibration tests on the plate. The others are the responses spectral density in g^2/cps for various masses at the center of the plate. For designation of each case, see "sampling" on the upper right corner of each diagram and refer to the following tabulation:

"Sampling" (Case No.)	Additional Mass, m_2 (Pounds)	Mass Ratio (m_2/m_1)
1-B-0	0	0
1-B-2	1.80	0.34
1-B-4	2.70	0.51
1-B-1	3.29	0.62
1-B-3	5.30	1.0
1-B-5	10.41	2.0
1-B-6	15.62	3.0
1-B-7	21.02	4.0

ACC. # 9
1B-0B

1

ENGINEERING DEVELOPMENT LABORATORY

without Acc' #10

TEST TITLE Mass Loading Test ~ Panel DATE 6-1-66
CHANNEL IDENTIFICATION Accel. #9 LR 2892
OVERALL 23 GRMS, FULL SCALE 40 G^2/CPS, SAMPLE LENGTH ___ SEC
RUN 1-B-0
BW_1 5 CPS 10 TO 100 CPS, SW. SP.1 ___ CPS/SEC, AV.T_1 ___ SEC
BW_2 10 CPS 100 TO 850 CPS, SW. SP.2 ___ CPS/SEC, AV.T_2 ___ SEC
BW_3 ___ CPS ___ TO ___ CPS, SW. SP.3 ___ CPS/SEC, AV.T_3 ___ SEC
CAL VOLTAGE ___ MVRMS = ___ G^2/CPS, OPERATOR ASK

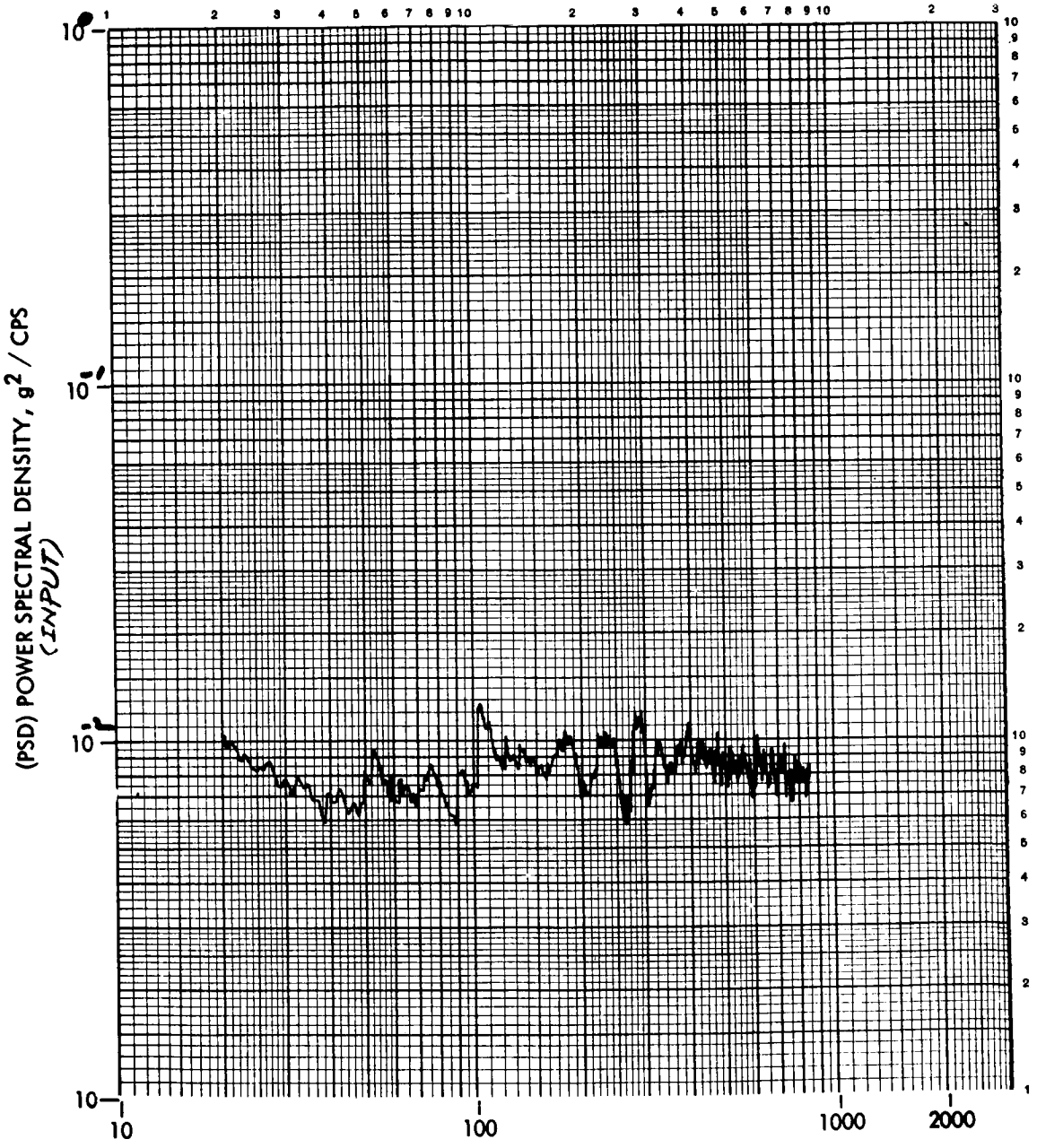

Enclosure ( )
Lab Memo No. S-37 1966

Figure -

MASS LOADING TEST-PANEL R1x97

Specimen:
S/N
P/N

Transducer: S/N
Control ( )
Response

TR
G RMS 13.3
Sampling: 1-B-0

RANDOM

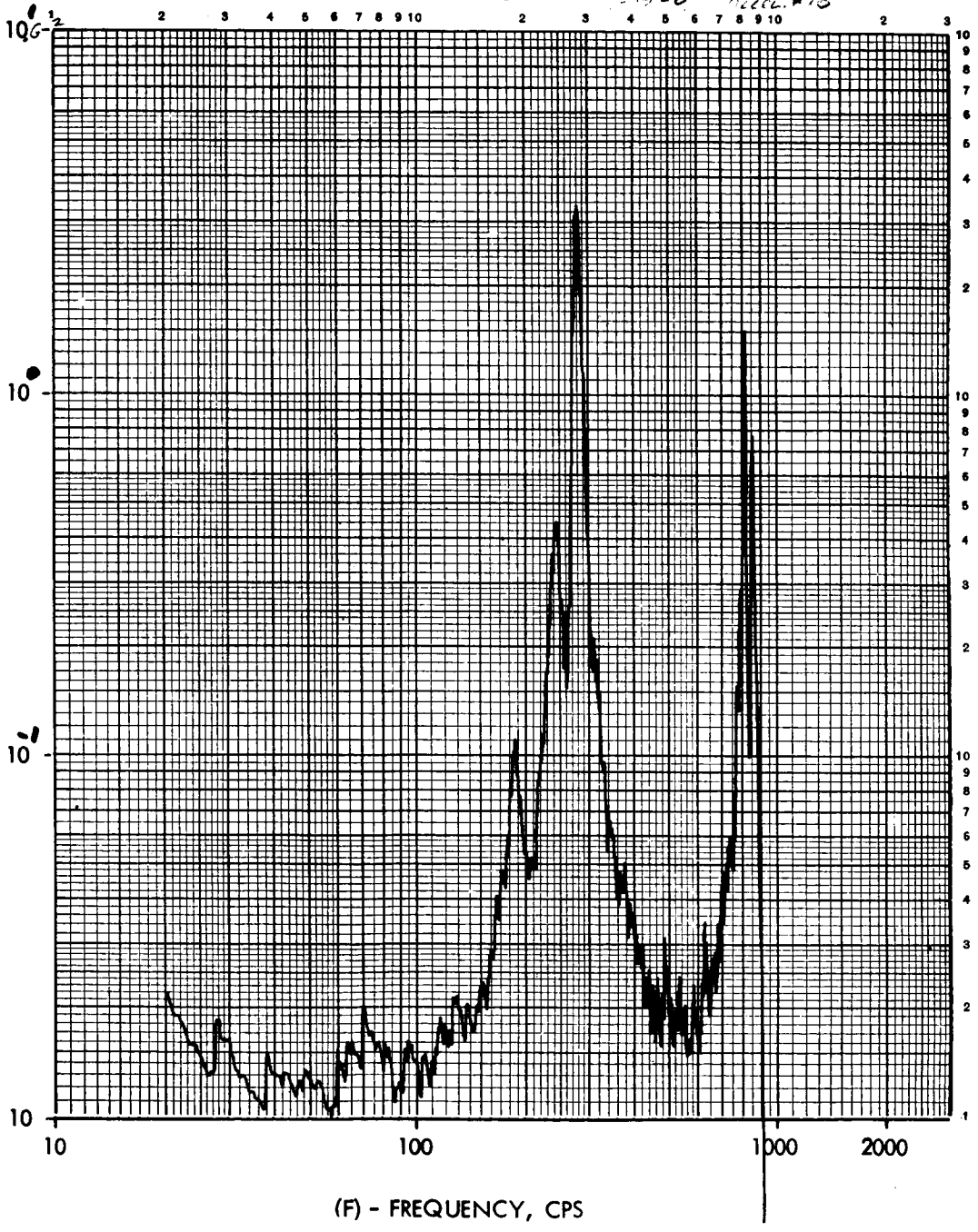

Enclosure ( )
Lab Memo No.
5-27-1966

Figure -

MASS LOADING TEST-PANEL

Specimen:
S/N
P/N

Transducer: S/N
Control ( )
Response #1 (#2)

TR
G RMS 5.3
Sampling : 1-8-1

RANDOM

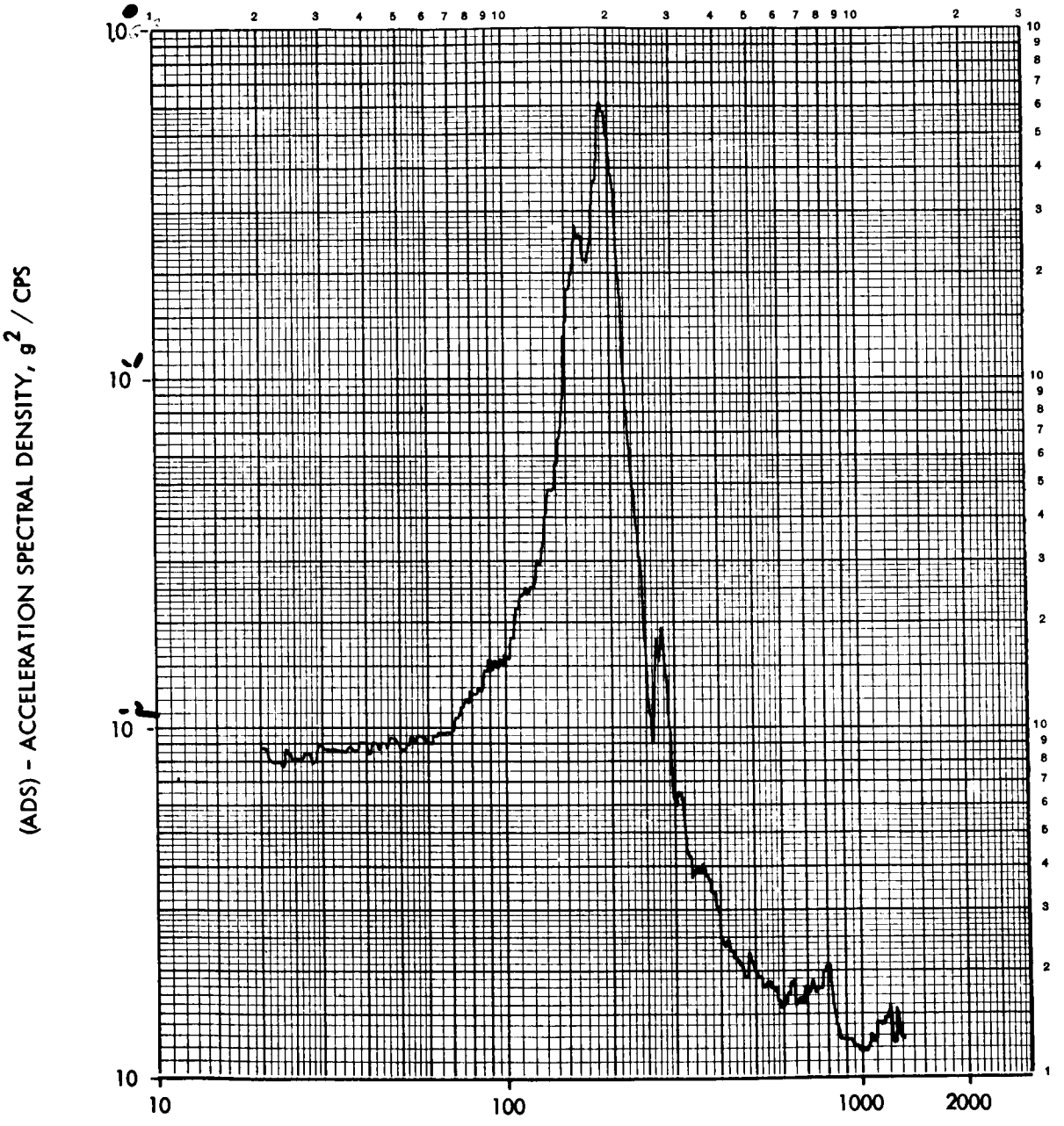

4

Enclosure ( )
Lab Memo No.
S-627-19

Figure -

MASS LOADING TEST ~ PANEL #2697

Specimen:
S/N
P/N

Transducer: S/N
Control ( )
Response ( )

TR
G RMS 7.0
Sampling: 1-B-2 NEW
1-B-2

RANDOM

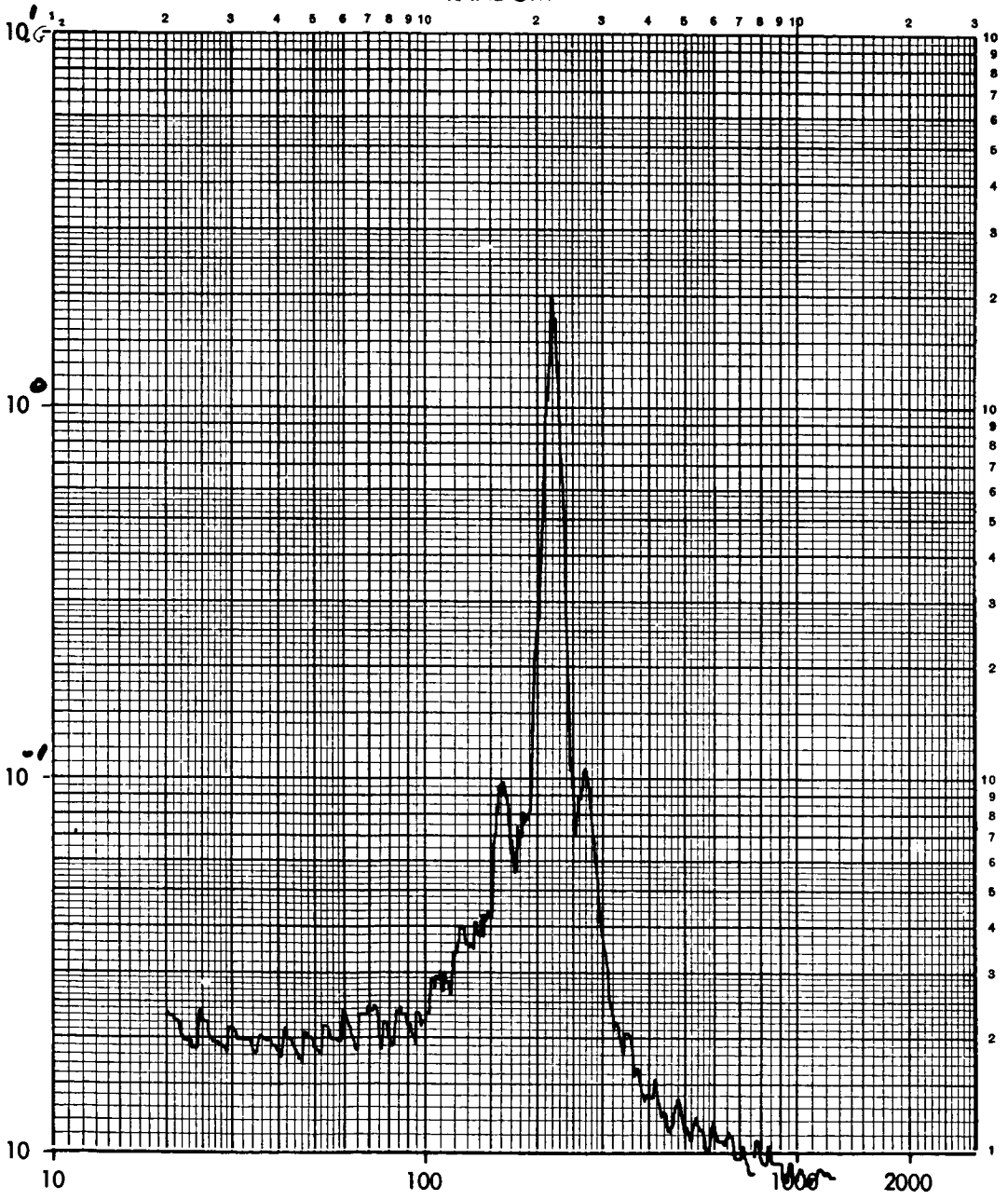

Enclosure ( )
Lab Memo No.
5-27 19 66

Figure -

MASS LOADING TEST ~ PANEL 4A-897

Specimen:
S/N
P/N

Transducer: S/N
Control ( )
Response #(10)

TR
G RMS 5.7
Sampling: 1-8-3
1-13-3

RANDOM

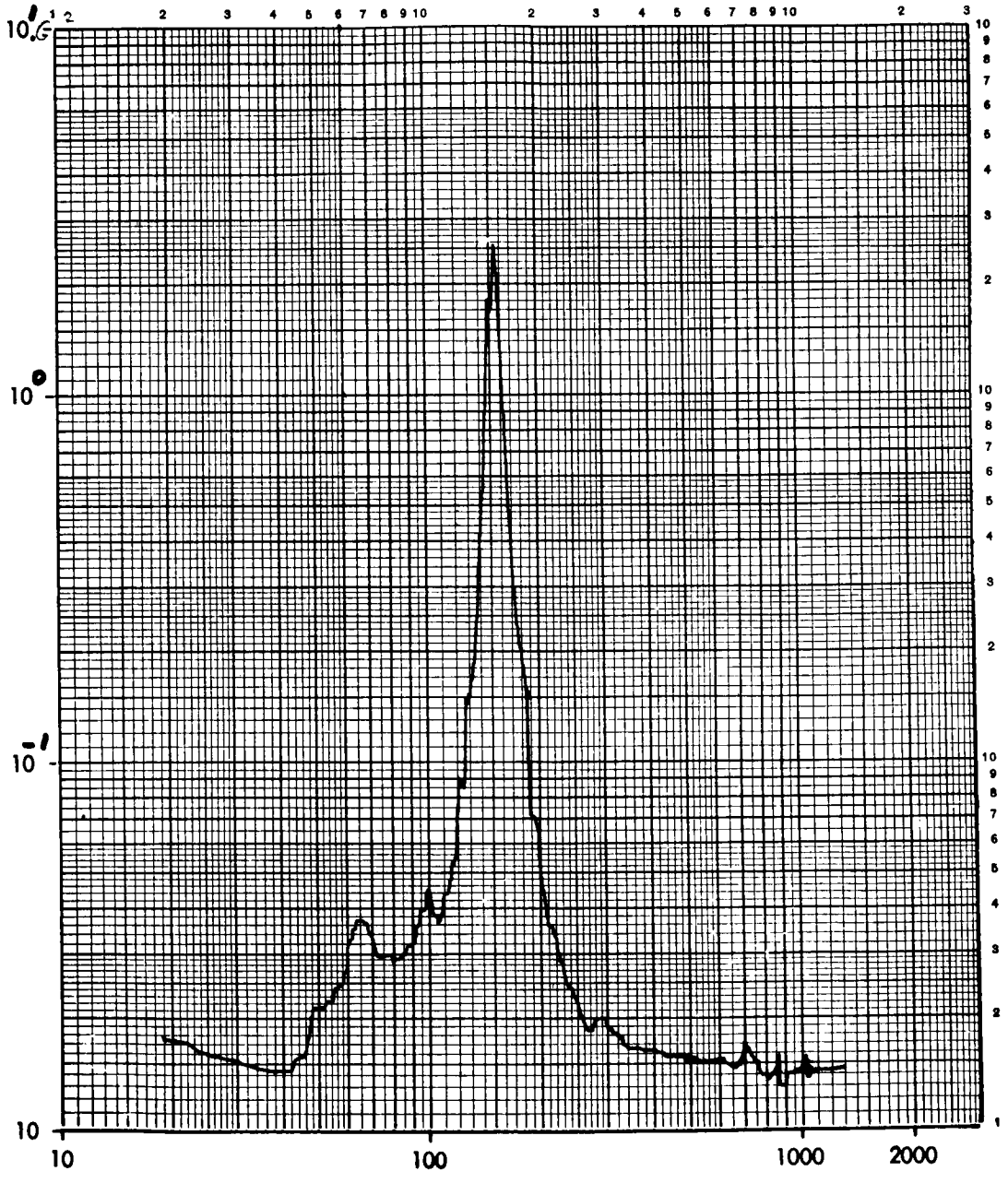

Enclosure ( ) 6
Lab Memo No. S-27 1966

Figure -

MASS LOADING TEST - PANEL

Specimen:
S/N
P/N

Transducer: S/N
Control ( )
Response (10)

TR
G RMS 6.0
Sampling 1-0-9

RANDOM

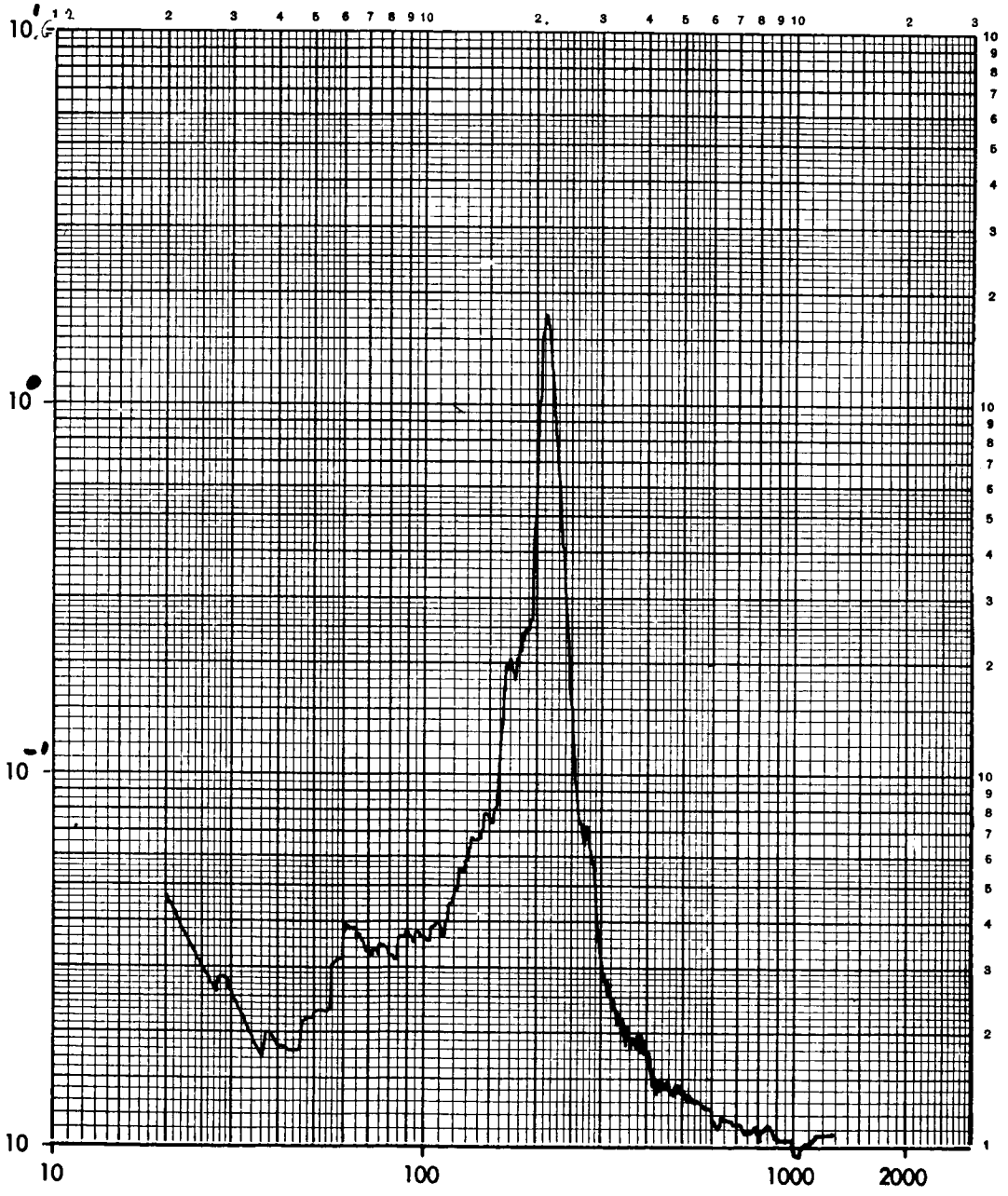

RCW

Enclosure ( )
Lab Memo No. 7
5-87 1966

Figure -

MASS LOADING TEST - PANEL (287)

Specimen:
S/N
P/N

Transducer: S/N
Control ( )
Response (10)

TR
G RMS 5.0
Sampling: 1-8-5
1-8-7

RANDOM

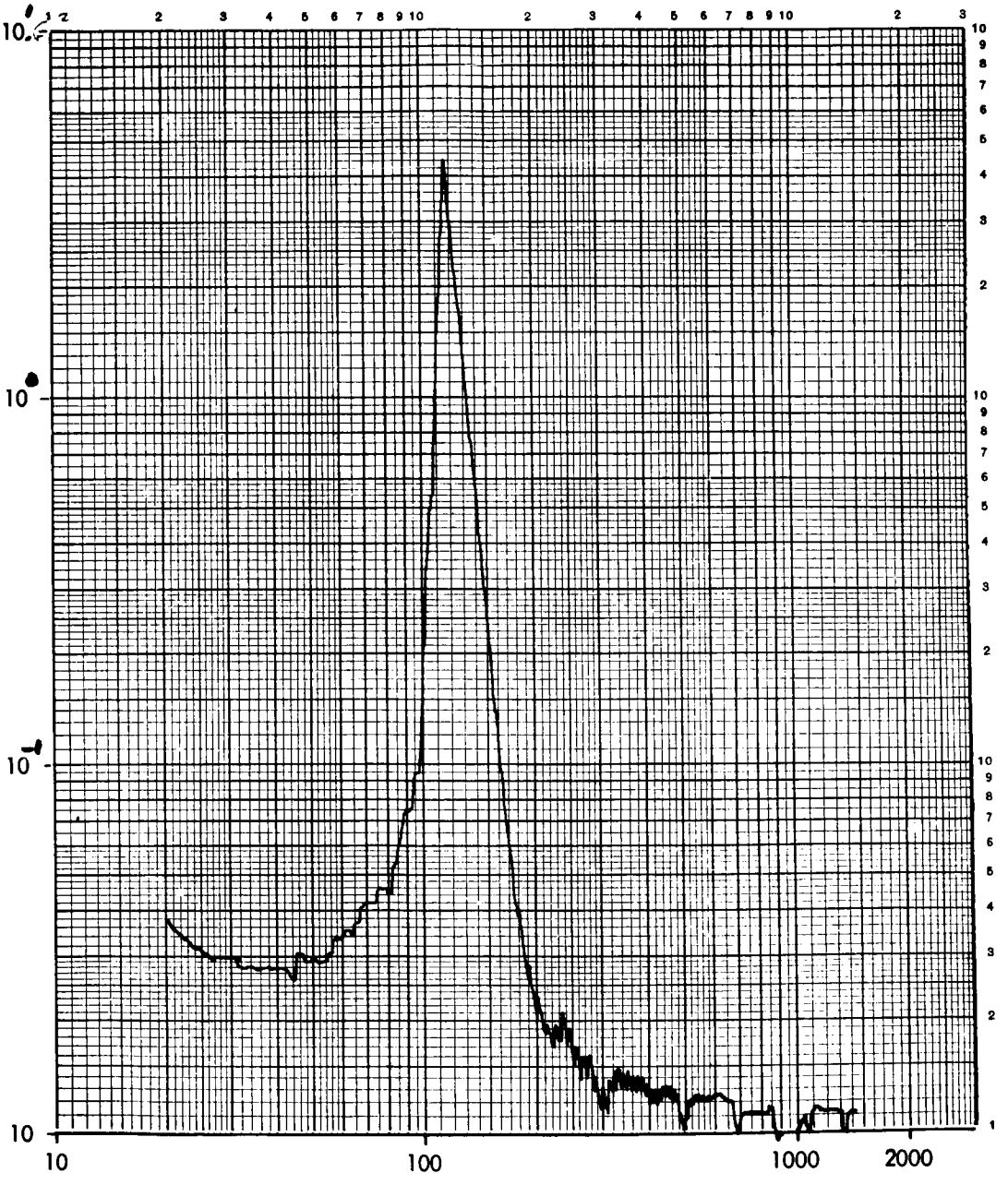

Enclosure ( )
Lab Memo No. S-[illegible]19[illegible]

Figure -

MASS LOADING TEST - PANEL [illegible]

Specimen:
S/N
P/N

Transducer: S/N
Control ( )
Response [illegible] ([illegible])

TR
G RMS 9.2
Sampling : 1-B-6

RANDOM

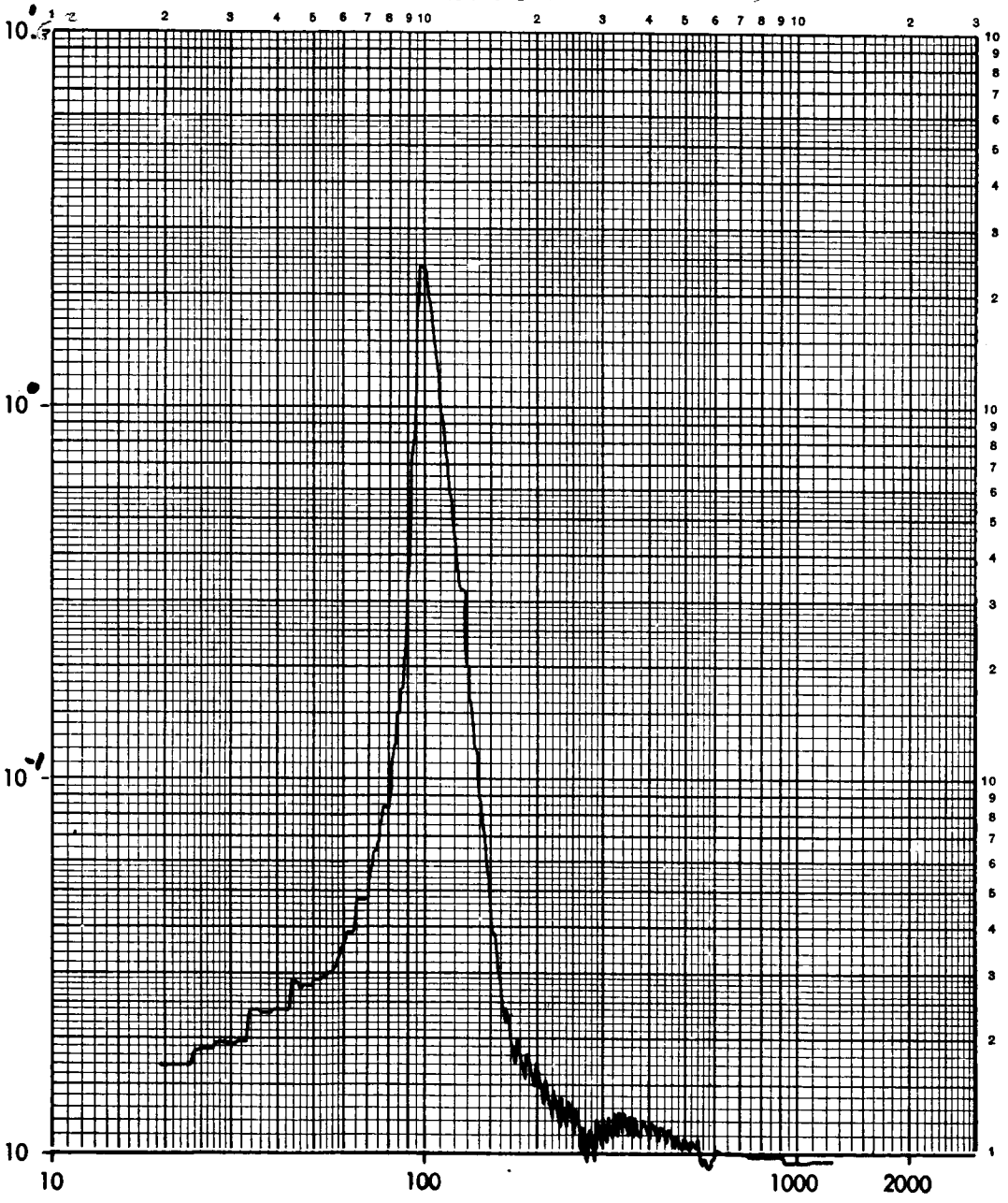

Enclosure ( )
Lab Memo No. 9
5-26 1966

Figure -

MASS LOADING TEST - PANEL

Specimen:
S/N
P/N

Transducer: S/N TR
Control ( ) G RMS 2.8
Response (W 40) Sampling 1-8-7

RANDOM